UNIVERSITÁ DEGLI STUDI DI PARMA

Dipartimento di Fisica e Scienze della Terra
Macedonio Melloni

Dottorato di ricerca in Fisica
Ciclo XXVIII

Studies on Wilson loops, correlators and localization in supersymmetric quantum field theories

Coordinatore:
Chiar.mo Prof. Cristiano Viappiani

Tutor:
Chiar.mo Prof. Luca Griguolo

Candidato:
Michelangelo Preti

Anno Accademico 2015-2016

Studies on Wilson loops, correlators and localization in supersymmetric quantum field theories

Michelangelo Preti

Supervisor: Prof. Luca Griguolo
Coordinator: Prof. Cristiano Viappiani

January 2016

Contents

Chapter 1

Overview and summary of the results

Relativistic quantum field theory describes consistently the electromagnetic force and the weak and strong nuclear interactions: these fundamental forces are successfully harmonized into a renormalizable gauge theory called the *Standard Model*. Unfortunately, gravity does not seem to enter into this framework. A consistent quantum theory of gravity is still lacking and its construction stands as one of the main problems of modern fundamental physics. Indeed there is no way of quantizing gravity due to its non-renormalizability. *String theory* is a promising candidate for this concern. Replacing the notion of point-like particles with one-dimensional strings it automatically includes as oscillation modes the Standard Model particles and a massless spin-two particle, identified with the graviton. A consistent bosonic string theory is constrained to live in a 26 dimensional space-time but, adding fermionic excitations, it gives rise to the ten-dimensional *superstring theory*.

Supersymmetry plays a central role both in superstring theory and in quantum field theory. While theoretically it provides a symmetric description of fermions and bosons, phenomenologically it could solve longstanding questions as hierarchy problem and dark matter origin. Supersymmetry is certainly not realized in nature at accessible energies but it can be seen as a powerful tool to drastically simplifies computation in field theories. In particular, including supersymmetry algebra into the field theory algebra, one is able to construct interesting theories with a lot of peculiar features. Furthermore, if one considers also the conformal invariance, the resulting theories, the so-called *superconformal field theories*, become enough constrained that exact computations of physical observables are accessible. The most studied superconformal field theories are the four-dimensional $\mathcal{N} = 4$ super Yang-Mills (SYM) and the three-dimensional $\mathcal{N} = 6$ super Chern-Simons theory with matter called ABJ(M). These two theories share a peculiar feature: they can be described as a string theory in the AdS/CFT framework.

The *AdS/CFT duality* is a powerful tool that gave and still gives a great contribution to the understanding of supersymmetric theories. It refers to the existence of dualities between theories with gravity and theories without gravity, and is also sometimes referred to as the gauge-gravity correspondence. This correspondence relates the weakly coupled regime of the gauge theory to the strongly coupled regime of the string theory and vice-versa. For some class of observables (called BPS), which preserve some supersymmetry of the theory, the actual value must be the same for all values of the coupling. For other observables, however, one needs to interpolate the results between the two regimes (even in some BPS cases). The prototype example of such a correspondence, as originally conjectured by Maldacena, is the equivalence between type IIB string theory compactified on $AdS_5 \times S^5$ and four-dimensional $\mathcal{N} = 4$ SYM theory. Another example is the duality between $\mathcal{N} = 6$ Super Chern-Simons theory with matter and string theory on $AdS_4 \times \mathbb{CP}^3$.

In both cases, *supersymmetric Wilson loops* provide a rich class of BPS observables that can be computed exactly through particular techniques, for instance *integrability* and *localization*. In particular, localization has been proven to be one of the most powerful tools in obtaining non perturbative results in quantum supersymmetric gauge theories. The key point is that supersymmetry algebras can be often deformed to accommodate background curvature on compact spaces and the resulting partition functions can be computed via a particular saddle-point procedure, known as the supersymmetric localization technique. Thanks to this procedure, an impressive number of new exact results have been derived for supersymmetric theories in different dimensions, mainly when formulated on spheres or products thereof.

This technique is enough flexible to compute also correlation functions of local operators and expectation values of non local observables, such as Wilson loops and 't Hooft loops. Actually the exact expression for circular 1/2 BPS Wilson loops in $\mathcal{N} = 4$ Super Yang-Mills theory was conjectured long before its concrete derivation through supersymmetric localization. This procedure in turn generalizes to a large class of $\mathcal{N} = 2$ theories, where Wilson loops can be also accurately studied through matrix model techniques.

Integrability technique gives non perturbative result from a completely different point of view. There is growing amount of evidences that $\mathcal{N} = 4$ SYM and ABJ(M) possess additional hidden symmetries at the quantum level that are not manifest in the Lagrangian formulation. These extra symmetries allow to describe gauge theories as an integrable system: indeed the single trace operator containing L fields in gauge theory mimes the spin-chain of length L. In this language one can use the Bethe equations and solve the spectrum obtaining the anomalous dimensions of the field theory operators. This technique can be applied to a large number of problems and in some situations may allow to access the strongly coupled regimes of gauge theories analytically. Furthermore, the AdS/CFT correspondence allows to compare these results.

As anticipated above, the Wilson loop is one of the most interesting observables in this context. It is a gauge invariant non-local operator, whose importance in non-

abelian gauge theories has been known for a long time. It is, namely, the holonomy of the gauge connection of the theory and in supersymmetric field theories can be a supersymmetric operator. In superconformal field theories the usual Wilson loop has additional couplings: in $\mathcal{N} = 4$ SYM it is coupled to some scalars and in ABJ(M) to scalars and fermions. For a suitable choice of these couplings the operator turns out to be supersymmetric and possesses a string theory description: indeed it is described, at large N and strong coupling, by a minimal surface in the bulk of AdS which ends on the contour of the Wilson loop. Calculating the expectation value of the circular Wilson loop on both sides of the correspondence has been one of the first successful tests of the duality.

In the case of $\mathcal{N} = 4$, the 1/2-BPS circle can be generalized to Wilson loops of arbitrary shapes with lower degree of supersymmetry. A particular family within this construction is composed by arbitrary loops lying on a two-sphere S^2 embedded into the Euclidean spacetime. These operators are generically 1/8-BPS, and their quantum correlators seem to be reproduced exactly by a purely perturbative calculation in bosonic 2D Yang-Mills (YM_2). The original conjecture was proved using supersymmetric localization. The computation in the two-dimensional theory can be exactly mapped to simple Gaussian matrix models, leading to an explicit evaluation of the correlators. More generally, localization should apply not only to the Wilson loops, but also to a whole sector of operators that are annihilated by shared supercharges. In particular it should concern a family of chiral primary operators inserted on S^2, leading to exact results for their correlators also in presence of Wilson loops. A careful computation of two-point functions and three-point functions of Wilson loop and chiral primaries on S^2 was performed using a Gaussian two and three-matrix models.

In this thesis we take instead a more conservative point of view and study the same correlation functions through the conventional diagrammatic expansion. Of course the first aim is to check the highly non-trivial reorganization of the perturbative series encoded into the two-matrix model result: localization automatically performs a number of divergences cancellation among different diagrams and combines finite contributions into nice expressions, written in terms of the geometry of the correlator. These effects are by no means obvious, especially when the position of the operator and the shape of the contour are arbitrary. The appearing of a gaussian matrix model suggests that only the combinatorics of perturbation theory should mind when bosonic propagators connecting points on the circuit are constant. In this case the contributions of the interactions, coming from internal loops and non-trivial vertices, should cancel among themselves. The first situation that we examine reproduces exactly this pattern: we consider a chiral operator inserted on the north-pole of S^2 and a Wilson loop placed on a latitude. The bosonic propagators are constant and we check explicitly the complete cancellation of the interacting diagrams at two-loops: we use dimensional regularization to tame the divergences appearing in the intermediate steps of the calculation and some Mellin-Barnes technology, adapted to our integration contours, to compute the relevant graphs. The resummation of the perturbative exchanges is then easily performed,

leading to the expected result. A more involved situation arises when the operator is inserted in a arbitrary point of one of the two hemispheres. The structure of the operator itself changes and the bosonic propagators suspended on the loop are no more constant, complicating the actual computation: in particular the terms involving three contour integrations cannot be reduced completely to double-integrals, as in the previous case. Moreover to evaluate the interacting diagrams we must resort to numerical integration. These diagrams interplay with the ladder ones to reproduces the matrix model result. In our computation we will consider chiral primaries of dimension $J = 2$: at two-loop this is not really a limitation, in fact one can extend the perturbative evaluation to the general case with some combinatorial effort[1]. Furthermore we will analyze explicitly the diagrams in the large N limit, taking into account just the planar contributions. In this way we will compare the perturbative results with the large N solution of matrix model, obtained from localization. The inclusion of non-planar terms can also be easily considered and we checked that they do not change the cancellation pattern.

Another important object appearing in gauge theories is the *cusp anomalous dimension* $\Gamma(\varphi)$, that was originally introduced in QCD as the ultraviolet divergence of a Wilson loop with Euclidean cusp angle φ. In supersymmetric theories these loops are not BPS due to the presence of the cusp. $\Gamma(\varphi)$ defines in the light-like limit $\varphi \to i\infty$ an universal observable: exact results have been derived in $\mathcal{N} = 4$ SYM through integrability that match both weak coupling expansions and string computations describing the strong coupling behavior. A related thermodynamic Bethe ansatz (TBA) approach, that goes beyond the light-like limit, is known: the cusp anomalous dimension can be generalized including an R-symmetry angle θ that controls the coupling of the scalars to the two halves of the cusp. This system interpolates between BPS configurations (describing supersymmetric Wilson loops) and generalized quark-antiquark potential: exact equations can be written applying integrability, and have been checked successfully at three loops. Moreover one can use localization in a suitable limit to obtain the exact form of the infamous Bremsstrahlung function, that controls the near-BPS behavior of the cusp anomalous dimension. The same result has been later directly recovered from the TBA equations and quantum spectral curve (QSC) method. It is clear that the generalized cusp anomalous dimension $\Gamma(\theta, \varphi)$ represents, in $\mathcal{N} = 4$ SYM, a favorable playground in which the relative domains of techniques as integrability and localization overlap.

The fundamental step that allowed to derive exact equations for $\Gamma(\theta, \varphi)$ from integrability was to consider the cusped Wilson loop with the insertion of L complex scalars Z on the tip. Importantly the scalars appearing in Z should be orthogonal to the combinations that couple to the Wilson lines forming the cusp. The anomalous dimension $\Gamma_L(\theta, \varphi)$ of the corresponding Wilson loop depends on L-unit of R-charge and a set of exact TBA equations can be written by for any value of L, θ and φ: setting $L = 0$ one of course recovers $\Gamma(\theta, \varphi)$. When $\varphi = \pm\theta$ the operator becomes BPS and its near-

[1]The basic combination at two-loop level always involve two-legs diagram, so $J = 2$ is the most general situation at this order.

BPS expansion in $(\varphi - \theta)$ can be studied directly from the integrability equations. The leading coefficient in this expansion is called the *Bremsstrahlung function* and when $L = 0$ its expression has been derived to all loops from localization. However the TBA equations and the quantum spectral curve (QSC) approach give a prediction for the Bremsstrahlung function $\mathcal{B}_L(\lambda, \varphi)$ at any L and φ.

In this thesis we use some localization results in $\mathcal{N} = 4$ SYM checking the prediction from integrability. Having an alternative derivation of the results may shed some light on the relations between these two very different methods. We consider in particular a 1/4 BPS Wilson loop (two longitudes) with contour lying on an S^2 subspace of $\mathbb{R}^4$, inserting at the north and south poles, where the BPS cusp ends, L "untraced" chiral primaries operators. From the analysis of the supersymmetries it turns out that the system is BPS. In this framework we can relate the near BPS limit of $\Gamma_L(\theta, \varphi)$ to a derivative of the wedge Wilson loop with local insertions and define a generalized Bremsstrahlung function $\mathcal{B}_L(\lambda, \varphi)$. Our central observation is that the combined system of our Wilson loop and the appropriate local operator insertions still preserves the relevant supercharges to apply the localization procedure allowing the computation of $\mathcal{B}_L(\lambda, \varphi)$ by a perturbative calculation in YM_2 on S^2. The problem of resumming in this case the perturbative series in YM_2 is still formidable and we limit ourselves to the first non-trivial perturbative order for any L. In so doing we recover, in closed form, the leading Lüscher correction to the ground state energy of the open spin chain, that describes the system in the integrability approach.

ABJ(M) theory also possesses integrable structures and a localization procedure for some classes of Wilson loops is known as well. Furthermore, its strong coupling limit is encoded into string theory on the $AdS_4 \times \mathbb{CP}^3$ background. However in this theory the weak/strong interpolation is non-trivial even for the simple circular 1/2 BPS Wilson loop. One can introduce cusped Wilson loops with generalized cusp anomalous dimension $\Gamma(\theta, \varphi)$ also in ABJ(M) theory. The two halves of the cusp must couple also to the fermions of the theory and not only to the gauge connections and scalars in order to have an 1/2 BPS object. The resulting cusped Wilson loop is not globally supersymmetric and therefore its exact evaluation seems very challenging. The analogous system in $\mathcal{N} = 4$ SYM can be tackled in a particular limit through Feynman diagrams resummation. It is a scaling limit where the scalars becomes dominant, and the leading order contribution is simply given by ladder diagrams made by scalar exchanges. These ladder diagrams can be summed up efficiently using a Bethe-Salpeter equation, that provides a very simple description. Its solution, in the small angle limit, reproduces at strong coupling the string theory calculation. The matching of the strong coupling limit of the Bethe-Salpeter solution with the string theory computation holds also at the nesxt to leading order. This fact is a bit surprising since there is no reason why the strong coupling and the scaling limits commute.

In this thesis we consider a similar limit in three-dimensional ABJ(M) theory, obtaining some exact results for $\Gamma(\theta, \varphi)$. The presence of fermionic couplings to the loop inherits

a surprising supersymmetric structure in the relevant Bethe-Salpeter equation. More precisely, the effective Schroedinger problem, associated to the integral equation that resums planar diagrams in $\mathcal{N} = 6$ Super Chern-Simons, enjoys an unexpected quantum mechanical supersymmetry. Since only the ground state matters in determining $\Gamma(\theta, \varphi)$, supersymmetry produces an exact expression for *any* value of the opening angle φ. This is in sharp contrast with the $\mathcal{N} = 4$ case, where an analytic solution for the Bethe-Salpeter equation exists only at $\varphi = 0$.

In the ABJM case ($N = M$) we get a very simple solution: the cusp anomalous dimension is exact at one-loop level, as in an abelian theory. The delicate balance between bosonic and fermionic contributions, encoded into the effective supersymmetric quantum mechanics, exponentiates without non-abelian correction the one-loop term. As a matter of fact we do not observe any transition between a weak-coupling and a strong-coupling regime, the observable behaving as in a free gauge theory. Consequently we cannot match our result directly with the semiclassical computations of string theory, suggesting that it exists, in this case, a problem with the order of limits.

In the ABJ case ($N \neq M$) the story is even more intriguing: the Bethe-Salpeter equation reduces to two coupled integral equations, resumming the $(N \times N)$ and the $(M \times M)$ sectors. The problem is solved by diagonalizing the system and we end up with a two-dimensional supersymmetric Schroedinger equation. The exact ground state is then obtained and we have to fix carefully the normalization of the wave functions in order to reconstruct the original cusped Wilson loops. This is done by using the boundary conditions of the original Bethe-Salpeter equation and the first non-trivial order of its perturbative expansion. The main result of our investigation is that, in the ABJ case, the original cusped Wilson loop, *i.e.* the trace of the superconnection, does not renormalize multiplicatively but it mixes at quantum level with the supertraced operator. As a consequence we end up with two independent cusp anomalous dimensions, related to the renormalization constants of the operator eigenstates (with respect to the mixing).

The structure of this thesis is the following. In the first three chapters we lay the foundations for understanding the results accomplished in chapters 5, 6 and 7. In Chapter 2 we review some basics facts about superconformal field theories and in particular for $\mathcal{N} = 4$ SYM and ABJ(M) theories. We mention also their relations with the string theories and the general features of supersymmetric localization and integrability. Chapter 3 is dedicated to the definition of supersymmetric Wilson loops with explicit examples of computation of their vacuum expectation value (vev): we consider a very well-known configuration, the circular Wilson loop. It is also shown how supersymmetric localization predicts the all-loop vev for some classes of loops in $\mathcal{N} = 4$ SYM and ABJ(M) theories. In Chapter 4 we define the Wilson line with a cusp and we discuss the main features of its anomalous dimension in superconformal theories. Chapters 5, 6 and 7 are based on my original work and illustrate my results. In Chapter 5 we present a weak-coupling computation of some correlation functions of Wilson loops and local operators checking the localization result in $\mathcal{N} = 4$ SYM theory. Chapter 6 is dedicated

to the computation of the leading order of the Bremsstrahlung function in $\mathcal{N} = 4$ SYM in presence of L chiral operators on the tip of the loop. In Chapter 7 we present the calculation of the cusp anomalous dimension in ABJ(M) theory, performing the scaling limit that selects only ladder diagrams and resumming of the perturbative series. Conclusions are drawn in 8, where we also suggest further developments and outlooks of our research. Technical aspects such as propagators and conventions, and also some very tedious computations, are summarized in appendices A, B, C and D.

Chapter 2

Introduction

One of the main reasons why we study supersymmetric field theories is that, due to impressive cancellations between fermion and boson corrections, we are able to compute analytically a lot of quantities of interest. Certain quantities that are small or vanish classically remain so also when radiative corrections are taken into account. Famous examples include the vanishing of the cosmological constant, the hierarchy problem or the issue of renormalization of quantum gravity. While supersymmetry solves most of these issues, it cannot be the complete answer, since it cannot be exactly realized in nature: it must be broken at experimentally accessible energies. Supersymmetric models are often easier to solve than non-supersymmetric ones since they are more constrained. Thus they may serve as toy models where certain analytic results can be obtained and as a qualitative guide to the behavior of more realistic theories. The study of supersymmetric versions of QCD has provided some insights in the understanding of scattering amplitudes, quarks confinement and the strong coupling phase not accessible with the standard perturbation theory. The key ingredient of these studies is a duality between a weakly and a strongly coupled theory (gauge/gravity duality or AdS/CFT correspondence). Furthermore in recent years, a lot of non-perturbative techniques allowed us to deeply understand supersymmetric gauge theories and their dualities. The most studied ones are *integrability* and *supersymmetric localization*.

This Chapter is organized in the following way: in Section 2.1 we will review some basic properties of field theories for what concerns classical and quantum symmetries. In particular we will discuss supersymmetry, conformal and superconformal invariance and their realization in four-dimensional and three-dimensional theories, namely $\mathcal{N} = 4$ super Yang-Mills and ABJ(M) theory. In Section 2.2 we will briefly present the AdS/CFT correspondence and its consequences. Finally in Section 2.3 we will review the main ideas behind supersymmetric localization and integrability.

2.1 Supersymmetric gauge theories

The determination of the symmetry group of a quantum field theory plays a fundamental role for its understanding. The implementation of the symmetries at the quantum level leads to a set of relations between the correlation functions (Ward identities). These relations can give us a lot of information about the spectrum of the theory and its renormalization properties. The generators of this symmetry, namely the conserved charges, can act also on the S-matrix elements of the theory, hence the symmetries that a theory possesses are directly related to its phenomenology.

In a four dimensional quantum field theory that is relevant for the description of fundamental interactions, the basic symmetries are:

- *Poincaré invariance*, that is the semi-direct product of translations and Lorentz transformations, with respective generators P_μ and $M_{\mu\nu}$. The algebra is the following

$$\begin{aligned}[M_{\mu\nu}, M_{\rho\sigma}] &= -i(g_{\mu\rho}M_{\nu\sigma} - g_{\mu\sigma}M_{\nu\rho} + g_{\nu\sigma}M_{\mu\rho} - g_{\nu\rho}M_{\mu\sigma}),\\ [M_{\mu\nu}, P_\lambda] &= i(P_\mu g_{\nu\lambda} - P_\nu g_{\mu\lambda}),\end{aligned} \tag{2.1}$$

  with $g_{\mu\nu}$ the Minkowski metric;

- *Internal global symmetries* with generators T_a obeying a Lie algebra with structure constant ${f_{ab}}^c$

$$[T_a, T_b] = i{f_{ab}}^c T_c; \tag{2.2}$$

- *Discrete symmetries* namely C, P and T *i.e* charge conjugation, parity and time-reversal.

2.1.1 Supersymmetry

In 1967, Coleman and Mandula [1] proved that there is no nontrivial way to unify an internal symmetry with the relativistic space-time symmetry. In more precise words, any symmetry group $\mathcal{G}$ containing the Poincaré group and an arbitrary internal symmetry group has the form of a direct product

$$\mathcal{G} = \text{Pioncaré } \times \text{ Internal symmetry.}$$

This theorem concerns the symmetries of the S-matrix. It is based on general hypothesis such as locality and unitarity, and on the assumption that the symmetries are described by Lie groups. However, in 1975, Haag, Lopuszanski and Sohnius [2] found a way out of this "no-go" theorem, through the relaxation of the assumption that the group of symmetries is a Lie group, whose generators obey a Lie algebra in the form of commutation rules. Indeed allowing spinorial charges and their anticommutation relations, they

introduced the so-called *Poincaré supersymmetry*. The Lie algebra becomes a *graded* Lie algebra or *superalgebra*. Their result is nevertheless very restrictive, in the sense that beyond the usual bosonic scalar generators, the only other possible ones are $\mathcal{N}$ fermionic generators of spin 1/2 Q^i_α with $\alpha = 1, 2$ and $i = 1, ..., \mathcal{N}$.

According to the result of Haag, Lopuszanski and Sohnius, one can extend the Poincaré algebra including $\mathcal{N}$ fermionic charges. In the superalgebra, supersymmetry exchange bosonic and fermionic degrees of freedom. The resulting general superalgebra is the so-called *super-Poincaré algebra*.

$$\begin{aligned}
[M_{\mu\nu}, M_{\rho\sigma}] &= -i(g_{\mu\rho}M_{\nu\sigma} - g_{\mu\sigma}M_{\nu\rho} + g_{\nu\sigma}M_{\mu\rho} - g_{\nu\rho}M_{\mu\sigma}), \\
[M_{\mu\nu}, P_\lambda] &= i(P_\mu g_{\nu\lambda} - P_\nu g_{\mu\lambda}), \qquad [T_a, T_b] = i f_{ab}{}^c T_c, \\
\left\{Q^i_\alpha, Q^j_\beta\right\} &= \epsilon_{\alpha\beta} Z^{ij}, \qquad \left\{Q^i_\alpha, \bar{Q}^j_{\dot\alpha}\right\} = 2\delta^{ij}\sigma^\mu_{\alpha\dot\alpha} P_\mu, \\
[Q^i_\alpha, M_{\mu\nu}] &= \frac{1}{2}(\sigma_{\mu\nu})_\alpha{}^\beta Q^i_\beta, \qquad [Q^i_\alpha, T_a] = (B_a)^i{}_j Q^j_\alpha.
\end{aligned} \tag{2.3}$$

with $Z^{ij} = A^{ij}_a T^a$ a bosonic operator commuting with all the other generators called *central charge*. The relation between the coefficients $B^{ik}_a A^{kj}_b = -A^{ik}_b (B^{kj}_a)^*$ relates the definition of the central charges with the action of the internal symmetries on the algebra.This graded algebra possesses a symmetry that transforms supercharges into each other. This group of automorphisms is called *R-symmetry* and in general it is $U(\mathcal{N})$.

2.1.2 Conformal symmetry

Now we will inspect the consequences coming from a bosonic extension of Poincaré invariance, the conformal group. There are many important field theories, like Yang-Mills theory in four dimensions, that are classically scale invariant. In some special cases, this symmetry holds also at the quantum level and, even when it does not, it can still be a useful tool. In fact, field theories generally exhibit a renormalization group flow from some ultra-violet to some infra-red fixed points, that turn both to be scale invariant.

Essentially, conformal field theories arise from the addition of scale invariance to Poincaré invariance, thus linking physics at different scales. This symmetry fixes the 2-point and 3-point correlation functions in the theory and gives strong constraints on the space-time dependence of the other correlators. Together with renormalization group and conformal invariance, Operator Product Expansion (OPE) represents another feature of many QFTs. In particular, in a local quantum field theories the product of two operators in a correlation function can be substituted with a linear combination of the other (in principle all) operators in the theory. This leads to an infinite set of relations between the correlators in the theory. Since a theory is resolved when all its correlation functions are known, the OPE relations remarkably reduce the number of

information needed to completely solve the theory. The OPE relations combined with conformal invariance allow to relate all the correlation functions in the theory to only the two and three point functions of conformal operators.

The conformal group is defined as the most general (locally) causal-preserving automorphisms. This is equivalent to invariance of the space-time metric $g_{\mu\nu}$ up to an arbitrary scale factor, that in general may be coordinate-dependent:

$$g_{\mu\nu}(x) \to e^{2\sigma(x)} g_{\mu\nu}(x). \tag{2.4}$$

Performing an infinitesimal coordinate transformation $x^\mu = x^\mu + \epsilon^\mu(x)$, for $d > 2$, we can write

$$\epsilon^\mu(x) = a^\mu + \Lambda^\mu{}_\nu x^\nu + \lambda x^\mu + b^\mu x^2 - 2x^\mu b \cdot x, \tag{2.5}$$

where each parameter corresponds to a different transformation. These transformations are

- *Translations* with generators P_μ and parameter a^μ;
- *Lorentz transformations* with generators $M_{\mu\nu}$ and parameter $\Lambda^\mu{}_\nu$;
- *Scale transformations* generated by the dilatation operator D and parametrized by λ;
- *Special conformal transformations* with generators K_μ and parameter b^μ.

The conformal algebra is then

$$\begin{aligned}
[M_{\mu\nu}, M_{\rho\sigma}] &= -i(g_{\mu\rho}M_{\nu\sigma} - g_{\mu\sigma}M_{\nu\rho} + g_{\nu\sigma}M_{\mu\rho} - g_{\nu\rho}M_{\mu\sigma}), \\
[M_{\mu\nu}, P_\lambda] &= i(P_\mu g_{\nu\lambda} - P_\nu g_{\mu\lambda}), \quad [M_{\mu\nu}, K_\lambda] = i(K_\mu g_{\nu\lambda} - K_\nu g_{\mu\lambda}), \\
[P_\mu, D] &= -iP_\mu, \quad [K_\mu, D] = iK_\mu, \quad [P_\mu, K_\nu] = 2i(M_{\mu\nu} - g_{\mu\nu}D).
\end{aligned} \tag{2.6}$$

Starting from a metric with signature (a, b) the conformal group is isomorphic to $SO(a+1, b+1)$, and it is an extension of the Poincaré group.

2.1.2.1 Primaries and correlation functions

In a Conformal invariant Field Theory (CFT) the fields belong to particular representations of the conformal algebra. To construct the representations we can use the induced representation method, so we need to postulate the behavior of a field Φ under Lorentz transformations, dilatations and special conformal transformations:

$$\begin{aligned}
[M_{\mu\nu}, \Phi(0)] &= \Sigma_{\mu\nu}\Phi(0), \\
[D, \Phi(0)] &= -i\Delta\Phi(0), \\
[K_\mu, \Phi(0)] &= 0
\end{aligned} \tag{2.7}$$

The first relation defines the spin of the field Φ, given the matrices $\Sigma_{\mu\nu}$ forming a finite dimensional representation of the Lorentz group. In the second line it is written the so-called *scaling dimension* Δ of field: in other words, under dilatation $x \to \lambda x$ we have $\Phi(x) \to \lambda^{\Delta}\Phi(\lambda x)$. The last line in (2.7) defines what is called a *primary field*. The conformal algebra (2.6) implies that the operator P_μ raises the scaling dimension of the field, while K_μ lowers it. In unitary CFTs there is a lower bound on the dimensions of the fields. This means that each representation of the conformal algebra must have some operator of lowest dimension, which must be annihilated by K_μ. Such operators (or fields) are called *conformal primary operators*, or simply primary fields. By acting on the primary fields with P_μ we can construct the whole (infinite) tower of operators with dimensions greater than Δ. These operators are the *conformal descendants* of the primary field Φ.

The two point function of two scalar primary operators, with scaling dimensions Δ_1 and Δ_2, is strongly constrained by conformal invariance and is given by

$$\langle \Phi_{\Delta_1}(x_1)\Phi_{\Delta_2}(x_2)\rangle = \frac{\delta_{\Delta_1,\Delta_2}C_{12}}{(x_{12}^2)^{\Delta}} \tag{2.8}$$

where $x_{12} = x_1 - x_2$, $\Delta_1 = \Delta_2 = \Delta$ and C_{12} a constant depending on the choice of normalization of Φ_1 and Φ_2.

A similar analysis may be performed on three-point functions. Covariance under rotations, translations and dilatations forces the dependence on the positions, special conformal transformations give constraints for the dependence on the scaling dimensions. Therefore we have

$$\langle \Phi_{\Delta_1}(x_1)\Phi_{\Delta_2}(x_2)\Phi_{\Delta_3}(x_3)\rangle = \frac{C_{123}}{(x_{12}^2)^{\frac{1}{2}(\Delta_1+\Delta_2-\Delta_3)}(x_{23}^2)^{\frac{1}{2}(\Delta_2+\Delta_3-\Delta_1)}(x_{13}^2)^{\frac{1}{2}(\Delta_1+\Delta_3-\Delta_2)}} \tag{2.9}$$

All the correlation functions of four or more operators can be reduced into a combination of three-point functions using the fact that the effect of the operator product could be computed by replacing the product with a linear combination of local operators. These observations can be combined in an equation, that defines the Operator Product Expansion (OPE)

$$\Phi_i(x)\Phi_j(0) = \sum_k C_{ij}{}^k(x)\Phi_k(0) \tag{2.10}$$

where the coefficients $C_{ij}{}^k(x)$ are numeric functions. The index k runs over all the local fields in the theory that have the same quantum numbers as the product of the two fields $\Phi_i(x)$ and $\Phi_j(0)$.

2.1.2.2 Renormalization group

In general one can express the generators of the conformal algebra as Noether charges defined from the *symmetric energy-momentum tensor* $\Theta_{\mu\nu}$ (related to the canonical one

$T_{\mu\nu}$). In order for this charges to be conserved, the $\Theta_{\mu\nu}$ must be symmetric, conserved and traceless:

$$\Theta_{\mu\nu} = \Theta_{\nu\mu}, \quad \partial^\mu \Theta_{\mu\nu} = 0, \quad \Theta^\mu_\mu = 0 \tag{2.11}$$

In particular the tracelessness condition is important to ensure conservation of the dilatation current D^μ (because $\Theta^\mu_\mu = \partial_\mu D^\mu$), associated to scale invariance. An alternative definition of the symmetric energy-momentum tensor i given by

$$\Theta_{\mu\nu} = 2\frac{\delta}{\delta g_{\mu\nu}} \int d^4x \, \mathcal{L} \tag{2.12}$$

This construction gives a manifestly symmetric and gauge-invariant tensor. In a scale-invariant gauge theory, the action is invariant under the transformation (2.4) and this variation can be expressed in terms of $\Theta_{\mu\nu}$ as follows

$$0 = \delta S = \frac{\delta S}{\delta g_{\mu\nu}} \delta g_{\mu\nu} = \frac{1}{2} \Theta^{\mu\nu} \delta g_{\mu\nu} \tag{2.13}$$

Since in a scale (conformal) transformation we have $\delta g_{\mu\nu} = 2\sigma g_{\mu\nu}$, the above equation implies $\Theta^\mu_\mu = 0$.

This holds at least at the classical level. We know that in general, when quantum corrections are included, classical symmetries are not symmetries anymore due to anomalies. Let us now analyze the problem from a renormalization group point of view. Assuming that the theory is renormalizable, we know that the Green functions of n operators $G_n(x_1, ..., x_n; \mu, g)$, at a given renormalization scale μ, satisfy the Callan-Symanzik equation

$$\left(\mu \frac{\partial}{\partial \mu} + \beta(g) \frac{\partial}{\partial g} + \sum_{i=1}^{n} \gamma_i(g, \mu) \right) G_n(x_1, ..., x_n; \mu, g) = 0 \tag{2.14}$$

with g the coupling constant and $\beta(g) = \mu \partial_\mu g$ the *β-function*. To each operator appearing in the n-point function is associated a quantity $\gamma_i(g, \mu)$, called *anomalous dimension* of the operator, that can be calculated by analyzing its two-point function. At quantum level the renormalized coupling constant assumes different values at different scales, then the scale invariance is no longer a symmetry of the theory. Under the scale transformation $x \to e^{-\sigma} x$, the variation of renormalized coupling and Lagrangian is

$$g \to g + \sigma \beta(g), \qquad \mathcal{L} \to \mathcal{L} + \sigma \beta(g) \frac{\partial}{\partial g} \mathcal{L} \tag{2.15}$$

Taking into account the definition (2.12), at quantum level we have

$$\partial_\mu D^\mu = \Theta^\mu_\mu = \beta(g) \frac{\partial}{\partial g} \mathcal{L} \tag{2.16}$$

Thus the quantum scale invariance of the theory is directly related to the vanishing of the β-function. If the trace of the symmetric energy-momentum tensor takes a non-zero

value as a result of quantum corrections (*i.e* the β-function does not vanish), we have to deal with the so-called *trace anomaly*.

Now we want to give a physical interpretation for the anomalous dimension $\gamma(g,\mu)$. Consider a conformal primary operator from an ordinary QFT viewpoint, its two point function depends only on the distance between the two points, and scales with dimension $2\Delta^{(0)}$, where $\Delta^{(0)}$ is the classical dimension of this operator. When the β-function is zero, the renormalized two-point function $G_2(x;\mu,g)$ satisfies the equation

$$\left(\mu\frac{\partial}{\partial\mu}+2\gamma_i(g)\right)G_2(x;\mu,g)=0 \tag{2.17}$$

Using the Euler's theorem for the homogeneous functions, one can find that

$$G_2(x;\mu,g)=\frac{C(g)}{(x^2)^{\Delta^{(0)}+\gamma(g)}\mu^{2\gamma(g)}} \tag{2.18}$$

Then we can interpret the anomalous dimension $\gamma(g)$ as the quantum correction to the eigenvalue of the dilatation operator.

The renormalization procedure passes through the introduction of an energy scale which breaks the scale invariance. Both the renormalized operators $\hat{\Phi}$ and the correlation functions depend on the scale μ. In particular the conformal primary operators of a quantum field theory are scale-dependent objects derived from the classical ones by the renormalization prescription

$$\Phi_\Delta(x)\to\hat{\Phi}_{\Delta(g)}(x;\mu,g),\quad \text{with}\quad \Delta\to\Delta(g)=\Delta^{(0)}+\gamma(g) \tag{2.19}$$

such that its two-point function is of the form of (2.18). We will see that the constraints imposed by conformal symmetry are such that the scale appears in the renormalized operator in exactly the same way it appears in all the correlation functions involving this field. Hence we can redefine a scale-independent renormalized operator whose correlation functions scale with its full (classical + anomalous) conformal dimension, and in which μ does not appear. Thus, there is no breaking of scale invariance in a conformal invariant quantum field theory. In other terms the presence of the renormalization scale μ can be eliminated, and it can be interpreted as a simple artifact of the perturbative expansion.

2.1.2.3 Operator mixing

Let us consider a basis of n bare operators $\{\Phi_i(x)\}$, with $i=1,...,n$, with the same quantum numbers at classical level. Their scaling dimensions $\Delta^{(0)}$ are all the same but the anomalous dimensions in general may be different from one operator to another. Although the theory is conformal, the correlation functions of these operators contain divergences. Then we define a set of bare regularized operators $\{\tilde{\Phi}_i(x,\epsilon)\}$ where ϵ is

a scheme-dependent regulator with dimension of a length. With these fields we can resolve the so-called *mixing problem*: namely find the correct renormalized operators and their respective anomalous dimensions. The two-point functions of these operators will have the form

$$\langle\tilde{\Phi}_i(x_1,\epsilon)\tilde{\Phi}_j(x_2,\epsilon)\rangle = f_{ij}\left(\frac{\epsilon^2}{x_{12}^2},g\right)\frac{1}{(x_{12}^2)^{\Delta^{(0)}}} \tag{2.20}$$

where f_{ij} is the non vanishing part of the correlator. The renormalized operator $\hat{\Phi}_a$ which have a well defined anomalous dimension $\gamma_a(g)$ is a linear combination of the regularized one

$$\hat{\Phi}_a(x,\mu) = Z_{ai}((\epsilon\mu)^2,g)\tilde{\Phi}_i(x,\epsilon) \tag{2.21}$$

where μ is the subtraction point and $Z_{ai}((\epsilon\mu)^2,g)$ is an invertible matrix called *mixing matrix*. In the basis in which f_{ij} is real and symmetric, Z has the property $Z^\dagger = Z^T$. Scale invariance implies that the two-point function of renormalized operator is

$$\langle\hat{\Phi}_a(x_1,\mu)\hat{\Phi}_b(x_2,\mu)\rangle = \frac{\delta_{ab}C_a(g)}{(x_{12}^2)^{\Delta^{(0)}+\gamma_a(g)}\mu^{2\gamma_a(g)}}, \tag{2.22}$$

where $C_a(g)$ are the finite normalizations of the 2-point functions of the renormalized operators.

Compatibility among equations (2.20), (2.21) and (2.22) imply the matrix equation

$$Z((\epsilon\mu)^2,g)f\left(\frac{\epsilon^2}{x_{12}^2},g\right)Z^\dagger((\epsilon\mu)^2,g) = (x_{12}^2\mu^2)^{-\Gamma(g)}C(g) \tag{2.23}$$

where $\Gamma(g) = \mathrm{diag}(\gamma_1(g),...,\gamma_n(g))$ and $C(g) = \mathrm{diag}(C_1(g),...,C_n(g))$. One can find that the constraints imposed by scale invariance of the renormalized operators imply that the mixing matrix must have the following form

$$Z((\epsilon\mu)^2,g) = (\epsilon^2\mu^2)^{-\frac{1}{2}\Gamma(g)}Z(g) \tag{2.24}$$

with $Z(g) = Z(1,g)$. In other terms, in a conformal quantum field theory we can define the renormalized operators of (2.21) as

$$\hat{\Phi}_a(x) = \lim_{\epsilon\to 0}(\epsilon^2)^{-\frac{1}{2}\gamma_a(g)}Z_{ai}(g)\tilde{\Phi}_i(x,\epsilon) \tag{2.25}$$

with two-point function

$$\langle\hat{\Phi}_a(x_1)\hat{\Phi}_b(x_2)\rangle = \frac{\delta_{ab}C_a(g)}{(x_{12}^2)^{\Delta_a(g)}}, \tag{2.26}$$

where $\Delta_a(g) = \Delta^{(0)} + \gamma_a(g)$. Now we can see the realization of what we anticipated in the previous section. Conformal invariance allows to remove the subtraction point, since

it implies the same constraints both on the mixing matrix and on the two-point functions of the renormalized operators. Using this property we can define scale invariant renormalized operators whose correlators still preserve conformal invariance, provided the quantum scaling dimension is $\Delta = \Delta^{(0)} + \gamma$. Nevertheless, by expanding Δ in powers of g, conformal invariance appears to be broken at each order since one needs to reintroduce the scale μ into the logarithms. Conformal (scale) invariance, however, guarantees that the scale appears only in logarithms and resums in powers.

2.1.3 Superconformal symmetry

We have analyzed the extension of the Poincaré group introducing supersymmetry and then conformal invariance. Now we want to combine these two symmetry groups giving rise to a larger (and stronger) invariance, the *superconformal invariance*.

Suppose to have a supersymmetric theory, that is also invariant under the full conformal group. We can act on the states (or the fields) of this theory with the generators of the conformal group as well with the supercharges. One can notice, by imposing the Jacobi identity, that the commutators between the generators K_μ, Q_α and $\bar{Q}_{\dot{\alpha}}$ cannot be vanishing. Thus one needs to introduce another spinorial generator S^i_α commuting with K_μ that plays the same role of Q^i_α for the Poincaré generator P_μ.

The full classification of the superconformal algebras in any dimension was given by Nahm [3]. In order to construct superconformal theories in space-time dimensions $d = 4, 3$, we are interested in the study of the superconformal group in four and three dimensions, with supergroups respectively $(P)SU(2,2|\mathcal{N})$ and $OSp(\mathcal{N}|4)$.

2.1.3.1 Superconformal symmetry in d=4

The complete $\mathcal{N}$-extended superconformal algebra in four dimensions further includes the following (anti) commutation relations, supplementing the algebra 2.6:

$$\begin{gathered}
\{Q^i_\alpha, \bar{Q}^j_{\dot{\alpha}}\} = 2\delta^{ij}\sigma^\mu_{\alpha\dot{\alpha}}P_\mu \qquad \{Q^i_\alpha, Q^j_\beta\} = \epsilon_{\alpha\beta}Z^{ij} \qquad \{S^i_\alpha, \bar{S}^j_{\dot{\alpha}}\} = 2\delta^{ij}\sigma^\mu_{\alpha\dot{\alpha}}K_\mu \\
\{Q^i_\alpha, S^j_\beta\} = 2\epsilon_{\alpha\beta}\delta^{ij}D - i(\sigma^{\mu\nu})_\alpha{}^\gamma\epsilon_{\gamma\beta}\delta^{ij}M_{\mu\nu} + B^{ij}_a T^a - 4i\epsilon_{\alpha\beta}\delta^{ij}R \\
[Q^i_\alpha, M_{\mu\nu}] = (\sigma_{\mu\nu})_\alpha{}^\beta Q^i_\beta \qquad [Q^i_\alpha, D] = \frac{1}{2}Q^i_\alpha \qquad [Q^i_\alpha, K^\mu] = i\sigma^\mu_{\alpha\dot{\alpha}}\bar{S}^{i\dot{\alpha}} \qquad [Q^i_\alpha, T_a] = B^i_{aj}Q^j_\alpha \\
[S^i_\alpha, M_{\mu\nu}] = (\sigma_{\mu\nu})_\alpha{}^\beta S^i_\beta \qquad [S^i_\alpha, D] = -\frac{1}{2}S^i_\alpha \qquad [S^i_\alpha, P^\mu] = -i\sigma^\mu_{\alpha\dot{\alpha}}\bar{Q}^{i\dot{\alpha}} \qquad [S^i_\alpha, T_a] = -B^i_{aj}S^j_\alpha \\
[Q^i_\alpha, R] = -i\left(\frac{4-\mathcal{N}}{4\mathcal{N}}\right)Q^i_\alpha \qquad [S^i_\alpha, R] = i\left(\frac{4-\mathcal{N}}{4\mathcal{N}}\right)S^i_\alpha \qquad [T_a, T_b] = if^c_{ab}T_c
\end{gathered} \tag{2.27}$$

The operator R in these relations is the generator of the $U(1)$ factor of the group $U(N) = SU(N) \times U(1)$ of the automorphisms of the algebra. The $\mathcal{N} = 4$ case is special because R commutes with Q_α and $\bar{Q}_{\dot{\alpha}}$. The chiral rotation operator R must therefore have the same action on all the states in the multiplet. For this reason the R-symmetry

group in the $\mathcal{N}=4$ case is $SU(4)$ and not $U(4)$ as would be expected from general arguments. For the same argument, the general superalgebra in $d=4$ is $SU(2,2|\mathcal{N})$ but in the special case of $\mathcal{N}=4$ it becomes $PSU(2,2|4)$.

2.1.3.2 Superconformal symmetry in d=3

We are interested in the study of the algebra of $OSp(\mathcal{N}|4)$ in the particular case of $\mathcal{N}=6$ supersymmetries as it will be clear in the following. For the $OSp(6|4)$ generators, we use $SU(2)$ spinor greek indices $\alpha=1,2$ and $SU(4)$ capital latin R-symmetry indices $I=\ 1,2,3,4$. The bosonic generators are the usual conformal group generators and the R-symmetry charge. Additionally, there are 24 supercharges with

$$Q_{IJ,\alpha}=-G_{JI,\alpha}, \qquad \text{and} \quad S^{KL,\beta}=-S^{LK,\beta} \tag{2.28}$$

It is convenient to write the algebra for the three dimensions in the spinor basis, using the following prescriptions

$$P_{\alpha\beta}=(\gamma^\mu)_{\alpha\beta}P_\mu, \quad K^{\alpha\beta}=(\bar{\gamma}^\mu)^{\alpha\beta}K_\mu, \quad M^\alpha{}_\beta=\frac{i}{2}(\gamma^\mu\bar{\gamma}^\nu)_\alpha{}^\beta M_{\mu\nu}. \tag{2.29}$$

The complete algebra includes the following non-vanishing (anti) commutation relations [4, 5]

$$\begin{aligned}
[M^\alpha{}_\beta, M^\gamma{}_\delta] =&\delta^\alpha_\delta M^\gamma{}_\beta-\delta^\gamma_\beta M^\alpha{}_\delta, \qquad [M^\alpha{}_\beta, P_{\gamma\delta}]=2\delta^\alpha_{\{\gamma}P_{\delta\}\beta}-\delta^\alpha_\beta P_{\gamma\delta},\\
[M^\alpha{}_\beta, K^{\gamma\delta}] =&-2\delta^{\{\gamma}_\beta K^{\delta\}\alpha}+\delta^\alpha_\beta K^{\gamma\delta}, \qquad [M^\alpha{}_\beta, Q_\gamma]=\delta^\alpha_\gamma Q_\beta-\frac{1}{2}\delta^\alpha_\beta Q_\gamma,\\
[M^\alpha{}_\beta, S^\gamma] =&-\delta^{\beta\gamma}S^\alpha+\frac{1}{2}\delta^\alpha_\beta S^\gamma, \qquad [K^{\alpha\beta}, P_{\gamma\delta}]=4\delta^{\{\alpha}_{\{\gamma}M^{\beta\}}_{\delta\}}+4\delta^{\{\alpha}_{\{\gamma}\delta^{\beta\}}_{\delta\}}D,\\
[K^{\alpha\beta}, Q_{KL,\gamma}] =&\frac{1}{2}\epsilon_{KLIJ}(\delta^\alpha_\gamma S^{IJ,\beta}+\delta^\beta_\gamma S^{IJ,\alpha}), \qquad [D, Q_\alpha]=-\frac{1}{2}Q_\alpha\\
[P_{\alpha\beta}, S^{KL,\gamma}] =&-\frac{1}{2}\epsilon^{KLIJ}(\delta^\gamma_\alpha Q_{IJ,\beta}+\delta^\gamma_\beta Q_{IJ,\alpha}), \qquad [D, S^\alpha]=\frac{1}{2}S^\alpha\\
[R^I{}_J, R^K{}_L] =&\delta^I_L R^K{}_J-\delta^K_J R^I{}_L, \qquad [R^I{}_J, Q_{KL}]=2\delta^I_{[L}Q_{K]J}-\frac{1}{2}\delta^I_J Q_{KL},\\
[R^I{}_J, S^{KL}] =&-2\delta^{[L}_J S^{K]I}+\frac{1}{2}\delta^I_J S^{KL},\\
\{Q_{IJ,\alpha}, Q_{KL,\beta}\} =&-\epsilon_{IJKL}P_{\alpha\beta}, \qquad \{S^{IJ,\alpha}, S^{KL,\beta}\}=-\epsilon^{IJKL}K^{\alpha\beta},\\
\{Q_{IJ,\alpha}, S^{KL,\beta}\} =&4\delta^\gamma_\beta\delta^{[K}_{[I}R^{L]}{}_{J]}+2\delta^K_{[J}\delta^L_{I]}M^\gamma{}_\beta+2\delta^K_{[J}\delta^L_{I]}\delta^\gamma_\beta D.
\end{aligned} \tag{2.30}$$

2.1.3.3 Primaries operators

In a conformal theory we have defined primaries as the operators annihilated by K_μ and descendants the operators derived from the action of a certain number of translations

P_μ on the primaries. In the superconformal algebra the fundamental objects are the supersymmetry charges Q_α and S_α and their conjugates. Therefore now the generators Q_α and $\bar{Q}_{\dot{\alpha}}$ raise the scaling dimension by $\frac{1}{2}$ and S_α and $\bar{S}_{\dot{\alpha}}$ lower the scaling dimension by $\frac{1}{2}$. Then we define *superconformal primary* the operator obeying the following relation

$$[S_\alpha, \Phi] = [\bar{S}_{\dot{\alpha}}, \Phi] = 0 \tag{2.31}$$

The repeated action of the charges Q_α and $\bar{Q}_{\dot{\alpha}}$ on a superconformal primary define an infinite tower of operators whose are called *superconformal descendants*.

The simplest superconformal primaries (for instance in $\mathcal{N} = 4$ SYM) are the single trace operators, which are of the form $\mathrm{str}\left(\Phi^{I_1}\Phi^{I_2}...\Phi^{I_n}\right)$, where "str" denotes the symmetrized trace over the gauge algebra and as a result of this operation, the above operator is totally symmetric in the $SO(6)$ R-indices I_j. In general, the above operators transform under a reducible representation. The irreducible operators may be obtained by isolating the traces over $SO(6)$ indices. Since $\mathrm{Tr}\Phi^I = 0$, the simplest operators is the *Konishi operator* $\mathrm{Tr}(\Phi^I\Phi^I)$.

The unitary representations of the superconformal algebra $PSU(2,2|4)$ may be labeled by the quantum numbers of the bosonic subgroup, listed below,

$$\begin{array}{ccc} SO(1,3) \times SO(1,1) \times SU(4) & & \\ (s_+, s_-) & \Delta & [r_1, r_2, r_3] \end{array} \tag{2.32}$$

where $s_\pm$ are positive or zero half integers, Δ is the positive or zero dimension and $[r_1, r_2, r_3]$ are the Dynkin labels of the representations of $SU(4)$.

In unitary representations, the dimensions Δ of the operators are bounded from below by the spin and $SU(4)$ quantum numbers. Such operators are scalars, so that the spin quantum numbers vanish, and the dimension is bounded from below by the $SU(4)$ quantum numbers (see [6]). One can classify the corresponding discrete representations finding the so-called *BPS multiplet* that corresponds to *chiral primary operators* (CPO). These operators are superconformal primaries annihilated also by some supersymmetries Q_α and $\bar{Q}_{\dot{\alpha}}$

$$[\{Q, S\}, \Phi] = 0 \tag{2.33}$$

This structure gives a lot of constraints that mean that such operators can not have quantum corrections to their scaling dimension. In Table 2.1 we summarize the complete classification of primary operators.

2.1.4 $\mathcal{N} = 4$ Super Yang-Mills (SYM)

Starting from the superconformal algebra in 4 dimensions, for any $1 \leq \mathcal{N} \leq 4$ there exists a gauge multiplet which transforms under the adjoint representation of the gauge group $SU(N)$. It turns out that for $\mathcal{N} = 1, 2$ there exist other multiplets which can

Operator type	$\#Q$	spin range	$SU(4)$ primary	dimension Δ
identity	16	0	$[0,0,0]$	0
1/2 BPS	8	2	$[0,k,0],\ \ k\geq 2$	k
1/4 BPS	4	3	$[\ell,k,\ell],\ \ \ell\geq 1$	$k+2\ell$
1/8 BPS	2	7/2	$[\ell,k,\ell+2m]$	$k+2\ell+3m,\ \ m\geq 1$
non-BPS	0	4	any	unprotected

Table 2.1: Characteristics of BPS and Non-BPS multiplets. The symbol $\#Q$ represent the number of preserved Poincaré supercharges

be considered as matter multiplets, whereas for $\mathcal{N}=4$ the gauge multiplet is the only possible multiplet. This $\mathcal{N}=4$ gauge multiplet is given by [7]

$$(A_\mu, \lambda^a_\alpha, \Phi^I) \tag{2.34}$$

where A_μ is a spin 1 gauge field, λ^a_α $(a=1,...,4)$ are Weyl spinor and Φ^I $(I=1,...,6)$ are real scalars. Under the R-symmetry group these transform as a singlet, a vector, and a rank-2 antisymmetric tensor respectively.

$\mathcal{N}=4$ supersymmetric Yang-Mills (SYM) theory in four dimensions was obtained for the first time in [8, 9] by applying the method of dimensional reduction to $\mathcal{N}=1$ super Yang-Mills in ten dimensions. The latter is the low energy effective theory coming from type I superstring theory and describes a $\mathcal{N}=1$ vector multiplet in ten dimensions consisting of one real vector and one Majorana-Weyl spinor.

The Lagrangian for the $\mathcal{N}=4$ SYM theory is given by

$$\begin{aligned} S_{SYM} = \int d^4x \mathrm{Tr}\Big\{ &\frac{-1}{2g^2_{\mathrm{YM}}} F_{\mu\nu}F^{\mu\nu} + \frac{\theta_i}{8\pi^2} F_{\mu\nu}\tilde{F}^{\mu\nu} - D_\mu\Phi^I D^\mu\Phi_I - i\bar{\lambda}^a\bar{\sigma}^\mu D_\mu\lambda_a \\ &+ g_{\mathrm{YM}} C^{ab}_I \lambda_a[\Phi^I,\lambda_b] + g_{\mathrm{YM}} C_{Iab}\bar{\lambda}^a[\Phi^I,\bar{\lambda}^b] + \frac{g^2_{\mathrm{YM}}}{2}[\Phi^I,\Phi^J]^2 \Big\} \end{aligned} \tag{2.35}$$

where g_{YM} is the Yang-Mills coupling constant, θ_i is the so-called *instanton angle*, $F_{\mu\nu}$ is the usual gauge field strength, D_μ is the usual covariant derivative, $\tilde{F}$ is the Hodge dual of F and the constants C^{ab}_I and C_{Iab} are the structure constants of $SU(4)$. The trace is over the gauge indices (which are suppressed in (2.35)) and it ensures gauge invariance of the action.

Classical and quantum symmetries

The action given by (2.35) is invariant under the supersymmetry transformations

(where, for clarity, we write the indices explicitly) given by:

$$\begin{aligned}
(\delta\Phi^I)^a_\alpha =& [Q^a_\alpha, \Phi^I] = C^{Iab}\lambda_{\alpha b}, \\
(\delta\lambda_{\beta b})^a_\alpha =& \{Q^a_\alpha, \lambda_{\beta b}\} = F^+_{\mu\nu}(\sigma^{\mu\nu})_{\alpha\beta} + [\Phi^I, \Phi^J]\epsilon_{\alpha\beta}(C_{IJ})^{\alpha\beta}, \\
(\delta\bar{\lambda}^b_{\dot\beta})^a_\alpha =& \{Q^a_\alpha, \bar{\lambda}^b_{\dot\beta}\} = C^{ab}_I \sigma^\mu_{\alpha\dot\beta} D_\mu \Phi^I, \\
(\delta A^\mu)^a_\alpha =& [Q^a_\alpha, A^\mu] = \sigma^\mu_{\alpha\dot\beta}\bar{\lambda}^{\dot\beta\alpha}
\end{aligned} \tag{2.36}$$

where F^+ is the self-dual part of the field strength and the constants $(C_{IJ})^{\alpha\beta}$ are related to the bilinears in the Clifford Dirac matrices of $SU(4)$.

This theory is classically conformally invariant; indeed, with the standard mass-dimensions of the fields given by $[A^\mu] = [\Phi^I] = 1$ and $[\lambda^a_\alpha] = 3/2$, it is easy to see from (2.35) that the coupling constant and the instanton angle have dimension $[g_{\rm YM}] = [\theta_i] = 0$ since the Lagrangian must have $[\mathcal{L}] = 4$ in natural units in 4-dimensions. The theory is thus scale invariant, which together with Poincaré invariance forms full conformal invariance.

Upon quantization one finds that the theory is UV finite. Indeed, using the informations about the field content of the theory, one can shows that the one-loop β-function is zero. For any $SU(N)$ gauge theory, the one-loop β-function for the gauge coupling $g_{\rm YM}$ is given by [10]

$$\beta^{(1)}(g_{\rm YM}) \equiv \mu\frac{\partial g_{\rm YM}}{\partial\mu} = -\frac{g^3_{\rm YM}}{16\pi^2}\left(\frac{11}{3}N - \frac{1}{6}\sum_i C_i - \frac{1}{3}\sum_j \tilde{C}_j\right) \tag{2.37}$$

where the first sum is over all real scalars with quadratic casimir C_i and the second sum is over all Weyl fermions with quadratic casimir $\tilde{C}_j$. All fields in $\mathcal{N} = 4$ SYM are in the adjoint, hence all casimirs are equal to N. Then, one can quickly see that with six real scalars and eight Weyl fermions $\beta^{(1)}(g_{\rm YM}) = 0$. Going beyond one-loop, the β-function of $\mathcal{N} = 4$ SYM theory was shown to be zero up to three loops using superspace arguments [11]. Subsequently it was argued, using light cone gauge, that the β-function is zero to all loops [12, 13] thus $\mathcal{N} = 4$ SYM theory is conformal invariant at quantum level.

In addition to superconformal symmetry, $\mathcal{N} = 4$ SYM exhibits a further symmetry, most easily expressed by first combining the coupling constant and the instanton angle as:

$$\tau \equiv \frac{\theta_i}{2\pi} + \frac{4\pi i}{g^2_{\rm YM}} \tag{2.38}$$

The quantum theory is invariant under $\theta_i \to \theta_i + 2\pi$, or $\tau \to \tau + 1$. The *Montonen-Olive conjecture* [14] states that the quantum theory is also invariant under the $\tau \to -1/\tau$. The combination of both symmetries yields the S-duality group $SL(2, \mathbb{Z})$, generated by

$$\tau \to \frac{a\tau + b}{c\tau + d} \qquad \text{with} \quad ad - bc = 1, \quad a, b, c, d \in \mathbb{Z} \tag{2.39}$$

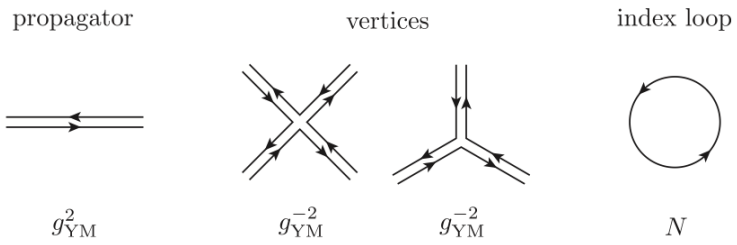

Figure 2.1: The double line notation.

Notice that when the instanton angle vanish, the S-duality transformation amounts to $g_{\rm YM} \to 1/g_{\rm YM}$, thereby exchanging strong and weak coupling.

The 't Hooft coupling

The only two free parameters of the theory are the Yang-Mills coupling $g_{\rm YM}$ and the rank of the gauge group N. Following the 't Hooft proposal [15], one can define a new constant as the combination of these two parameters and expand the theory with respect to it in the large N limit. Namely

$$\lambda \equiv g^2_{\rm YM} N \qquad \text{with} \quad \lambda \text{ fixed, } \mathrm{N} \to \infty \tag{2.40}$$

where λ is the so-called 't Hooft coupling.

The 't Hooft expansion corresponds to keeping λ fixed and perform an expansion of the observables in power of N. It turns out that different powers of N correspond to different topologies. This fact is more clear by adopting a double line notation for the gauge propagator and the vertices. It is not difficult to find the powers of N and λ appearing in a given diagram D with no external lines. The contributions of the gauge propagator and the vertices are displayed in Figure 2.1. Moreover, every index loop contributes with a power of N. Suppose that E is the number of propagators (edges) of D connecting two vertices, V is the number of vertices and F is the number of index loops (faces), then one can show that:

$$D \propto \left(\frac{\lambda}{N}\right)^E \left(\frac{N}{\lambda}\right)^V N^F = N^{F-E+V} \lambda^{E-V} \tag{2.41}$$

The exponent of N is the topological invariant

$$\chi = F - E + V = 2 - 2g \tag{2.42}$$

called *Euler characteristic*. g denotes the *genus* of the surface that corresponds to the number of handles. Then we can decompose physical quantities of the theory in a

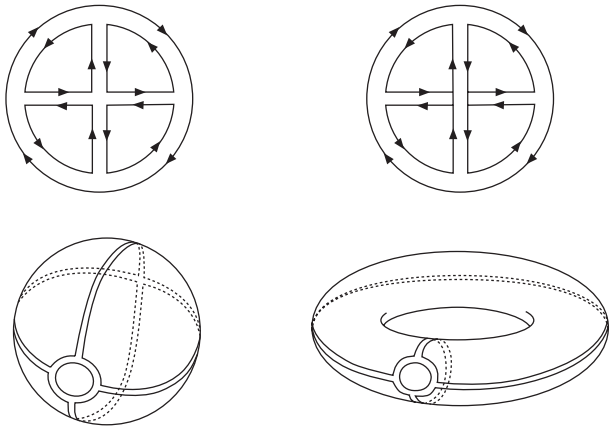

Figure 2.2: Examples of diagrams with or without crossing lines and their relative topologies.

double expansion in the 't Hooft coupling λ and $1/N^2$

$$\mathcal{Z} = \sum_{g=0}^{\infty} N^{2-2g} \sum_{n=0}^{\infty} c_{g,n} \lambda^n = \sum_{g=0}^{\infty} N^{2-2g} f_g(\lambda) \tag{2.43}$$

where $f_g(\lambda)$ is the sum of Feynman diagrams that can be drawn in a surface of genus g. It is easy to see that when taking the limit $N \to \infty$ the dominant contributions come from the diagrams of lowest genus. These are the diagrams that can be drawn in a plane (or on a sphere) without crossing lines, referred to as *planar*. The diagrams with one or more crossing lines, have the topology of a surface with g handles, namely a g-torus. An example for both a planar and a non-planar diagram is shown in Figure 2.2.

2.1.5 $\mathcal{N} = 6$ Super Chern-Simons with matter (ABJ(M))

Highly supersymmetric three-dimensional conformal field theories are interesting for various reasons. One is the construction of the theory describing the worldvolume of membranes in M-theory (M2-branes) at low energies as we will see in the next section. Another motivation to study three-dimensional conformal field theories is that they could describe interesting conformal fixed points in condensed matter systems.

Recentely Aharony, Bergman, Jafferis and Maldacena (ABJM) [16] constructed a three-dimensional Chern-Simons theory with gauge group $U(N) \times U(N)$, and proved that this theory has explicitly $\mathcal{N} = 6$ supersymmetry. In the same year, Aharony, Bergman and Jafferis proposed also a generalized version of ABJM with gauge group $U(N) \times U(M)$, with the same matter content and interactions as in [16], but with $M \neq N$ [17]. For these reason we refer to the generalized theory as ABJ and in the particular case of $M = N$ as ABJM.

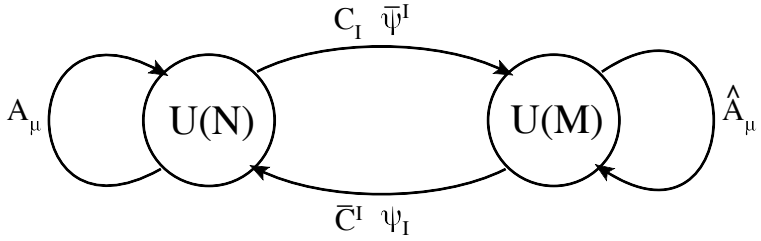

Figure 2.3: Quiver diagram for ABJ(M) theory.

The field content of the theory can be schematically represented in the quiver in Figure 2.3. Regarding the gauge index structure, we denote by i, $\hat{i}$ the gauge indices in the fundamental of the first and the second gauge group respectively. The gauge sector consists of two gauge fields $(A_\mu)_i{}^j$ and $(\hat{A}_\mu)_{\hat{i}}{}^{\hat{j}}$ belonging respectively to the adjoint of $U(N)$ and $U(M)$. The matter sector instead contains the complex fields $(C_I)_i{}^{\hat{j}}$ and $(\bar{C}^I)_{\hat{i}}{}^j$ as well as the fermions $(\psi_I)_{\hat{i}}{}^j$ and $(\bar{\psi}^I)_i{}^{\hat{j}}$. The fields $(C, \bar{\psi})$ transform in the $(\mathbf{N}, \bar{\mathbf{M}})$ of the gauge group $U(N) \times U(M)$ while the pair $(\bar{C}, \psi)$ lives in the $(\bar{\mathbf{N}}, \mathbf{M})$. The additional capitol index $I = 1, 2, 3, 4$ belongs to the R-symmetry group $SU(4)$. In order to quantize the theory at the perturbative level, we have introduced the covariant gauge fixing function $\partial_\mu A^\mu$ for both gauge fields and two sets of ghosts $(\bar{c}, c)$ and $(\bar{\hat{c}}, \hat{c})$. Now we can write the ABJ(M) action as the sum of the following terms

$$S_{\text{ABJ(M)}} = S_{\text{CS}} + S_{\text{gf}} + S_{\text{Matter}} + S^F_{\text{int}} + S^B_{\text{int}} \tag{2.44}$$

namely the Chern-Simons action, the gauge-fixing action, the matter term and two interaction actions that consist in a $\psi^2 C^2$ Yukawa-type potential and the sextic scalar potential. Therefore we work with the following Euclidian space action

$$\begin{aligned}
S_{\text{CS}} =& -i\frac{\kappa}{4\pi}\int d^3x \epsilon^{\mu\nu\rho}\left[\text{Tr}(\text{A}_\mu\partial_\nu\text{A}_\rho + \tfrac{2}{3}\text{iA}_\mu\text{A}_\nu\text{A}_\rho) - \text{Tr}(\hat{\text{A}}_\mu\partial_\nu\hat{\text{A}}_\rho + \tfrac{2}{3}\text{i}\hat{\text{A}}_\mu\hat{\text{A}}_\nu\hat{\text{A}}_\rho)\right], \\
S_{\text{gf}} =& \frac{\kappa}{4\pi}\int d^3x \left[\tfrac{1}{\xi}\text{Tr}\left(\partial_\mu\text{A}_\mu\right)^2 + \text{Tr}\left(\partial_\mu\bar{\text{c}}\text{D}_\mu\text{c}\right) - \tfrac{1}{\xi}\text{Tr}(\partial_\mu\hat{\text{A}}_\mu)^2 + \text{Tr}\left(\partial_\mu\bar{\hat{\text{c}}}\text{D}_\mu\hat{\text{c}}\right)\right], \\
S_{\text{Matter}} =& \int d^3x \left[\text{Tr}\left(\text{D}_\mu\text{C}_\text{I}\text{D}^\mu\bar{\text{C}}^\text{I}\right) + \text{iTr}\left(\bar{\psi}^\text{I}\not{D}\psi_\text{I}\right)\right],
\end{aligned} \tag{2.45}$$

and the following potentials

$$\begin{aligned}
S^F_{\text{int}} =& -\frac{2\pi i}{\kappa}\int d^3x \left[\text{Tr}(\bar{\text{C}}^\text{I}\text{C}_\text{I}\psi_\text{J}\bar{\psi}^\text{J}) - \text{Tr}(\text{C}_\text{I}\bar{\text{C}}^\text{I}\bar{\psi}^\text{J}\psi_\text{J}) + 2\text{Tr}(\text{C}_\text{I}\bar{\text{C}}^\text{J}\bar{\psi}^\text{I}\psi_\text{J})\right. \\
&\left. -2\text{Tr}(\bar{\text{C}}^\text{I}\text{C}_\text{J}\psi_\text{I}\bar{\psi}^\text{J}) - \epsilon_{\text{IJKL}}\text{Tr}(\bar{\text{C}}^\text{I}\bar{\psi}^\text{J}\bar{\text{C}}^\text{K}\bar{\psi}^\text{L}) + \epsilon^{\text{IJKL}}\text{Tr}(\text{C}_\text{I}\psi_\text{J}\text{C}_\text{K}\psi_\text{L})\right], \\
S^B_{\text{int}} =& -\frac{4\pi^2}{3\kappa^2}\int d^3x \left[\text{Tr}(\text{C}_\text{I}\bar{\text{C}}^\text{I}\text{C}_\text{J}\bar{\text{C}}^\text{J}\text{C}_\text{K}\bar{\text{C}}^\text{K}) + \text{Tr}(\bar{\text{C}}^\text{I}\text{C}_\text{I}\bar{\text{C}}^\text{J}\text{C}_\text{J}\bar{\text{C}}^\text{K}\text{C}_\text{K})\right. \\
&\left. +4\text{Tr}(\text{C}_\text{I}\bar{\text{C}}^\text{J}\text{C}_\text{K}\bar{\text{C}}^\text{I}\text{C}_\text{J}\bar{\text{C}}^\text{K}) - 6\text{Tr}(\text{C}_\text{I}\bar{\text{C}}^\text{J}\text{C}_\text{J}\bar{\text{C}}^\text{I}\text{C}_\text{K}\bar{\text{C}}^\text{K})\right],
\end{aligned} \tag{2.46}$$

where $\epsilon^{1234} = \epsilon_{1234} = 1$ and κ is the Chern-Simons level. The matter covariant derivatives are defined as

$$\begin{aligned} D_\mu C_I =& \partial_\mu C_I + i(A_\mu C_I - C_I \hat{A}_\mu), \qquad D_\mu \bar{C}^I = \partial_\mu \bar{C}^I - i(\bar{C}^I A_\mu - \hat{A}_\mu \bar{C}^I), \\ D_\mu \psi_I =& \partial_\mu \psi_I + i(\hat{A}_\mu \psi_I - \psi_I A_\mu), \qquad D_\mu \bar{\psi}^I = \partial_\mu \bar{\psi}^I - i(\bar{\psi}^I \hat{A}_\mu - A_\mu \bar{\psi}^I). \end{aligned} \tag{2.47}$$

Classical and quantum symmetries

The action given by (2.44) is invariant under the supersymmetry transformations given by:

$$\begin{aligned} \delta A_\mu &= \frac{4\pi i}{k} \bar{\theta}^{IJ\alpha} (\gamma_\mu)_\alpha^{\ \beta} \left(C_I \psi_{J\beta} + \frac{1}{2} \epsilon_{IJKL} \bar{\psi}^K_\beta \bar{C}^L \right), \\ \delta \hat{A}_\mu &= \frac{4\pi i}{k} \bar{\theta}^{IJ\alpha} (\gamma_\mu)_\alpha^{\ \beta} \left(\psi_{J\beta} C_I + \frac{1}{2} \epsilon_{IJKL} \bar{C}^L \bar{\psi}^K_\beta \right), \\ \delta C_K &= \bar{\theta}^{IJ\alpha} \epsilon_{IJKL} \bar{\psi}^L_\alpha, \\ \delta \bar{C}^K &= 2 \bar{\theta}^{KL\alpha} \psi_{L\alpha}, \\ \delta \psi^\beta_K &= -i \bar{\theta}^{IJ\alpha} \epsilon_{IJKL} (\gamma^\mu)_\alpha^{\ \beta} D_\mu \bar{C}^L \\ &\qquad + \frac{2\pi i}{k} \bar{\theta}^{IJ\beta} \epsilon_{IJKL} \big(\bar{C}^L C_P \bar{C}^P - \bar{C}^P C_P \bar{C}^L \big) + \frac{4\pi i}{k} \bar{\theta}^{IJ\beta} \epsilon_{IJML} \bar{C}^M C_K \bar{C}^L, \\ \delta \bar{\psi}^K_\beta &= -2i \bar{\theta}^{KL\alpha} (\gamma^\mu)_{\alpha\beta} D_\mu C_L - \frac{4\pi i}{k} \bar{\theta}^{KL}_\beta (C_L \bar{C}^M C_M - C_M \bar{C}^M C_L) - \frac{8\pi i}{k} \bar{\theta}^{IJ}_\beta C_I \bar{C}^K C_J, \end{aligned} \tag{2.48}$$

where they are written only in terms of the parameters $\bar{\theta}$ and not θ, by using the following relation

$$\theta_{IJ} = \frac{1}{2} \epsilon_{IJKL} \bar{\theta}^{KL}. \tag{2.49}$$

The supersymmetry parameters are antisymmetric, $\bar{\theta}^{IJ} = -\bar{\theta}^{JI}$, and obey the reality condition $\bar{\theta}^{IJ} = (\theta_{IJ})^*$.

Classically the theory is scale invariant; indeed, with the standard mass dimensions of the fields given by $[A_\mu] = [\hat{A}_\mu] = [\psi_I] = 1$ and $[C_I] = 1/2$, it is easy to see from the action (2.44) that the Chern-Simons level has dimension $[\kappa] = 0$ since the Lagrangian must have $[\mathcal{L}] = 3$ in natural units in 3-dimensions. Thus the theory is conformal invariant.

The global symmetry group of ABJ(M) theory, for Chern-Simons level $\kappa > 2$ [1], is given by the orthosymplectic supergroup $OSp(6|4)$ [16, 18] (see the algebra in Section 2.1.3.2). The bosonic part of $OSp(6|4)$ are the R-symmetry group $SO(6) \sim SU(4)$ and the 3d conformal group $Sp(4) \sim SO(2,3)$. The fermionic part generates the $\mathcal{N} = 6$ supersymmetry transformations. Finally, the ABJM theory also possesses a discrete, parity-like symmetry. This might be surprising since the Chern-Simons action is not

[1] We are ignoring the symmetry enhancement to $OSp(8|4)$ at $\kappa = 1$ and $\kappa = 2$, because we will work in the 't Hooft limit where κ is large.

invariant but changes sign under a canonical parity transformation. The trick to make the model parity invariant is to accompany the "naive" parity transformation by the exchange of the two gauge group factors. The total transformation is a symmetry because the Chern-Simons terms for the two gauge group factors have opposite signs. Furthermore, in the ABJ case, the generalized parity invariance of the ABJM theory is explicitly broken, because now the two gauge group factors cannot be exchanged anymore.

The 't Hooft coupling

In the ABJ(M) theory the Chern-Simons level κ acts like a coupling. In particular we can define the coupling constant $g^2_{\rm CS} \equiv \frac{1}{\kappa}$ that plays a similar role of g^2_{YM} in $\mathcal{N} = 4$ SYM, though of course κ has to be an integer to preserve non-abelian gauge symmetry. As in the previous sections, the theory can be restricted to the planar sector by taking the 't Hooft limit which introduces the effective couplings

$$\lambda_1 \equiv g^2_{\rm CS} N = \frac{N}{\kappa}, \quad \lambda_2 \equiv g^2_{\rm CS} M = \frac{M}{\kappa} \qquad \text{with } \kappa, \mathrm{M}, \mathrm{N} \to \infty \tag{2.50}$$

In the ABJM case the theory has only one 't Hooft coupling $\lambda = \lambda_1 = \lambda_2$ and it has special properties as we will see in the following sections.

2.2 AdS/CFT correspondence

The AdS/CFT correspondence is one of the most significant results that string theory has produced. It refers to the existence of dualities between theories with gravity and theories without gravity, and is also sometimes referred to as the *gauge-gravity correspondence*. The prototype example of such a correspondence, as originally conjectured by Maldacena [19], is the exact equivalence between type IIB string theory compactified on $AdS_5 \times S^5$, and four-dimensional $\mathcal{N} = 4$ SYM theory. The abbreviation AdS_5 refers to an anti-de Sitter space in five dimensions, S^5 refers to a five-dimensional sphere. Anti-de Sitter spaces are maximally symmetric solutions of the Einstein equations with a negative cosmological constant. The large symmetry group of 5d anti-de Sitter space matches precisely with the group of conformal symmetries of the $\mathcal{N} = 4$ SYM theory. The term AdS/CFT correspondence has its origin in this particular example, CFT being an abbreviation for conformal field theory. Since then, many other examples of gauge theory/gravity dualities have been found. In particular we are also interested in the duality between 3d superconformal field theories and string/M-theory.

The AdS/CFT correspondence is related with two deep ideas. The first of these is the idea that large N gauge theories is equivalent to a string theory [15]. The perturbative expansion of a large N gauge theory in $1/N$ and λ has the form (2.43) and

this is similar to the loop expansion in string theory

$$\mathcal{Z}_{\text{string}} = \sum_{g=0}^{\infty} g_s^{2g-2} \mathcal{Z}_g \tag{2.51}$$

with the string coupling g_s equal to $1/N$. Through some peculiar mechanism, Feynman diagrams of the gauge theory are turned into surfaces that represent interacting strings [20]. Notice that the AdS/CFT correspondence is indeed an example of a weak/strong coupling duality. Depending on the choice of parameters, either AdS or the CFT provides a weakly/strongly coupled description of the system, but never both at the same time. Therefore, the AdS/CFT correspondence can be applied in two directions. We can use string theory to learn about gauge theory, and viceversa.

The second is the idea of holography [21, 22]. This idea has its origin in the study of the thermodynamics of black holes. It was shown by Bekenstein and Hawking [23, 24] that black holes can be viewed as thermodynamical systems with a temperature and an entropy. The temperature is related to the black body radiation emitted by the black hole, whereas the entropy is given by $S = A/4G_N$, with G_N the Newton constant and A the area of the horizon of the black hole. With these definitions, Einstein's equations of general relativity are consistent with the laws of thermodynamics. Since in statistical physics entropy is a measure for the number of degrees of freedom of a theory, it is rather surprising to see that the entropy of a black hole is proportional to the area of the horizon. If gravity would behave like a local field theory, one would have expected an entropy proportional to the volume. A consistent picture is reached if gravity in d dimensions is somehow equivalent to a local field theory in $d-1$ dimensions. Both have an entropy proportional to the area in d dimensions, which is the same as the volume in $d-1$ dimensions. The analogy of this situation to that of an hologram, which stores all information of a 3d image in a 2d picture, led to the name holography. The AdS/CFT correspondence is holographic, because it states that quantum gravity in five dimensions (forgetting the compact five sphere) is equivalent to a local field theory in four dimensions.

The correspondence AdS_5/CFT_4

The derivation of the AdS/CFT correspondence given in [19] crucially involves the notion of D-branes. D-branes are certain extended objects in string theory, that were introduced by Polchinski in [25]. They are labeled by the number of dimensions of the object, so that a D0 brane is like a particle, a D1 brane is like a string, a D2 brane is like a membrane, etc. There are two ways to think about D-branes. On one hand, they are solitonic solutions of the equations of motion of low-energy closed string theory an on the other hand they are objects in open string theory with the property that open strings can end on them. Open strings have a finite tension T, and their center of mass cannot be taken arbitrarily far away from the D-brane. As a consequence, the degrees

$\mathcal{N}=4$ conformal SYM all N, $g_{\rm YM}$ $g_s = g^2_{\rm YM}/(4\pi)$	$\Leftrightarrow$	Full Quantum Type IIB string theory on $AdS_5 \times S^5$ $L^4 = 4\pi g_s N \alpha'^2$
't Hooft limit of $\mathcal{N}=4$ SYM $\lambda = g^2_{\rm YM} N$ fixed, $N \to \infty$ $1/N$ expansion	$\Leftrightarrow$	Classical Type IIB string theory on $AdS_5 \times S^5$ g_s string loop expansion
Large λ limit of $\mathcal{N}=4$ SYM (for $N \to \infty$) $\lambda^{-1/2}$ expansion	$\Leftrightarrow$	Classical Type IIB supergravity on $AdS_5 \times S^5$ α' expansion

Table 2.2: Different regimes of the AdS/CFT conjecture in order of decreasing strength

of freedom of the open string can effectively only propagate in a direction parallel to the brane: one says that they are confined to the brane, or that they live on the brane. The open string spectrum can be reproduced directly from the soliton in the closed string description via a collective coordinate quantization.

To derive the AdS/CFT correspondence, one starts with a stack of D3-branes. This has a description both in terms of open and closed strings. Next, one takes a suitable low-energy limit of the system, which involves taking the string length scale $l_s \to 0$. The open string description reduces to $\mathcal{N}=4$ SYM theory, whereas the closed string description reduces to string theory on $AdS_5 \times S^5$.

Summing up all these ideas, we have

$\mathcal{N}=4$ SYM in $d=4$ with gauge group $SU(N)$ and coupling $g_{\rm YM}$	$\Longleftrightarrow$	Type IIB superstring theory on $AdS_5 \times S^5$ (both with radius L) with 5-form flux N and string coupling g_s

with the following identifications between the parameters of both theories

$$g_s = \frac{g^2_{\rm YM}}{4\pi}, \qquad L^4 = 4\pi g_s N \alpha'^2 \tag{2.52}$$

with the *Regge slope* α' defined as the inverse of the string tension or the square of the string length scale l_s. The equivalence between the two theories includes a precise map between the states (and fields) on the superstring side and the local gauge invariant operators on the $\mathcal{N}=4$ SYM side, as well as a correspondence between the correlators in both theories. The string coupling may be re-expressed in terms of the 't Hooft coupling as $g_s = \lambda/(4\pi N)$. Since λ is being kept fixed, the 't Hooft limit corresponds to weak coupling string perturbation theory (see Table 2.2). A key necessary ingredient for the AdS/CFT correspondence to hold is that the global unbroken symmetries of the two theories be identical. The continuous global symmetry of $\mathcal{N}=4$ SYM theory was

previously shown to be the superconformal group $PSU(2,2|4)$. Recall that the bosonic subgroup arises as the product of the conformal group $SO(2,4)$ in 4-dimensions by the $SU(4)$ automorphism group of the $\mathcal{N}=4$ Poincaré supersymmetry algebra. This bosonic group is immediately recognized on the AdS side as the isometry group of the $AdS_5 \times S^5$ background. The completion into the full supergroup arises on the AdS side because 16 of the 32 Poincaré supersymmetries are preserved by the array of N parallel D3-branes, and in the AdS limit, are supplemented by another 16 conformal supersymmetries. Thus, the global symmetry $PSU(2,2|4)$ matches on both sides of the AdS/CFT correspondence.

$\mathcal{N}=4$ SYM theory also has Montonen-Olive or S-duality symmetry, realized on the complex coupling constant τ as in (2.39). On the AdS side, this symmetry is a global discrete symmetry of Type IIB string theory. Thus, S-duality is also a symmetry of the AdS side of the AdS/CFT correspondence. Notice that, however, that S-duality is a useful symmetry only in the strongest form of the AdS/CFT conjecture. As soon as one takes the large N limit while keeping λ fixed, S-duality no longer has a consistent action. This may be seen for $\theta_i = 0$, where it maps $g_{\rm YM} \to 1/g_{\rm YM}$ and thus $\lambda \to N^2/\lambda$.

Matching global symmetries is of course just the first step; we need a precise prescription for each operator $\mathcal{O}(x)$ in $\mathcal{N}=4$ SYM to be identified with a field $\Phi(x)$ in the bulk of AdS_5. This prescription can then be used to compute correlation functions on both sides of the correspondence. The specification for matching correlation functions in the AdS/CFT correspondence was given in [26, 27] and is usually called *Witten prescription*. It matches the generating functional on the field theory side with the string partition function

$$\langle e^{\int d^4x \Phi_0(x)\mathcal{O}(x)} \rangle_{CFT} = \mathcal{Z}_{\rm string}[\Phi(x,z)|_{z=0} = \Phi_0(x)] \tag{2.53}$$

where $\Phi_0(x)$ specifies the boundary values of the field $\Phi(x)$. Although, calculating the string partition function in general is hard to manage, one has to recall that in the large N and large λ limit (2.53) simplifies as (see Table 2.2)

$$\mathcal{Z}_{\rm string} \approx e^{-S_{\rm Sugra}} \tag{2.54}$$

allowing for predictions of the CFT correlation functions at strong coupling.

The correspondence AdS_4/CFT_3

The duality between 3d conformal field theory and string theory in the AdS_4 background is much more tricky. The most natural choice of M- theory with compactifications involving AdS_4 , *i.e.* the $AdS_4 \times S^7$ solution, it is dual to the three-dimensional gauge field theory with the superconformal symmetry $OSp(8|4)$.

To construct a Lagrangian satisfying the requirements above, the key is to find a proper way to introduce the gauge fields to the free theory with global $U(N)$ symmetry.

In 2004, J.Schwarz [28] suggested that the kinetic term of gauge field should be taken to be Chern-Simons type, instead of the F^2 type, to make sure no new propagating degrees of freedom are added. Moreover, since the Chern-Simons term is of dimension three, the coefficient of this term is dimensionless, in accordance with the requirement that the classical theory should be scale invariant. Under certain assumptions, he also found that there was no Chern-Simons theories with the desired $\mathcal{N} = 8$ supersymmetries. To construct the three-dimensional supersymmetric CFT with $OSp(8|4)$ symmetry, one has to change one or some of his assumptions, which was done by Bagger/Lambert and by Gustavsson.

In 2007, a world-volume theory for stacks of multiple M2-branes was found by Bagger and Lambert [29, 30] and separately by Gustavsson [31] (BLG). The BLG theory is an $\mathcal{N} = 8$ superconformal Chern-Simons theory based on an algebraic structure called a three-algebra, with a basis T^a and a totally antisymmetric triple product:

$$[T^a, T^b, T^c] = f_d^{abc} T^d \tag{2.55}$$

For a specific realization of the three-algebra, related to the Lie algebra $SO(4)$, it was later shown in [32] that it is possible to rewrite the theory as an ordinary $SU(2) \times SU(2)$ gauge theory, without any reference to the three-algebra structure constants. This realization, however, seems to be the only finite-dimensional one, which means that the BLG theory can only describe stacks of two M2-branes. As a solution to this problem, Aharony, Bergman, Jafferies and Maldacena (ABJM) were led to formulate another world-volume theory for stacks of M2-branes. The ABJM theory is described in Section 2.1.5.

Following their work, Bagger and Lambert [33] rewrote the classical action in the 3-algebra form by relaxing constraints on the original structure constants. They also proved that the BLG action could be a special case of the ABJM action when the supersymmetry is enhanced to $\mathcal{N} = 8$ for levels $\kappa = 1, 2$. In fact, for level κ, the theory is conjectured to describe M2 branes in an $\mathbb{R}^8/\mathbb{Z}_\kappa$ orbifold[2] background. A stack of M2 branes on $\mathbb{R}^8$ or $\mathbb{R}^8/\mathbb{Z}_2$ has $\mathcal{N} = 8$ supersymmetry which matches the number of supersymmetries enhanced in ABJM theory with $\kappa = 1, 2$.

The near-horizon geometry is given by M-theory on $AdS_4 \times S^7/\mathbb{Z}_\kappa$. Notice that it is an eleven-dimensional space. Due to the $\mathbb{Z}_\kappa$ action, it is natural to write the sphere S^7 as an S^1 fibration over $\mathbb{CP}^3$: roughly speaking $S^7/\mathbb{Z}_\kappa \simeq \mathbb{CP}^3 \times S^1/\mathbb{Z}_\kappa$. The radius of the circle S^1 depends on κ and the effect of the orbifold is to reduce the volume by a factor κ. In particular when κ is very large, effectively the space is ten-dimensional, *i.e.* $AdS_4 \times \mathbb{CP}^3$. Explicitly, the circle radius is given by $L_{S^1} \sim \frac{(N\kappa)^{1/6}}{\kappa}$. Thus, when such radius is very large, namely when $N \gg \kappa^5$, then the theory is strongly coupled and the proper description is in terms of the M-theory. Vice versa, when the radius is very small, *i.e.* $N \ll \kappa^5$, then it can be effectively used a description in terms of IIA superstrings living on $AdS_4 \times \mathbb{CP}^3$.

[2] An orbifold is a coset G/H where H is a group of discrete symmetries [34].

AdS_5/CFT_4		AdS_4/CFT_3
IIB on $AdS_5 \times S^5$	AdS side	IIA on $AdS_4 \times \mathbb{CP}^3$
$\mathcal{N}=4$ SYM in 4d	CFT side	$\mathcal{N}=6$ CS-matter in 3d
$\lambda = g^2_{\rm YM} N$	't Hooft coupling	$\lambda = \frac{N}{\kappa}$
$T = \frac{L^2}{2\pi\alpha'} = \frac{\sqrt{\lambda}}{2\pi}$	String tension	$T = \frac{L^2}{2\pi\alpha'} = 2^{5/2}\pi\sqrt{\lambda}$
$g_s = \frac{g^2_{\rm YM}}{4\pi}$	String coupling	$g_s = \left(32\pi^2 \frac{N}{k^5}\right)^{1/4}$
$SU(N)$	gauge group	$U(N) \times U(N)$
$PSU(2,2\|4)$	global symmetry	$OSp(6\|4)$

Table 2.3: Summarized comparison between the two gauge/string dualities.

As in the previous case one can write down a map between the parameters of the two theories. The two parameters N and κ, which describe the number of M2-branes and the order of the orbifold group, are contained in the effective string tension and in the string coupling. They are given by

$$T = \frac{L^2}{2\pi\alpha'} = 2^{5/2}\pi \left(\frac{N}{\kappa}\right)^{\frac{1}{2}}, \qquad g_s = \left(32\pi^2 \frac{N}{\kappa^5}\right)^{\frac{1}{4}}. \tag{2.56}$$

Again, from the behavior of the string coupling, we can see the two regimes of strong coupling (M-theory) and weak coupling (string limit approximation). In the 't Hooft limit, the theory is weakly coupled and the parameters are

$$T \sim \sqrt{\lambda}, \qquad g_s \sim \left(\frac{\lambda^5}{N^4}\right)^{\frac{1}{4}}. \tag{2.57}$$

Let us see how the global symmetries are realized on the string scenario. The isometry group of AdS_4 is indeed $SO(3,2)$. Thus once more, the conformal group enters on the string theory side as a symmetry of the background. The same is true also for the projective space $\mathbb{CP}^3$: the corresponding isometry group is $SU(4)$.

Finally, in Table 2.3, we summarize the most relevant results of the dualities wehave considered above, namely AdS_5/CFT_4 and AdS_4/CFT_3.

2.3 Non-perturbative techniques

2.3.1 Supersymmetric localization

Supersymmetric localization is a very powerful tool that allows us to exactly compute the partition function and the expectation value of certain operators in supersymmetric theories. It has been used for a long time in cohomological and topological field theories and more recently it has been applied directly to physical theories, for instance to 4d

$\mathcal{N}=2$ theories by Nekrasov [35, 36], in $\mathcal{N}=2$ theory on the sphere S^4 by Pestun [37] and in 3d superconformal Chern-Simons matter theories by Kapustin, Willett and Yaakov [38].

The key point is that supersymmetry algebras can be often deformed to accommodate background curvature on compact spaces and the resulting partition functions can be computed via a particular saddle-point procedure, known as the supersymmetric localization technique. The technique is enough flexible to compute also correlation functions of local operators and expectation values of non local observables, such as Wilson loops [37, 38] and 't Hooft loops [39, 40]. This procedure in turn generalizes to a large class of $\mathcal{N}=2$ theories, where Wilson loops can be also accurately studied [41, 42, 43] through matrix model techniques.

Suppose we have a fermionic symmetry $\mathcal{Q}$ of the action such that $\mathcal{Q}S=0$. Since $\mathcal{Q}$ is fermionic, its square is either zero or a bosonic symmetry δ_B of the action. Consider the following deformed path-integral

$$\mathcal{Z}(t)=\int \mathcal{D}\Phi\; e^{-S[\Phi]-t\mathcal{Q}V[\Phi]}, \qquad \text{with} \quad \delta_{\mathrm{B}}\mathrm{V}=0 \tag{2.58}$$

which depends on a parameter t and where V is some functional. If the measure is $\mathcal{Q}$-invariant, *i.e.* the fermionic symmetry (and consequently δ_B) is non-anomalous, $\mathcal{Z}$ does not depend by t

$$\frac{\partial\mathcal{Z}(t)}{\partial t}=-\int \mathcal{D}\Phi\; \mathcal{Q}V\; e^{-S-t\mathcal{Q}V}=-\int \mathcal{D}\Phi\; \mathcal{Q}\; \left(Ve^{-S-t\mathcal{Q}V}\right)=0. \tag{2.59}$$

In other words, the symmetry $\mathcal{Q}$ acts as a total derivative and if there are no boundary terms at infinity in field space, the integral of a total derivative is zero. This argument still holds if we insert $\mathcal{Q}$-invariant operators $\mathcal{Q}\mathcal{O}[\Phi]$, then:

- the partition function or VEV does not depend on parameters in front of $\mathcal{Q}$-exact terms in the action;
- VEVs only depend on the $\mathcal{Q}$-cohomology class of the operators;
- the partition function or VEV is not modified by the deformation term $\mathcal{Q}V$.

Now we need to specify a contour in field space on which the path-integral is performed, and the contour must be such that the path-integral is convergent for all values of t.

When t becomes zero, $\mathcal{Z}(0)$ is the original path-integral we want to compute. Suppose we can find some V such that the bosonic part of $\mathcal{Q}V$ is ≥ 0 along the contour. Then, in the limit $t\to\infty$ all field configurations for which $\mathcal{Q}V[\Phi]>0$ are infinitely suppressed. Therefore the path-integral *localizes* to the bosonic zeros Φ_0 of $\mathcal{Q}V$ (which are also stationary points). Let us parametrize the fields around Φ_0 as[3]

$$\Phi=\Phi_0+t^{-1/2}\hat{\Phi} \tag{2.60}$$

[3]We choose the specific power $t^{-1/2}$ because when the deformation term dominates at large t, the kinetic term should be canonically normalized with no powers of t.

Expanding the action around Φ_0, we have

$$S + t\mathcal{Q}V = S[\Phi_0] + (\mathcal{Q}V)^{(2)}[\Phi_0]\hat{\Phi}^2 + O(t^{-1/2}) \tag{2.61}$$

therefore only the on-shell action S_0 and the quadratic expansion of $\mathcal{Q}V$ around the fixed point matters. Then we obtain the localization formula

$$\mathcal{Z} = \int_{\text{BPS}} \mathcal{D}\Phi_0 e^{-S[\Phi_0]} \mathcal{Z}_{1-\text{loop}}[\Phi_0] \tag{2.62}$$

by Gaussian integration where the so-called *1-loop determinant*

$$\mathcal{Z}_{1-\text{loop}}[\Phi_0] = \text{SDet}[(\mathcal{Q}\text{V})^{(2)}]_{\Phi_0} \tag{2.63}$$

is the ratio of the fermionic and bosonic determinants and it can be thought of as a measure on the subspace of fixed points. This formula is exact and if the space of fixed points $\{\Phi_0\}$ is finite-dimensional, then we have reduced the path-integral to an ordinary integral and we may be able to solve it.

It turns out that one localizes on some BPS configurations. We can make a canonical choice for V

$$V = \sum_{\text{fermions } \psi} (\mathcal{Q}\Psi)^\dagger \Psi \tag{2.64}$$

If the bosonic part of $\mathcal{Q}V$ is non-negative along the contour and $\delta_B V = 0$, then the fixed points are essentially

$$\mathcal{Q}\Psi = 0 \tag{2.65}$$

which are the BPS equations. The computation of the 1-loop determinant in general might seem exceedingly hard but, because there is supersymmetry, one have to expect huge cancellations among the eigenvalues.

Matrix models

In some cases (and in particular in the cases we will see in the following chapters) the solution of (2.65) is constant and the theory in the localization *locus* can be treated as a zero-dimensional field theory, namely a matrix model. The basic field is an Hermitian $N \times N$ matrix M with action

$$S[M] = \frac{1}{2}\text{Tr}\, M^2 + \sum_{p\geq 3} \frac{g_p}{p} \text{Tr}\, M^p. \tag{2.66}$$

with g_p is a coupling constant depending on p. This action has the gauge symmetry $M \to UMU^\dagger$, where U is a $U(N)$ matrix. The partition function of the theory is given by

$$\mathcal{Z} = \frac{1}{\text{Vol}(U(N))} \int [dM]\, e^{-\frac{1}{g}S[M]} \tag{2.67}$$

where g is another coupling constant such that each propagator gives a power of g, while each interaction vertex with p legs gives a power of g_p/g. The factor $\mathrm{Vol}(U(N))$ is the volume factor of the gauge group that arises after fixing the gauge. The measure in the path integral is given by

$$[dM] = 2^{\frac{N(N-1)}{2}} \prod_{i=1}^{N} dM_{ii} \prod_{1\leq i<j\leq N} d\mathrm{Re}\, M_{ij} d\mathrm{Im}\, M_{ij}. \tag{2.68}$$

where the numerical factor in (2.68) is introduced to obtain a convenient normalization.

A particularly simple example is the *Gaussian matrix model*, defined by the partition function

$$\mathcal{Z}_G = \frac{1}{\mathrm{Vol}(U(N))} \int [dM]\, e^{-\frac{1}{2g}\mathrm{Tr}\, M^2}. \tag{2.69}$$

The normalized vevs of a gauge-invariant functional $f(M)$ in the Gaussian matrix model is given by

$$\langle f(M)\rangle_G = \frac{1}{\mathcal{Z}} \int [dM]\, f(M)\, e^{-\frac{1}{2g}\mathrm{Tr}\, M^2} \tag{2.70}$$

This model is exactly solvable, and the vevs (2.70) can be computed systematically.

2.3.2 Integrability

There is growing amount of evidence that some gauge theories Yang-Mills theories and Chern-Simons-matter theories possess additional hidden symmetries at the quantum level that are not manifest in the Lagrangian formulation. Remarkably, in certain regimes this extra symmetry allows to describe gauge theories as an integrable system. In such situations the integrable structure may allow to overcome the difficulties of accessing the strongly coupled regimes of gauge theories analytically. To understand how integrability appears in gauge theories it is convenient to study $\mathcal{N} = 4$ SYM theory which provides an ideal testing ground. In particular, there is strong evidence that this theory is integrable in the 't Hooft limit. Furthermore, the AdS/CFT duality allows to actually compare results obtained using integrability methods to the strongly and weakly coupled regimes.

The spin-chain picture

In 2003 Minahan and Zarembo [44] established a crucial equivalence between the one loop dilatation operator in the $SO(6)$ sector of the theory and the Heisenberg spin chain Hamiltonian. Let us review why and how it works and the consequences brought by this relation. In Section 2.1.2.3 we have seen the relation between the two-point function of renormalized fields/operators and their anomalous dimension and in Section 2.1.3.3 we

have seen how to construct composite operators. If $g_{\rm YM}$ is small ($\gamma << \Delta_0$) one can approximate the two-point function as

$$\langle \mathcal{O}(x)\bar{\mathcal{O}}(y)\rangle \approx \frac{1}{|x-y|^{2\Delta_0}}(1-\gamma\log\Lambda^2|x-y|^2), \tag{2.71}$$

where Λ is the cutoff. For operators made up only of scalar fields with no covariant derivatives, all fields have bare dimension 1 and the bare dimension of the operator is $\Delta_0 = L$, namely the number of scalar fields inside the trace.

Let us now investigate what happens as we let $N \to \infty$ (see Section (2.1.4)). For the most general scalar single-trace operator in this sector

$$\mathcal{O}_{I_1,I_2\ldots I_L}(x) = \frac{(4\pi^2)^{L/2}}{\sqrt{C_{I_1,I_2\ldots I_L}}\,N^{L/2}}\mathrm{Tr}(\Phi_{\rm I_1}(\rm x)\Phi_{\rm I_2}(\rm x)\ldots\Phi_{\rm I_L}(\rm x))\,, \tag{2.72}$$

where $C_{I_1,I_2\ldots I_L}$ is a symmetry factor, one finds up to one loop the following correlator

$$\begin{aligned}\langle \mathcal{O}_{I_1,I_2\ldots I_L}(x)\bar{\mathcal{O}}^{J_1,J_2\ldots J_L}(y)\rangle = &\frac{1}{|x-y|^{2L}}\frac{(\delta^{J_1}{}_{I_1}\delta^{J_2}{}_{I_2}\ldots\delta^{J_L}{}_{I_L}+\text{cycles})}{\sqrt{C_{I_1,I_2\ldots I_L}C_{J_1,J_2\ldots J_L}}}\\ &\times\left[1-\frac{\lambda}{16\pi^2}\log(\Lambda^2|x-y|^2)\sum_{\ell=1}^{L}(1-C-2P_{\ell,\ell+1}+K_{\ell,\ell+1})\right],\end{aligned} \tag{2.73}$$

where C is a constant and "cycles" refers to the $L-1$ uniform shifts of the J_k indices. $P_{\ell,\ell+1}$ is the exchange operator, and as its name implies it exchanges the flavor indices of the ℓ and the $\ell+1$ sites inside the trace:

$$P_{\ell,\ell+1}\,\delta^{J_1}_{I_1}\ldots\delta^{J_\ell}_{I_\ell}\delta^{J_{\ell+1}}_{I_{\ell+1}}\ldots\delta^{J_L}_{I_L} = \delta^{J_1}_{I_1}\ldots\delta^{J_{\ell+1}}_{I_\ell}\delta^{J_\ell}_{I_{\ell+1}}\ldots\delta^{J_L}_{I_L}\,. \tag{2.74}$$

$K_{\ell,\ell+1}$ is the trace operator which contracts the flavor indices of neighboring fields:

$$K_{\ell,\ell+1}\,\delta^{J_1}_{I_1}\ldots\delta^{J_\ell}_{I_\ell}\delta^{J_{\ell+1}}_{I_{\ell+1}}\ldots\delta^{J_L}_{I_L} = \delta^{J_1}_{I_1}\ldots\delta_{I_\ell I_{\ell+1}}\delta^{J_\ell J_{\ell+1}}\ldots\delta^{J_L}_{I_L}\,. \tag{2.75}$$

Because of the $P_{\ell,\ell+1}$ and $K_{\ell,\ell+1}$, there is operator mixing at the one-loop level.

If we compare this result to (2.71), we see that because of the operator mixing the anomalous dimension γ should be replaced with an operator $\Gamma^{(1)}$ as follows

$$\Gamma^{(1)} = \frac{\lambda}{16\pi^2}\sum_{\ell=1}^{L}(1-C-2P_{\ell,\ell+1}+K_{\ell,\ell+1})\,. \tag{2.76}$$

The one-loop anomalous dimensions are the eigenvalues of $\Gamma^{(1)}$.

The entire class of scalar single trace operators of length L can be mapped to a Hilbert space which itself is a tensor product of finite dimensional Hilbert spaces

$$\mathcal{V}_1\otimes\mathcal{V}_2\cdots\otimes\mathcal{V}_\ell\otimes\cdots\otimes\mathcal{V}_L\,. \tag{2.77}$$

Each $\mathcal{V}_\ell$ is the Hilbert space for an $SO(6)$ vector representation. The tensor product is the same Hilbert space as that of a one-dimensional spin-chain with L sites, where at each site there is an $SO(6)$ vector "spin".

The operator $\Gamma^{(1)}$ in (2.76) acts linearly on this space. Furthermore, it is Hermitian and commutes with the shift associated to the cyclicity of the trace. Thus, we can treat Γ as a Hamiltonian on the spin-chain. The energy eigenstates then correspond to the possible anomalous dimensions for the scalar operators. Because $P_{\ell,\ell+1}$ and $K_{\ell,\ell+1}$ act on neighboring fields, the spin-chain Hamiltonian only has nearest neighbor interactions between the spins.

Any chiral primary operator (CPO) $\mathcal{O}_L^{\rm CPO}$, which is in the $L^{\rm th}$ symmetric traceless representation of $SO(6)$, is eigenstate of $\Gamma^{(1)}$. In particular one can prove that $P_{\ell,\ell+1}\mathcal{O}_L^{\rm CPO} = \mathcal{O}_L^{\rm CPO}$ for any ℓ and $K_{\ell,\ell+1}\mathcal{O}_L^{\rm CPO} = 0$. Therefore,

$$\Gamma^{(1)}\,\mathcal{O}_L^{\rm CPO} = \frac{\lambda}{16\,\pi^2}\sum_{\ell=1}^{L}(1 - C - 2)\mathcal{O}_L^{\rm CPO} \tag{2.78}$$

However, the dimension of $\mathcal{O}_L^{\rm CPO}$ is protected, meaning that its anomalous dimension is zero ($\Gamma^{(1)}\,\mathcal{O}_L^{\rm CPO} = 0$). Hence, we find that $C = -1$ and $\Gamma^{(1)}$ becomes [44]

$$\Gamma^{(1)} = \frac{\lambda}{8\,\pi^2}\sum_{\ell=1}^{L}\left(1 - P_{\ell,\ell+1} + \frac{1}{2}\,K_{\ell,\ell+1}\right)\,. \tag{2.79}$$

The Hamiltonian for the spin-chain that corresponds to $\Gamma^{(1)}$ is integrable[4], then the system is solvable, at least in principle. In [45, 46] Beisert and Staudacher generalize the 1-loop Hamiltonian to all single-trace operator. Going beyond one-loop, one finds that the n-loop contribution to the anomalous dimension can involve up to n neighboring fields in an effective Hamiltonian [47, 48, 49]. Therefore, as λ becomes larger these longer range interactions become more and more important, such that at strong coupling the spin-chain is effectively long range. In this case the Hamiltonian is not known above the first few loop orders [47, 48, 50].

Heisenberg spin-chain and magnons

Let us now restrict our single trace operators to the $SU(2)$ closed sector. The two independent complex scalar fields Z and X transform under a doublet of $SU(2)$, hence

[4]One needs to construct the R-matrix $R_{12}(u)$ which acts on a tensor product of two vector spaces $\mathcal{V}_1 \otimes \mathcal{V}_2$ (see (2.77)) and the transfer matrix $T(u)$ constructed from the R-matrix as $T(u) = R_{01}(u)R_{02}(u)...R_{0L}(u)$. The parameter u is the spectral parameter. If a system is integrable, then the R-matrix satisfies the Yang-Baxter equation

$$R_{12}(u)R_{13}(u+v)R_{23}(v) = R_{23}(v)R_{13}(u+v)R_{12}(u) \tag{2.80}$$

and $T(u)$ is called *Yangian* which is the algebra of $2L$ set of charges of an integrable system.

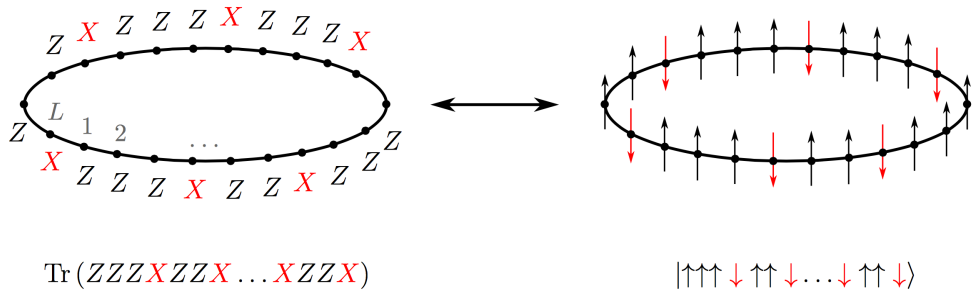

Figure 2.4: A single trace operator and its interpretation as spin chain.

we can label the Z field as spin up ($\uparrow$) and the X field as spin down ($\downarrow$) as in Figure 2.4. The $SU(2)$ sector has the Hamiltonian

$$\Gamma^{(1)}_{SU(2)} = \frac{\lambda}{8\pi^2}\sum_{\ell=1}^{L}(1 - P_{\ell,\ell+1})\,. \tag{2.81}$$

In terms of spin operators the Hamiltonian can be rewritten as

$$\Gamma_{SU(2)} = \frac{\lambda}{8\pi^2}\sum_{\ell=1}^{L}\left(\frac{1}{2} - 2\,\vec{S}_\ell\cdot\vec{S}_{\ell+1}\right)\,. \tag{2.82}$$

Remarkably, $\Gamma_{SU(2)}$ is the Hamiltonian of the *Heisenberg spin-chain* with L lattice sites. The total spin $\vec{S} = \sum_\ell \vec{S}_\ell$ commutes with Γ so the energy eigenstates are simultaneously total spin eigenstates.

Because of the sign of the $\vec{S}_\ell\cdot\vec{S}_{\ell+1}$ term the spin-chain is ferromagnetic and the ground state has all spins aligned, with total spin $L/2$. This is the symmetric representation, which corresponds to the chiral primary operator. The operators which are not chiral primaries correspond to excitations about the ground state. They have total spin that is less than $L/2$. Let us start with a ground state which we write as $|\uparrow\uparrow\uparrow\ldots\uparrow\uparrow\rangle$. This corresponds to the chiral primary $\mathcal{O}^{\rm CPO}_L$ described above. Let us now consider the states where one spin is down. The action on a state with a down spin at a particular position ℓ is

$$\begin{aligned}&\Gamma_{SU(2)}|\uparrow\ldots\overset{\ell}{\uparrow\downarrow}\uparrow\ldots\uparrow\rangle\\ &= \frac{\lambda}{8\,\pi^2}\left(2\,|\uparrow\ldots\overset{\ell}{\uparrow\downarrow}\uparrow\ldots\uparrow\rangle - |\uparrow\cdots\overset{\ell-1}{\downarrow}\uparrow\uparrow\ldots\uparrow\rangle - |\uparrow\ldots\uparrow\uparrow\overset{\ell+1}{\downarrow}\ldots\uparrow\rangle\right).\end{aligned} \tag{2.83}$$

From this it is easy to see that the eigenstates are

$$|p\rangle \equiv \frac{1}{\sqrt{L}}\sum_{\ell=1}^{L} e^{ip\ell}|\uparrow\uparrow\cdots\overset{\ell}{\downarrow}\ldots\uparrow\uparrow\rangle \tag{2.84}$$

where

$$\Gamma_{SU2}|p\rangle = \varepsilon(p)\,|p\rangle\,, \qquad \varepsilon(p) = \frac{\lambda}{2\,\pi^2}\,\sin^2\frac{p}{2}\,. \tag{2.85}$$

The state $|p\rangle$ is called a single *magnon* state with momentum p. The dispersion is $\varepsilon(p)$ and the magnon momentum is $p = 2\pi n/L$. The single magnon state is quite trivial because the only allowed state is the $p = 0$ state and we find no operators that are not chiral primaries with only a single X field. The first non-trivial case occurs with two down spins. One can prove that the allowed values for p_1 and p_2 are $p_1 = -p_2 = 2\pi n/(L-1)$ and the possible eigenvalues for the two magnon state are

$$\gamma = \frac{\lambda}{\pi^2}\sin^2\frac{\pi n}{L-1}\,. \tag{2.86}$$

For M magnons one then sets up a state

$$|p_1, p_2, \ldots p_M\rangle = \sum_{\ell_1<\ell_2\ldots\ell_M} e^{ip_1\ell_1+ip_2\ell_2+\cdots+ip_M\ell_M}\,|\,\ldots\overset{\ell_1}{\downarrow}\ldots\overset{\ell_2}{\downarrow}\ldots\ldots\overset{\ell_M}{\downarrow}\ldots\rangle + \ldots \tag{2.87}$$

with $p_1 > p_2 \cdots > p_M$ and where the last set of dots refers to the other possible orderings for the magnons, with appropriate phase factors. Defining the rapidity variable u, where $e^{ip} = \frac{u+i/2}{u-i/2}$ and putting the magnons on a circle with L sites we then find the quantization condition for the j^{th} magnon

$$\left(\frac{u_j+i/2}{u_j-i/2}\right)^L = \prod_{k\neq j}^{M}\frac{u_j-u_k+i}{u_j-u_k-i}\,. \tag{2.88}$$

with the S-matrix for magnons of rapidity u_j and u_k is $S_{jk} = \frac{u_j-u_k-i}{u_j-u_k+i}$. The energy of the state is

$$\gamma = \sum_{j=1}^{M}\varepsilon(u_j) = \frac{\lambda}{8\,\pi^2}\sum_{j=1}^{M}\frac{1}{u_j^2+1/4}. \tag{2.89}$$

The equations in (2.88) were first derived by Bethe many years ago [51] and are called the *Bethe equations* for the Heisenberg spin-chain.

The integrability of the $SU(2)$ scalar sector of $\mathcal{N}=4$ is not confined to the one loop order, it has been proven its integrability up to three loops in [47]. In the limit of long spin chain an all loop Asymptotic Bethe Ansatz (ABA) for the $SU(2)$ sector has been proposed in [52] and generalized to the full $PSU(2,2|4)$ spin chain [53].

Wrapping corrections and Thermodynamic Bethe Ansatz

The Bethe ansatz yields reliable results for the anomalous dimensions in the asymptotic limit only $L \to \infty$. Since the range of the interaction grows with the perturbative

original model	mirror model
$(t, x) \equiv (y = it, x)$	$(y, x = i\tau) \equiv (\tau, y)$
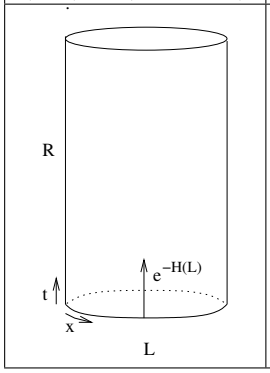	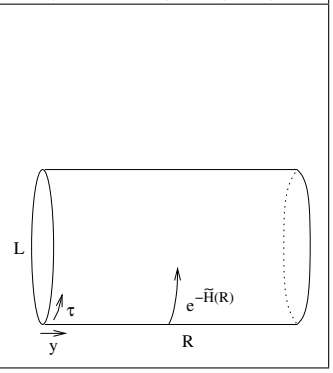

Table 2.4: The relation between the original and the mirror model.

order, for finite length L of the spin-chain, at λ^{L+1} order the interaction stretches all around the spin-chain and the Bethe-ansatz need to be corrected. Then, contributions from the *wrapping interactions* have to be added. They were first introduced and used in [54, 55], for the four-loop anomalous dimension of the Konishi operator. The four-loop contribution has also been obtained from a generalized Lüscher formula [56].

The matching of the Feynman diagram and Lüscher based calculations provides the first test of AdS/CFT and the underlying integrability beyond the asymptotic limit. It is also reproduced by the recently proposed Y-system [57, 58], which is derived from the *Thermodynamic Bethe Ansatz* (TBA) [59, 60, 61, 62] and is a candidate to capture the full planar spectrum of $\mathcal{N} = 4$ SYM theory.

The first step towards computing the finite size spectrum of our model will be to compute the ground state energy. This can be done exactly thanks to an idea by Zamolodchikov [63]. The ground state energy is the leading low temperature contribution to the Euclidean partition function

$$\mathcal{Z}(R, L) \sim e^{-RE_0} \qquad \text{with } R = \frac{1}{T} \to \infty \tag{2.90}$$

This partition function can be computed from our original quantum field theory by Wick-rotating $t \to y = it$ and considering a path integral over fields periodic in y with period R. In geometrical terms we are putting the theory on a torus which in the zero temperature limit degenerates to a cylinder. Analytically continuing $y \to t = -iy$ we have a theory where the role of space and time have been interchanged with respect to the original theory. This new theory is the so-called *mirror theory* (see Table 2.4). In principle we can compute the Euclidean partition function both through our original model at size L and temperature $1/R$ and through the mirror model at size R and temperature $1/L$ ($\mathcal{Z}(L, R) = \tilde{\mathcal{Z}}(R, L)$).

To compute the ground state energy of a model then, we can equivalently compute

the infinite volume partition function of the mirror model at finite temperature or just its Helmholtz free energy $\tilde{F}$ since $\mathcal{Z} = e^{-L\tilde{F}}$. More precisely, recalling equation (2.90), the ground state energy is the free energy density of the mirror model

$$E_0 = \frac{\tilde{F}}{R}. \tag{2.91}$$

The key point is that we are considering the mirror model in the infinite volume limit where we can use the Asymptotic Bethe Ansatz.

Finally one can find the ground state energy solving the following integral

$$E_0 = -\sum_Q \int_{-\infty}^{\infty} \frac{du}{4\pi} \partial_u \tilde{p}_Q \log\left(1 + Y_Q\right) \tag{2.92}$$

where $\tilde{p}_Q$ is the momentum in the mirror space and Y_Q is the so-called *Y-function* that is in relation with the particle density. The nonlinear integral equation which determines the Y-function is called the *Thermodynamic Bethe Ansatz equation* (the choice of the letter "Y" is due to the fact that the TBA equation, in certain cases, can be treated as a *Y-system* which can be represented diagrammatically by graphs [64]). This implicit solution is a starting point of a systematic large and small volume expansion and can be used to derive TBA equations for excited states by analytical continuation.

Chapter 3

Supersymmetric Wilson loops in $\mathcal{N} = 4$ SYM and ABJ(M)

The Wilson loop, introduced by Wilson in [65], is one of the most general gauge invariant observable in Yang-Mills theories and therefore plays an important role in studying the general structure. Furthermore, it is the building block of lattice gauge theories, where it can be also used to study non-perturbative phenomenons. In any gauge theory the Wilson loop operator is defined as the traced holonomy of the gauge connection $A_\mu(x) = A^a_\mu(x)T^a$

$$W[C] \equiv \frac{1}{\dim_{\mathcal{R}}} \mathrm{Tr}_{\mathcal{R}} \mathcal{P} \exp\left[i \oint_C dx^\mu \, A_\mu(x) \right] \tag{3.1}$$

where $\dim_{\mathcal{R}}$ is the dimension of the representation $\mathcal{R}$ and the curve C is parametrized by the vector x^μ. The symbol $\mathcal{P}$ denotes the *path-ordering* of the integrand: in practice it ensures gauge invariance of the Wilson loop. The definition of path ordering, for instance for $\tau_1 > \tau_2$, is the following:

$$\begin{aligned} \mathcal{P} \exp\left[i \oint_C dx^\mu \, A_\mu(x) \right] = \mathbb{1} + i \int_a^b d\tau_1 (\dot{x}_1^\mu A_\mu(x_1)) \\ - \int_a^b d\tau_1 \int_a^{\tau_1} d\tau_2 (\dot{x}_1^\mu \dot{x}_2^\nu A_\mu(x_1) A_\nu(x_2)) + ... \end{aligned} \tag{3.2}$$

where $x_i^\mu = x^\mu(\tau_i)$, $\dot{x}_i^\mu = \partial_{\tau_i} x_i^\mu$ with $\tau \in [a, b]$. In other words, the action of $\mathcal{P}$ ensures that the integrals are nested instead of being independent of each other.

Now let us imagine creating a quark-antiquark pair at a (spatial) distance R, at time $t = 0$. Their masses are taken to infinity, so we may expect them to be static (no kinetic energy). After a large time T we let them rejoin and annihilate. The static potential of this configuration is encoded in the Wilson loop when the contour C is a

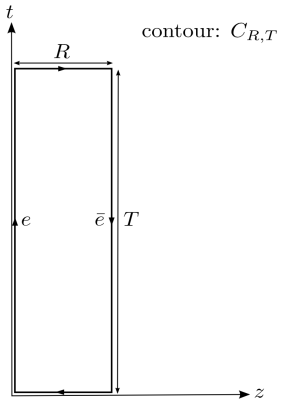

Figure 3.1: contour

rectangular loop $C_{R,T}$ (see Figure 3.1) in the limit of large T

$$V(R) = -\lim_{T\to\infty} \frac{1}{T} \log\left(\langle W[C_{R,T}]\rangle\right) . \tag{3.3}$$

The closed loop $C_{R,T}$ has two geometrical characteristics, the total length of the loop $L = 2(R+T)$ and the area of the minimal surface $A = RT$ spanned by the loop. When the loop size is scaled up to infinity, the dominant behavior is a exponential decay according to a perimeter law or an area law respectively:

$$\begin{aligned} \lim_{R\to\infty} \langle W[C_{RT}]\rangle \sim e^{-kL} \qquad &\Rightarrow \qquad V(R) = 2k \\ \lim_{R\to\infty} \langle W[C_{RT}]\rangle \sim e^{-\sigma A} \qquad &\Rightarrow \qquad V(R) = \sigma R \end{aligned} \tag{3.4}$$

where k may be interpreted as a self-energy and σ is the strong coupling *string tension* of the "string" associated to the *flux tube* between the two charges. The first line of the (3.4) obeys to the perimeter law and the energy of a quark-antiquark pair saturates to a constant. This is the so-called *Coulomb phase*. Instead, the area law of the second line leads to a potential proportional to the separation R between the charges. Hence they cannot be separated to infinite distance with any finite amount of energy. This is the so-called *confinement phase*.

The confining and non-confining phases of gauge theories are thus distinguished by the behavior of the Wilson loop expectation value (*Wilson criterion*): the Wilson loop in gauge theories plays the role of the *order parameter* for confinement.

In this Chapter we will see in sections 3.1 and 3.2 how to construct a supersymmetric Wilson loop operator in $\mathcal{N} = 4$ SYM and ABJ(M) theories. In particular we will define some families of Wilson loops that preserve a fraction of the original supersymmetry, depending on the geometry of C. In Section 3.3 we will give practical examples of Wilson loops in perturbation theory: in particular we will consider the vacuum expectation

value of the circular Wilson loop in $\mathcal{N}=4$ SYM and ABJ(M) theory. The same observable can be computed in a non-perturbative way: in Section 3.4 we will present some general results given by supersymmetric localization.

3.1 Supersymmetric Wilson loops in $\mathcal{N}=4$ SYM

In $\mathcal{N}=4$ SYM the ordinary Wilson loop (3.1) has been generalized to the so-called *Maldacena-Wilson loop* [66]

$$W[C]=\frac{1}{\dim_{\mathcal{R}}}\mathrm{Tr}_{\mathcal{R}}\mathcal{P}\exp\left[\oint_C d\tau(i\dot{x}^\mu A_\mu+|\dot{x}|\Theta_I\Phi^I)\right] \tag{3.5}$$

Here, $x^\mu(\tau)$ parameterizes the contour C in $\mathbb{R}^4$ and Θ_I is a six-vector ($\Theta_I\Theta^I=1$) which specifies a point on S^5 and in general it can depend on τ. This operator measures the holonomy of an heavy W-boson whose mass results from spontaneous breaking of the $SU(N+1)$ gauge symmetry into $SU(N)\times U(1)$ in $\mathcal{N}=4$ SYM theory. As one can see from (3.5), in contrast to the ordinary Wilson loop the Maldacena-Wilson loop not only couples to the gauge field of the theory but also to the six adjoint scalars. The origin of these additional couplings can be understood by considering an ordinary Wilson loop in ten-dimensional $\mathcal{N}=$ 1 SYM theory and performing a dimensional reduction down to four spacetime dimensions (following the same procedure adopted to obtain $\mathcal{N}=4$ SYM from the ten-dimensional theory). Using this procedure, one can find a bigger class of Wilson loop with an arbitrary scalar coupling $\dot{y}_I$. A loop of this form belongs to the Maldacena-Wilson loops if the contour satisfies the following additional constraint

$$\dot{x}^2=\dot{y}^2 \qquad \dot{y}_I=|\dot{x}|\Theta_I \tag{3.6}$$

As we will see, this light-likeness condition is crucial, since it is related to nearly all the nice properties that Maldacena-Wilson loop operators have.

The supersymmetry variation of the Wilson loop is (we have chosen a loop in the fundamental representation)

$$\delta_\epsilon W[C]=\frac{1}{N}\mathrm{Tr}\mathcal{P}\oint d\tau\bar{\lambda}(i\Gamma^\mu\dot{x}_\mu+\Gamma^I\Theta_I|\dot{x}|)\epsilon\exp\left[\oint d\tau'(i\dot{x}^\mu A_\mu+|\dot{x}|\Theta_I\Phi^I)\right] \tag{3.7}$$

where $\Gamma^M=(\Gamma^\mu,\Gamma^I)$ are the ten-dimensional Dirac matrices. The transformations of the bosonic field $A^M=(A^\mu,\Phi^I)$ are

$$\begin{aligned}\delta_\epsilon A_\mu =&\bar{\lambda}\Gamma_\mu\epsilon\,,\\ \delta_\epsilon\Phi^I =&\bar{\lambda}\Gamma^I\epsilon\,,\end{aligned} \tag{3.8}$$

where the parameter of transformation ϵ is a ten-dimensional Majorana-Weyl spinor. Some fraction of the total supersymmetry will be preserved if

$$(i\Gamma^\mu\dot{x}_\mu+\Gamma^I\Theta_I|\dot{x}|)\epsilon=0 \tag{3.9}$$

The equation (3.9) has eight independent solutions for any given τ. In general, these solutions will depend on τ, so an arbitrary Wilson loop is only locally supersymmetric. The requirement to achieve global supersymmetry, *i. e.* a constant ϵ, induces a constraint on $x_\mu(\tau)$ and $\Theta_I(\tau)$. The number of linearly independent ϵ's that satisfy (3.9) determines the number of conserved supercharges.

When Θ_I does not depend on τ, the condition (3.9) has not solution, unless C is a straight line. Indeed, choosing parameterization of the contour C such that $|\dot{x}| = 1$ and differentiating (3.9) with respect to τ, we get:

$$i\Gamma^\mu \ddot{x}_\mu \epsilon = 0\,, \tag{3.10}$$

which implies that $\ddot{x}$ is identically zero. In that case $W[C]$ is a BPS operator that commutes with all the Poincaré supercharges (1/2 BPS). Consistently with this property, it should be protected from radiative corrections and we have

$$\langle W[C_{\rm sl}]\rangle = 1 \tag{3.11}$$

The 1/2 BPS straight line is related to the circular Wilson loop by a conformal transformation (an inversion). The circle has similar features of the straight line, but its quantum expectation value is non-trivial as we will see in the following sections. The circular Wilson loop is still 1/2 BPS but preserves a mixture of Poincaré and conformal supercharges.

For a general loop with varying Θ_I and a curved contour C, (3.9) constitutes an infinite set of algebraic equations for sixteen unknown quantities. However they can have still non-trivial solutions for certain x_μ and Θ_I. In Section 3.1.1 and 3.1.2 we will review two general classes of supersymmetric Wilson loops that differ for the choice of the coupling to the scalars. These operators are the so-called *Zarembo Wilson loop* (or *Q-invariant Wilson loop*) and the *DGRT Wilson loop*.

Maldacena-Wilson loop in the AdS/CFT correspondence

The Maldacena-Wilson loop (3.5) is the natural operator that one is led to use in the AdS/CFT framework. It was proposed in [66, 67] that the Wilson loop is defined by an open string ending on the loop at the boundary of AdS (see also [68]). To compute the expectation value of the Wilson loop operator in string theory one has to generalize the prescription (2.53), since the Wilson loop is a non local operator. The mapping between the non-local Wilson loop operator in the gauge theory and the string partition function $\mathcal{Z}_{\rm string}[C]$ is

$$\langle W[C]\rangle = \mathcal{Z}_{\rm string}[C] \tag{3.12}$$

More explicitly, one should compute the partition function for an open string in the $AdS_5 \times S^5$ background with the boundary conditions defined by the physical contour:

the string ends on the loop at the boundary on AdS_5, drawing on S^5 the scalar coupling Θ_I.

In the large N limit and large 't Hooft coupling, recalling equation (2.54), the expectation value of the Wilson loop can be computed in the classical supergravity approximation. In this limit the string action is described by a *minimal surface* of area $A[C]$ and we have

$$\langle W[C] \rangle \simeq \exp\left(-A[C]\right) \tag{3.13}$$

Due to the curvature of AdS_5, the minimal surface does not stay near the boundary, but goes deep into the interior of space, where the area element can be made smaller. The behavior of the Wilson loop, for large area, is that of a conformal theory and it does not imply confinement.

The area of the minimal surface can be obtained by extremizing the *Nambu-Goto action*

$$A[C] = S_{NG} = \frac{1}{2\pi\alpha'} \int d\sigma d\tau \sqrt{-\text{Det } G_{MN}(\partial_\alpha X^M \partial_\beta X^N)} \tag{3.14}$$

In the definition of the Nambu-Goto action, G_{MN} is the ten-dimensional background metric and the X^M are the string coordinates in ten dimensional space time; the set $\{\tau, \sigma\}$ parametrizes the string worldsheet. This area in general is divergent, the infinite part was identified as due to the mass of the W-boson and subtracted [66, 69]. Furthermore, it turns out that minimal surfaces terminating at the boundary of AdS_5 correspond only to loops that satisfy the constraint (3.6).

Finally, there are three universal predictions of the AdS/CFT correspondence for Wilson loops: in the strong 't Hooft coupling limit the Wilson loop expectation value exponentiates, the exponent is proportional to $\sqrt{\lambda}$ and the coefficient is positive, thus

$$\langle W[C] \rangle = \exp(\sqrt{\lambda} \times \text{positive number}) \qquad \lambda \to \infty \tag{3.15}$$

Corrections to the Wilson loop in the large λ limit come from the string fluctuations and are suppressed when λ is large. An expansion which includes them perturbatively is an ordinary α' expansion of the world-sheet sigma model and, for AdS string, goes in powers of $1/\sqrt{\lambda}$.

3.1.1 The Zarembo construction

In [70] Zarembo proposed a simple ansatz, for which (3.9) reduces to a finite number of equations. The ansatz amounts in requiring that the position of the loop in S^5 follows the tangent vector $\dot{x}^\mu$ of the space-time contour C. Thus we can write the following condition for the scalar coupling

$$\Theta_I = M_I^\mu \frac{\dot{x}_\mu}{|\dot{x}|} \tag{3.16}$$

where the rectangular matrix M_I^μ can be regarded as a projection operator:

$$M_I^\mu M_I^\nu = \delta^{\mu\nu} \tag{3.17}$$

With this choice of Θ_I, the Maldacena-Wilson loop becomes

$$W_Z[C] = \frac{1}{N}\mathrm{Tr}\mathcal{P}\exp\left[\oint_C dx_\mu (iA^\mu + M_I^\mu \Phi^I)\right] \tag{3.18}$$

The supersymmetry equation (3.9) reduces to the following four algebraic equations

$$(\Gamma^\mu - iM_I^\mu \Gamma^I)\epsilon = 0 \tag{3.19}$$

Expanding the terms in the supersymmetry variation we find that a general curve in $\mathbb{R}^4$ preserves one Poincaré supersymmetry [70], thus it is called 1/16 BPS. This family of Wilson loops is often called therefore *Q-invariant*. The supersymmetry is enhanced if the contour C has a special shape. Consider, for instance, a spatial Wilson loop which lies in a three-dimensional time slice $x^0 = 0$. In this case only three of the four constraints (3.19) can be imposed and the loop preserves two Poincaré supersymmetries. Thus the loop is called 1/8 BPS. If the contour C lies in a two-dimensional plane, the number of supersymmetries again doubles and so on. Therefore this construction guarantees that a curve in $\mathbb{R}^1$ is 1/2 BPS, in $\mathbb{R}^2$ it is 1/4 BPS, in $\mathbb{R}^3$ it is 1/8 BPS and in $\mathbb{R}^4$ it is 1/16 BPS.

One can explicitly check that the VEV of this class of Wilson loops is trivial

$$\langle W_Z[C]\rangle = 1\,. \tag{3.20}$$

In the original work of Zarembo this has been checked at weak coupling at order λ^2 for a general curve. The basic ingredient in this calculation is the equality of the scalar and the vector propagator in Feynman gauge. For the circle and a line this result was also confirmed from an AdS calculation in the original work (minimal surface vanishes). In that paper it was conjectured that planar Wilson loops, which preserve 1/4 of the original supersymmetries do not receive quantum corrections, which was proven in [71] and [72]. The absence of quantum corrections for the case of a general Wilson loop in the Zarembo construction was finally proven in [73] on the string theory side of the correspondence.

3.1.2 The DGRT construction

In this Section we will review the family of supersymmetric Wilson loops introduced in [74, 75] by Drukker, Giombi, Ricci and Trancanelli. These operators are called *DGRT Wilson loops* and they are Wilson loops which are restricted to S^3. These loops are similar to the ones constructed by Zarembo, but their expectation values, in general, are complicated functions of g_{YM} and N. They may be viewed as generalizations of the 1/2 BPS circle.

The Zarembo construction can be associated to a topological twist of $\mathcal{N}=4$ SYM, where one identifies an $SO(4)$ subgroup of the $SO(6)$ R-symmetry group with the Euclidean Lorentz group. Under this twist four of the scalars become a space-time vector $M_I^\mu \Phi^I$ that modify the gauge connection. The simplest way to determine the new class of operators, is by considering a different twist, where three of the scalars are transformed into a self-dual tensor $\phi_{\mu\nu} = \sigma^i_{\mu\nu} M^i{}_I \Phi^I$ and the modified gauge connection becomes

$$A_\mu \to A_\mu + i\phi_{\mu\nu} x^\nu \,. \tag{3.21}$$

where the matrix $M^i{}_I$ is a 3×6 matrix with $M^1{}_1 = M^2{}_2 = M^3{}_3 = 1$ and all the other entries zero. The tensor $\sigma^i_{\mu\nu}$ are related to the invariant one-forms on S^3

$$\begin{aligned}
\sigma_1^{R,L} &= 2[\pm(x^2dx^3 - x^3dx^2) + (x^4dx^1 - x^1dx^4)] \\
\sigma_2^{R,L} &= 2[\pm(x^3dx^1 - x^1dx^3) + (x^4dx^2 - x^2dx^4)] \\
\sigma_3^{R,L} &= 2[\pm(x^1dx^2 - x^2dx^1) + (x^4dx^3 - x^3dx^4)]
\end{aligned} \tag{3.22}$$

where σ_i^R are the right one-forms and σ_i^L are the left one-forms. Choosing the scalar coupling to rely on the right-forms

$$\sigma_i^R = 2\sigma^i_{\mu\nu} x^\mu dx^\nu \,, \tag{3.23}$$

the Wilson loop can be rewritten in the following way

$$\begin{aligned}
W_{\mathrm{DGRT}}[C] =& \frac{1}{\dim_{\mathcal{R}}} \mathrm{Tr}_{\mathcal{R}} \mathcal{P} \exp\left[\oint_C \left(iA + \frac{1}{2}\sigma_i^R M^i{}_I \Phi^I\right)\right] \\
=& \frac{1}{\dim_{\mathcal{R}}} \mathrm{Tr}_{\mathcal{R}} \mathcal{P} \exp\left[\oint_C dx^\mu (iA_\mu - \sigma^i_{\mu\nu} x^\nu M^i{}_I \Phi^I)\right] \,.
\end{aligned} \tag{3.24}$$

One could try to couple the remaining scalars Φ^4, Φ^5 and Φ^6 with the left-form σ_i^L, but it turns out that the resulting Wilson loop is not supersymmetric. The operator $W_{\mathrm{DGRT}}[C]$ will be supersymmetric only if we restrict the loop to be on a three-dimensional sphere embedded in $\mathbb{R}^4$ with unit radius[1].

The supersymmetry variation of the Wilson loop (3.7), in the 4+6-dimensional notation, is then proportional to

$$\delta_\epsilon W_{\mathrm{DGRT}}[C] \propto (i\dot{x}^\mu \gamma_\mu - \sigma^i_{\mu\nu} \dot{x}^\mu x^\nu M^i_I \rho^I \gamma^5)\epsilon(x) \tag{3.25}$$

where γ_μ and ρ^I are respectively the gamma matrices of $SO(4)$ and $SO(6)$, the Poincaré and R-symmetry groups, and they are taken to commute with each-other. The quantity $\epsilon(x)$ is the conformal Killing spinor given in $\mathbb{R}^4$ by two arbitrary constant 16-component Majorana-Weyl spinors as

$$\epsilon(x) = \epsilon_0 + x^\mu \gamma_\mu \epsilon_1 \tag{3.26}$$

[1] In general it is simple to generalize to other radii by putting the radius factors where they are required by dimensionality.

where ϵ_0 is related to the Poincaré supersymmetries while ϵ_1 is related to the superconformal ones.

Requiring that the variation (3.25) vanishes for arbitrary curves on S^3 leads to the two equations

$$\begin{aligned} \gamma_{\mu\nu}\epsilon_1 + i\sigma^i_{\mu\nu}\rho^i\gamma^5\epsilon_0 = 0 \\ \gamma_{\mu\nu}\epsilon_0 + i\sigma^i_{\mu\nu}\rho^i\gamma^5\epsilon_1 = 0 \end{aligned} \tag{3.27}$$

Solving the equations (3.27) means to decompose the ϵ's into their chiral and anti-chiral part and count how many equations are independent. For a generic curve on S^3 we have only two independent constraints for the ϵ's. Notice that in singling out three of the scalars the R-symmetry group $SU(4)$ is broken down to $SU(2)_A \times SU(2)_B$,where $SU(2)_A$ corresponds to rotations of Φ^1, Φ^2, Φ^3 while $SU(2)_B$ rotates Φ^4, Φ^5 and Φ^6. The Wilson loops (3.24) preserve the two supercharges

$$\bar{\mathcal{Q}}^a = \epsilon^{\dot{\alpha}\dot{a}}(\bar{Q}^a_{\dot{\alpha}\dot{a}} - \bar{S}^a_{\dot{\alpha}\dot{a}}) \tag{3.28}$$

where $\dot{a}$ and a are respectively $SU(2)_A$ and $SU(2)_B$ indices. Then an arbitrary Wilson loop on S^3 preserves 1/16 of the original supersymmetries and it is called 1/16 BPS.

For special curves, when there are extra relations between the coordinates and their derivatives, there will be more independent solutions of (3.27) and the Wilson loops will preserve more supersymmetries.

3.1.2.1 The submanifold S^2

An infinite class of operators with a lot of interesting features is obtained restricting the loops to lie on a great S^2 inside S^3 (the 2-sphere is defined by the condition $x^4 = 0$). By definition, the one-forms of the maximal S^2 are no longer independent

$$\sigma^L_i = -\sigma^R_i = -2\epsilon_{ijk}x^k dx^k\,, \tag{3.29}$$

then the Wilson loop, for instance in the fundamental representation of the gauge group, explicitly becomes:

$$W[C] = \frac{1}{N}\mathrm{Tr}\mathcal{P}\exp\oint_C d\tau\left[i\dot{x}^\mu A_\mu - \epsilon_{\mu\nu\rho}\dot{x}^\mu x^\nu \Phi^\rho\right]. \tag{3.30}$$

Using the relation between the one-forms, one can check directly that the condition $\delta_\epsilon W_{\mathrm{DGRT}}[C] = 0$ (3.25) is solved not only by the antichiral spinors but also by spinors with positive chirality that can be combined as follows

$$i\gamma_{ij}\epsilon_1 = \epsilon_{ijk}\rho_i\gamma^5\epsilon_0 \tag{3.31}$$

At variance with the general S^3 case, we see that the constraints are not chiral and hence the supersymmetries are doubled. The generic Wilson loop on S^2 will therefore gives a 1/8 BPS operator. The four supercharges may be written explicitly as

$$\mathcal{Q}^a = (i\sigma_2)^{\alpha}{}_{\dot{a}}(\bar{Q}^{\dot{a}a}_{\alpha} + \bar{S}^{\dot{a}a}_{\alpha})\,, \qquad \bar{\mathcal{Q}}^a = \epsilon^{\dot{\alpha}\dot{a}}(\bar{Q}^a_{\dot{\alpha}\dot{a}} - \bar{S}^a_{\dot{\alpha}\dot{a}}) \tag{3.32}$$

where σ_i are the Pauli matrices.

In the following we discuss some examples of special loops inside S^2 preserving some extra supersymmetries.

The great circle (equator)

The 1/2 BPS circular Wilson loop is included in the DGRT construction as a special example, this is simply a great circle on the S^2 (in the S^3 case is the same). Consider a circle in the (1,2)-plane with parametrization:

$$x^{\mu}(\tau) = \{\cos\tau, \sin\tau, 0, 0\} \tag{3.33}$$

The invariant one-form (3.29) are

$$\sigma_i^R = 2\{0, 0, 1\}d\tau\,, \tag{3.34}$$

then the corresponding Wilson loop is coupled only with Φ^3

$$W[C_{\text{eq.}}] = \frac{1}{N}\text{Tr}\mathcal{P}\exp\left[\oint_{C_{\text{eq.}}} d\tau(i\dot{x}^{\mu}A_{\mu} + \Phi^3)\right]\,. \tag{3.35}$$

As a consequence, the relation (3.31) leads to the single constraint

$$\rho^3\gamma^5\epsilon_0 = i\gamma_{12}\epsilon_1\,, \tag{3.36}$$

and therefore the loop preserves 16 (8 chiral and 8 anti-chiral) supercharges and is indeed a 1/2 BPS operator. Using (3.36) we may write down the sixteen supercharges as

$$\mathcal{Q}^A = i\gamma_{12}Q^A + (\rho^3 S)^A\,, \qquad \bar{\mathcal{Q}}^A = i\gamma_{12}\bar{Q}_A - (\rho^3\bar{S})_A\,. \tag{3.37}$$

where $A = 1, ..., 4$ and for simplicity the Lorentz indices are omitted.

Latitude

More generally we can take the loop to be a non-maximal circle, *i.e.* a latitude of the S^2. A latitude with angle θ_0 is parametrized as follows

$$x^{\mu}(\tau) = \{\sin\theta_0\cos\tau, \sin\theta_0\sin\tau, \cos\theta_0, 0\} \tag{3.38}$$

The scalar coupling can be computed using the (3.29) and we have

$$\sigma_i^R = 2\sin\theta_0\{-\cos\theta_0\cos\tau, -\cos\theta_0\sin\tau, \sin\theta_0\}d\tau, \tag{3.39}$$

leading to the corresponding Wilson loop

$$W[C_{\text{lat.}}] = \frac{1}{N}\text{Tr}\mathcal{P}\exp\left[\oint_{C_{\text{lat.}}} d\tau\left(i\dot{x}^\mu A_\mu - \sin\theta_0\cos\theta_0(\cos\tau\Phi^1 + \sin\tau\Phi^2) + \sin^2\theta_0\Phi^3\right)\right]. \tag{3.40}$$

When $\theta_0 = \pi/2$, the loop is a 1/2 BPS maximal circle and when $\theta_0 = 0$ the curve reduces to a point (the north pole). This family of loops is essentially the same as the operators considered in [76]: they are related by a conformal transformation.

As can be seen from (3.39), such an operator couples to three scalars; it can be shown that the supersymmetry equations will give only two independent constraints. Indeed, the two supersymmetry conditions are the following

$$\begin{aligned}\cos\theta_0(\gamma_{12}+\rho_{12})\epsilon_1 =& 0\,,\\ (i\gamma_{12}+\gamma_3\rho^2\gamma^5\cos\theta_0(\gamma_{23}+\rho_{23}))\epsilon_1 =& \rho^2\gamma^5\epsilon_0\,.\end{aligned} \tag{3.41}$$

If $\cos\theta_0 \neq 0$, one has two independent constraints and the loop preserves 1/4 of the supersymmetries. Thus the Wilson loop preserves the following eight supercharges

$$\begin{aligned}\mathcal{Q}^a_{(1)} =& (i\sigma_2)^\alpha{}_{\dot{a}}(\bar{Q}^{\dot{a}a}_\alpha + \bar{S}^{\dot{a}a}_\alpha)\,, \qquad \bar{\mathcal{Q}}^a_{(1)} = \epsilon^{\dot{\alpha}\dot{a}}(\bar{Q}^a_{\dot{\alpha}\dot{a}} - \bar{S}^a_{\dot{\alpha}\dot{a}})\\ \mathcal{Q}^a_{(2)} =& \frac{1}{\sin\theta_0}(\sigma_3\epsilon)^{\dot{\alpha}\dot{a}}(\bar{Q}^a_{\dot{\alpha}\dot{a}} - \bar{S}^a_{\dot{\alpha}\dot{a}}) + \cot\theta_0(i\sigma_2)^\alpha{}_{\dot{a}}(\bar{Q}^{\dot{a}a}_\alpha - \bar{S}^{\dot{a}a}_\alpha)\\ \mathcal{Q}'^a_{(2)} =& \frac{1}{\sin\theta_0}(\sigma_1)^\alpha{}_{\dot{a}}(\bar{Q}^{\dot{a}a}_\alpha + \bar{S}^{\dot{a}a}_\alpha) + \cot\theta_0\epsilon^{\dot{\alpha}\dot{a}}(\bar{Q}^a_{\dot{\alpha}\dot{a}} + \bar{S}^a_{\dot{\alpha}\dot{a}})\end{aligned} \tag{3.42}$$

Two longitudes (wedge)

Consider a loop made of two arcs connected on the poles of the sphere S^2 with an arbitrary longitude angle δ. We can parameterize the loop in the following way

$$\begin{aligned}x^\mu_l =& \{\sin\tau, 0, \cos\tau, 0\}\,, & 0\leq\tau\leq\pi\,,\\ x^\mu_r =& \{-\cos\delta\sin\tau, -\sin\delta\sin\tau, \cos\delta, 0\}\,, & \pi\leq\tau\leq 2\pi\,.\end{aligned} \tag{3.43}$$

where l and r denote the left and right edge of the loop. The scalar coupling can be computed using the (3.29) and we have

$$\begin{aligned}\sigma^R_{i\,(l)} =& 2\{0,1,0\}d\tau\,,\\ \sigma^R_{i\,(r)} =& 2\{\sin\delta, -\cos\delta, 0\}d\tau\,.\end{aligned} \tag{3.44}$$

then the corresponding Wilson loop is composed by the following two operators

$$\begin{aligned}W[C^{(l)}_{\text{wed.}}] =& \frac{1}{N}\text{Tr}\mathcal{P}\exp\left[\oint_{C_{\text{eq.}}} d\tau(i\dot{x}^\mu A_\mu + \Phi^2)\right]\,,\\ W[C^{(r)}_{\text{wed.}}] =& \frac{1}{N}\text{Tr}\mathcal{P}\exp\left[\oint_{C_{\text{eq.}}} d\tau(i\dot{x}^\mu A_\mu + \sin\delta\Phi^1 - \cos\delta\Phi^2)\right]\,.\end{aligned} \tag{3.45}$$

Notice that such an operator is related by a stereographic projection to a Wilson loop of the type invariant under Q [70] given by two semi-infinite rays on the plane with an opening angle δ (cusped Wilson loop). We will see that such kind of loops have a lot of interesting properties in the section 4.2 and in the rest of the thesis.

Each arc, being (half) a maximal circle, is 1/2 BPS and will produce a single constraint. The system, as long as $\sin\delta \neq 0$, has to satisfy the following equations

$$\rho^2\gamma^5\epsilon_0 = i\gamma_{31}\epsilon_1\,, \qquad \rho^1\gamma^5\epsilon_0 = i\gamma_{23}\epsilon_1\,. \tag{3.46}$$

The loop will preserve 1/4 of the supersymmetries: when $\sin\delta = 0$, the second equation in (3.46) disappears and the loop becomes 1/2 BPS (for $\delta = 0$, the loop is the maximal circle and for $\delta = \pi$, the loop is made of two coincident half circles with opposite orientations).

Thus the eight supercharges which annihilate the Wilson loop made of two longitudes are

$$\begin{aligned} \mathcal{Q}^a_{(1)} =& (i\sigma_2)^{\alpha}{}_{\dot{a}}(Q^{\dot{a}a}_{\alpha} + S^{\dot{a}a}_{\alpha})\,, \qquad & \bar{\mathcal{Q}}^a_{(1)} = \epsilon^{\dot{\alpha}\dot{a}}(\bar{Q}^a_{\dot{\alpha}\dot{a}} - \bar{S}^a_{\dot{\alpha}\dot{a}}) \\ \mathcal{Q}^a_{(2)} =& (\sigma_1)^{\alpha}{}_{\dot{a}}(Q^{\dot{a}a}_{\alpha} - S^{\dot{a}a}_{\alpha})\,, \qquad & \bar{\mathcal{Q}}^a_{(2)} = (\sigma_3\epsilon)^{\dot{\alpha}\dot{a}}(\bar{Q}^a_{\dot{\alpha}\dot{a}} + \bar{S}^a_{\dot{\alpha}\dot{a}}) \end{aligned} \tag{3.47}$$

Starting from (3.25), one can construct other families of supersymmetric Wilson loops which preserve more supersymmetries for particular contours. These contours are: Hopf fibers, curves in the Hopf base, curves on a torus and curves close to points.

3.2 Supersymmetric Wilson loops in ABJ(M)

As we have seen in Section 2.1.5 and 2.2, ABJ(M) theory provides an exciting arena where studying the duality AdS_4/CFT_3. In this theory it is possible to define Wilson loop operators, which in the dual string theory are given by semi-classical string surfaces [66, 67]. The most symmetric string of this type preserves half of the supercharges of the vacuum and its dual operator in the field theory must be an 1/2 BPS Wilson loop.

The definition of BPS Wilson loops in ABJ(M) theory is more complex than the four-dimensional case. Bosonic Wilson loop operators constructed initially in $\mathcal{N} = 2, 3$ theories by Gaiotto and Yin (GY) in [77] and then studied in ABJ(M) in [78, 79, 80], preserve only 1/6 of the supercharges and are therefore not viable candidates to be the dual of this classical string. In [81], Drukker and Trancanelli (DT) proposed a new type of Wilson loop that couples both to the bosonic and fermionic fields of the theory. The construction of this operator uses the quiver structure of the theory and turns out to be 1/2 BPS. This operator is dual to the half-BPS string solution found in [78, 80].

In ABJ(M) theory there are more general BPS DT-type Wilson loops, lying along arbitrary curves and preserving fewer supersymmetries. These loops have been proposed in [82] and they generalize the straight line and the circle constructed in [81]: they can

be considered the analogous of the Zarembo and DGRT loops in three-dimensional $\mathcal{N}=6$ super Chern-Simons-matter theories. They are also related to several quantities of interest as studied in [83, 84, 85, 86].

3.2.1 The 1/6 BPS construction

In order to determine the supersymmetric Wilson loop in the AdS/CFT framework, we restrict the theory in the ABJM case. Thus the theory has two gauge groups of equal rank N and opposite level κ and $-\kappa$.

In ABJM there are quite a few possibilities to construct gauge-invariant Wilson loop operators: one choice would simply be the standard Wilson loop operator in one of the gauge groups. As in the $\mathcal{N}=4$ SYM case, such a Wilson loop is not supersymmetric. In the four dimensional theory a supersymmetric Wilson loop couples also to an adjoint scalar field (3.5). Here there are no adjoint fields, but one can use two bi-fundamental fields to construct a composite in the adjoint

$$W_{\mathcal{R}}[C]=\frac{1}{\dim_R}\mathrm{Tr}_{\mathcal{R}}\mathcal{P}\exp\left[\int_C d\tau\left(i\dot{x}^\mu A_\mu+\frac{2\pi}{\kappa}|\dot{x}|M_J^I C_I\bar{C}^J\right)\right] \tag{3.48}$$

where M_J^I is a matrix whose properties will be determined by supersymmetry.

Using the supersymmetry transformation (2.48), one can consider the supersymmetry variation of the Wilson loop (3.48) and impose that it vanishes for a suitable choice of the parameter θ. One then finds the following condition

$$\begin{aligned}\delta_\theta W_{\mathcal{R}}\sim\theta^{IJ\alpha}[-\dot{x}_\mu\sigma^\mu_{\alpha\beta}\delta_I^P+|\dot{x}|\delta_{\alpha\beta}M_I^P]C_P(\psi_J)^\beta\\ +\epsilon_{IJKL}\theta^{IJ\alpha}[\dot{x}_\mu\sigma^\mu_{\alpha\beta}\delta_P^K+|\dot{x}|\delta_{\alpha\beta}M_P^K](\bar{\psi}^L)^\beta\bar{C}^P=0\end{aligned} \tag{3.49}$$

For a supersymmetric loop both terms in the above have to vanish separately.

Let us consider a straight space-like Wilson line: it turns out that this Wilson line operator is invariant under two of the 12 Poincaré supersymmetries and two of the 12 superconformal supersymmetries, *i.e.* the loop is 1/6 BPS. Under a conformal transformation a line will be mapped to a circle, which will therefore posses the same number of supersymmetries. The conformal transformation mapping the line to the circle mixes the super-Poincaré and superconformal charges, hence the circular Wilson loop is invariant under a linear combination of Q and S.

In (3.48) we choose one of the gauge groups, but a similar operator $\hat{W}_{\mathcal{R}}[C]$ exists also in the other group[2]. In that case the scalar bilinear will be in the opposite order. More generally, one can take any combination of the two Wilson loops in any representation of each of the gauge groups. It turns out with explicit computations in planar perturbation

[2]In the ABJ case the rank of the two groups are different then we will have two operators $W_{\mathcal{R}_N}$ and $\hat{W}_{\mathcal{R}_M}$ depending on different representations of the gauge groups.

theory, that the operator identifiable with appropriate Type IIA fundamental string configurations is the sum of W and $\hat{W}$ ([78, 80]).

The puzzling fact is that this operator, as we have seen, preserve only 4 supercharges but a fundamental string ending along a straight line on the boundary of AdS_4 and localized on $\mathbb{CP}^3$ preserves 12 supercharges. In order to match with the gauge theory observable one has to smear the string over a $\mathbb{CP}^1$, breaking indeed the supersymmetry down to 1/6. But the question remains what is the gauge theory dual to a localized fundamental string. The solution to this problem will be the argument of the next section.

3.2.2 The Drukker-Trancanelli construction

The central idea of [81] to construct 1/2 BPS lines and circles is to embed the natural gauge connection of $U(N) \times U(M)$ of ABJ into a superconnection of the form

$$\mathcal{L}(\tau) \equiv -i \begin{pmatrix} i\mathcal{A} & \sqrt{\frac{2\pi}{k}}|\dot{x}|\eta_I \bar{\psi}^I \\ \sqrt{\frac{2\pi}{k}}|\dot{x}|\psi_I \bar{\eta}^I & i\hat{\mathcal{A}} \end{pmatrix} \quad \text{with} \quad \begin{cases} \mathcal{A} \equiv A_\mu \dot{x}^\mu - \frac{2\pi i}{k}|\dot{x}| M_J{}^I C_I \bar{C}^J \\ \hat{\mathcal{A}} \equiv \hat{A}_\mu \dot{x}^\mu - \frac{2\pi i}{k}|\dot{x}| \hat{M}_J{}^I \bar{C}^J C_I, \end{cases} \tag{3.50}$$

belonging to the super-algebra of $U(N|M)$. The coordinate x^μ parametrizes the curve along which the loop operator is supported and $M_J{}^I$, $\hat{M}_J{}^I$, η_I^α and $\bar{\eta}_\alpha^I$ parameterize the possible local couplings. A lot of the form of $\mathcal{L}$ is dictated by dimensional analysis and by the index structure of the fields. In three dimensions the scalars have dimension 1/2, so they should appear as bilinears, which are in the adjoint and therefore enter in the diagonal blocks together with the gauge fields. The fermions have dimension 1 and should appear linearly. Since they transform in the bi-fundamental, they are naturally placed in the off-diagonal entries of the matrix. Note that η_I^α and $\bar{\eta}_\alpha^I$ are Grassmann even, so that the off-diagonal blocks of $\mathcal{L}$ are Grassmann odd and $\mathcal{L}$ is a supermatrix[3]. The above supermatrix $\mathcal{L}$ is in general $(N+M) \times (N+M)$: the upper-left block is $N \times N$ and the lower-right is $M \times M$.

For a given path C, it is possible to compute the holonomy of the superconnection (3.50)

$$W[C] \equiv \mathcal{P} \exp\left(i \int_C d\tau \, \mathcal{L}(\tau) \right). \tag{3.51}$$

When the contour is a straight-line , all the couplings can be chosen to be independent of τ in order to preserve the invariance under translations along the line. Further restrictions on scalar and fermionic couplings follow from R−symmetry and supersymmetry requirements. Indeed the requirement of having an unbroken $SU(3)$ R-symmetry restricts the coupling to be of the form

$$\eta_I^\alpha = n_I \eta^\alpha \,, \quad \bar{\eta}_\alpha^I = \bar{n}^I \bar{\eta}_\alpha \,, \quad M_J{}^I = p_1 \delta_J^I - 2 p_2 n_j \bar{n}^I \,, \quad \hat{M}_J^I = q_1 \delta_J^I - 2 q_2 n_j \bar{n}^I \tag{3.52}$$

[3]The origin of the superconnection was also investigated from the point of view of the low- energy dynamics of heavy W-bosons in [87].

where n_I and $\bar{n}^I$ are two complex conjugated vectors which transform in the fundamental and anti-fundamental representation and determine the embedding of the $SU(3)$ subgroup in $SU(4)$. By rescaling η^α and $\bar{\eta}_\alpha$, we can always choose $n_I \bar{n}^I = 1$. The parameters p_1 and q_i in the definition of M and $\hat{M}$ instead control the eigenvalues of the two matrices.

The free parameters appearing in (3.52) can be then constrained by imposing that the resulting Wilson loop is globally supersymmetric. Actually, imposing $\delta_{\text{susy}}\mathcal{L}(\tau) = 0$ gives rise to loop operators which are merely bosonic ($\eta = \bar{\eta} = 0$) and at most 1/6 BPS. The weaker condition of invariance under supersymmetry up to a super-gauge transformation brings out the 1/2 BPS solution

$$\delta_{\text{susy}}\mathcal{L}(\tau) = \partial_\tau G + i\{\mathcal{L}, G] \tag{3.53}$$

with G an anti-diagonal supermatrix.

The condition (3.53) for the anti-diagonal entries first constrains the form of the spinors η and $\bar{\eta}$ to obey the two conditions

$$(\dot{x}^\mu \gamma_\mu)_\alpha{}^\beta = \frac{1}{(\eta\bar{\eta})}|\dot{x}|(\eta^\beta \bar{\eta}_\alpha + \eta_\alpha \bar{\eta}^\beta)\,, \qquad (\eta^\beta \bar{\eta}_\alpha + \eta_\alpha \bar{\eta}^\beta) = (\eta\bar{\eta})\delta_\alpha^\beta \tag{3.54}$$

and then fixes the value of the parameters p_i and q_i appearing in (3.52) to 1. The requirement (3.53) for the diagonal entries does not yield new conditions, simply fixing the normalization

$$\eta\bar{\eta} = 2i \tag{3.55}$$

In particular the vectors n_I and $\bar{n}^I$ continue to be unconstrained.

Combining the supersymmetry transformation (2.48) and the condition (3.53), one can find that a Wilson loop lying on a straight line preserve 6 Poincaré supercharges and 6 superconformal supercharges. Thus the loop is 1/2 BPS (the same for the circle).

For (finite) closed path one has to carefully consider the boundary conditions obeyed by the gauge functions to obtain a gauge invariant object. For instance, in the circle case one has to take the trace of (3.51). For an infinite open circuit, such as the straight line, the naive statement that the fields vanish when $\tau = \pm\infty$ allows two possible supersymmetric operators

$$\begin{aligned} \mathcal{W}_- =& \frac{1}{N-M}\text{Str}\left[\mathcal{P}\text{exp}\left(-i\int d\tau \mathcal{L}(\tau)\right)\right] \\ \mathcal{W}_+ =& \frac{1}{N+M}\text{Tr}\left[\mathcal{P}\text{exp}\left(-i\int d\tau \mathcal{L}(\tau)\right)\right]. \end{aligned} \tag{3.56}$$

In the following, if not specified, we will consider the second possibility, since it is connected through a conformal transformation to BPS closed loops.

Relation with $\mathcal{W}_{1/6}$

The purely bosonic 1/6 BPS circle, defined in Section 3.2.1, is obtained by choosing $\eta_I(\tau) = \bar{\eta}^I(\tau) = 0$: it requires, in turn, a different choice of the bosonic matrices *i.e* ${M_J}^I = {\hat{M}_J}^I = \mathrm{diag}(-1,-1,1,1)$. In spite of the different BPS degree, the 1/2 BPS circle is cohomologically equivalent at classical level to the 1/6 BPS [81]. The key point, in order to establish the equivalence of the two observables, is to notice that the difference between the DT Wilson loop $\mathcal{W}^{1/2}_{\mathcal{R}}$ and the 1/6 BPS Wilson loop $\mathcal{W}^{1/6}_{\mathcal{R}}$ can be cast into a Q-exact term

$$\dim_{\mathcal{R}} \mathcal{W}^{1/2}_{\mathcal{R}} - \left(\dim_{\mathcal{R}_N} \mathcal{W}^{1/6}_{\mathcal{R}_N} + \dim_{\mathcal{R}_M} \hat{\mathcal{W}}^{1/6}_{\mathcal{R}_M}\right) = QV. \tag{3.57}$$

Here Q is a particular supercharge that generates transformations leaving invariant both operators. Its explicit expression and the precise form of V are reported in [81]. The relation (3.57) implies that the expectation values of the two loops are equal

$$\langle \mathcal{W}^{1/2}_{\mathcal{R}} \rangle = \frac{1}{\dim_{\mathcal{R}}} \left(\dim_{\mathcal{R}_N} \langle \mathcal{W}^{1/6}_{\mathcal{R}_N} \rangle + \dim_{\mathcal{R}_M} \langle \hat{\mathcal{W}}^{1/6}_{\mathcal{R}_M} \rangle\right). \tag{3.58}$$

Actually the presence of quantum infinities needs a regularization procedure, that could potentially affect the classical cohomological equivalence. On the other hand it is well known that in pure Chern-Simons theory Wilson loops depend in a very specific way from a regularization choice, the so called *framing* [88], and a global phase appears in the quantum evaluation, parameterizing the different possibilities. The non-perturbative evaluation of the BPS Wilson loops in ABJ(M) seems to display a similar phenomenon.

3.2.2.1 Generalization for an arbitrary contour

As in the four-dimensional case one can construct two families of supersymmetric Wilson loops for arbitrary shape generalizing the straight line and the circle constructed in [81]. The strategy is to derive a general set of algebraic and differential conditions that correspond to preserve locally a fraction of supersymmetry. Then one have to impose that solutions of these constraints can be combined into a conformal Killing spinor,

$$\bar{\Theta}^{IJ} = \bar{\theta}^{IJ} - (x \cdot \gamma)\bar{\epsilon}^{IJ} \tag{3.59}$$

with $\bar{\theta}^{IJ}$ and $\bar{\epsilon}^{IJ}$ constant spinors. In this Section we will briefly review the results of [82].

Supersymmetric Wilson loop on $\mathbb{R}^3$ (Zarembo-like loops)

The first construction concerns a family of Wilson loops of arbitrary shape, which preserve at least a super-Poincaré charge, *i.e.* a supercharge with $\bar{\epsilon}^{IJ} = 0$. In this

sense these operators can be viewed as the three dimensional companion of the loops discussed by Zarembo in [70]. They can be also considered a generalization of the BPS straight-line constructed by Drukker and Trancanelli in [81].

One can make the following ansatz for the reduced vector couplings (3.52)

$$\bar{n}^I = (\eta \bar{s}^I)\,, \qquad n_I = (s_I \eta\eta) \tag{3.60}$$

Here $\bar{s}$ are four τ-independent spinors and η and $\bar{\eta}$ are determined by (3.54). The normalization condition $\bar{n}^I n_I = 1$ is equivalent to the following completeness relation on the spinors s and $\bar{s}$

$$\bar{s}^I_\beta s^\alpha_I = \frac{1}{2i}\delta^\alpha_\beta \tag{3.61}$$

The general solution of the supersymmetry conditions can be written as follows

$$\bar{\Theta}^{IJ} = \bar{\theta}^{IJ} = \bar{v}^J \bar{s}^I - \bar{v}^I \bar{s}^J\,, \qquad \text{with} \quad \bar{v}^I s_{I\beta} = 0 \tag{3.62}$$

It follows that these loops are in general 1/12 BPS.

Summarizing this family of supersymmetric Wilson loops of arbitrary shape on $\mathbb{R}^3$ has the following couplings

$$\begin{gathered} \eta^\alpha_I = i s^\beta_I \left(\mathbb{1} + \frac{\dot{x}\cdot\gamma}{|\dot{x}|}\right)^\alpha_\beta, \qquad \bar{\eta}^I_\alpha = i \left(\mathbb{1} + \frac{\dot{x}\cdot\gamma}{|\dot{x}|}\right)^\beta_\alpha \bar{s}^I_\beta, \\ M_K{}^J = \hat{M}_K{}^J = \left(\delta^J_K - 2i s_K \bar{s}^J - 2i \frac{\dot{x}^\mu}{|\dot{x}|} s_K \gamma_\mu \bar{s}^J\right), \end{gathered} \tag{3.63}$$

and which are invariant under the Poincarè supercharges (3.62).

Supersymmetric Wilson loop on S^2 (DGRT-like loops)

The second family of Wilson loops is defined for an arbitrary curve on the unit sphere S^2. The central idea is again a guess for the reduced vector couplings n_I and $\bar{n}_I$. Specifically one shall consider a deformation of the ansatz (3.60)

$$\bar{n}^I = r(\eta U \bar{s}^I) \qquad \text{and} \qquad n_I = \frac{1}{r}(s_I U^{-1} \bar{\eta}), \tag{3.64}$$

where s^I_α and $\bar{s}^I_\alpha$ are again four τ-independent spinors obeying the completeness relation (3.61). The parameter r is a function of τ and the matrix U is an element of $SU(2)$ constructed with the coordinates $x^\mu(\tau)$ of the circuit, namely

$$U = \cos\alpha\ \mathbb{1} + i \sin\alpha\ (x^\mu \gamma_\mu), \tag{3.65}$$

with α free constant parameter.

The preserved supercharges can be parametrized as follows

$$\bar{\Theta}^{IJ} = [\cos\alpha\, \mathbb{1} + i \sin\alpha\ (x^\mu \gamma_\mu)]\bar{\theta}^{IJ} = U\bar{\theta}^{IJ}. \tag{3.66}$$

It follows that these loops are in general 1/6 BPS.

Summarizing this family of supersymmetric Wilson loops of arbitrary shape on S^2 has coupling as follows

$$\begin{aligned}
\eta_I^\beta =& \frac{i}{r_0} e^{\frac{i}{2}(\sin 2\alpha)s} \left[s_I (\cos\alpha\ \mathbb{1} - i \sin\alpha\ (x^\mu \gamma_\mu)) \left(\mathbb{1} + \frac{\dot{x}\cdot\gamma}{|\dot{x}|} \right) \right]^\beta , \\
\bar{\eta}_\beta^I =& i r_0 e^{-\frac{i}{2}(\sin 2\alpha)s} \left[\left(\mathbb{1} + \frac{\dot{x}\cdot\gamma}{|\dot{x}|} \right) (\cos\alpha\ \mathbb{1} + i \sin\alpha\ (x^\mu \gamma_\mu))\, \bar{s}^I \right]_\beta , \\
M_K{}^J =& \hat{M}_K{}^J = \left[\delta_K^J - 2i s_K \bar{s}^J - 2i \cos 2\alpha \left(s_K \frac{\dot{x}\cdot\gamma}{|\dot{x}|} \bar{s}^J \right) - 2i \sin 2\alpha \left(s_K \gamma^\lambda \bar{s}^J \right) \epsilon_{\lambda\mu\nu} x^\mu \dot{x}^\nu \right] .
\end{aligned} \tag{3.67}$$

Notice that for $\alpha = 0$ we recover the couplings (3.63). In this sense one can consider this class of loops as a deformation of those considered in the previous section. There is a second interesting value of α, *i.e.* $\alpha = \frac{\pi}{4}$, for which the Zarembo-like term vanishes and the scalars couple only to the invariant forms. For this value of α we also recover the 1/2 BPS circle discussed in [81]. One is then tempted to identify these operators as the three dimensional companions of the so-called DGRT loops [74, 75]. For generic α, the situation is more intricate.

3.3 Supersymmetric Wilson loops in perturbation theory

The circular Wilson loop is one of the most studied, both in $\mathcal{N} = 4$ SYM and in ABJ(M). In this Section we will derive its vev using perturbation theory, obtaining some hints for a non-perturbative analysis of the system. Since in perturbation theory we have to deal with intermediate divergencies, in the following we use to use dimensional regularization.

3.3.1 Circular Wilson loop in $\mathcal{N} = 4$ SYM

In general the vacuum expectation value (vev) of a supersymmetric Wilson loop in in perturbation theory in $\mathcal{N} = 4$ SYM is given by the following expansion

$$\langle W[C] \rangle = 1 + \frac{g_{\rm YM}^2 N}{4\pi^2} \oint_C d\tau_1\, d\tau_2 \frac{|\dot{x}(\tau_1)||\dot{x}(\tau_2)| - \dot{x}(\tau_1)\cdot\dot{x}(\tau_2)}{|x(\tau_1) - x(\tau_2)|^2} + \cdots , \tag{3.68}$$

where we have used the $\mathcal{N} = 4$ propagators of Appendix A. For a loop without cusps or self-intersections $\langle W[C] \rangle$ is finite. The explicit two-loop computation shows that a cancellation between the contributions of the scalar and vector fields occurs and similar mechanisms are expected to act at any order. The case of cusps and self-intersections has been discussed briefly in [69].

In order to compare the result with the prediction of the AdS/CFT correspondence, we are interested in the large N limit perturbative expansion. Thus we want to compute only planar diagrams at any order of the 't Hoof coupling $\lambda = g^2_{\rm YM}N$.

Consider the circular Wilson loop with unitary radius of (3.35) with parametrization (3.33). As we have seen in Section 3.1.2.1, this loop is coupled with only the scalar field Φ^3 and it is 1/2 BPS. The vev of this loop was studied in great detail by Erickson, Semenoff and Zarembo in [89]. The ultraviolet singularities cancel to order λ^2 for any smooth loop: in this particular case we observe a further cancellation, all the contribution to the vev comes from the Feynman diagrams without vertices, the so-called *ladder diagrams*. In [89], the authors conjecture that the vertex diagrams cancellation is true at any order, predicting the all-loop behavior of the vev.

Summing the planar ladder graphs

First, consider the $2n$-th order term in the Taylor expansion of the loop

$$\frac{1}{N}\int_0^{2\pi} d\tau_1 \int_0^{\tau_1} d\tau_2 ... \int_0^{\tau_{2n-1}} d\tau_{2n}\ \mathrm{Tr}\Big[\big\langle (iA_\mu(\tau_1)\dot{x}^\mu(\tau_1) + \Phi^3(\tau_1))... \\ ...(iA_\mu(\tau_{2n})\dot{x}^\mu(\tau_{2n}) + \Phi^3(\tau_{2n}))\big\rangle\Big] \tag{3.69}$$

where the τ-dependence is explicit. We are interested in all Wick contractions which represent planar diagrams. Note that for the circular loop any contraction gives the same contribution

$$\langle (iA_\mu\dot{x}^\mu + \Phi^3)^{ab}_{\tau_1}(iA_\mu\dot{x}^\mu + \Phi^3)^{cd}_{\tau_2}\rangle = \frac{g^2_{\rm YM}\delta^{ad}\delta^{bc}}{4\pi^2 N}\frac{1-\dot{x}(\tau_1)\cdot\dot{x}(\tau_2)}{|x(\tau_1)-x(\tau_2)|^2} = \frac{g^2_{\rm YM}\delta^{ad}\delta^{bc}}{8\pi^2 N} \tag{3.70}$$

Computing also the color factor given by the trace over the δ's, the sum of ladder diagrams with n propagators is

$$\frac{(\lambda/4)^n}{(2n)!}\times N_n \tag{3.71}$$

where N_n is the number of planar graphs with n internal lines and the factor $1/(2n)!$ is the result of the integrations over τ_i.

Now one have to count the number of planar graphs with n internal lines. Any such diagram with $n+1$ propagators can be uniquely decomposed as

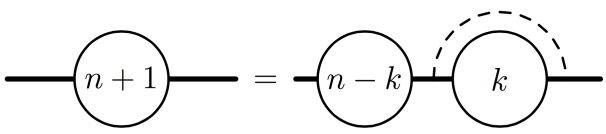

The number of such diagrams N_{n+1} satisfies the recursion relation

$$N_{n+1} = \sum_{k=0}^{n} N_{n-k} N_k \tag{3.72}$$

with $N_0 = 1$. The generating function f is defined by

$$f(z) = \sum_{n=0}^{\infty} N_n z^n \tag{3.73}$$

and satisfies $zf^2(z) = f(z) - 1$. Thus

$$f(z) = \frac{1 - \sqrt{1-4z}}{2z} = \sum_{n=0}^{\infty} \frac{(2n)!}{(n+1)!n!} z^n \quad \Rightarrow \quad N_n = \frac{(2n)!}{(n+1)!n!} \tag{3.74}$$

where the sign of the square root is chosen by requiring that f is finite for $z = 0$. Therefore from (3.71) and (3.74), the ladder contribution to the vev of circular Wilson loop is

$$\langle W[C] \rangle_{\text{lad.}} = \sum_{n=0}^{\infty} \frac{\lambda^n}{2^{2n}(n+1)!n!} = \frac{2}{\sqrt{\lambda}} I_1(\sqrt{\lambda}) \tag{3.75}$$

where I_1 is the modified Bessel function of the first order.

The result (3.75) is true at any value of λ, then one can consider the large λ behavior

$$\langle W[C] \rangle_{\text{lad.}} \xrightarrow{\lambda \to \infty} \frac{e^{\sqrt{\lambda}}}{(\pi/2)^{1/2} \lambda^{3/2}} \tag{3.76}$$

that is the same of the AdS/CFT prediction [90]

$$\langle W[C] \rangle_{\text{Sugra}} \sim e^{\sqrt{\lambda}} \tag{3.77}$$

Finally, since the Wick contraction are position-independent, the problem is mapped in a zero dimensional theory. Recalling (2.70), one can compute the vev of $W[C]$ with the following large N matrix-model

$$\langle W[C] \rangle_{\text{lad.}} = \left\langle \frac{1}{N} \text{Tr} e^M \right\rangle = \frac{1}{\mathcal{Z}} \int [dM] \frac{1}{N} \text{Tr} e^M \exp\left[-\frac{2}{g^2_{\text{YM}}} \text{Tr} M^2 \right] \tag{3.78}$$

where

$$\mathcal{Z} = \int [dM] \exp\left[-\frac{2}{g^2_{\text{YM}}} \text{Tr} M^2 \right] \tag{3.79}$$

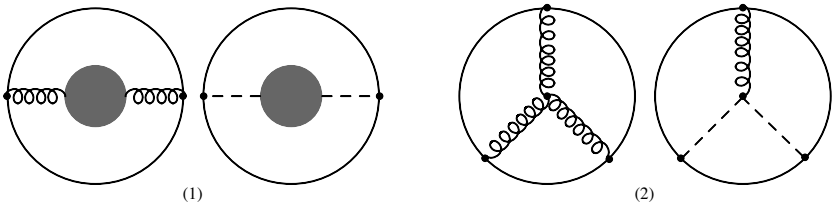

Figure 3.2: Interaction diagrams at order λ^2: (1) one-loop corrections to the gluon and scalar propagators (bubbles), (2) diagrams with one internal vertex (spiders)

The cancellation of diagrams with vertices

Now we consider, up to order λ^2, the contribution of interaction diagrams. We have two kinds of diagrams: the "*bubble*" diagrams (see Figure 3.2.(1)) and the "*spider*" diagrams (see Figure 3.2.(2)).

Expanding the loop to the second order and using the one-loop corrected propagators of Appendix A, one can find the contribution of the bubble diagrams

$$\Sigma_2 = -\frac{\lambda^2\Gamma^2(\omega-1)}{2^7\pi^{2\omega}(2-\omega)(2\omega-3)}\oint d\tau_1\, d\tau_2 \frac{|\dot{x}(\tau_1)|\,|\dot{x}(\tau_2)| - \dot{x}(\tau_1)\cdot\dot{x}(\tau_2)}{\big[(x(\tau_1)-x(\tau_2))^2\big]^{2\omega-3}}. \tag{3.80}$$

The diagrams with only an internal vertex come from the Taylor expansion of the loop to the third order contracted with the 3-gluon or the scalar-gluon vertices. Summing up these diagrams we have

$$\begin{aligned}\Sigma_3 = -\frac{g^4N^2}{4}\oint d\tau_1\, d\tau_2\, d\tau_3\, \epsilon(\tau_1\,\tau_2\,\tau_3)(|\dot{x}(\tau_1)||\dot{x}(\tau_3)| - \dot{x}(\tau_1)\cdot\dot{x}(\tau_3))\\ \times\, \dot{x}(\tau_2)\cdot\frac{\partial}{\partial x(\tau_1)}\int d^{2\omega}w\,\Delta(x(\tau_1)-w)\Delta(x(\tau_2)-w)\Delta(x(\tau_3)-w)\end{aligned} \tag{3.81}$$

where ϵ is the path ordering symbol defined by $\epsilon(\tau_1\tau_2\tau_3) = 1$ if $\tau_1 > \tau_2 > \tau_3$ and antisymmetric under any transposition of τ_i. Introducing the short-hand notation $x_i = x(\tau_i)$ and using the Feynman parameters, one can compute the integral over w and obtain

$$\begin{aligned}\Sigma_3 = \lambda^2\frac{\Gamma(2\omega-2)}{2^7\pi^{2\omega}}\int_0^1 d\alpha\, d\beta\, d\gamma\,(\alpha\beta\gamma)^{\omega-2}\delta(1-\alpha-\beta-\gamma)\oint d\tau_1\, d\tau_2\, d\tau_3\,\epsilon(\tau_1\,\tau_2\,\tau_3)\\ \times\,\frac{\big(|\dot{x}_1||\dot{x}_3| - \dot{x}_!\cdot\dot{x}_3\big)\big(\alpha(1-\alpha)\dot{x}_2\cdot x_1 - \alpha\gamma\dot{x}_2\cdot x_3 - \alpha\beta\dot{x}_2\cdot x_2\big)}{\big[\alpha\beta|x_1-x_2|^2 + \alpha\gamma|x_1-x_3|^2 + \beta\gamma|x_3-x_2|^2\big]^{2\omega-2}}\end{aligned} \tag{3.82}$$

Introducing the definition $\tau_{ij} = \tau_i - \tau_j$, in the circular case one can find

$$\Sigma_3 = \lambda^2\frac{\Gamma^2(\omega-1)}{2^{2\omega+4}\pi^{2\omega}(2\omega-3)(2-\omega)}\oint d\tau_1\, d\tau_2\,\frac{1}{[1-\cos\tau_{12}]^{2\omega-4}} + \mathcal{O}(2\omega-4). \tag{3.83}$$

and

$$\Sigma_2 = -\lambda^2 \frac{\Gamma^2(\omega-1)}{2^{2\omega+4}\pi^{2\omega}(2-\omega)(2\omega-3)} \oint d\tau_1\, d\tau_2\, \frac{1}{[1-\cos\tau_{12}]^{2\omega-3}}. \tag{3.84}$$

Then the contributions (3.83) e (3.84) cancel exactly when $2\omega = 4$

$$\langle W[C]\rangle_{\text{int.}} = \Sigma_2 + \Sigma_3 = 0\,. \tag{3.85}$$

As we will see the cancellation of interaction diagrams conjectured by Erickson, Semenoff and Zarembo will be proved by Pestun in [37]. Then the result (3.75) turn to be exact.

3.3.2 Circular Wilson loop in ABJ(M)

As we have seen in Section 3.2.2.1, we are able to construct a circular Wilson loop 1/2 BPS in ABJ(M) as in the four-dimensional case. Thus we want to compute the vacuum expectation value up to two-loop in perturbation theory.

The vev of the Wilson loop is by definition

$$\langle W_{\mathcal{R}}\rangle = \frac{1}{\dim_{\mathcal{R}}} \int \mathcal{D}[A,\hat{A},C,\bar{C},\psi,\bar{\psi}]\ \mathrm{e}^{-S_{\text{ABJ(M)}}}\ \mathrm{Tr}_{\mathcal{R}}\left[\mathrm{P}\exp\left(i\oint_C d\tau\,\mathcal{L}(\tau)\right)\right], \tag{3.86}$$

where $S_{ABJ(M)}$ stands for the action for $ABJ(M)theory$ (2.44) in euclidean space. In the following $\mathcal{R}$ is taken to be the fundamental representation ($\dim_{\mathcal{R}} = N+M$) and C to be the circle of unit radius parametrized by $x^\mu(\tau) = \{\cos\tau, \sin\tau, 0\}$.

To begin with, we shall only consider the upper left $N \times N$ block of the supermatrix appearing in (3.86). For this sector the trace in (3.86) is obviously taken in the fundamental representation $\mathbf{N}$ of $U(N)$. The expectation value of the lower diagonal block can be then obtained from the above analysis by replacing N with M. A two-loop computation requires to expand the path-exponential in (3.86) up to the fourth order. The expansion of the upper block at this order will include both contributions of bosonic and fermionic type:

$$\begin{aligned}
\mathbb{W}_{\mathbf{N}} = \mathrm{Tr}_{\mathbf{N}}\Bigg[1 &+ i\int_C d\tau_1 \mathcal{A}_1 - \int_C d\tau_{1>2}\left(\mathcal{A}_1\mathcal{A}_2 - (\eta\bar{\psi})_1(\psi\bar{\eta})_2\right)\\
&- i\int_C d\tau_{1>2>3}\left(\mathcal{A}_1\mathcal{A}_2\mathcal{A}_3 + \frac{2\pi}{k}[(\eta\bar{\psi})_1(\psi\bar{\eta})_2\mathcal{A}_3 + (\eta\bar{\psi})_1\hat{\mathcal{A}}_2(\psi\bar{\eta})_3 + \mathcal{A}_1(\eta\bar{\psi})_2(\psi\bar{\eta})_3]\right)\\
&+ \int_C d\tau_{1>2>\,3>\,4}\left(\left(\frac{2\pi}{\kappa}\right)^2(\eta\bar{\psi})_1(\psi\bar{\eta})_2(\eta\bar{\psi})_3(\psi\bar{\eta})_4 + \mathcal{A}_1\mathcal{A}_2\mathcal{A}_3\mathcal{A}_4 -\right.\\
&- \left(\frac{2\pi}{\kappa}\right)\mathcal{A}_1\mathcal{A}_2(\eta\bar{\psi})_3(\psi\bar{\eta})_4 - \left(\frac{2\pi}{\kappa}\right)\mathcal{A}_1(\eta\bar{\psi})_2\hat{\mathcal{A}}_3(\psi\bar{\eta})_4 - \left(\frac{2\pi}{\kappa}\right)(\eta\bar{\psi})_1\hat{\mathcal{A}}_2\hat{\mathcal{A}}_3(\psi\bar{\eta})_4 -\\
&\left.- \left(\frac{2\pi}{\kappa}\right)\mathcal{A}_1(\eta\bar{\psi})_2(\psi\bar{\eta})_3\mathcal{A}_4 - \left(\frac{2\pi}{\kappa}\right)(\eta\bar{\psi})_1\hat{\mathcal{A}}_2(\psi\bar{\eta})_3\mathcal{A}_4 - \left(\frac{2\pi}{\kappa}\right)(\eta\bar{\psi})_1(\psi\bar{\eta})_2\mathcal{A}_3\mathcal{A}_4\right)\Bigg].
\end{aligned} \tag{3.87}$$

In (3.87) we have introduced a shorthand notation for the circuit parameter dependence of the fields, namely $\mathcal{A}_i = \mathcal{A}(x_i)$ with $x_i = x(\tau_i)$. Above we have suppressed the spinor and $SU(4)_R$ indices ($\eta\bar{\psi} \equiv \eta_I^\alpha \bar{\psi}_\alpha^I$ and $\psi\bar{\eta} \equiv \psi_I^\alpha \bar{\eta}_\alpha^I$) and we have used that $|\dot{x}| = 1$ for our parametrization.

The explicit couplings in the circular case can be recast from (3.67) for $\alpha = \pi/4$: in particular for the bosonic couplings we have $M_J{}^I = \hat{M}_J{}^I = \text{diag}(-1, 1, 1, 1)$. and for the fermionic couplings $\eta_I(\tau)$ and $\bar{\eta}^I(\tau)$ we have the following factorized structure

$$\eta_I^\alpha = (e^{\frac{i\tau}{2}} \quad -ie^{-\frac{i\tau}{2}}) \begin{pmatrix} 1 \\ 0 \\ 0 \\ 0 \end{pmatrix} \qquad \bar{\eta}_\alpha^I = (1\ 0\ 0\ 0) \begin{pmatrix} ie^{-\frac{i\tau}{2}} \\ -e^{\frac{i\tau}{2}} \end{pmatrix}, \tag{3.88}$$

The vev of this loop was studied in great detail in [91, 92, 93] and in this Section we will review briefly the main results.

Bosonic diagrams

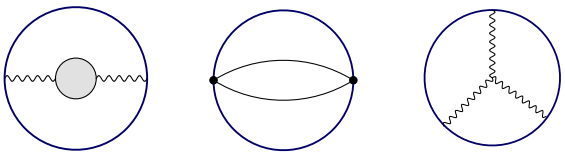

(a) B_1 (b) B_2 (c) B_3

Figure 3.3: Bosonic diagrams up to order $1/\kappa^2$.

Any diagram involving a tree-level gauge propagator ranging between two points of the circle yields zero[4]. We are working in the DRED scheme then all the tadpole-like graphs vanish. However at one-loop there are no bosonic diagrams and at two loops the terms $\mathcal{A}_1\mathcal{A}_2$ and $\mathcal{A}_1\mathcal{A}_2\mathcal{A}_3$ of (3.87) produce the three graphs in Figure 3.3.

Since the constant matrix $M_I{}^J$, governing the scalar couplings, appears quadratically in diagrams B_1 and B_2, they are identical to the those computed in [78] for the 1/6 BPS circle and we can borrow their result

$$B_1 + B_2 = \frac{\pi^2}{\kappa^2} \frac{N^2 M}{N + M}. \tag{3.89}$$

The next step is to consider the monomial $\mathcal{A}_1\mathcal{A}_2\mathcal{A}_3$. At this order only the gauge field in $\mathcal{A}$ is relevant. This graph also appears in pure Chern-Simons theory and its value

[4]This type of graphs will always contain a Levi-Civita tensor contracted with three linear dependent vectors (see propagators in Appendix A).

only depends on the topology of the loop [94]. Translated in the language relevant for ABJ(M) Wilson loops it is given by

$$B_3 = -\frac{N^3}{N+M}\frac{\pi^2}{6\kappa^2}. \tag{3.90}$$

Thus the bosonic contribution of the upper-left block (denoted by $\uparrow$) at two-loop is

$$\langle W^{(B)}[C_{\text{cir.}}]\rangle^{(2)}_{\uparrow} = B_1 + B_2 + B_3 = \frac{\pi^2}{\kappa^2(N+M)}(N^2M - \frac{N^3}{6}). \tag{3.91}$$

Now, summing up (3.91) with the contribution of the lower-right block (exchanging the gauge group ranks M and N) we find the total bosonic contribution to the vev of the circular Wilson loop

$$\begin{aligned}\langle W^{(B)}[C_{\text{cir.}}]\rangle^{(2)} =& \langle \mathcal{W}_B[C_{\text{cir.}}]\rangle^{(2)}_{\uparrow} + \langle \mathcal{W}_B[C_{\text{cir.}}]\rangle^{(2)}_{\downarrow} \\ =& -\frac{\pi^2}{6\kappa^2}(N^2+M^2-7MN)\,.\end{aligned} \tag{3.92}$$

Fermionic diagrams

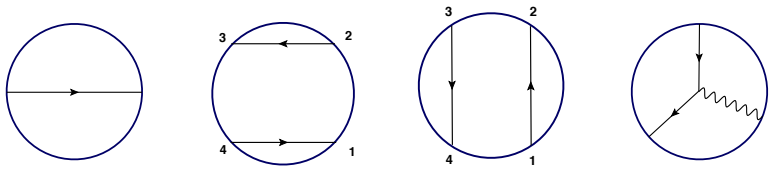

(a) F_1 (b) F_2 (c) F_3 (d) F_4

Figure 3.4: Fermionic diagrams up to order $1/\kappa^2$.

It remains to compute the diagrams which involve fermions propagating along the contour. We have three type of contributions represented in Figure 3.4: from the monomial $\bar{\psi}_1\psi_2$ we have the so-called single exchange diagram F_1; from the four fermion terms we obtains the double-exchange diagrams F_2 and F_3; finally from the monomials $\psi\bar{\psi}A$ we have the vertex diagram F_4.

The single-exchange diagram is given by

$$F_1 = \left(\frac{2\pi}{\kappa}\right)\int_0^{2\pi} d\tau_1 \int_{\tau_1}^{2\pi} d\tau_2\ \langle \text{Tr}[(\eta\bar{\psi})_1(\psi\bar{\eta})_2]\rangle = \frac{MN4^{\epsilon}\pi^{\epsilon+2}\sec(\pi\epsilon)}{\kappa\Gamma(\epsilon)} = 0 \qquad \epsilon \to 0 \tag{3.93}$$

where we have used the DRED regularization scheme in which $d = 3 - 2\epsilon$. Notice that, as in the bosonic part, the fermionic one-loop expectation value is zero.

The contour integral describing the double-exchange diagrams is given by

$$-\left(\frac{2\pi}{\kappa}\right)^2 \oint_C d\tau_{4>\ldots>1}\left[M^2N\underset{F_2}{\langle(\bar\eta\psi)_2(\bar\psi\eta)_1)\rangle}\langle(\psi\bar\eta)_4(\eta\bar\psi)_3\rangle - N^2M\underset{F_3}{\langle(\psi\bar\eta)_2(\eta\bar\psi)_3\rangle}\langle(\psi\bar\eta)_4(\eta\bar\psi)_1\rangle\right], \tag{3.94}$$

where we have already performed the trace over the gauge index. Using the explicit expression of the fermion propagator given in Appendix A and computing the integrals, we obtain:

$$F_2 + F_3 = \frac{\pi^2}{\kappa^2}\frac{MN}{M+N}\left(M+\frac{1}{2}N\right). \tag{3.95}$$

The last diagram is quite tricky because it involves an integration over the position of a gauge-spinor-spinor vertex. These diagrams arise from the three cubic monomials in the second line of (3.87) Wick-contracted with the vertex from the lagrangian (2.44), *i.e*

$$\begin{aligned} F_4 = \left(\frac{2\pi}{\kappa}\right)^2 \frac{1}{M+N}\int_0^{2\pi} d\tau_{3>2>1}\ \Big[&N^2M(\eta_{1L}\gamma_\nu\gamma^\mu\gamma_\lambda\bar\eta_2^L)\epsilon_{\mu\rho\sigma}\dot x_3^\rho\ \Gamma^{\nu\lambda\sigma} + \\ &+ N^2M(\eta_{2L}\gamma_\lambda\gamma^\mu\gamma_\nu\bar\eta_3^L)\epsilon_{\mu\rho\sigma}\dot x_1^\rho\ \Gamma^{\sigma\lambda\nu} + NM^2(\eta_{1L}\gamma_\lambda\gamma^\mu\gamma_\nu\bar\eta_3{}^L)\epsilon_{\mu\rho\sigma}\dot x_2^\rho\ \Gamma^{\lambda\sigma\nu}\Big], \end{aligned} \tag{3.96}$$

where we have also performed the trace over all the gauge indices. The function $\Gamma^{\lambda\mu\nu}$ is a short-hand notation which hides the three-point function defined by the integral

$$\Gamma^{\lambda\mu\nu}(x_1,x_2,x_2) = \left(\frac{\Gamma(\frac{1}{2}-\epsilon)}{4\pi^{3/2-\epsilon}}\right)^3 \partial_{x_1^\lambda}\partial_{x_2^\mu}\partial_{x_3^\nu}\int \frac{d^{3-2\epsilon}w}{(x_{1w}^2)^{1/2-\epsilon}(x_{2w}^2)^{1/2-\epsilon}(x_{3w}^2)^{1/2-\epsilon}}. \tag{3.97}$$

Using the relations in Appendix A for the gamma matrices and for the bilinears $(\eta\gamma\gamma\gamma\bar\eta)$, one can reduce the integral (3.96) into simpler pieces. Since there are a lot of cancellations, it is useful summing up the upper and lower blocks of the loop from the beginning. Performing the integrals we have

$$F_{4\uparrow} + F_{4\downarrow} = -2\frac{\pi^2}{\kappa^2}MN \tag{3.98}$$

Finally as in the bosonic case, we can sum up all the fermionic contributions from the two blocks. The total fermionic part of the vev of the circular Wilson loop up to two-loop is given by

$$\langle W^{(F)}[C_{\text{cir.}}]\rangle^{(2)} = -\frac{1}{2}\frac{\pi^2}{\kappa^2}MN\,. \tag{3.99}$$

Summing up all the contributions

Summing up the bosonic and the fermionic vev's, and considering the "0-order" of the perturbation theory namely the traces of the identities in the fundamental representations, we obtain the complete Wilson loop

$$\begin{aligned}\langle \mathcal{W}[C_{\text{cir.}}]\rangle =& 1 + \langle W^{(B)}[C_{\text{cir.}}]\rangle^{(2)} + \langle W^{(F)}[C_{\text{cir.}}]\rangle^{(2)} + ... \\ =& 1 - \frac{\pi^2}{6\kappa^2}(N^2 + M^2 - 4MN) + ... \\ =& 1 - \frac{\pi^2}{6}(\lambda_1^2 + \lambda_2^2 - 4\lambda_1\lambda_2) + ...\end{aligned} \tag{3.100}$$

where in the last line we have used the 't Hooft coupling defined in (2.50).

3.4 Non-perturbative results: localization

From the above computations of the vev of circular Wilson loops one can notice a lot of interesting features as the apparently "magical" cancellations between diagrams. This fact was a starting point for a deeper analysis of this operator and the more general families of which it belongs. It turns out that using supersymmetric localization, one can obtain non-perturbative results for these loop operators in a relatively simple way.

3.4.1 From $\mathcal{N} = 4$ SYM to YM_2

As we have seen in Section 3.3.1, the authors of [89] conjectured that the ladder graphs compute the exact large N behavior of the circular Wilson loop and proposed some evidence (a 2 loop calculation) to this effect. We will give some arguments supporting the validity of this result to all orders.

In [90] the authors proposed some arguments to obtain the vacuum expectation value of the circular Wilson loop from the following Gaussian matrix model for finite N

$$\langle W(C_{\text{cir.}})\rangle = \left\langle \frac{1}{N}\text{Tr}e^M \right\rangle = \frac{1}{Z}\int [dM]\frac{1}{N}\text{Tr}e^M \exp\left[-\frac{2N}{\lambda}\text{Tr}M^2\right] \tag{3.101}$$

with solution

$$\begin{aligned}\langle W(C_{\text{cir.}})\rangle =& \frac{1}{N}L_{N-1}^1\left(-\frac{\lambda}{4N}\right)e^{\frac{\lambda}{8N}} \\ =& \frac{2}{\sqrt{\lambda}}I_1(\sqrt{\lambda}) + \frac{\lambda}{48N^2}I_2(\sqrt{\lambda}) + \frac{\lambda^2}{1280N^4}I_4(\sqrt{\lambda}) + ...\end{aligned} \tag{3.102}$$

where L_i^j are the Laguerre polynomials. At leading order in $1/N$ we recover the result (3.75). Notice, indeed, that the matrix model (3.78) is the same of (3.101) in the large N limit.

Since we have seen the relation between the 1/2 BPS circular Wilson loop and the general class of loops on the two-sphere (DGRT), we are interested to know if a general matrix model at finite N exists for arbitray shape of the loop. The solution to this point has been conjectured in [75] and [95] where the authors proposed a relation between Wilson loop in $\mathcal{N}=4$ SYM and the same operator in the zero-instanton sector of pure two-dimensional Yang-Mills (YM_2).

Let us consider a loop restricted to a unit S^2 as in Section 3.1.2.1, where the scalar coupling reduces to (3.29). Expanding the exponent to second order in the fields and computing the expectation value will give the contractions of the gauge fields and the scalars as in (3.68). That combined "gauge+scalar" propagator is not generically a constant, as in the case of the 1/2 BPS circle, a fact which led to the identification of that operator with the zero-dimensional Gaussian matrix model of (3.78). But still, instead of having mass-dimension 2 as expected in a four-dimensional theory, it is dimensionless. This is the first indication that this effective propagator may serve as a vector propagator in two dimensions.

To see that this is a vector propagator on S^2 we will change coordinates and parameterize the sphere in terms of complex coordinates z and $\bar{z}$ as

$$\vec{x} = \frac{1}{1+z\bar{z}}\left(z+\bar{z},\, -i(z-\bar{z}),\, 1-z\bar{z}\right) . \tag{3.103}$$

In these coordinates, the S^2 metric takes the Fubini-Study form

$$ds^2 = \frac{4\, dz d\bar{z}}{(1+z\bar{z})^2} . \tag{3.104}$$

For the gauge theory on the sphere consider the Feynman gauge, so the kinetic action is

$$L = \frac{\sqrt{g}}{g_{2d}^2}\left[\frac{1}{4}(F_{ij}^a)^2 - \frac{1}{2}(\nabla^i A_i^a)^2\right] = -\frac{\sqrt{g}}{g_{2d}^2}(g^{z\bar{z}})^2\left[(\nabla_z \tilde{A}_{\bar{z}}^a)^2 + (\nabla_{\bar{z}}\tilde{A}_z^a)^2\right] , \tag{3.105}$$

where $\sqrt{g} = -ig^{\bar{z}z}$. In the last equality we have ignored interaction terms, and the covariant derivatives are taken with respect to the metric (3.104). The constant g_{2d} is the coupling in this framework and the propagators are

$$\begin{aligned} \Delta_{zz}^{ab}(z,w) &= \delta^{ab}\frac{g_{2d}^2}{2\pi}\frac{1}{(1+z\bar{z})}\frac{1}{(1+w\bar{w})}\frac{\bar{z}-\bar{w}}{z-w} , \\ \Delta_{\bar{z}\bar{z}}^{ab}(z,w) &= \delta^{ab}\frac{g_{2d}^2}{2\pi}\frac{1}{(1+z\bar{z})}\frac{1}{(1+w\bar{w})}\frac{z-w}{\bar{z}-\bar{w}} , \end{aligned} \tag{3.106}$$

The first line of (3.106) satisfies

$$\frac{4}{g_{2d}^2}(g^{z\bar{z}})^2\nabla_{\bar{z}}^2\Delta_{zz}^{ab}(z,w) = \delta^{ab}\frac{1}{\sqrt{g}}\delta^2(z-w) , \tag{3.107}$$

and similarly for $\Delta_{\bar{z}\bar{z}}$. By doing the change of variables to the complex coordinates (3.103), one can then see that the effective propagator agrees with the 2d vector propagators (3.106) when the 2d and Yang-Mills couplings are related by

$$g_{2d}^2 = -2\frac{g_{\rm YM}^2}{A}\,. \tag{3.108}$$

where A is the total area of the 2-sphere, then g_{2d} has 2 dimensions of mass.

One can associate the gauge field in x to the effective propagator in S^2

$$A_i = \frac{g_{2d}^2}{2\pi}\int dy^j \left(\frac{1}{2}\delta_{ij} - \frac{(x-y)_i(x-y)_j}{(x-y)^2}\right)\,, \tag{3.109}$$

and the resulting field-strength, gotten by differentiation and projection in the directions tangent to the sphere, is

$$F_{ij} = -\frac{g_{2d}^2}{2\pi}\int ds\,\frac{-\dot{y}_i y_j + \dot{y}_j y_i}{(x-y)^2}\,. \tag{3.110}$$

The associated dual scalar $\tilde{F} = \frac{1}{2}\epsilon_{ijk}F_{ij}x_k$ reads

$$\tilde{F} = -\frac{g_{2d}^2}{2\pi}\int ds\,\frac{\varepsilon_{ijk}\,\dot{y}^i y^j x^k}{(x-y)^2} = g_{2d}^2\frac{A_2}{A}\,. \tag{3.111}$$

where A_2 is the area of the part of the sphere enclosed by the loop and not including x. Clearly this is a constant unless x crosses the loop. Then it is simple to evaluate the Wilson loop at the quadratic order using Stokes' theorem. We get

$$\langle W\rangle = 1 - \frac{N}{4}\int_{\Sigma_1}\tilde{F} + O(g_{2d}^4) = 1 - g_{2d}^2 N\,\frac{A_1 A_2}{4A} + O(g_{2d}^4)\,, \tag{3.112}$$

and the result is the product of the areas of the two parts of the sphere separated by the loop and it clearly does not depend on the order of the y and x integrals. Computing higher order graphs for loops of arbitrary shape is quite tricky. Two-dimensional YM is a soluble theory [96, 97] and one can use known results and compare them to some results in four dimensions, including some strong-coupling results from the AdS dual of $\mathcal{N}=4$.

The above perturbative calculation of the Wilson loop in two dimensions is very similar to the one performed by Staudacher and Krauth in [98]. There the calculation has been done on the plane exploiting the light-cone gauge, while here we have shown the calculation on S^2 employing a different gauge. One may change to the light-cone gauge on the sphere by taking $A_{\bar{z}} = 0$ and then, using the same prescription, the propagator for A_z would double the one in (3.106). The Staudacher-Krauth propagator is the flat-space limit of this last one, and it is possible to sum up all the ladders, finding for the Wilson loop

$$\langle W\rangle = \frac{1}{N}L_{N-1}^1\left(\frac{g_{2d}^2 A_1}{2}\right)\exp\left[-\frac{g_{2d}^2 A_1}{4}\right]\,, \tag{3.113}$$

where A_1 is the area enclosed by the loop. It is equal to the expectation value of a Wilson loop in the Gaussian matrix model. This expression has an obvious generalization to S^2 with the simple replacement $A_1 \to 4A_1A_2/A$, where the combination of the areas is the same as appeared in (3.112).

Those formulas do not agree with the exact solution of YM in two dimensions. In [99] Bassetto and Griguolo showed that (3.113) may be extracted from the exact result by restricting to the zero-instanton sector following the expansion of [100]. It was therefore concluded that the perturbative calculation of [98], using the light-cone gauge, does not capture non-perturbative effects.

The result of the perturbative two-dimensional YM implies that the vev of four-dimensional Wilson loops is

$$\langle W \rangle = \frac{1}{N} L^1_{N-1}\left(-\frac{\lambda}{N}\,\frac{A_1A_2}{A^2}\right)\exp\left[\frac{\lambda}{2N}\,\frac{A_1A_2}{A^2}\right]. \tag{3.114}$$

where the 't Hooft is $\lambda = g^2_{\rm YM}N$. The expansion of this expression to order $g^2_{\rm YM}$ agrees with the aforementioned result (3.112).

One can notice that with the following rescaling of the coupling constant

$$\lambda \to \tilde{\lambda} = 4\lambda\,\frac{A_1A_2}{A^2} \tag{3.115}$$

the vacuum expectation value of any Wilson loop on the sphere is equal to the vev of the circular Wilson loop with the suitable coupling constant. In particular we are able to derive the vev's at large N of the BPS Wilson loops mentioned in Section 3.1.2.1 with the following maps:

$$\langle W_{\rm DGRT}\rangle = \frac{2}{\sqrt{\tilde{\lambda}}} I_1(\sqrt{\tilde{\lambda}}) \qquad \begin{cases} \tilde{\lambda} = \lambda & \text{Equator} \\ \tilde{\lambda} = \lambda \sin^2\theta_0 & \text{Latitude} \\ \tilde{\lambda} = \lambda \frac{\delta(2\pi-\delta)}{\pi^2} & \text{Wedge} \end{cases} \tag{3.116}$$

that coincide with the perturbative results of [75]. This result is only a conjecture. In [37] and [101] Pestun gave an interpretation of this 4d-2d correspondence in terms of supersymmetric localization.

3.4.1.1 Pestun supersymmetric localization

We consider the same geometrical setup of [101] where, extending the work [37], it was shown how to use localization in the context of the 1/8 BPS Wilson loops of [74, 75, 95] to obtain from $\mathcal{N} = 4$ SYM the two-dimensional theory on S^2, which was called in [101] *almost* 2d Yang-Mills theory. This theory is related to the Yang-Mills-Higgs theory [102, 103, 104, 105].

In [101] a set of supersymmetric equations was derived from the appropriate fermionic symmetry of the Wilson loop operators, and there it was shown that the smooth solutions of these equations are parameterized by certain field configurations on S^2.

Let us consider the space-time to be the four-sphere S^4, which can be interpreted as the one-point compactification of $\mathbb{R}^4$. Then we represent the S^4 as a warped $S^2 \times S^1$ fibration over an interval I, such that the metric takes the form

$$ds^2 = d\xi^2 + \sin^2\xi(d\theta^2 + \sin^2\theta d\phi^2) + \cos^2\xi d\tau^2. \tag{3.117}$$

The $\xi \in [0, \pi/2]$ is the coordinate on the interval I, the τ is the coordinate on S^1 fiber, and (θ, ϕ) are the usual polar coordinates on the S^2 fiber. At $\xi = 0$ the S^2 fiber shrinks to zero size, at $\xi = \pi/2$ the S^1 fiber shrinks to zero size. The relevant 1/8-BPS Wilson loops studied in [95, 75, 74, 106, 107, 108, 109] are located at the largest S^2 fiber at $\xi = \pi/2$.

The fermionic charge Q used in the localization computation [37] squares to a combination of a $U(1)$ rotation along the S^1 direction τ and a rotation in a $U(1)$ subgroup of the $SO(6)$ R-symmetry of $\mathcal{N} = 4$ SYM. By the arguments introduced in Section 2.3.1, the field theory localizes to the equations $Q\psi = 0$ where ψ are fermionic fields of the theory. In the $\mathcal{N} = 4$ theory one gets sixteen equations, one for each component of ψ. Then it can be seen that nine equations tell us that all fields are covariantly constant along the S^1 fiber. At this step the 4d theory localizes to a 3d theory on the S^1 quotient of the S^4. This quotient has the topology and the natural metric of the solid three-dimensional ball with boundary, which we denote as B^3. The metric on B^3 is given by the first two terms in (3.117), which is just the metric on a three-dimensional semi-sphere.

The remaining seven supersymmetric equations are 3d equations on B^3 for the 3d gauge field and five scalar fields (one of six scalar fields of $\mathcal{N} = 4$ SYM does not appear in the 3d equations). The equations are invariant under a diagonal $SO(3)$ subgroup of $SO(3)_{Lorentz} \times SO(3)_R$, where $SO(3)_R$ is a subgroup of the $SO(6)_R$ R-symmetry group. The scalars which transform under $SO(3)_R$ are denoted by Φ_1, Φ_2, Φ_3 (these are the three scalars which couple to the 1/8 BPS Wilson loops [74, 95, 75]). The remaining two scalar fields are labeled as Φ_4 and Φ_5. It is convenient to represent the Φ_i scalar fields as three components of adjoint valued one-form Φ.

Now we want to write down the YM action in the three-dimensional ball B^3. Following the arguments of [101], one have

$$S_{YM}(B^3) = S_{susy}(B^3) + \frac{\pi}{g^2_{\rm YM}} \int_{S^2} d\Omega\, \Phi_n^2 \tag{3.118}$$

where Φ_n is the normal component to the S^2 of the one-form Φ, namely $\Phi_n = n^i \Phi_i$ with $n^i = x^i/|x|$, and $d\Omega$ is the standard volume form of S^2. On supersymmetric configuration $S_{susy}(B^3)$ vanishes, thus the $\mathcal{N} = 4$ SYM theory localizes to the two-

dimensional theory on S^2 with the action

$$S_{2d} = \frac{\pi}{g^2_{\rm YM}} \int_{S^2} d\Omega \, \Phi_n^2 = \frac{\pi}{g^2_{\rm YM}} \int_{S^2} d\Omega \, (d_A^{*2d} \Phi_t)^2 \tag{3.119}$$

where Φ_t denotes an adjoined-valued one-form on S^2 obtained from the components of Φ_i tangential to S^2. Then for supersymmetric configurations $d_A^{*2d}\Phi_t = -\Phi_n$.

The Wilson loop operator (3.24) descends to the Wilson loop operator in the two-dimensional theory

$$W_{\mathcal{R}}[C] = {\rm Tr}_{\mathcal{R}} \mathcal{P} \exp \left[\int (A - i * \Phi_t) \right] = {\rm Tr}_R \mathcal{P} \exp \left[\int \tilde{A}_{\mathbb{C}} \right] \tag{3.120}$$

which is the holonomy of the complexified connection $\tilde{A}_{\mathbb{C}} = A - i * \Phi_t$.

Let be $F_{\tilde{A}_{\mathbb{C}}}$ the curvature of $\tilde{A}_{\mathbb{C}}$, then

$$F_{\tilde{A}_{\mathbb{C}}} = d\tilde{A}_{\mathbb{C}} + \tilde{A}_{\mathbb{C}} \wedge \tilde{A}_{\mathbb{C}} = F_A - \Phi_t \wedge \Phi_t - i d_A \Phi_t \tag{3.121}$$

At the localized configuration we have $F_A - \Phi_t \wedge \Phi_t = 0$, then

$$d_A \Phi_t = i F_{\tilde{A}_{\mathbb{C}}} \tag{3.122}$$

Finally the action of the two-dimensional theory (3.119) is equivalent to the action of the bosonic Yang-Mills for complexified connection $\tilde{A}_{\mathbb{C}}$

$$S_{2d} = \frac{1}{2g^2_{2d}} \int_{S^2} d\Omega \, (*_{2d} F_{\tilde{A}_{\mathbb{C}}})^2 \tag{3.123}$$

where the two-dimensional coupling constant is denoted g_{2d}

$$g^2_{2d} = -\frac{g^2_{\rm YM}}{2\pi} \tag{3.124}$$

in agreement with the conjecture of [74, 75, 95].

Since perturbative correlation functions of holomorphic observables do not depend on deformation of the contour of integration, we conclude that the expectation value of Wilson loop observables (3.120) perturbatively coincides with the expectation values of Wilson loops in the zero-instanton sector two-dimensional Yang-Mills.

3.4.2 Localization in ABJ(M) theory

As in the $\mathcal{N} = 4$ SYM case, one is interested to define some tools in ABJ(M) to extract non-perturbative information from the theory. Also in ABJ(M) theory, the localization technique plays a central role. As we have seen before, the structure of the theory is

quite involved, then we don't know if there is a similar localization procedure as in the four-dimensional case for the generalized BPS Wilson loop on S^2 (see Section 3.2.2.1).

Kapustin, Willett and Yaakov in [38] proposed the following matrix model for the partition function of the $\mathcal{N}=6$ superconformal Chern-Simons theory on S^3

$$\begin{aligned}\mathcal{Z} &= \int \prod_{a=1}^{N} d\lambda_{1a}\, e^{i\pi\kappa\lambda_{1a}^2} \prod_{b=1}^{M} d\lambda_{2b}\, e^{-i\pi\kappa\lambda_{2b}^2} \\ &\times \frac{\prod_{a<b}^{N} \sinh^2(\pi(\lambda_{1a}-\lambda_{1b}))\prod_{a<b}^{M}\sinh^2(\pi(\lambda_{2a}-\lambda_{2b}))}{\prod_{a=1}^{N}\prod_{b=1}^{M}\cosh^2(\pi(\lambda_{1a}-\lambda_{2b}))}\end{aligned} \tag{3.125}$$

where $\lambda_{1,2}$ are the 't Hooft coupling (2.50). They studied also the expectation values of $\mathcal{W}_{\mathcal{R}_N}^{1/6}$ and $\hat{\mathcal{W}}_{\mathcal{R}_M}^{1/6}$ in the fundamental representations. These operators are directly obtained by inserting in (3.125) the functions

$$w_N^{1/6} = \frac{1}{N}\sum_{a=1}^{N} e^{2\pi\lambda_{1a}} \quad \text{and} \quad \hat{w}_M^{1/6} = \frac{1}{M}\sum_{a=1}^{M} e^{2\pi\lambda_{2a}} \tag{3.126}$$

corresponding to the $U(N)$ and $U(M)$ pieces respectively. The computation of the 1/2 BPS Wilson loop, in the fundamental representation F, is instead equivalent to the insertion in (3.125) of the operator [110]

$$w_F^{1/2} = \frac{1}{N+M}\left(\sum_{a=1}^{N} e^{2\pi\lambda_{1a}} + \sum_{a=1}^{M} e^{2\pi\lambda_{2a}}\right). \tag{3.127}$$

As we have seen in Section 3.2.2, a particular combination of the vacuum expectation values of the two 1/6 BPS Wilson loops are equal to the vev of the 1/2 BPS Wilson loop (see equation (3.58)) since they are related by a Q-exact term. The localization procedure implies therefore the same relation and, in particular

$$\langle \mathcal{W}_F^{1/2}\rangle_{\mathcal{Z}} = \frac{N\langle \mathcal{W}_N^{1/6}\rangle_{\mathcal{Z}} + M\langle \hat{\mathcal{W}}_M^{1/6}\rangle_{\mathcal{Z}}}{N+M}, \tag{3.128}$$

where with $\langle\ \rangle_{\mathcal{Z}}$ we have denoted the quantum avarages obtained from the matrix model eq. (3.125). In deriving eq. (3.128) it has been assumed that the regularization procedure preserves the cohomological relation: it is therefore tempting to analyze the framing dependence of this result. The 1/6 BPS case was discussed at perturbative level in [78], employing conventional DRED regularization at framing $f=0$. As suggested in [38], comparing the explicit two-loop expression with the expansion of the matrix model average at the same order, one discovers that

$$\begin{aligned}\langle \mathcal{W}_N^{1/6}\rangle_{\mathcal{Z}} &= e^{\frac{i\pi}{k}N}\,\langle \mathcal{W}_N^{1/6}\rangle^{f=0} \\ \langle \hat{\mathcal{W}}_M^{1/6}\rangle_{\mathcal{Z}} &= e^{-\frac{i\pi}{k}M}\,\langle \hat{\mathcal{W}}_M^{1/6}\rangle^{f=0}.\end{aligned} \tag{3.129}$$

Then localization computes the Wilson loop at framing $f = 1$. The matrix model average for the 1/2 BPS Wilson loop is given by

$$\langle \mathcal{W}_F^{1/2} \rangle_{\mathcal{Z}} = e^{\frac{i\pi}{k}(N-M)} \langle \mathcal{W}_F^{1/2} \rangle^{f=0} . \tag{3.130}$$

In particular, for the 1/2 BPS circular Wilson loop, the matrix model average [110] can be expanded perturbatively

$$\langle \mathcal{W}_F^{1/2} \rangle_{\mathcal{Z}} = 1 + i\frac{\pi}{\kappa}(N-M) - \frac{2}{3}\frac{\pi^2}{\kappa}^2 (N^2 - \frac{5}{2}MN + M^2 - \frac{1}{4}) + \mathcal{O}(\frac{1}{\kappa^3}) \tag{3.131}$$

Now using the relation (3.130), we can find the vev at framing $f = 0$, *i.e.* the outcome of the perturbative analysis via Feynman diagrams

$$\langle \mathcal{W}_F^{1/2} \rangle^{f=0} = 1 - \frac{\pi^2}{6\,\kappa^2} \left(N^2 + M^2 - 4NM \right) + \mathcal{O}(1/\kappa^3) , \tag{3.132}$$

that corresponds exactly to the expected result of perturbation theory (3.100). Notice that the relation implies that the 1/2 BPS Wilson loop at framing $f = 0$ is not given, at quantum level, by the sum of the two (bosonic) 1/6 BPS Wilson loops. This means, in particular, that fermionic interactions should play a crucial role, at perturbative level, to find agreement with the localization procedure.

The complete solution of the matrix model was investigated in [111, 110, 112] to obtain exact results in the large N limit, producing a non-trivial interpolating function between the weak and the strong coupling regimes of the theory.

Chapter 4

The cusp anomalous dimension

In Chapter 3 we have defined the Wilson loop operator and we have studied some examples of smooth supersymmetric Wilson loops and their properties. In this Chapter we will explore the case of Wilson loops with a discontinuity in the contour. These operators have an anomalous dimension called *cusp anomalous dimension* and we will see how it is related with a lot of interesting physical quantities.

We will start with a review of renormalization properties of a Wilson loop in section 4.1 also pointing out the main features of its anomalous dimension. This function is related to a great number of physical observables and plays a central role in the duality Wilson loops/amplitudes. In Section 4.2 we will construct the cusped Wilson loop operator in $\mathcal{N} = 4$ SYM and ABJ(M) theories. We will also discuss how to extract the cusp anomalous dimension from its expectation value.

4.1 Cusped Wilson loop and its anomalous dimension

Let us summarize the renormalization properties of the Wilson loops. In a generic gauge theory with ultraviolet divergences, the gauge field A_μ and the coupling constant g are renormalized by multiplicative counterterms. These subtractions do not depend on the contour C of the loop, then we focus on the divergences inherent to the Wilson loop.

Renormalization properties of smooth Wilson loops are studied by Gervais, Neveu [113], Polyakov [114] and Vergeles, Dotsenko [115]. They become finite after the coupling renormalization

$$\hat{W}[C] = e^{\epsilon L[C]} W[C] \tag{4.1}$$

where $\hat{W}$ is the loop operator after the change $g \to \hat{g}$ and ϵ stands for the ultraviolet cutoff used to regularize the Wilson loop. The exponential perimeter factor in (4.1) is associated with the renormalization of the mass of an heavy test particle propagating along the loop. It does not emerge in dimensional regularization. An additional

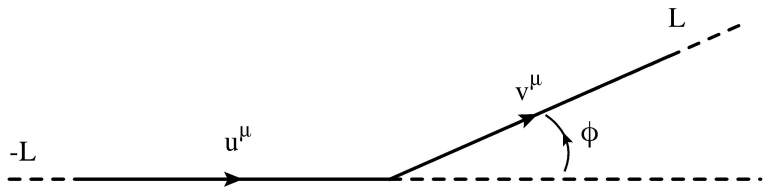

Figure 4.1: The cusped Wilson line with euclidea angle φ

logarithmic divergence appears when the loop has a cusp as it was first observed by Polyakov in [114].

The cusped Wilson loop, represented in Figure 4.1, has a great number of applications to physical processes. For instance in QCD, it represents the world trajectory of a heavy quark which changes its velocity suddenly at the location of the cusp. In that case, UV (short-distance) divergences associated to each cusp appear. The ultraviolet divergence is related to the bremsstrahlung radiation of soft gluons emitted by the quark during its sudden change in velocity. For euclidean kinematics, or when it is away from the light-cone in Minkowski space, the usual cusped Wilson loop is multiplicatively renormalizable, as was shown by Brandt, Neri and Sato in [116],

$$\hat{W}[C] = Z_{\text{cusp}}(g, \varphi) W[C] \tag{4.2}$$

where the divergent function Z_{cusp} depends only locally on the contour C through the cusp angle φ defined as

$$\begin{aligned} \cos\varphi &= \frac{u \cdot v}{|u||v|} \qquad \text{Euclidean space} \\ \cosh\varphi &= \frac{u \cdot v}{|u||v|} \qquad \text{Minkowski space} \end{aligned} \tag{4.3}$$

with u^μ and v^μ the vectors parametrizing the two rays of the cusp as in Figure 4.1. The locality of the counterterms persists when there are several cusps with angles φ_i. In that case, the renormalization function

$$Z_{\text{cusp}}(g, \{\varphi_1, ..., \varphi_n\}) = Z_{\text{cusp}}(g, \varphi_1) Z_{\text{cusp}}(g, \varphi_2) ... Z_{\text{cusp}}(g, \varphi_n) \tag{4.4}$$

factorizes into a product of renormalization factors, one for each cusp. Thus, there are no "anomalous" divergences that depend non-locally on the contour.

In [117, 118] a renormalisation group equation for Wilson loops with cusps was derived. It reads

$$\left(\mu \frac{\partial}{\partial \mu} + \beta(\hat{g}) \frac{\partial}{\partial \hat{g}} + \Gamma_{\text{cusp}}(\hat{g}, \varphi) \right) \hat{W} = 0 \tag{4.5}$$

where, as in the local operator case presented in 2.1.2.2, the anomalous dimension is

$$\Gamma_{\text{cusp}} = \mu \frac{\partial}{\partial \mu} \log Z_{\text{cusp}} \,. \tag{4.6}$$

One can derive from (4.5) a renormalization group equation for Z_{cusp} that implies the exponentiation of the divergent part of the Wilson loop (see a similar case for local operators in Section 2.1.2.3)

Additional divergences can appear if one considers instead of a closed contour C an open line. In that case one looses gauge independence, and there are logarithmic divergences associated to the endpoints. In the following we do not consider these spurious effects and concentrate on the true cusp divergences. We introduce an UV regulator ϵ shielding the tip of the contour and an IR regulator L cutting the infinite length of the line: the Wilson loop develops a logarithmic divergence of the form

$$\langle W[C_{\text{cusp}}]\rangle \propto e^{-\Gamma_{\text{cusp}} \log \frac{L}{\epsilon}} . \tag{4.7}$$

We list some of the important properties of Γ_{cusp}:

- It characterizes the IR divergences that arise when we scatter massive colored particles. Here φ is the boost angle between two external massive particle lines. For each consecutive pair of lines in the color ordered diagram we get a factor of the form (4.7), where L and ϵ are respectively an IR and UV regulators. The angle is given by (4.3). This relation is general for any gauge theory.

- The IR divergences of massless particles are characterized by γ_{cusp} which is the coefficient of the large φ behavior of the cusp anomalous dimension in Minkowski space

  $$\Gamma_{\text{cusp}}(g, i\varphi) \xrightarrow{\varphi\to\infty} \varphi\, \gamma_{\text{cusp}} \tag{4.8}$$

  This is the anomalous dimension of a light-like, or null, Wilson loop and it was computed in perturbation theory at weak coupling in [117, 119, 120]. It is also related [121, 117, 122, 123] to the anomalous dimensions of twist-two conformal operators [124, 125, 126] with large spin. More recently, in $\mathcal{N} = 4$ SYM it was studied in[127, 128, 129]. It is determined exactly by an integral equation [130].

- In conformal gauge theories, by the plane to cylinder map, this quantity is identical to the energy of a static quark and anti-quark sitting on a spatial three sphere at an angle $\delta = \pi - \varphi$.

  $$\Gamma_{\text{cusp}}(g, \varphi) = V(g, \varphi) \tag{4.9}$$

  see Figure 4.2. In particular, in the small δ limit we get the same answer as the quark-antiquark potential in flat space computed with the prescription (3.3)

  $$\Gamma_{\text{cusp}}(g, \varphi) = \frac{V(g)}{\delta} \qquad \text{with} \quad \delta \to 0 \tag{4.10}$$

  where $V(g)$ is the coefficient of the quark-antiquark potential, for a quark and an antiquark at distance R in flat space.

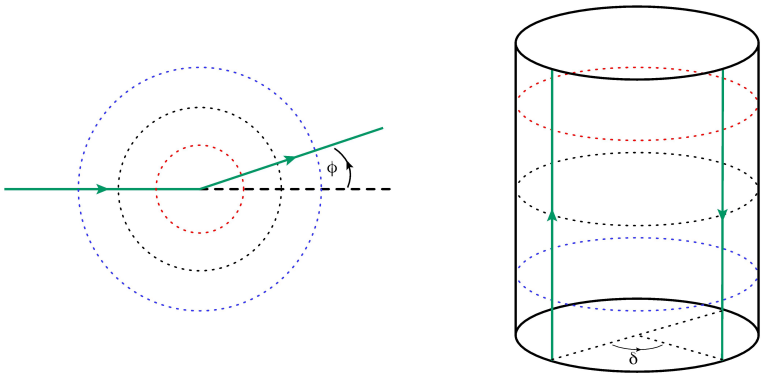

Figure 4.2: The plane-to-cylinder map

- In the small φ limit, having $\Gamma_{\text{cusp}}(g,0)=0$, the cusp anomalous dimension can be shown to go as φ^2 and it is possible to define, in the conformal case, the so-called Bremsstrahlung function $\mathcal{B}$ by

$$\Gamma_{\text{cusp}}(g,\varphi) \sim -\varphi^2 \mathcal{B}(g) \qquad \varphi \to 0 \tag{4.11}$$

  The order φ^2 correction is related to the energy loss of an accelerated quark. In $\mathcal{N}=4$ SYM, $\mathcal{B}$ can be computed exactly using localization, see [131] and [132]. Moreover, one can derive a set of integral equations that also determines $\mathcal{B}$ linking localizazion and integrability results.

Another motivation to study the cusp anomalous dimension comes from its relation with scattering amplitudes. In $\mathcal{N}=4$ SYM scattering amplitudes are also functions of the angles between particles and are related to polygonal light-like Wilson loops by a very powerful duality. Obtaining exact results for the cusp anomalous dimension is useful to learn about the general structure of the amplitude problem [133, 134, 135].

4.2 Cusped Wilson loop in supersymmetric gauge theories

As we have seen in Section 3.1, the locally supersymmetric Wilson loop includes a coupling to the scalar fields specified by a direction in the internal space Θ_I. The same behavior is present in the three-dimensional case presented in 3.2. When one wants to study the cusped Wilson line in supersymmetric field theories, it seems natural to deform the loop operator adding information about R-symmetry. In practice, defining in general the direction in the internal space with the six-vector $\vec{\Theta}$, instead of considering the same vector $\vec{\Theta}$ on the two lines that make the cusp, we can take two vectors $\vec{\Theta}$ and $\vec{\Theta}'$. This introduces a second angle defined as

$$\cos\theta = \vec{\Theta}\cdot\vec{\Theta}' \tag{4.12}$$

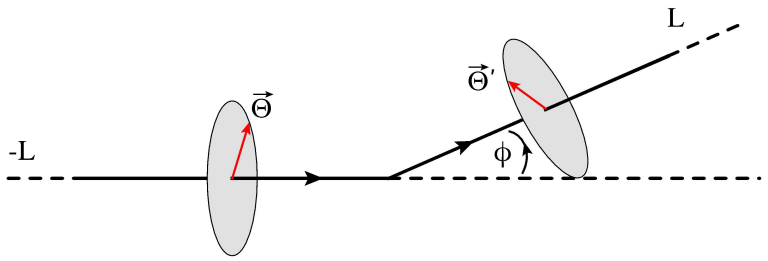

Figure 4.3: The generalized cusped Wilson line.

The anomalous dimension of this cusped loop is the so-called *generalized cusp anomalous dimension* $\Gamma_{\text{cusp}}(g, \varphi, \theta)$ which is a function of two angles θ and φ. The generalized cusp has the same properties of the Γ_{cusp} introduced in the previous Section and, for instance in $\mathcal{N} = 4$ SYM, it characterizes the planar IR divergences that arise when massive W-bosons scatter. Those massive particles can be obtained by setting some Higgs vev's to be non-zero. Then the angle θ is the angle between the Higgs vev's associated to consecutive massive particles. This generalized cusp anomalous dimension was computed in $\mathcal{N} = 4$ SYM to leading and subleading order in weak and strong coupling in [69] and [136, 137] respectively and in ABJ(M) theory in [83, 138].

Despite the loop operator in general is not BPS, there are some configurations in which this property still holds. As we have seen the not-deformed loop turns out to be trivial when the euclidean angle φ vanishes, indeed the contour is a BPS straight line. In the generalized case we have additional possibilities: in fact the loop in Figure 4.3 is BPS when $\varphi = \pm\theta$. In particular, as we will see, in $\mathcal{N} = 4$ SYM the loop is 1/4 BPS and in ABJ(M) is 1/6 BPS.

The leading order term in the expansion of $\Gamma_{\text{cusp}}(g, \varphi, \theta)$ around the supersymmetric value (*near BPS expansion*) is

$$\Gamma_{\text{cusp}}(g, \varphi, \theta) = -(\varphi^2 - \theta^2)\mathcal{H}(g, \varphi) + \mathcal{O}((\varphi^2 - \theta^2)^2) \qquad \text{when} \quad \theta \simeq \pm\varphi \tag{4.13}$$

The $\mathcal{H}$ function turns out to be the same of $\mathcal{B}(g)$ in equation (4.11) for $\varphi = 0$.

In [139, 140] a TBA system of integral equations is derived for $\Gamma_{\text{cusp}}(\varphi, \theta)$. This is done via the standard approach of integrability and a limit of those integral equations computes the function $\mathcal{B}$. Thus the cusp anomalous dimension at small angles allows us to connect results computed using integrability with results computed using localization and perturbation theory.

4.2.1 Cusped Wilson loop in $\mathcal{N} = 4$ SYM

4.2.1.1 The quark-antiquark potential

We first replace the theory on $\mathbb{R}^4$ with the theory on $S^3 \times \mathbb{R}$ (related by the exponential map as represented in Figure 4.2). Now consider a pair of antiparallel lines separated by an angle $\delta = \pi - \varphi$ on S^3. For $\varphi = 0$ the two lines are antipodal and mutually BPS, while for $\varphi \to \pi$ the lines get very close together. If one "zoom in", we get a situation very similar to the original antiparallel lines in flat space. In this framework, the expectation value of the Wilson loop calculates the effective potential $V(g, \varphi, \theta)$ between a generalized quark-antiquark pair.

The effective potential depends on the 't Hooft coupling in large N limit and can be expanded in a perturbative series at weak coupling or in an expansion around a classical string solution at strong coupling as follows

$$V(\lambda, \varphi, \theta) = \Gamma_{\text{cusp}}(\lambda, \varphi, \theta) = \begin{cases} \sum_{l=1}^{\infty} \left(\frac{\lambda}{16\pi^2}\right)^l \Gamma^{(l)}_{\text{weak}}(\varphi, \theta) & \lambda << 1 \\ \\ \frac{\sqrt{\lambda}}{4\pi} \sum_{l=0}^{\infty} \left(\frac{4\pi}{\sqrt{\lambda}}\right)^l \Gamma^{(l)}_{\text{strong}}(\varphi, \theta) & \lambda >> 1 \end{cases} \tag{4.14}$$

The one-loop result $\Gamma^{(1)}_{\text{weak}}$ was found in perturbation theory in [69] and it is

$$\Gamma^{(1)}_{\text{weak}} = -2\frac{\cos\theta - \cos\varphi}{\sin\varphi}\varphi \equiv -2\xi\varphi \tag{4.15}$$

To check the result one can focus on the BPS case $\theta = \pm\varphi$, indeed $\Gamma^{(1)}_{\text{weak}}(\varphi, \pm\varphi) = 0$ because ξ vanish in BPS limit. One can argue that at a given perturbative order l, we have

$$\Gamma^{(l)}_{\text{weak}} = \sum_{k=1}^{l} \xi^k f^{(l)}_k(\varphi) \tag{4.16}$$

where $f^{(l)}_k(\varphi)$ are functions of φ with uniform trascendentality. This behavior is obviously compatible with the BPS condition at any perturbative order. As another test, for large imaginary angle the leading behavior matches the perturbative expansion of the cusp anomalous dimension γ_{cusp}. The second order was computed in [137] in perturbation theory, the third order from a leading infrared (soft) divergence of amplitudes or form factors involving massive particles in [141] for $\theta = 0$. Moreover in [141, 142], the authors have developed some tools to compute the cusp anomalous dimension in a limit that selects only ladder diagrams with can be resummed with the help of a Bethe-Salpeter (this argument will have a central role in Chapter 7 in a ABJ(M)). An explicit computation of the cusp anomalous dimension at the fourth perturbative order is given in [143]. All these perturbative computations are in agreement with the expansion (4.16) and with the non perturbative integrability result for γ_{cusp} in the light-like

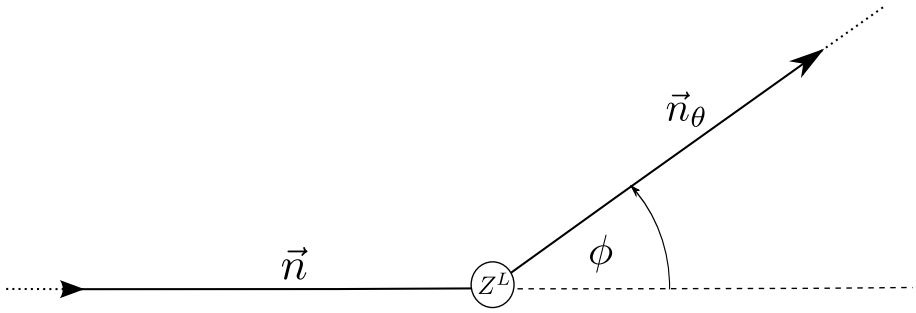

Figure 4.4: The generalized cusped Wilson line with L operator insertions on the tip.

limit. The strong coupling limit was computed in [137], at the first sub-leading order. It comes from fluctuations around the classical string solution dual to the Wilson loops with arbitrary θ and φ.

In the limit $\varphi \to \pi$ and $\theta = 0$ the curves approach to two antiparallel lines at a distance R. With the prescription $\delta = \pi - \varphi = R$ with $\delta << 1$, one recovers from $\Gamma^{(l)}_{\text{weak}}$ and $\Gamma^{(l)}_{\text{strong}}$ the usual result for this configuration in two regimes of the coupling. Recently in [144], the authors have constructed a closed system of equations describing the quark-antiquark potential at any coupling in planar $\mathcal{N} = 4$ SYM theory based on the Quantum Spectral Curve (QSC) method. They have studied analytically the generalized quark-antiquark potential in the limit of large imaginary twist, representing the angle θ, and have obtained the exact result. The QSC reduces to a one-dimensional Schroedinger equation establishing a link between the Q-functions and the solution of the Bethe-Salpeter equation of [141].

4.2.1.2 The cusp anomalous dimension from TBA

Let us consider the problem of computing the anomalous dimension of operators inserted along a Wilson loop of length T, for example an insertion of L complex scalar fields Z on the contour in the point $\tau = 0$. The resulting operator is BPS if the inserted operator does not couple with the loop. The straight Wilson loop is invariant under dilatations, so we can characterize the operators by their dimension under dilatations. These operators have dimension $\Delta_0 = L$.

The operator Z^L can be associated to a spin chain and one can solve the problem of computing the scaling dimension (for large L) considering virtual magnons propagating along the chain as we have seen in Section 2.3.2. The new aspect is that the magnons can be reflected from the boundaries at the end of the chain. To proceed, one need to determine the boundary reflection matrix to all orders in the coupling. At this stage one has completely solved the problem for operators with large L. Up to corrections of order $e^{-(\text{const.})L}$, one can find the energy by solving the appropriate Asymptotic Bethe equations of the type (2.88).

Now one can rotate one of the Wilson line (boundary) by an angle θ, restoring the generalized cusp system. This rotation will simply act on the indices of the reflection matrix via a global transformation. This operator is no longer BPS but its energy is very small when L is very large, *i.e.* it has zero energy up to $e^{-(\text{const.})L}$ corrections. These are called Lüscher (or wrapping) corrections.

As a non trivial check one can compute the first correction to the ground state energy al large L. This correction is given by a Lüscher-type formula. If we want to restore L to be finite, one have to consider the problem in the mirror picture (see Section 2.3.2 and Table 2.4). In the mirror theory magnons propagate over a Euclidean time L (length of the strip) between chains of length T. The two boundary conditions, now lead to two boundary states that create magnons that propagate along the strip. The leading order correction at weak coupling is a term proportional to λ^{1+L}. This has the interesting implication that this leading wrapping correction appears at $L+1$ loops, in other words it appears when the range of interaction is bigger than the size of the spin chain. Thus the leading order of the ground state energy of the spin-chain, the so-called *leading Lüscher term*, is [139, 140]

$$\begin{aligned} E_{\text{lead.}} &= \left(\frac{\lambda}{16\pi^2}\right)^{1+L} \Gamma_{\text{weak}}^{(1+L)}(\varphi,\theta) \\ &= -\left(\frac{\lambda}{16\pi^2}\right)^{1+L} \frac{\cos\theta-\cos\varphi}{\sin\varphi} \frac{(-1)^L(4\pi)^{1+2L}}{(1+2L)!} B_{1+2L}\left(\frac{\pi-\varphi}{2\pi}\right) + \mathcal{O}(\lambda^{2+L}) \end{aligned} \tag{4.17}$$

where $B_l(x)$ are the Bernoulli polynomials of degree l. In Chapter 6 we will present this result from a different point of view. In particular for $L=0$, the one loop contribution $\Gamma_{\text{weak}}^{(1)}$ of (4.15) comes from such a term. Notice that the leading Lüscher term also appears surprisingly in a very different subject as the leading Regge limit of the horizontal ladder diagram in [141].

Finally, one can write down a Thermodynamic Bethe Ansatz equation that describes the all-loop finite L configuration. This follows the standard route for getting the energies of states of an integrable field theory with a boundary. The boundary states are given in terms of the analytic continuation of the boundary reflection matrix. The TBA system of equations arises from evaluating this exact overlap between the two boundary states. The resulting Y function is [139, 140]

$$Y_Q = 4\lambda_Q(\cos\varphi-\cos\theta)^2 \frac{\sin^2 Q\varphi}{\sin^2\varphi} e^{-(2L+1)\tilde{E}_Q} \tag{4.18}$$

where $\tilde{E}_Q$ is the energy of the bound state of the magnon Q. We have seen in Section 2.3.2 that the ground state energy of the spin-chain is given by (2.92): given the Y-function, the energy of the ground state (and in this case the cusp anomaly) is completely determined (at least in principle). One notable example is the solution of the TBA for the near BPS limit of the energy that will be the central argument of Chapter 6.

4.2.1.3 The Bremsstrahlung function

The near-BPS expansion of the generalized cusp is characterized by the function $\mathcal{H}$ defined by the equations (4.13). First we consider the 1/4 BPS Wilson loop introduced in Section 3.1.2.1 and obeying the matrix model (3.101) with solution (3.114) and (3.116) at large N. It has a parameter θ_0 that is the latitude angle. As we have seen the vev of the latitude Wilson loop is given by the same expression as the circular one, but with a redefined coupling constant. In other words

$$\langle W[C_{\theta_0}](\lambda)\rangle = \langle W[C_{\text{cir.}}](\tilde{\lambda})\rangle \tag{4.19}$$

Expanding the equation around $\theta_0 = 0$, $\tilde{\lambda} \sim \lambda(1-\theta_0^2)$ (see (3.116)) we have

$$\frac{\langle W[C_{\theta_0}]\rangle - \langle W[C_{\theta_0=0}]\rangle}{\langle W[C_{\theta_0=0}]\rangle} = -\theta_0^2 \lambda \partial_\lambda \log\langle W[C_{\text{cir.}}](\lambda)\rangle \tag{4.20}$$

Taking the above derivative is the same as computing the two-point function of the scalar field inserted into the Wilson loop. This particular two-point function of the scalar field also gives the expansion of the cusp anomalous dimension around $\varphi = \theta = 0$. One can relate the derivative of the circular Wilson loop with the derivative of the circular Wilson loop [131]

$$\mathcal{B}(\lambda) = \frac{1}{2\pi}\lambda\partial_\lambda \log\langle W[C_{\text{cir.}}]\rangle \tag{4.21}$$

or, performing the change of the coupling for the latitude, we have

$$\mathcal{B}(\lambda) = -\frac{1}{4\pi^2}\partial_{\theta_0}^2 \log\langle W[C_{\theta_0}]\rangle_{\theta_0=0} \tag{4.22}$$

In the more general case when the BPS condition is $\theta = \pm\varphi \neq 0$, one have to deal with the wedge Wilson loop $W[C_\varphi]$. In this case (3.115) becomes

$$\tilde{\lambda} = \lambda\left(1 - \frac{\varphi^2}{\pi^2}\right) \tag{4.23}$$

and the vev of this Wilson loop is then

$$\langle W[C_\varphi](\lambda)\rangle = \langle W[C_{\text{cir.}}](\tilde{\lambda})\rangle \tag{4.24}$$

Deforming one edge of the contour with a displacement in an orthogonal direction and computing the variation of the vev with respect to this displacement it has been shown [131]

$$\partial_\varphi\langle W[C_\varphi]\rangle = -2\mathcal{H}(\tilde{\lambda},\varphi) = -4\frac{\varphi}{\left(1-\frac{\varphi^2}{\pi^2}\right)}\mathcal{B}(\tilde{\lambda}) \tag{4.25}$$

One can recall the localization result (3.114) for the DGRT Wilson loops and find an exact solution for he Bremsstrahlung function: we have [131, 132]

$$\mathcal{B}(\tilde{\lambda}) = \frac{1}{16\pi^2 N}\frac{L_{N-1}^2\left(-\frac{\tilde{\lambda}}{4N}\right) - L_{N-2}^2\left(-\frac{\tilde{\lambda}}{4N}\right)}{L_{N-1}^1\left(-\frac{\tilde{\lambda}}{4N}\right)} \tag{4.26}$$

and in the large N limit

$$\mathcal{B}(\tilde{\lambda}) = \frac{1}{4\pi^2}\sqrt{\tilde{\lambda}}\frac{I_2(\sqrt{\tilde{\lambda}})}{I_1(\sqrt{\tilde{\lambda}})} \tag{4.27}$$

Notice that the result (4.27) is very similar to the result of the correlation function of a DGRT Wilson loop and a CPO operator of scaling dimension $\Delta = 2$ as noticed in [132]. The computation of such a kind of correlators will be the central argument of the next chapter.

4.2.2 Cusped Wilson loop in ABJ(M)

In view of these developments in the four-dimensional theory, it appears natural to wonder if similar results could also be obtained for other superconformal gauge theories with integrable structures, the natural candidate being ABJ(M) (see Section 2.1.5). Supersymmetric configurations of Wilson loop, supported on straight lines and circles, were presented and also a localization formula, reducing the computation to an explicit matrix model average (see 3.4.2). In ABJ(M) the study of the cusp anomalous dimension is quite tricky: BPS lines and circles appear in two fashions, distinguished by the degree of preserved supersymmetries. Actually both loops turn out to be in the same cohomology class, differing by a BRST exact term with respect the localization complex (see 3.2.2). In this Section we review the perturbative approach for the cusped Wilson loop in ABJ(M) and the relation between the loop operators and the quantities studied in four dimensions, namely the quark-antiquark potential, the generalized cusp anomalous dimension and the Bremsstrahlung function.

4.2.2.1 Cusped Wilson line in perturbation theory

We start by considering the theory on the Euclidean space-time. We shall consider two rays in the plane (1, 2) intersecting at the origin. The angle between the rays is $\pi - \varphi$, such that for $\varphi = 0$ they form a continuous straight line. The path is given by the following parametrization

$$x^\mu(\tau) = \{0, \tau\cos\frac{\varphi}{2}, |\tau|\sin\frac{\varphi}{2}\}, \qquad -\infty \leq \tau \leq \infty \tag{4.28}$$

The couplings to the scalars and the fermions are determined by the relations (3.52) and (3.54). On the other hand the R-symmetry part of the couplings is arbitrary and in fact n and $\bar{n}$ are totally unconstrained (see (3.52)). We can generalize the coupling with the internal symmetry, choosing a parametrization such that

$$n_i \cdot \bar{n}_j = \begin{cases} 1 & i = j \\ \cos\frac{\theta}{2} & i \neq j \end{cases} \tag{4.29}$$

with the indices $i, j = 1, 2$ refer to the two edges of the cusp.

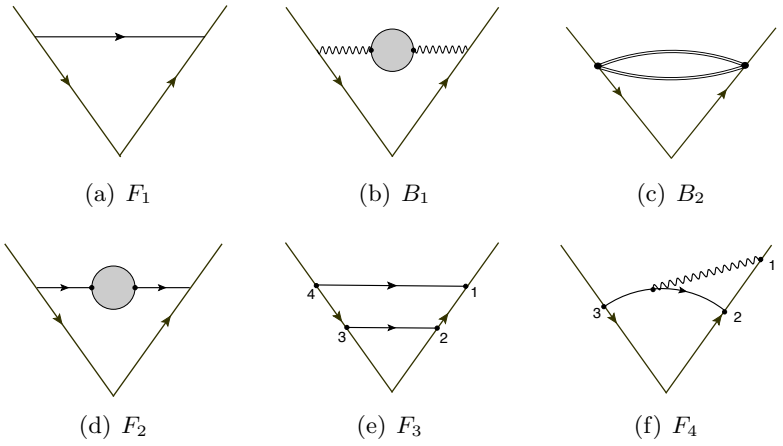

(a) F_1 (b) B_1 (c) B_2

(d) F_2 (e) F_3 (f) F_4

Figure 4.5: Fermionic and bosonic contributions to the vacuum expectation value of the cusped Wilson line in ABJ(M). Notice that every diagram represents a family of graphs with several fashions depending on the order of the expansion of the edges.

The perturbative computation is quite similar to the circular case analyzed in section 3.3.2. Indeed, using the expansion (3.87), one can compute the contribution to the vev up to two loops. The evaluation of the diagrams obviously encounter UV divergences which originate from the part of the integration region where the propagator endpoints coincide. To tame these divergences one have to use dimensional regularization, namely the DRED scheme, shifting the dimension to $d = 3 - 2\epsilon$. Note that this breaks the conformal invariance introducing a mass scale $\mu^{2\epsilon}$ that keeps the action dimensionless. We will also need an explicit IR regulator L, representing the finite length of the two rays forming the cusp.

All the non-zero diagrams for the cusped Wilson line up to two loops are depicted in Figure 4.5. The one-loop contribution, as in the circular case, came from the fermionic diagram F_1 only

$$\begin{aligned} F_1 &= \left(\frac{2\pi}{\kappa}\right)\mu^{2\epsilon}\int_{\tau_2<\tau_1} d\tau_1 d\tau_2\ \langle \mathrm{Tr}_{\mathbf{N}}\left[(\eta\bar{\psi})_1(\psi\bar{\eta})_2\right]\rangle \\ &= \left(\frac{2\pi}{\kappa}\right) MN\left(\frac{\Gamma(1/2-\epsilon)}{4\pi^{3/2-\epsilon}}\right)(\mu L)^{2\epsilon}\left[\frac{1}{\epsilon}\left(\frac{\cos\frac{\theta}{2}}{\cos\frac{\varphi}{2}}-2\right)-2\frac{\cos\frac{\theta}{2}}{\cos\frac{\varphi}{2}}\log\left(\sec\left(\frac{\varphi}{2}\right)+1\right)\right]. \end{aligned} \tag{4.30}$$

where propagators and general rules for the fermions and bilinears are in appendix A.

Differently by the four-dimensional case, since the scalar fields have the bilinear structure $C\bar{C}$, the first merely scalar contribution arises at two loops. Indeed

$$B_2 = MN^2\left(\frac{2\pi}{\kappa}\right)^2\frac{\Gamma^2\left(\frac{1}{2}-\epsilon\right)}{16\pi^{3-2\epsilon}}\int_\Gamma d\tau_{1>2}\ \frac{|\dot{x}_1||\dot{x}_2|\mathrm{Tr}(M_1M_2)}{((x-y)^2)^{1-2\epsilon}}. \tag{4.31}$$

and combined with the one-loop correction to the gauge propagator we have:

$$\begin{aligned} B_1 + B_2 =& - MN^2 \left(\frac{2\pi}{\kappa}\right)^2 \frac{\Gamma^2\left(\frac{1}{2}-\epsilon\right)}{4\pi^{3-2\epsilon}} \left(\cos\varphi - \cos^2\frac{\theta}{2}\right) \int_0^L d\tau_1 \int_{-L}^0 d\tau_2 \frac{1}{((x-y)^2)^{1-2\epsilon}} \\ =& - g(\epsilon) \left(\cos\varphi - \cos^2\frac{\theta}{2}\right) \frac{1}{\epsilon} \frac{\varphi}{\sin\varphi} \end{aligned} \tag{4.32}$$

where we have used the short-hand notation

$$g(\epsilon) = MN \left(\frac{2\pi}{\kappa}\right)^2 \frac{\Gamma^2\left(\frac{1}{2}-\epsilon\right)}{16\pi^{3-2\epsilon}} (\mu L)^{4\epsilon} \tag{4.33}$$

The diagram F_2 in proportional to $(N-M)$ then when we will sum the traces in the two blocks of the observable, it vanishes. The double exchange diagrams F_3 and the vertex diagrams F_4 are more subtle: the computation of their divergent part is discussed in detail in [83]:

$$\begin{aligned} F_1 + F_2 =& + \frac{g(\epsilon)}{2\epsilon^2} \left(\frac{\cos\frac{\theta}{2}}{\cos\frac{\varphi}{2}} - 2\right)^2 + \frac{2g(\epsilon)}{\epsilon} \frac{\cos\frac{\theta}{2}}{\cos\frac{\varphi}{2}} \left(2 - \frac{\cos\frac{\theta}{2}}{\cos\frac{\varphi}{2}}\right) \log\left(\sec\frac{\varphi}{2} + 1\right) \\ &+ \frac{2g(\epsilon)}{\epsilon} \log\left(\cos\frac{\varphi}{2}\right) \left(\frac{\cos\frac{\theta}{2}}{\cos\frac{\varphi}{2}} - 1\right) - (B_1 + B_2) + O(1). \end{aligned} \tag{4.34}$$

Summing up all the results we obtain the upper-left block of the bare observable. The final result appears surprising since in the limit $\varphi = \theta = 0$ a non-vanishing and divergent result persists, contradicting the naive expectation that the BPS infinite line is trivial. To understand the result and to extract from it the truly gauge-invariant cusp divergence, one have to deal with the renormalization of (cusped) Wilson loops in gauge theories (we extensively discuss this point in Chapter 7). The renormalized upper-left block of the observable is (we will consider from now on the case $N = M$)

$$\begin{aligned} W_\uparrow^{\text{Ren.}} =& 1 + \left(\frac{2\pi}{\kappa}\right) N \left(\frac{\Gamma(\frac{1}{2}-\epsilon)}{4\pi^{3/2-\epsilon}}\right) (\mu L)^{2\epsilon} \left[\frac{1}{\epsilon}\left(\frac{\cos\frac{\theta}{2}}{\cos\frac{\varphi}{2}} - 1\right) - 2\frac{\cos\frac{\theta}{2}}{\cos\frac{\varphi}{2}} \log\left(\sec\left(\frac{\varphi}{2}\right) + 1\right) + \log 4\right] \\ &+ \left(\frac{2\pi}{\kappa}\right)^2 N^2 \left(\frac{\Gamma\left(\frac{1}{2}-\epsilon\right)}{4\pi^{3/2-\epsilon}}\right)^2 (\mu L)^{4\epsilon} \left[\frac{1}{\epsilon} \log\left(\cos\frac{\varphi}{2}\right)^2 \left(\frac{\cos\frac{\theta}{2}}{\cos\frac{\varphi}{2}} - 1\right) + O(1)\right], \end{aligned} \tag{4.35}$$

and the final result for the traced operator can be find summing up the two blocks (that are actually equal at this order) as

$$\mathcal{W}_+^{\text{Ren.}} = \frac{1}{2}(W_\uparrow^{\text{Ren.}} + W_\downarrow^{\text{Ren.}}) \tag{4.36}$$

The quark-antiquark potential is recovered by taking the limit $\varphi \to \pi$ and following the prescription of [137]

$$V_N(R) = \frac{N}{k}\frac{1}{R} - \left(\frac{N}{k}\right)^2 \frac{1}{R} \log\left(\frac{T}{R}\right). \tag{4.37}$$

We observe a logarithmic, non-analytic term in T/R at the second non-trivial order that, as in four dimensions, is expected to disappear when resummation of the perturbative series is performed. We can also perform the opposite limit, taking large imaginary φ, and we recover the universal cusp anomaly

$$\gamma_{\text{cusp}} = \frac{N^2}{k^2}, \tag{4.38}$$

that is the result obtained directly from the light-like cusp [145].

4.2.2.2 The Bremsstrahlung function

As in four-dimensions, one can study the cusp anomalous dimension around its BPS configuration. In [146], the authors proposed an expression for the all-loop Bremsstrahlung function associated to 1/6 BPS lines, that as we have seen are purely bosonic. They considered the planar limit and the BPS point $\varphi = 0$:

$$\mathcal{B}_{1/6} = \frac{1}{4\pi^2}\partial_m \log\langle W_m\rangle \,\big|_{m=1} \tag{4.39}$$

where W_m is the 1/6 BPS Wilson loop wrapping the great circle of the S^3 wound m times. $\langle W_m\rangle$ has been computed exactly through localization and the resulting Bremsstrahlung function can be expanded at weak and strong coupling

$$\begin{aligned}
\mathcal{B}_{1/6} =& \frac{\lambda^2}{2} - \frac{\pi^2\lambda^4}{2} + \frac{47\pi^4\lambda^6}{72} - \frac{17\pi^6\lambda^8}{18} + ... && \lambda << 1 \\
\mathcal{B}_{1/6} =& \frac{\sqrt{2\pi^2\lambda}}{4\pi^2} - \frac{1}{4\pi^2} + \left(\frac{1}{4\pi^2} - \frac{5}{96}\right)\frac{1}{\sqrt{2\pi^2\lambda}} + ... && \lambda >> 1
\end{aligned} \tag{4.40}$$

One could also consider the Bremsstrahlung function associated to 1/2 BPS lines and trying to use some kind of latitude Wilson loop to perform an exact computation, as it has been done in $\mathcal{N} = 4$ SYM. In 3.2.2.1 a "DGRT-like" extension of the Wilson loops in ABJ(M) has been obtained: by exploiting that construction, a Bremsstrahlung function for the 1/2 BPS cusped Wilson line in ABJM has been proposed in [85]

$$\mathcal{B}_{1/2} = \frac{1}{4\pi^2}\partial_\nu \log\langle W_F(\nu)\rangle \,\big|_{\nu=1}; \tag{4.41}$$

here ν is a parameter describing the position of the latitude in space-time and in R-symmetry space ($\nu = 1$ corresponds to the 1/2 BPS circle). The above proposal was supported by perturbative computations and, using the cohomological equivalence between 1/6 BPS and 1/2 BPS loops, the previous prescription can be rephrased in terms of bosonic Wilson loops W_B: a prediction for $\mathcal{B}_{1/2}$ at strong and weak coupling is then possible

$$\begin{aligned}
\mathcal{B}_{1/2} =& \frac{\lambda}{8} - \frac{\pi^2}{48}\lambda^3 + \frac{\pi^4}{60}\lambda^5 - \frac{841\pi^6}{40320}\lambda^7 + ... && \lambda << 1 \\
\mathcal{B}_{1/2} =& \frac{\sqrt{2\lambda}}{4\pi} - \frac{1}{4\pi^2} - \frac{1}{96\pi}\frac{1}{\sqrt{2\lambda}} + ... && \lambda >> 1
\end{aligned} \tag{4.42}$$

In [138] and in [86] this result has been checked at strong-coupling, from string theory, at leading and one-loop order respectively. We are currently trying to check the weak coupling expansion against a direct three-loop evaluation of the 1/2-BPS cusp anomalous dimension. This work is in progress [147].

Chapter 5

Correlators of Wilson loops and chiral primary operators

In Section 3.1.2.1, we have seen that in $\mathcal{N} = 4$ SYM, one can define a particular family of supersymmetric Wilson loops lying on a two-sphere S^2 embedded into the Euclidean spacetime. These operators are generically 1/8-BPS and, with supersymmetric localization arguments, one finds that their quantum correlators is reproduced exactly by a purely perturbative calculation in bosonic 2D Yang-Mills. The computation in the two-dimensional theory can be exactly mapped to simple Gaussian multi-matrix models, leading to an explicit evaluation of the correlators. The relation to 2D YM has been thoroughly checked [109, 148, 108, 149] and extended to the inclusion of 't Hooft loops [150].

More generally localization should apply not only to the Wilson and 't Hooft loops, but to a whole sector of operators that are annihilated by shared supercharges. Furthermore it should concern a family of chiral primary operators inserted on S^2 [106], leading to exact results for their correlators also in presence of Wilson loops. The correlation function of a local operator and a Wilson loop in this sector was firstly computed in [106], supporting and extending the original conjecture of [151] for the correlator of a 1/2-BPS Wilson loop and a chiral primary (see also [152] for the study of the 1/4 BPS case). The correspondence with the zero-instanton sector of two-dimensional YM was checked at tree level, finding consistency with the localization result. In a further development [153] the investigation of the protected sector was extended to the realm of three-point functions mapping the correlator to a Gaussian three-matrix model. Large R-charge and strong coupling limits were also explored, in order to make contact with the string picture, and interesting results have been obtained considering one "heavy" and one "light" primary [154, 155]. These calculations should be considered important for recent advances on three-point functions study through AdS/CFT duality and integrability [156].

In this Chapter we will study the same correlation functions, considered in [106], through the conventional diagrammatic expansion. In Section 5.1 we recall the multi-matrix model describing the correlation functions of Wilson loop and local operators. In Section 5.2 we outline the computation of the correlation function between a chiral primary inserted at the north-pole and a latitude Wilson loop: in particular we organize the diagrams and write down the result for the building blocks that cancel among themselves. In Section 5.3 we consider the case of a chiral primary in an arbitrary position. We show that, computing the expectation value of the ladder diagrams, a position dependent term arises. In this case it is crucial that the sum of interaction diagrams does not vanish but exactly cancels the unexpected contribution, reproducing the matrix-model answer. This Chapter is based on [157].

5.1 Correlation function on S^2 as Gaussian multi-matrix model

The Wilson loops that we consider in this Chapter are generically 1/8-BPS operators constructed in [75] and introduced in Section 3.1.2.1. They are supported on arbitrary closed curves on a S^2 embedded into the Euclidean four-dimensional space. The relevant two-sphere is defined in Cartesian coordinates as

$$x_4 = 0, \qquad \sum_{i=1}^{3} x_i^2 = R^2. \tag{5.1}$$

In the following we will take $R = 1$[1]. For any contour C parametrized by $x^\mu$the explicit form of the operator is given by (3.30).

This is not the end of the story: we can also insert an arbitrary number of local operators on the same S^2 still preserving two supercharges. The local operators doing the job are the following

$$\mathcal{O}_J(x) = \left(\frac{2\pi}{\sqrt{\lambda}}\right)^J \frac{1}{\sqrt{J}} \mathrm{Tr}\Big(x_k \Phi^k(x) + i\Phi^4(x)\Big)^J. \qquad x_k \in S^2\,, \quad k = 1,2,3. \tag{5.2}$$

They are of course ordinary chiral primaries, the orientation in the scalar space being simply correlated with the position of the insertion on S^2. The two-point function of these operators is position independent, as can be easily shown from the direct definition, and it holds

$$\langle \mathcal{O}_J(x)\, \mathcal{O}_{J'}(x) \rangle = \delta_{JJ'}. \tag{5.3}$$

More generally all the n-point functions $\langle \mathcal{O}_{J_1}(x_1) \mathcal{O}_{J_2}(x_2) ... \mathcal{O}_{J_n}(x_n) \rangle$ are position independent [158] and tree-level exact. Any collection of these operators on S^2 also preserves four supercharges. In presence of the Wilson loops (3.30), the system becomes invariant

[1] The dependence from the radius of the two-sphere can be easily reintroduced.

under two supercharges [106] and mixed correlation functions of Wilson loops and local operators can depend non-trivially on the coupling constant, as we will discuss in the next sections. The two preserved supercharges can be combined [106] to obtain the fermionic charge used in the localization procedure of [101]. Mixed correlators of Wilson loops and local operators should therefore be exactly computed by the perturbative sector two-dimensional Yang-Mills theory on S^2 [99], according to the proposal of [75].

Two-dimensional Yang-Mills theory can be exactly solved on any Riemann surface, both using lattice [159] and localization [160] techniques and its zero-instanton sector is described by certain Gaussian matrix models [107]. The relevant four-dimensional correlators can be mapped to

$$\begin{aligned}&\langle W_{\mathcal{R}_1}[C_1]W_{\mathcal{R}_2}[C_2]...\mathcal{O}_{J_1}(x_1)\mathcal{O}_{J_2}(x_2)...\rangle \\ &\qquad = \frac{1}{\mathcal{Z}}\int [dX][dY]\mathrm{Tr}_{\mathcal{R}_1}e^{X_1}\mathrm{Tr}_{\mathcal{R}_2}e^{X_2}...\mathrm{Tr}Y_1^{J_1}\mathrm{Tr}Y_2^{J_2}...e^{S[X,Y]},\end{aligned} \tag{5.4}$$

where the matrix model action $S[X,Y]$ is a quadratic form in X_i,Y_i with coefficients depending on the areas singled out by the Wilson loops and the topology of the system. We remarks that localization, and consequently the matrix model description, does not need the large N limit.

The special case of (5.4) where one consider a single Wilson loop have been studied and checked in the previous sections. In [108, 149] correlators of two Wilson loops were considered and explicit computations at order g_{YM}^6 have confirmed the matrix model result. The generic n-point function for local operators has been studied in [106] where also the mixed correlator between a Wilson loop and a local operator has been computed and studied in different regimes. Three-point functions have been instead carefully scrutinized in [153], expecially at strong coupling and in relation with string computations. Here we concentrate our attention on the mixed two-point correlators:

$$\langle W_{\mathcal{R}}[\mathcal{C}]\mathcal{O}_J(x_1)\rangle = \frac{1}{\mathcal{Z}}\int [dX][dY]\mathrm{Tr}_{\mathcal{R}}e^{X}\mathrm{Tr}Y^J e^{-\frac{A^2}{2g_{YM}}\mathrm{Tr}\left(\frac{A_1}{A_2}Y^2-\frac{2i}{A_2}XY\right)}. \tag{5.5}$$

Here $A_{1,2}$ are the areas single out by the loop on S^2 with $A = A_1 + A_2$ and the local operator is inserted into A_1.

Taking the trace of the Wilson loop (3.30) in the fundamental representation and considering the large N limit, the matrix integral (5.5) can be readily done obtaining

$$\langle W_{\mathcal{R}}[\mathcal{C}]\mathcal{O}_J(x_1)\rangle = \frac{1}{N}\frac{\sqrt{J}}{2^J}\left(\frac{A_2}{A_1}\right)^{\frac{J}{2}} I_J(\sqrt{\tilde{\lambda}}), \tag{5.6}$$

where $\tilde{\lambda} = 4\lambda A_1 A_2/A^2$. We will check this expression at second order in perturbation theory. For loops of arbitrary shape and arbitrary operator insertion this result cannot be recovered simply by resumming the ladder exchanges. On the other hand, to perform a concrete computation, we must limit ourselves to some particular configuration, keeping enough generality to observe non-trivially emerging of the matrix model

answer. We will consider two cases: in the first one the operator is inserted at the north pole and the loop is placed at an arbitrary latitude. Propagators are constant and interactions should cancel. We then consider a second configuration, where the operator is inserted at an arbitrary point and the loop is wrapped at the equator: here, as we will see, interactions are expected to contribute non-trivially to the final result. In both cases we consider the large N limit, in which just planar contributions are taken into account. The inclusion of non-planar terms do not change the cancellation pattern and just modify, at subleading order in N, the final result, as expected from the matrix model picture.

5.2 Perturbative computations I: latitude Wilson loop with an operator insertion at the north-pole of S^2

We begin by considering the correlation function between a Wilson loop lying on a latitude of S^2 and a chiral primary operator inserted at the north pole. In our coordinate system the north pole is $x_N = (0, 0, 1, 0)$ and, as a consequence, the CPO operator assumes a very simple form because just two scalars (Φ^3, Φ^4) appear in its explicit expression. It is useful instead to write the Wilson loop through a generalized connection

$$W[C] = \frac{1}{N}\mathrm{Tr}\mathcal{P}\exp\oint d\tau\ \mathcal{A}(x(\tau)), \tag{5.7}$$

where $\mathcal{A}(x(\tau))$ is the connection introduced in (3.40)

$$\mathcal{A}(x(\tau)) = (iA_\mu \dot{x}^\mu + \sin^2\theta_0\,\Phi^3 - \sin\theta_0\cos\theta_0(\sin\tau\,\Phi^2 + \cos\tau\,\Phi^1)). \tag{5.8}$$

Here θ_0 is the latitude angle in standard polar coordinates and for symmetry reasons we will restrict its range to $[0, \pi/2]$. The position on the latitude is parametrized by τ, ranging from 0 to 2π, and we will denote, in the case of multiple integrations, $x(\tau_i) = x_i$, $\Phi^I(x_i) = \Phi^I_i$ and $\mathcal{A}(x_i) = \mathcal{A}_i$. Using the usual propagators in appendix A, one can notice that the effective propagators entering the actual computation do not depend on the positions along the latitude. More explicitly

$$\begin{aligned}\langle \mathcal{A}_i^{ab}\,\mathcal{A}_j^{cd}\rangle &= \frac{\tilde{\lambda}}{16\pi^2}\frac{\delta^{ad}\delta^{bc}}{N},\\ \langle \mathcal{A}_i^{ab}\,\Phi^{I\,cd}(x_N)\rangle &= \frac{\tilde{\lambda}}{16\pi^2}\frac{\delta_{I3}}{1-\cos\theta_0}\frac{\delta^{ad}\delta^{bc}}{N},\end{aligned} \tag{5.9}$$

where $\tilde{\lambda} = 4\lambda A_1 A_2/A^2 = \lambda\sin^2\theta_0$ for this loop.

5.2.1 Ladder contribution I

Ladder diagrams are the easiest class of perturbative contributions to our correlation function and as in [89], we are able to resum their expectation value to all loop. As the

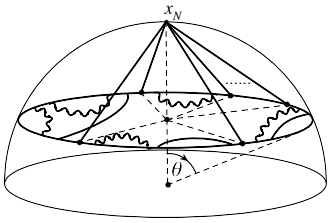

Figure 5.1: A typical ladder diagram for latitude-north pole correlation function.

generalized connection does not depend on the scalar field Φ^4 (see (5.8)), the operator $\mathcal{O}_J$ effectively reduces to

$$\mathcal{O}_J(x_N) = \left(\frac{2\pi}{\sqrt{\lambda}}\right)^J \frac{1}{\sqrt{J}} \mathrm{Tr}\left(\Phi_N^3\right)^J, \tag{5.10}$$

where we use the notation $\Phi_N^3 = \Phi^3(x_N)$.

We have

$$\langle W[C]\mathcal{O}_J(x_N)\rangle_{\text{ladder}} = \frac{1}{N}\sum_{n=0}^{\infty}\int_0^{2\pi} d\tau_1 ... \int_0^{\tau_{2n+J-1}} d\tau_{2n+J} \left\langle \mathrm{Tr}(\mathcal{A}_1 ... \mathcal{A}_{2n+J})\, \mathcal{O}_J(x_N)\right\rangle, \tag{5.11}$$

where n counts the number of ladder insertions in the Wilson loop. Using the effective propagators (5.9) we get

$$\langle \mathrm{Tr}(\mathcal{A}_1 ... \mathcal{A}_{2n+J})\, \mathrm{Tr}(\Phi_N^3)^J\rangle = \left(\frac{\tilde{\lambda}}{16\pi^2}\right)^{n+J} \left(\frac{1}{1-\cos\theta_0}\right)^J N_{\text{tot}}, \tag{5.12}$$

where N_{tot} is the total number of planar graphs. Any such diagram originates from Wick contractions of this kind

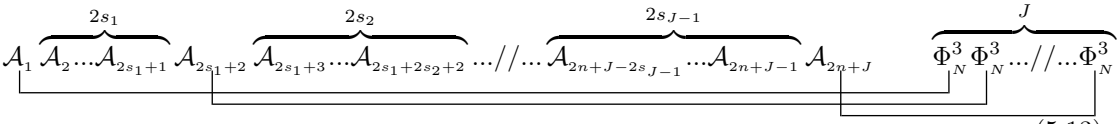

(5.13)

where $\sum_{i=1}^{J-1} s_i = n$ and the $2s$ generalized connections $\mathcal{A}_i$ under the brackets have to be contracted among themselves. According to [89], as we have seen in Section (3.3.1), the number of these planar contractions is

$$N_s = \frac{(2s)!}{(s+1)!s!}. \tag{5.14}$$

Therefore the total number of planar graphs is

$$N_{\text{tot}} = (2n+J)\sum_{s_1=0}^{n} N_{s_1} \sum_{s_2=0}^{n-s_1} N_{s_2} \sum_{s_3=0}^{n-s_1-s_2} ...//... \sum_{s_{J-1}=0}^{n-\sum_{i=1}^{J-2} s_i} N_{s_{J-1}} N_{n-\sum_{i=1}^{J-2} s_i - s_{J-1}}, \tag{5.15}$$

where the factor $(2n+J)$ comes from the cyclicity of the trace. Using the recurrence relation (3.72), we can perform the sum over s_{J-1}, obtaining

$$\begin{aligned}&(2n+J)\sum_{s_1=0}^{n}\frac{2s_1!}{s_1!(s_1+1)!}\sum_{s_2=0}^{n-s_1}\frac{2s_2!}{s_2!(s_2+1)!}\sum_{s_3=0}^{n-s_1-s_2}...//...\\&\times\left[\sum_{s_{J-2}=0}^{n-\sum_{i=1}^{J-3}s_i+1}N_{s_{J-2}}N_{n-\sum_{i=1}^{J-3}s_i+1-s_{J-2}}-\frac{(2n-2\sum_{i=1}^{J-3}s_i+2)!}{(n-\sum_{i=1}^{J-3}s_i+1)!(n-\sum_{i=1}^{J-3}s_i+2)!}\right].\end{aligned}\tag{5.16}$$

Iterating this process $(J-3)$-times, we get

$$N_{\text{tot}}=\frac{J(2n+J)!}{n!(n+J)!}.\tag{5.17}$$

Substituting this result into the (5.12) and performing the trivial integrations, we can write

$$\begin{aligned}\langle W[C]\,\mathcal{O}_J(x_N)\rangle_{\text{ladder}}=&\frac{1}{N}\frac{\sqrt{J}}{2^J}\left(\frac{A_2}{A_1}\right)^{J/2}\sum_{n=0}^{\infty}\frac{1}{n!(n+J)!}\left(\frac{\sqrt{\tilde{\lambda}}}{2}\right)^{2n+J}\\=&\frac{1}{N}\frac{\sqrt{J}}{2^J}\left(\frac{A_2}{A_1}\right)^{J/2}I_J(\sqrt{\tilde{\lambda}}).\end{aligned}\tag{5.18}$$

where $\frac{A_2}{A_1}=\cot^2\frac{\theta_0}{2}$. Thus the sum of all ladder contribution reproduces the localization result (5.6).

In the following we will restrict our investigation to the case $J=2$ and at order λ^2. This choice will simplify our analysis and at two-loop level does not represent a real limitation: no new class of perturbative diagrams would enter the computation and the general case should be tamed by simple combinatorics. Indeed the ladder contribution for $J=2$ at order λ^2 is

$$\langle W[\mathcal{C}]\mathcal{O}_2(x_N)\rangle_{\text{ladder}}=\frac{1}{N}\frac{\tilde{\lambda}^2}{192\sqrt{2}}\left(\frac{A_2}{A_1}\right),\tag{5.19}$$

5.2.2 Interacting contributions I

We discuss now the effect of interaction vertices to the correlation function at order λ^2: it is the crucial part of the computation. We expect indeed that their total contribution sums to zero since, for the particular configuration we are considering, ladder diagrams are enough to recover the matrix model expression, as shown by (5.19) and in general by (5.18). The different interacting diagrams are grouped in four classes, denoted by **H**, **X**, **IY** and **O**, symbols that actually resemble their graphical form (see Figure (5.2)).

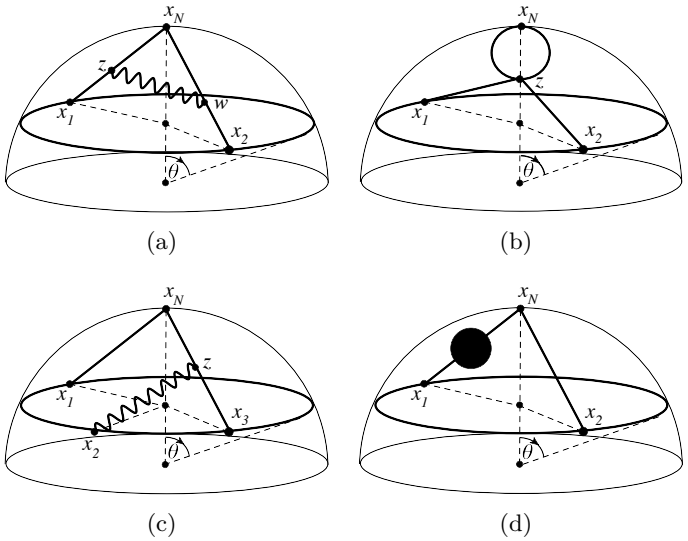

Figure 5.2: Diagrams with interaction vertices at order λ^2: (a) **H**-contribution, (b) **X**-contribution, (c) **IY**-contribution and (d) **O**-contribution; z and w denote the position of interaction vertices.

The H-contribution: We first consider the diagrams of type **H**: the interaction vertices are connected here by a gluon propagator and its form is

$$-\frac{2}{(2\pi)^2\lambda}\int_0^{2\pi} d\tau_1 \int_0^{\tau_1} d\tau_2 \int d^4z\, d^4w\, D(z-w)\, \langle \mathrm{Tr}(\mathcal{A}_1\mathcal{A}_2)\, \mathrm{Tr}(\Phi_z^I \partial_z^\mu \Phi_z^I [\Phi_w^J, \partial_w^\mu \Phi_w^J])\, \mathcal{O}_2(x_N)\rangle, \tag{5.20}$$

where $D(x-y) = \frac{1}{(x-y)^2}$. Due to the explicit form of the CPO and of the Wilson loop we have non vanishing contributions from $I = J = 3$. Defining the composite operator $\mathcal{O}_2(x_N)$ via point-splitting

$$(\Phi(x_N))^2 = \lim_{\substack{y_1\to x_N \\ y_2\to x_N}} \Phi(y_1)\Phi(y_2), \tag{5.21}$$

a straightforward manipulation leads to

$$\begin{aligned}
\mathbf{H} =& \frac{\tilde{\lambda}^2}{2^2\sqrt{2}(2\pi)^8 N}\int_0^{2\pi} d\tau_1 \int_0^{\tau_1} d\tau_2 \int d^4z\, d^4w\, D(z-w) \\
&\times \Big[\Big(\partial_{x_1} - \partial_{y_1}\Big)\cdot\Big(\partial_{x_2} - \partial_{y_2}\Big) D(z-y_1)D(w-y_2)D(z-x_1)D(w-x_2) \\
&+ \Big(\partial_{x_2} - \partial_{y_1}\Big)\cdot\Big(\partial_{x_1} - \partial_{y_2}\Big) D(w-y_1)D(z-y_2)D(z-x_1)D(w-x_2)\Big] \\
=& \frac{(2\pi)^2\tilde{\lambda}^2}{2^2\sqrt{2}N}\int_0^{2\pi} d\tau_1 \int_0^{2\pi} d\tau_2\, (\partial_{x_1} - \partial_{y_1})\cdot(\partial_{x_2} - \partial_{y_2})\, \mathcal{H}(x_1, y_1; x_2, y_2).
\end{aligned} \tag{5.22}$$

Here we have used the symmetry $z \leftrightarrow w$, symmetrized the expression in the exchange $x_1 \leftrightarrow x_2$ and defined

$$\mathcal{H}(x_1,x_2;x_3,x_4) = \int \frac{d^4z\, d^4w}{(2\pi)^{10}} D(z-x_1)D(z-x_2)D(z-w)D(w-x_3)D(w-x_4). \quad (5.23)$$

Taking advantage of the identity [161]

$$\begin{aligned}
&(\partial_{x_1}-\partial_{y_1})\cdot(\partial_{x_2}-\partial_{y_2})\,\mathcal{H}(x_1,y_1;x_2,y_2) \\
&\quad= \frac{1}{(x_1-y_1)^2(x_2-y_2)^2}\Bigg[\mathcal{X}(x_1,y_1,x_2,y_2)\Big((x_1-x_2)^2(y_1-y_2)^2-(x_1-y_2)^2(x_2-y_1)^2\Big) \\
&\qquad+\frac{1}{(2\pi)^2}\Big(\mathcal{G}(x_1;x_2,y_2)-\mathcal{G}(y_1;x_2,y_2)+\mathcal{G}(x_2;x_1,y_1)-\mathcal{G}(y_2;x_1,y_1)\Big)\Bigg],
\end{aligned} \quad (5.24)$$

where

$$\begin{aligned}
\mathcal{G}(x_1;x_2,x_3) &= \mathcal{Y}(x_1,x_2,x_3)[(x_1-x_3)^2-(x_1-x_2)^2], \\
\mathcal{X}(x_1,x_2,x_3,x_4) &= \frac{1}{(2\pi)^8}\int \frac{d^4z}{(z-x_1)^2(z-x_2)^2(z-x_3)^2(z-x_4)^2}, \\
\mathcal{Y}(x_1,x_2,x_3) &= \frac{1}{(2\pi)^6}\int \frac{d^4z}{(z-x_1)^2(z-x_2)^2(z-x_3)^2} \equiv \mathcal{I}_1(x_1-x_3,x_2-x_3),
\end{aligned} \quad (5.25)$$

and setting $y_1 = y_2 = x_N$ we arrive at

$$\begin{aligned}
\mathbf{H} = &-\frac{\tilde{\lambda}^2}{2^2\sqrt{2}N}\oint d\tau_1 d\tau_2\; \mathcal{X}(x_1,x_N,x_2,x_N)+ \\
&+\frac{\tilde{\lambda}^2}{2^2\sqrt{2}N}\frac{1}{1-\cos\theta_0}\oint d\tau_1 d\tau_2\,\Big[\mathcal{I}_1(x_1-x_N,x_2-x_N)+\mathcal{I}_1(0,x_2-x_N)\Big] \\
&-\frac{\tilde{\lambda}^2}{2^3\sqrt{2}N}\frac{1}{(1-\cos\theta_0)^2}\oint d\tau_1 d\tau_2\;\; \mathcal{I}_1(x_1-x_2,x_N-x_2)\,(x_1-x_2)^2.
\end{aligned} \quad (5.26)$$

The X-contribution: The **X** diagram comes entirely from the four-point scalar vertex

$$\frac{1}{2\lambda}\int_0^{2\pi} d\tau_1 \int_0^{\tau_1} d\tau_2 \int d^4z\, \langle \mathrm{Tr}(\mathcal{A}_1\mathcal{A}_2)\; \mathrm{Tr}([\Phi_z^I,\Phi_z^J]^2)\; \mathcal{O}_2(x_N)\rangle. \quad (5.27)$$

The only non vanishing terms arise from $\mathcal{A}_i = \Phi_i^3$ and $I,J = 3,4$, giving directly

$$\mathbf{X} = \frac{(2\pi)^2\tilde{\lambda}^2}{2^2\sqrt{2}N}\int_0^{2\pi} d\tau_1 \int_0^{2\pi} d\tau_2\; \mathcal{X}(x_N,x_N,x_1,x_2). \quad (5.28)$$

The IY-contribution: We examine the most elaborate part of the two-loop computation, involving the presence of three distinct contour integrations

$$\frac{i2}{3\lambda}\oint d\tau_1 d\tau_2 d\tau_3\,\eta(\tau_1,\tau_2,\tau_3)\int d^4z\,\langle \mathrm{Tr}(\mathcal{A}_1\mathcal{A}_2\mathcal{A}_3)\,\mathrm{Tr}(\partial_z^\nu\Phi_z[A_z^\nu,\Phi_z])\,\mathcal{O}_2(x_N)\rangle, \tag{5.29}$$

where to take into account the appropriate ordering we have defined

$$\eta(\tau_1,\tau_2,\tau_3)=\theta(\tau_1-\tau_2)\theta(\tau_2-\tau_3)+\text{cyclic permutations}. \tag{5.30}$$

Computing the contractions we get

$$\begin{aligned}\mathbf{IY}=&-\frac{\tilde\lambda^2}{2^2\sqrt{2}N}\oint d\tau_1 d\tau_2 d\tau_3\,\epsilon(\tau_1,\tau_2,\tau_3)\,\dot x_2^\mu\,D(x_1-x_N)\\&\times\int\frac{d^4z}{(2\pi)^6}\,D(x_2-z)\Big[D(x_N-z)\partial_z D(x_3-z)-\partial_z D(x_N-z)D(x_3-z)\Big],\end{aligned} \tag{5.31}$$

with

$$\epsilon(\tau_1,\tau_2,\tau_3)=\eta(\tau_1,\tau_2,\tau_3)-\eta(\tau_2,\tau_1,\tau_3). \tag{5.32}$$

Performing an integration by parts, we can rewrite **IY** as

$$\begin{aligned}\mathbf{IY}=&\frac{\tilde\lambda^2}{2^2\sqrt{2}N}\oint d\tau_1 d\tau_2 d\tau_3\,\epsilon(\tau_1,\tau_2,\tau_3)\,\dot x_2^\mu\,D(x_1-x_N)(2\partial_3+\partial_2)\mathcal{Y}(x_2,x_3,x_N)\\=&\frac{\tilde\lambda^2}{2^2\sqrt{2}N}\frac{1}{1-\cos\theta_0}\Big\{\oint d\tau_1 d\tau_3\Big[\mathcal{I}_1(x_1-x_N,x_3-x_N)-\mathcal{I}_1(0,x_3-x_N)\Big]\\&+\oint d\tau_1 d\tau_2 d\tau_3\,\epsilon(\tau_1,\tau_2,\tau_3)\,\dot x_2^\mu\,\partial_3\mathcal{I}_1(x_3-x_N,x_2-x_N)\Big\},\end{aligned} \tag{5.33}$$

where we have used

$$\frac{\partial}{\partial\tau_2}\epsilon(\tau_1,\tau_2,\tau_3)=2(\delta(\tau_2-\tau_3)-\delta(\tau_1-\tau_2)). \tag{5.34}$$

The triple integral can be massaged exploiting the trivial identity

$$\frac{\tilde\lambda^2}{2^2\sqrt{2}N}\frac{1}{1-\cos\theta_0}\oint d\tau_1 d\tau_2 d\tau_3\,\frac{d}{d\tau_2}\Big[\epsilon(\tau_1,\tau_2,\tau_3)\,\mathcal{I}_2(x_3-x_N,x_2-x_N)\Big]=0, \tag{5.35}$$

where the function $\mathcal{I}_2$ is defined in the appendix A. Upon subtracting (5.35) to (5.33) we obtain

$$\begin{aligned}\mathbf{IY}=\frac{\tilde\lambda^2}{2^2\sqrt{2}N}\frac{1}{1-\cos\theta_0}\Big\{&\oint d\tau_1 d\tau_3\Big[\mathcal{I}_1(x_1-x_N,x_3-x_N)-\mathcal{I}_1(0,x_3-x_N)\Big]\\&-2\oint d\tau_1 d\tau_3\Big[\mathcal{I}_2(x_3-x_N,x_3-x_N)-\mathcal{I}_2(x_3-x_N,x_1-x_N)\Big]\\&+\oint d\tau_1 d\tau_2 d\tau_3\,\epsilon(\tau_1,\tau_2,\tau_3)\,\dot x_2^\mu\,V_\mu(x_3-x_N,x_2-x_N)\Big\},\end{aligned} \tag{5.36}$$

with

$$V^{\mu}(x,y) \equiv \partial_x^{\mu}\,\mathcal{I}_1(x,y) - \partial_y^{\mu}\,\mathcal{I}_2(x,y). \tag{5.37}$$

With the help of equation (A.15) we find

$$\dot{x}_2^{\mu}\,V_{\mu}(x_3-x_N,x_2-x_N) = -\frac{1}{32\pi^4(x_3-x_N)^2}\frac{d}{dt_2}\Bigg[\mathrm{Li}_2\left(1-\frac{(x_3-x_2)^2}{(x_2-x_N)^2}\right) + \frac{1}{2}\log^2\left[\frac{(x_3-x_2)^2}{(x_2-x_N)^2}\right] - \frac{1}{2}\log^2\left[\frac{(x_3-x_2)^2}{(x_3-x_N)^2}\right]\Bigg]. \tag{5.38}$$

Inserting this result into (5.36) and integrating by parts we arrive at the final expression

$$\begin{aligned}\mathbf{IY} = \frac{\tilde{\lambda}^2}{2^2\sqrt{2}N}\frac{1}{1-\cos\theta_0}\Bigg\{ &\oint d\tau_1 d\tau_3\left[\mathcal{I}_1(x_1-x_N,x_3-x_N)-\mathcal{I}_1(0,x_3-x_N)\right]\\ &-2\oint d\tau_1 d\tau_3\left[\mathcal{I}_2(x_3-x_N,x_3-x_N)-\mathcal{I}_2(x_3-x_N,x_1-x_N)\right]\\ &-\frac{1}{2^6\pi^4}\frac{1}{1-\cos\theta_0}\oint d\tau_1 d\tau_3\left[\mathrm{Li}_2\left(1-\frac{\sin^2\theta_0}{1-\cos\theta_0}(1-\cos\tau_{31})\right)-\frac{\pi^2}{6}\right]\Bigg\},\end{aligned} \tag{5.39}$$

where $\tau_{ij}=\tau_i-\tau_j$.

The O-contribution: The last interacting diagram comes from the self-energy of the scalar propagator: borrowing directly the result from [89], we write down

$$\mathbf{O} = -\frac{\tilde{\lambda}^2}{2\sqrt{2}N}\frac{1}{1-\cos\theta_0}\oint d\tau_1 d\tau_2\ \mathcal{I}_1(0,x_2-x_N). \tag{5.40}$$

5.2.3 Summing up interactions I

Adding up the contributions of all the interacting diagrams we obtain:

$$\begin{aligned}\langle W[\mathcal{C}]\mathcal{O}_2(x_N)\rangle_{\mathrm{int}} = \mathbf{H}+\mathbf{O}+\mathbf{X}+\mathbf{IY} = &\\ -\frac{\tilde{\lambda}^2}{2^3\sqrt{2}N}\frac{1}{(1-\cos\theta_0)^2}&\oint d\tau_1\,d\tau_2\ \ \mathcal{I}_1(x_1-x_2,x_N-x_2)\,(x_1-x_2)^2\\ +\frac{\tilde{\lambda}^2}{2\sqrt{2}N}\frac{1}{1-\cos\theta_0}&\oint d\tau_1\,d\tau_2\ \left[\mathcal{I}_1(x_1-x_N,x_2-x_N)+\mathcal{I}_2(x_2-x_N,x_1-x_N)\right]\\ -\frac{\tilde{\lambda}^2}{2\sqrt{2}N}\frac{1}{1-\cos\theta_0}&\oint d\tau_1\,d\tau_2\ \left[\mathcal{I}_2(x_2-x_N,x_2-x_N)+\mathcal{I}_1(0,x_2-x_N)\right]\\ -\frac{\tilde{\lambda}^2}{2^8\pi^4\sqrt{2}N}\frac{1}{(1-\cos\theta_0)^2}&\oint d\tau_1 d\tau_2\left[\mathrm{Li}_2\left(1-\frac{\sin^2\theta_0}{1-\cos\theta_0}(1-\cos\tau_{21})\right)-\frac{\pi^2}{6}\right].\end{aligned} \tag{5.41}$$

Remarkably, no triple contour integration is present in this final expression. The integrals in (5.41), denoted by $P_{1,2,3,4}$, are evaluated in appendix B.1. Using these results we find

$$\langle W[\mathcal{C}]\mathcal{O}_2(x_N)\rangle_{\rm int} = -\frac{\tilde{\lambda}^2}{2^3\sqrt{2}N}\frac{1}{(1-\cos\theta_0)^2}\left[P_1 - \frac{1-\cos\theta_0}{4}(P_2-P_3) + \frac{P_4}{2^5\pi^4} - \frac{1}{3\cdot 2^4}\right] = 0 \tag{5.42}$$

for any θ_0, as expected. We confirm therefore that at order λ^2, the correlator of the latitude Wilson loop with $\mathcal{O}_2$ at the north-pole is

$$\langle W[\mathcal{C}]\mathcal{O}_2(x_N)\rangle = \langle W[\mathcal{C}]\mathcal{O}_2(x_N)\rangle_{\rm ladder} = \frac{1}{N}\frac{\tilde{\lambda}^2}{192\sqrt{2}}\left(\frac{A_2}{A_1}\right). \tag{5.43}$$

5.3 Perturbative computations II: equator Wilson loop with an operator insertion at an arbitrary point of S^2

In this Section we consider the correlation function of a Wilson loop shaped on the equator of S^2 (3.35) and the CPO operator (5.2) inserted on the sphere at the point $x_{\mathcal{O}} = (\sin\phi, 0, \cos\phi)$ (one of the coordinates can be taken to zero by symmetry reasons). Without loss of generality, we also assume that the operator is located in the north hemisphere, and we consider $0 \leq \phi \leq \pi/2$. Thus the CPO depends on the three scalars Φ^I, with $I = 1, 3, 4$ and the Wilson loop is written as an integral of the generalized connection as in (5.7) with

$$\mathcal{A}(x(\tau)) = (iA_\mu \dot{x}^\mu + \Phi^3). \tag{5.44}$$

The effective propagators are now the following:

$$\begin{aligned} \langle \mathcal{A}_i^{ab}\, \mathcal{A}_j^{cd}\rangle &= \frac{\lambda}{16\pi^2}\frac{\delta^{ad}\delta^{bc}}{N}, \\ \langle \mathcal{A}_i^{ab}\, \Phi^{I\,cd}(x_{\mathcal{O}})\rangle &= \frac{\lambda}{16\pi^2} f(\tau_i)\cos\phi\frac{\delta^{ad}\delta^{bc}}{N}\,\delta_{I3}, \end{aligned} \tag{5.45}$$

where

$$f(\tau_i) = \frac{1}{1-\sin\phi\cos\tau_i}. \tag{5.46}$$

Notice that a new and relevant feature appears in this case: effective propagators connecting the CPO and the Wilson loop depend explicitly on the integration parameters τ_i. As we will see soon, this aspect complicates considerably the computations and, crucially, destroys the naive matrix model picture based on summing up ladder diagrams and neglecting interaction vertices. Unfortunately we will not able to perform all the calculations analytically and we will resort to numerical integration for one particular contribution. We again limit ourselves to CPO with $J = 2$.

5.3.1 Ladder contribution II

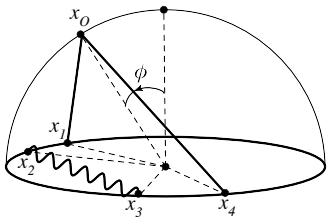

Figure 5.3: Ladder diagram for equator-arbitrary point correlation function at order λ^2.

At the order λ^2, the ladder contribution arises from

$$\langle W[\mathcal{C}]\mathcal{O}_2(x_\mathcal{O})\rangle_{\text{ladder}} = \frac{1}{N}\int_0^{2\pi} d\tau_1 \int_0^{\tau_1} d\tau_2 \int_0^{\tau_2} d\tau_3 \int_0^{\tau_3} d\tau_4 \,\langle \text{Tr}(\mathcal{A}_1\mathcal{A}_2\mathcal{A}_3\mathcal{A}_4)\,\mathcal{O}_2(x_\mathcal{O})\rangle. \tag{5.47}$$

By performing the contractions and using (5.45), we find

$$\frac{\lambda^2\cos^2\phi}{2^9\sqrt{2}\pi^4 N}\int_0^{2\pi} d\tau_1 ... \int_0^{\tau_3} d\tau_4 \left[f(\tau_1)f(\tau_4)+f(\tau_1)f(\tau_2)+f(\tau_2)f(\tau_3)+f(\tau_3)f(\tau_4)\right]. \tag{5.48}$$

By simply changing the integration order, we can evaluate two integrals, ending up with

$$\begin{aligned}&\frac{\lambda^2\cos^2\phi}{2^9\sqrt{2}\pi^4 N}\int_0^{2\pi} d\tau_1\, f(\tau_1)\int_0^{\tau_1} d\tau_2\, f(\tau_2)\left[(\tau_1-\tau_2)^2+2\pi^2-2\pi(\tau_1-\tau_2)\right]\\ =&\frac{\lambda^2\cos^2\phi}{2^9\sqrt{2}\pi^4 N}\left[\mathcal{J}_2\mathcal{J}_0-\mathcal{J}_1^2+\pi^2\mathcal{J}_0^2-2\pi\mathcal{J}_1\mathcal{J}_0+4\pi\tilde{\mathcal{J}}\right],\end{aligned} \tag{5.49}$$

where $\mathcal{J}_n$ e $\tilde{\mathcal{J}}$ are defined and computed in appendix B.2. Using these results we get

$$\begin{aligned}&\langle W[\mathcal{C}]\mathcal{O}_2(x_\mathcal{O})\rangle_{\text{ladder}} =\\ &=\frac{\lambda^2}{192\sqrt{2}N}-\frac{\lambda^2}{2^6\sqrt{2}\pi^2}\left[\log\left(\frac{2\sigma}{1+\sigma}\right)^2+\log\left(\frac{1+\sigma}{2}\right)^2+2\text{Li}_2\left(\frac{1-\sigma}{2}\right)+2\text{Li}_2\left(\frac{\sigma-1}{2\sigma}\right)\right],\end{aligned} \tag{5.50}$$

where $\sigma=\sqrt{\frac{1+\sin\phi}{1-\sin\phi}}$.

The first term in the above expression already gives the matrix model result, *i.e.* the second order term in the expansion of the Bessel function $I_2(\sqrt{\lambda})$. Therefore the remaining term

$$\mathbf{L}\equiv-\frac{\lambda^2}{2^6\sqrt{2}\pi^2}\left[\log\left(\frac{2\sigma}{1+\sigma}\right)^2+\log\left(\frac{1+\sigma}{2}\right)^2+2\text{Li}_2\left(\frac{1-\sigma}{2}\right)+2\text{Li}_2\left(\frac{\sigma-1}{2\sigma}\right)\right] \tag{5.51}$$

should cancel the interacting contributions.

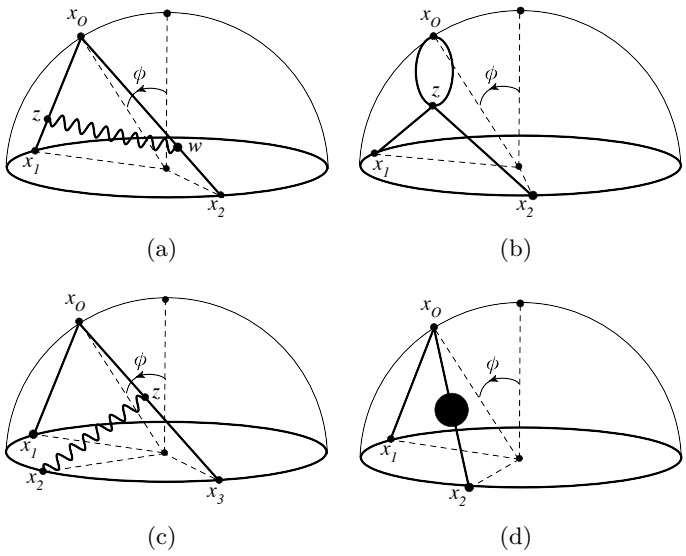

Figure 5.4: Diagrams with interaction vertices at order λ^2: (a) **H**-contribution, (b) **X**-contribution, (c) **IY**-contribution and (d) **O**-contribution; z and w denote the position of interaction vertices.

5.3.2 Interacting contributions II

We attempt here the computation of the diagrams containing interaction vertices: due to the asymmetry of our configuration we will not be able to obtain an expression only in terms of double-integrals, as in the previous case. We have truly to face triple contour integrations, and moreover part of the job must be done numerically.

The H, X and O contributions: The procedure to evaluate the diagrams **H**, **O** e **X** is very similar to the previous case. Their structure remains basically unchanged, the only relevant difference being the appearance of contour dependent propagators. We get

$$\begin{aligned}\mathbf{H} = &-\frac{(2\pi)^2\lambda^2\cos^2\phi}{2^2\sqrt{2}N}\oint d\tau_1 d\tau_2\ \mathcal{X}(x_1,x_{\mathcal{O}},x_2,x_{\mathcal{O}})\\ &+\frac{\lambda^2\cos^2\phi}{2^2\sqrt{2}N}\int_0^{2\pi}d\tau_1\, f(\tau_1)\int_0^{2\pi}d\tau_2\,\Big[\mathcal{I}_1(x_1-x_{\mathcal{O}},x_2-x_{\mathcal{O}})+\mathcal{I}_1(0,x_2-x_{\mathcal{O}})\Big]\\ &-\frac{\lambda^2\cos^2\phi}{2^3\sqrt{2}N}\int_0^{2\pi}d\tau_1\, f(\tau_1)\int_0^{2\pi}d\tau_2\, f(\tau_2)\ \mathcal{I}_1(x_1-x_2,x_{\mathcal{O}}-x_2)\,(x_1-x_2)^2,\end{aligned} \tag{5.52}$$

$$\mathbf{X} = \frac{(2\pi)^2\lambda^2\cos^2\phi}{2^2\sqrt{2}N}\oint d\tau_1 d\tau_2\ \mathcal{X}(x_{\mathcal{O}}, x_{\mathcal{O}}, x_1, x_2), \tag{5.53}$$

$$\mathbf{O} = -\frac{\lambda^2\cos^2\phi}{2\sqrt{2}N}\int_0^{2\pi} d\tau_1\, f(\tau_1)\int_0^{2\pi} d\tau_2\ \mathcal{I}_1(0, x_2 - x_{\mathcal{O}}), \tag{5.54}$$

with the functions $\mathcal{X}$ and $\mathcal{I}_1$ defined in (5.25).

The IY-contribution: We have seen in the previous section, that the **IY** diagram contains triple integrations along the circuit. In that case we have been able, through some judicious manipulation, to reduce the problem to double integrals. Now, with the CPO operator in an arbitrary position on the sphere, this technique works only partially.

Repeating the same steps as in Section 5.2 we arrive at the expression

$$\mathbf{IY} = \frac{\lambda^2\cos^2\phi}{2^2\sqrt{2}N}\oint d\tau_1\, f(\tau_1)\Big\{\oint d\tau_3\left[\mathcal{I}_1(x_1 - x_{\mathcal{O}}, x_3 - x_{\mathcal{O}}) - \mathcal{I}_1(0, x_3 - x_{\mathcal{O}})\right] + \oint d\tau_2 d\tau_3\,\epsilon(\tau_1,\tau_2,\tau_3)\,\dot{x}_2^{\mu}\,\partial_3\mathcal{I}_1(x_3 - x_{\mathcal{O}}, x_2 - x_{\mathcal{O}})\Big\}. \tag{5.55}$$

We can still massage the triple integral using an identity similar to (5.35), obtaining

$$\mathbf{IY} = \frac{\lambda^2\cos^2\phi}{2^2\sqrt{2}N}\oint d\tau_1\, f(\tau_1)\Big\{\oint d\tau_3\left[\mathcal{I}_1(x_1 - x_{\mathcal{O}}, x_3 - x_{\mathcal{O}}) - \mathcal{I}_1(0, x_3 - x_{\mathcal{O}})\right] - 2\oint d\tau_3\Big[\mathcal{I}_2(x_3 - x_{\mathcal{O}}, x_3 - x_{\mathcal{O}}) - \mathcal{I}_2(x_3 - x_{\mathcal{O}}, x_1 - x_{\mathcal{O}})\Big] + \oint d\tau_2 d\tau_3\,\epsilon(\tau_1,\tau_2,\tau_3)\,\dot{x}_2^{\mu}\,V_{\mu}(x_3 - x_{\mathcal{O}}, x_2 - x_{\mathcal{O}})\Big\}. \tag{5.56}$$

Using again (A.15), we end up with

$$\begin{aligned}\mathbf{IY} = \frac{\lambda^2\cos^2\phi}{2^2\sqrt{2}N}\oint d\tau_1\, f(\tau_1)\Big\{&\oint d\tau_3\left[\mathcal{I}_1(x_1 - x_{\mathcal{O}}, x_3 - x_{\mathcal{O}}) - \mathcal{I}_1(0, x_3 - x_{\mathcal{O}})\right] \\ &- 2\oint d\tau_3\Big[\mathcal{I}_2(x_3 - x_{\mathcal{O}}, x_3 - x_{\mathcal{O}}) - \mathcal{I}_2(x_3 - x_{\mathcal{O}}, x_1 - x_{\mathcal{O}})\Big] \\ &- \frac{1}{2^6\pi^4}\oint d\tau_3\, f(\tau_3)\left[\mathrm{Li}_2\Big(1 - (1-\cos\tau_{31})f(\tau_1)\Big) - \frac{\pi^2}{6}\right] \\ &+ \frac{1}{2^7\pi^4}\oint d\tau_2 d\tau_3\,\epsilon(\tau_1,\tau_2,\tau_3)\, f(\tau_3)\,\cot\left(\frac{\tau_{32}}{2}\right)\log\left(\frac{f(\tau_3)}{f(\tau_2)}\right)\Big\}.\end{aligned} \tag{5.57}$$

Unfortunately, in this case the awkward triple integral cannot be avoided.

5.3.3 Summing up interactions II

The evaluation of the whole interacting contributions requires some care: first of all let us collect the different diagrams

$$\begin{aligned}\langle W[\mathcal{C}]\mathcal{O}_2(x_{\mathcal{O}})\rangle_{\rm int} = \mathbf{H}+\mathbf{O}+\mathbf{X}+\mathbf{IY} = \\ -\frac{\lambda^2\cos^2\phi}{2^3\sqrt{2}N}\oint d\tau_1 d\tau_2\, f(\tau_1)\, f(\tau_2)\;\; \mathcal{I}_1(x_1-x_2, x_{\mathcal{O}}-x_2)\,(x_1-x_2)^2 \\ +\frac{\lambda^2\cos^2\phi}{2\sqrt{2}N}\oint d\tau_1 d\tau_2\, f(\tau_1)\,\Big[\mathcal{I}_1(x_1-x_{\mathcal{O}}, x_2-x_{\mathcal{O}})+\mathcal{I}_2(x_2-x_{\mathcal{O}}, x_1-x_{\mathcal{O}})\Big] \\ -\frac{\lambda^2\cos^2\phi}{2^8\pi^4\sqrt{2}N}\oint d\tau_1 d\tau_2\, f(\tau_1)\, f(\tau_2)\Big[\mathrm{Li}_2\Big(1-(1-\cos\tau_{21})f(\tau_1)\Big)-\frac{\pi^2}{6}\Big] \\ -\frac{\lambda^2\cos^2\phi}{2\sqrt{2}N}\oint d\tau_1 d\tau_2\, f(\tau_1)\,\Big[\mathcal{I}_2(x_2-x_{\mathcal{O}}, x_2-x_{\mathcal{O}})+\mathcal{I}_1(0, x_2-x_{\mathcal{O}})\Big] \\ +\frac{\lambda^2\cos^2\phi}{2^9\pi^4\sqrt{2}N}\oint d\tau_1 d\tau_2 d\tau_3\,\epsilon(\tau_1,\tau_2,\tau_3)\, f(\tau_1)\, f(\tau_3)\,\cot\Big(\frac{\tau_{32}}{2}\Big)\log\Big(\frac{f(\tau_3)}{f(\tau_2)}\Big).\end{aligned} \tag{5.58}$$

Using the definitions in appendix A we can simplify this expression noticing that

$$\begin{aligned}\Big[\mathcal{I}_2(x_2-x_{\mathcal{O}}, x_2-x_{\mathcal{O}})+\mathcal{I}_1(0, x_2-x_{\mathcal{O}})\Big] =& -\lim_{\epsilon\to 0}\frac{\csc(\pi\epsilon)(\Gamma(\epsilon)-2\Gamma(1-\epsilon)\Gamma(2\epsilon))}{128\pi^{3+2\epsilon}[(x_2-x_{\mathcal{O}})^2]^{1+2\epsilon}\Gamma(1-\epsilon)} \\ =& \frac{1}{2^7\pi^4}f(\tau_2)\frac{\pi^2}{6}.\end{aligned} \tag{5.59}$$

Then we rewrite (5.58) as a sum of two terms

$$\begin{aligned}\langle W[\mathcal{C}]\mathcal{O}_2(x_{\mathcal{O}})\rangle_{\rm int} = \\ \left.\begin{aligned}&-\frac{\lambda^2\cos^2\phi}{2^3\sqrt{2}N}\oint d\tau_1 d\tau_2\, f(\tau_1)\, f(\tau_2)\;\; \mathcal{I}_1(x_1-x_2, x_{\mathcal{O}}-x_2)\,(x_1-x_2)^2 \\ &+\frac{\lambda^2\cos^2\phi}{2\sqrt{2}N}\oint d\tau_1 d\tau_2\, f(\tau_1)\,\Big[\mathcal{I}_1(x_1-x_{\mathcal{O}}, x_2-x_{\mathcal{O}})+\mathcal{I}_2(x_2-x_{\mathcal{O}}, x_1-x_{\mathcal{O}})\Big] \\ &-\frac{\lambda^2\cos^2\phi}{2^8\pi^4\sqrt{2}N}\oint d\tau_1 d\tau_2\, f(\tau_1)\, f(\tau_2)\Big[\mathrm{Li}_2\Big(1-(1-\cos\tau_{21})f(\tau_1)\Big)\Big]\end{aligned}\right\}\text{A} \\ +\frac{\lambda^2\cos^2\phi}{2^9\pi^4\sqrt{2}N}\oint d\tau_1 d\tau_2 d\tau_3\,\epsilon(\tau_1,\tau_2,\tau_3)\, f(\tau_1)\, f(\tau_3)\,\cot\Big(\frac{\tau_{32}}{2}\Big)\log\Big(\frac{f(\tau_3)}{f(\tau_2)}\Big). \qquad \text{B}\end{aligned} \tag{5.60}$$

The integrals A and B are computed in appendix B.3. In particular B has been evaluated analytically obtaining $B = -2\mathbf{L}$, where $\mathbf{L}$ is given in (5.51). The term A has been

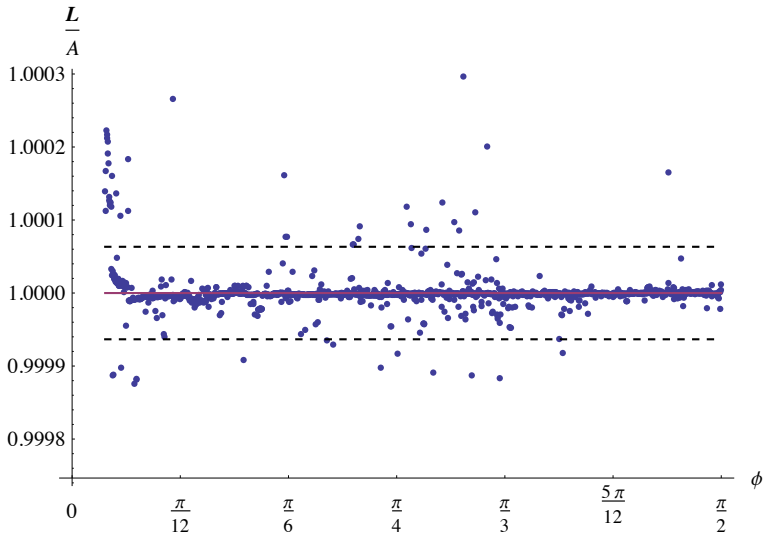

Figure 5.5: Numerical evaluation of the ratio $\frac{\mathbf{L}}{\mathrm{A}}$ as a function of ϕ obtained with Wolfram Mathematica routine NIntegrate. The red line is the linear fit of the data and the dashed lines are the upper and lower limit of the Confidence Interval.

calculated numerically for different values of the angle ϕ. In Figure 5.5 we plot the ratio $\frac{\mathbf{L}}{\mathrm{A}}$ and from this analysis we conclude that $\mathrm{A} = \mathbf{L}$ [2].

The contribution of the interacting diagrams is therefore

$$\langle\, W[\mathcal{C}]\mathcal{O}_2(x_{\mathcal{O}})\,\rangle_{\text{int}} = -\mathbf{L}. \tag{5.61}$$

Finally, summing up the interacting and the ladder contributions, we obtain

$$\langle\, W[\mathcal{C}]\mathcal{O}_2(x_{\mathcal{O}})\,\rangle = \langle\, W[\mathcal{C}]\mathcal{O}_2(x_{\mathcal{O}})\,\rangle_{\text{int}} + \langle\, W[\mathcal{C}]\mathcal{O}_2(x_{\mathcal{O}})\,\rangle_{\text{ladder}} = \frac{\lambda^2}{192\sqrt{2}N} \tag{5.62}$$

that perfectly fits into the localization result.

[2]For $\phi < \frac{\pi}{32}$ the value of A is much less than its error, while $\mathbf{L}$ is an exact quantity. Thus in Figure 5.5 we drop the points in that range.

Chapter 6

Bremsstrahlung function and leading Lüscher term in $\mathcal{N} = 4$ SYM from localization

As we have seen, the investigation of integrable structures [128] (or the Quantum Spectral Curve approach [162]) and the use of supersymmetric localization [37] have produced a huge number of results that are beyond perturbation theory and can be successfully compared with AdS/CFT expectations. It is certainly interesting to understand the relation between these two approaches, when the same quantities can be computed in both ways.

One of this quantities is the cusp anomalous dimension $\Gamma(\varphi)$ introduced in chapter 4. In the light-like limit a lot of results have been derived in $\mathcal{N} = 4$ SYM through integrability [163] that match both weak coupling expansions [164] and string computations describing the strong coupling behavior [165]. A related TBA approach, that goes beyond the light-like limit, was later proposed [139, 140]: the cusp anomalous dimension can be generalized including an R-symmetry angle θ that controls the coupling of the scalars to the two halves of the cusp [137]. Exact equations can be written applying integrability, and have been checked successfully at three loops [139]. For a recent approach using the QSC see [166]. Moreover one can use localization in a suitable limit to obtain the exact form of the infamous Bremsstrahlung function [131], that controls the near-BPS behavior of the cusp anomalous dimension (see also [132] for a different derivation). The same result has been later directly recovered from the TBA equations [167, 168] and QSC method [169, 166]. It is clear that the generalized cusp anomalous dimension $\Gamma(\theta, \varphi)$ represents, in $\mathcal{N} = 4$ SYM, a favorable playground in which the relative domains of techniques as integrability and localization overlap.

The Chapter is organized as follows: in Section 6.1 we recall the main ideas and the results of the near BPS limit of the cusp anomalous dimension using a TBA appoach.

In Section 6.2 we present the construction of the wedge Wilson loop in $\mathcal{N} = 4$ SYM with the relevant operator insertions. We discuss the BPS nature of these observables and their mapping to two-dimensional Yang-Mills theory on S^2 in the zero-instanton sector. The relation with the generalized Bremsstrahlung function is also established. In Section 6.3 we set up the perturbative calculation of the first non-trivial contribution to the near-BPS limit of $\Gamma_L(\theta, \varphi)$, first considering the case $L = 1$ and then presenting the computation for general L. We recover the weak coupling contribution to the Lüscher term as expected. In Section 6.4 we perform the $L = 1$ computation using Feynman diagrams in $\mathcal{N} = 4$ SYM: this is a check of our construction and also exemplifies the extreme complexity of the conventional perturbative calculations. This Chapter is based on [170].

6.1 The generalized Bremsstrahlung function from TBA

We have seen in Section 4.2.1.2 that a fully nonperturbative description for the value of Γ_{cusp} was obtained in a remarkable development by Drukker [140] and by Correa, Maldacena and Sever [139]. They proposed an infinite system of TBA integral equations which compute this quantity at arbitrary 't Hooft coupling λ and for arbitrary angles. In order to implement the TBA approach, the cusp anomalous dimension was generalized for the case when a local operator with R-charge L is inserted at the cusp as in Figure 4.4. The deformed anomalous dimension $\Gamma_L(\lambda, \theta, \varphi)$ corresponding to such Wilson loop is captured by the TBA equations exactly at any value of L. For $L = 0$ the usual quark-antiquark potential is recovered. The number of field insertions plays the role of the systems volume in the TBA description, and $\Gamma_L(\lambda, \theta, \varphi)$ is obtained as the vacuum state energy.

While the infinite system of these TBA equations is rather complicated, having the two angles as continuous parameters opens the possibility to look for simplifications in some limits where an exact analytical solution may be expected. Thus one can focus on the near-BPS limit when $\theta \approx \varphi$. As we have seen in Section 4.2, for $\theta \approx \varphi$ the configuration is BPS and the anomalous dimension vanishes. In Section 4.2.1.3 the small deviations from this supersymmetric case are known for $L = 0$ at any λ and N using results from localization methods (see equation (4.26) and (4.27)).

The existence of such explicit result suggests that the cusp TBA system should simplify dramatically when $\theta \approx \varphi$. Even though the full set of TBA equations was simplified a bit in this limit as described in [139], the result is still an enormously complicated infinite set of integral equations. Remarkably, it turned out that these equations admit an exact analytical solution. It was obtained in [167] for the particular near-BPS configuration where $\theta = 0$ and φ is small. The result of [167] covers all values of L and λ and for $L = 0$ reproduces the localization result.

In [168], the authors extend the results of [167] to the generic near-BPS limit, namely they consider the case when $\theta \approx \varphi$, but θ is arbitrary and is an extra parameter

in the result. They apply the methods developed for the spectral problem to reduce the Y-system to a finite set of equations, known as FiNLIE [171].

The final result is quite simple and takes the form

$$\Gamma_L = \frac{\varphi-\theta}{4}\partial_\varphi \log \frac{\det \mathcal{M}_{2L+1}}{\det \mathcal{M}_{2L-1}}, \tag{6.1}$$

where $\mathcal{M}_N$ is an $N+1\times N+1$ matrix defined as follows

$$\mathcal{M}_N = \begin{pmatrix} I_1^\varphi & I_0^\varphi & \cdots & I_{2-N}^\varphi & I_{1-N}^\varphi \\ I_2^\varphi & I_1^\varphi & \cdots & I_{3-N}^\varphi & I_{2-N}^\varphi \\ \vdots & \vdots & \ddots & \vdots & \vdots \\ I_N^\varphi & I_{N-1}^\varphi & \cdots & I_1^\varphi & I_0^\varphi \\ I_{N+1}^\varphi & I_N^\varphi & \cdots & I_2^\varphi & I_1^\varphi \end{pmatrix} \tag{6.2}$$

and the φ-deformed Bessel functions I_n^θ are

$$I_n^\varphi = \frac{1}{2} I_n\left(\sqrt{\tilde{\lambda}}\right)\left[\left(\sqrt{\frac{\pi+\varphi}{\pi-\varphi}}\right)^n - (-1)^n\left(\sqrt{\frac{\pi-\varphi}{\pi+\varphi}}\right)^n\right], \qquad \tilde{\lambda} = \lambda\left(1-\tfrac{\varphi^2}{\pi^2}\right). \tag{6.3}$$

At $L=0$ the result reproduces the localization prediction. For $L>0$ the (6.1) complements and generalizes the calculation of [167] as an integrability-based prediction for localization techniques.

6.2 Loop operators in $\mathcal{N}=4$ SYM and YM_2: an alternative route to the generalized Bremsstrahlung function

In Section 3.1.2.1 we have reviewed, in $\mathcal{N}=4$ SYM theory, an infinite family of loop operators which share, independently of the contour, $\frac{1}{8}$ of the original supersymmetries of the theory. These loop operators are the DGRT Wilson loop defined by equation (3.30).

We have also seen that the expectation value of this class of observables is captured by the matrix model governing the zero-instanton sector of two dimensional Yang-Mills on the sphere:

$$\begin{aligned}\langle W^{(2d)}\rangle =& \frac{1}{\mathcal{Z}}\int DM \frac{1}{N}\mathrm{Tr}\left(e^{iM}\right)\exp\left(-\frac{A}{g_{2d}^2 A_1 A_2}\mathrm{Tr}(M^2)\right) = \\ =& \frac{1}{N} L_{N-1}^1\left(\frac{g_{2d}^2 A_1 A_2}{2A}\right)\exp\left(-\frac{g_{2d}^2 A_1 A_2}{4A}\right),\end{aligned} \tag{6.4}$$

where A_1, A_2 are the areas singled out by the Wilson loop and $A = A_1 + A_2 = 4\pi$ is the total area of the sphere. The result in $\mathcal{N}=4$ SYM (see (3.101)) is then obtained with the following map

$$g_{2d}^2 \mapsto -\frac{2g_{\mathrm{YM}}^2}{A}. \tag{6.5}$$

Above g_{2d} and $g_{\rm YM}$ are respectively the two and four dimensional Yang-Mills coupling constants.

The knowledge of the exact expectation value for this family of Wilson loops has been a powerful tool to test the AdS/CFT correspondence in different regimes. In particular, here, we want to investigate the connection, originally discussed in [131], between these observables and the so-called Bremsstrahlung function.

Consider, in fact, the generalized cusp anomaly $\Gamma(\theta,\varphi)$ defined in 4.2.1, namely the coefficient of the logarithmic divergence for a Wilson line that makes a turn by an angle φ in actual space-time and by an angle θ in the $R-$symmetry space of the theory. When $\theta=\pm\varphi$ the Wilson line becomes supersymmetric and $\Gamma(\theta,\varphi)$ identically vanishes. In this limit the operator is, in fact, a particular case of the $\frac{1}{4}$ BPS loops discussed by Zarembo in [70]. In [131] a simple and compact expression for the first order deviation away from the BPS value was derived. When $|\theta-\varphi|\ll 1$, we can write

$$\Gamma(\theta,\varphi)\simeq-(\varphi-\theta)\mathcal{H}(\lambda,\varphi)+O((\varphi-\theta)^2) \tag{6.6}$$

where

$$\mathcal{H}(\lambda,\varphi)=\frac{2\varphi}{1-\frac{\varphi^2}{\pi^2}}\mathcal{B}(\tilde{\lambda})\qquad\text{with}\quad\tilde{\lambda}=\lambda\left(1-\frac{\varphi^2}{\pi^2}\right). \tag{6.7}$$

In (6.7) $\mathcal{B}(\tilde{\lambda})$ is given by the Bremsstrahlung function of $\mathcal{N}=4$ SYM theory.

The expansion (6.6) was obtained in [131] by considering a small deformation of the so-called $\frac{1}{4}$ BPS wedge. It is a loop in the class defined by (3.30) which consists of two meridians separated by an angle $\pi-\varphi$. As we have seen in Section 4.2.1, the analysis in [131] shows that $\mathcal{H}(\lambda,\varphi)$ can be computed as the logarithmic derivative of the expectation value of the BPS wedge with respect to the angle φ

$$\mathcal{H}(\lambda,\varphi)=-\frac{1}{2}\partial_\varphi\log\langle\mathcal{W}_{\rm wedge}(\varphi)\rangle=-\frac{1}{2}\frac{\partial_\varphi\langle\mathcal{W}_{\rm wedge}(\varphi)\rangle}{\langle\mathcal{W}_{\rm wedge}(\varphi)\rangle}. \tag{6.8}$$

The quantity $\langle\mathcal{W}_{\rm wedge}(\varphi)\rangle$ is given by the matrix model (6.4) with the replacement (6.5). In other words $\langle\mathcal{W}_{\rm wedge}(\varphi)\rangle=\langle\mathcal{W}_{\rm circle}(\tilde{\lambda})\rangle$ where $\tilde{\lambda}$ is defined in (6.7).

The results (6.7) and (6.8) were also recovered in [167, 168] by solving the TBA equations, obtained in [139], for the cusp anomalous dimension in the BPS limit. This second approach based on integrability naturally led to consider a generalization $\Gamma_L(\theta,\varphi)$ for the cusp anomalous dimension, where one has inserted the scalar operator Z^L on the tip of the cusp[1]. In [168] it was shown that the whole family $\Gamma_L(\theta,\varphi)$ admits an expansion of the type (6.6) when $|\theta-\varphi|\ll 1$:

$$\Gamma_L(\theta,\varphi)\simeq-(\varphi-\theta)\mathcal{H}_L(\lambda,\varphi)+O((\varphi-\theta)^2) \tag{6.9}$$

[1] The scalar Z is the holomorphic combination of two scalars, which do not couple to the Wilson line.

with

$$\mathcal{H}_L(\lambda,\varphi)=\frac{2\varphi}{1-\frac{\varphi^2}{\pi^2}}\mathcal{B}_L(\lambda,\varphi)\,. \tag{6.10}$$

The function $\mathcal{B}_L(\lambda,\varphi)$ is a generalization of the usual Bremsstrahlung function and its value for any L in the large N limit was derived in [168].

Below, we want to show that expansion (6.9) and in particular the function $\mathcal{B}_L(\lambda,\varphi)$ can be evaluated exploiting the relation between the Wilson loops (3.30) and YM_2 as done in [131] for the case $L=0$.

6.2.1 BPS wedge on S^2 with scalar insertions in $\mathcal{N}=4$ SYM

The first step is to construct a generalization of the $\frac{1}{4}$ BPS wedge in $\mathcal{N}=4$ SYM, whose vacuum expectation value is still determined by a suitable observable in YM_2. We start by considering the contour depicted in Figure 6.1, namely the wedge composed

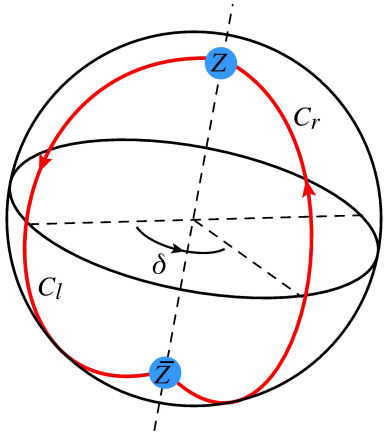

Figure 6.1: Pictorial description of the observable (6.15): the $\frac{1}{4}$ BPS wedge with operator insertions in the north and the south pole.

by two meridians C_l and C_r, the first in the (x_1,x_3) plane and the second in a plane with longitude angle δ:

$$\begin{aligned} C_l \quad &\mapsto \quad x_l^\mu=(\sin\tau,0,\cos\tau) && 0\le\tau\le\pi,\\ C_r \quad &\mapsto \quad x_r^\mu=(-\cos\delta\sin\sigma,-\sin\delta\sin\sigma,\cos\sigma) && \pi\le\sigma\le 2\pi. \end{aligned} \tag{6.11}$$

On the two meridians the Wilson loop couples to two different combinations of scalars. Indeed the effective gauge connections on the two sides are given by

$$\mathcal{A}_l=\dot{x}_l^\mu A_\mu-i\Phi^2\,,\qquad \mathcal{A}_r=\dot{x}_r^\mu A_\mu-i\sin\delta\Phi^1+i\cos\delta\Phi^2. \tag{6.12}$$

We now consider the insertion of local operators in the loop and focus our attention on those introduced in [158] and studied in detail in [153] and in the previous chapter.

They are given by:

$$\mathcal{O}_L(x) = \left(x_\mu \Phi^\mu + i\Phi^4\right)^L , \tag{6.13}$$

where x_μ are the cartesian coordinate of a point on S^2 and the index μ runs from 1 to 3. Any system of these operators preserves at least four supercharges. When the Wilson loops (3.30) are also present, the combined system is generically invariant under two supercharges ($\frac{1}{16}$ BPS) [106]. Here we choose to insert two of these operators: one in the north pole $[x^\mu_N = (0,0,1)]$ and the other in the south pole $[x^\mu_S = (0,0,-1)]$. In these special positions they reduce to the holomorphic and the anti-holomorphic combination of two of the scalar fields which do not couple to the loop

$$\mathcal{O}_L(x_N) = \left(\Phi^3 + i\Phi^4\right)^L \equiv Z^L , \qquad \mathcal{O}_L(x_S) = \left(-\Phi^3 + i\Phi^4\right)^L \equiv (-1)^L \bar{Z}^L . \tag{6.14}$$

Then the generalization of the $\frac{1}{4}$ BPS wedge which is supposed to capture the generalized Bremsstrahlung function $\mathcal{B}_L(\lambda,\varphi)$ is simply given by

$$\mathcal{W}_L(\delta) = \mathrm{Tr}\left[Z^L \ \mathrm{Pexp}\left(\int_{C_l} \mathcal{A}_l d\tau\right) \ \bar{Z}^L \ \mathrm{Pexp}\left(\int_{C_r} \mathcal{A}_r d\sigma\right)\right] . \tag{6.15}$$

The operators (6.15) preserve $\frac{1}{8}$ of the supercharges. Applying the same argument given in [131], one can argue (since the relevant deformation never involves the poles) that

$$\mathcal{H}_L(\lambda,\varphi) = \frac{2\varphi}{1-\frac{\varphi^2}{\pi^2}}\,\mathcal{B}_L(\lambda,\varphi) = \frac{1}{2}\partial_\delta \log\langle \mathcal{W}_L(\delta)\rangle\Big|_{\delta=\pi-\varphi} . \tag{6.16}$$

6.2.2 The wedge on S^2 with field strength insertions in YM_2

Next we shall construct a *putative* observable in YM_2, which computes the vacuum expectation of $\mathcal{W}_L(\delta)$. Following [75], we map the Wilson loop of $\mathcal{N}=4$ SYM into

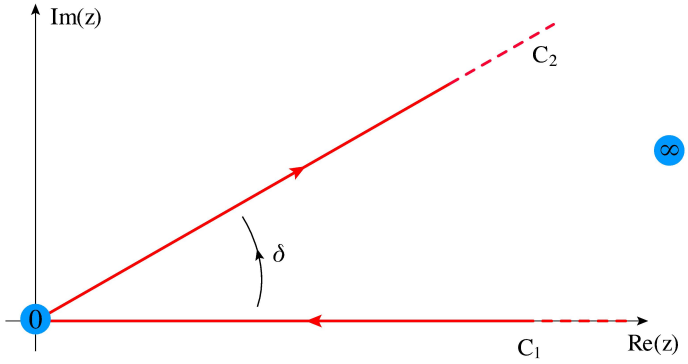

Figure 6.2: Wedge on S^2 in stereographic coordinates. The blue blobs denote the operator insertions.

a loop operator of YM_2 defined along the same contour C on S^2. Since we use the

complex stereographic coordinates $z = x + iy$ to parametrize the sphere, the wedge will appear as an infinite cusp on the plane where the origin represents the north pole, while the infinity is identified with the south pole (see Figure 6.2). The two straight-lines C_1 and C_2 are then given by

$$\begin{array}{lcll} C_1 & \mapsto & z(t) = t & t \in [\infty, 0]\,, \\ C_2 & \mapsto & w(s) = e^{i\delta} s & s \in [0, \infty]\,. \end{array} \tag{6.17}$$

In these coordinates the metric on S^2 takes the usual conformally flat form

$$ds^2 = \frac{4 dz d\bar{z}}{(1 + z\bar{z})^2}\,. \tag{6.18}$$

The wedge Wilson loop is mapped into

$$\mathcal{W}_C = \frac{1}{N} \mathrm{Tr} \left[\mathrm{Pexp} \left(\oint_C d\tau\ \dot{z} \tilde{A}_z(z) \right) \right]\,, \tag{6.19}$$

where $C = C_1 \cup C_2$ (see Figure 6.2). In (6.19) we have used the notation $\tilde{A}$, to distinguish gauge field in $d = 2$ from its counterpart A in $d = 4$.

The two dimensional companion of the operator (6.13) was found in [153] through a localization argument. These local operators are mapped into powers of the field strength $\tilde{F}$ of the two-dimensional gauge field $\tilde{A}$:

$$\mathcal{O}_L(x) \mapsto \left(i\ {}^*\tilde{F}(z) \right)^L\,. \tag{6.20}$$

Here the * denotes the usual hodge dual on the sphere. Combining the above ingredients the observable in YM_2 which computes the vacuum expectation value of (6.15) is

$$\mathcal{W}_L^{(2d)}(\delta) = \mathrm{Tr} \left[\left(i\ {}^*\tilde{F}(0) \right)^L\ \mathrm{Pexp} \left(\int_{C_2} \dot{w} \tilde{A}_w ds \right)\ \left(i\ {}^*\tilde{F}(\infty) \right)^L\ \mathrm{Pexp} \left(\int_{C_1} \dot{z} \tilde{A}_z dt \right) \right]. \tag{6.21}$$

Constructing a matrix model for the observable (6.21) in the zero instanton sector is neither easy nor immediate. In fact the usual topological Feynman rules for computing quantities in YM_2 are tailored for the case of correlators of Wilson loops. The insertion of local operators along the contour was not considered previously and the rules for this case are still missing. Therefore, in the next section, to test the relation between the function $\mathcal{H}_L(\lambda, \varphi)$ and the vacuum expectation value of (6.21) implied by (6.16), *i.e.*

$$\mathcal{H}_L(\lambda, \varphi) = \frac{2\varphi}{1 - \frac{\varphi^2}{\pi^2}}\, \mathcal{B}_L(\lambda, \varphi) = \frac{1}{2} \partial_\delta \log \langle \mathcal{W}_L^{(2d)}(\delta) \rangle \Big|_{\substack{\delta = \pi - \varphi \\ g_{2d}^2 = -2g^2/A}}\,, \tag{6.22}$$

we shall resort to standard perturbative techniques.

6.3 Perturbative computation of the Lüscher term from YM_2 on the sphere

In this Section we compute the first non-trivial perturbative contribution to the generalized Bremsstrahlung function $\mathcal{B}_L(\lambda,\varphi)$, in the planar limit, using perturbation theory in YM_2. It coincides with the weak coupling limit of the Lüscher term, describing wrapping corrections in the integrability framework. We believe it is instructive to present first the computation for $L=1$, where few diagrams enter into the calculation and every step can be followed explicitly. Then we turn to general L, exploiting some more sophisticated techniques to account for the combinatorics.

6.3.1 General setting for perturbative computations on S^2

For perturbative calculations on the two dimensional sphere, it is convenient to use the holomorphic gauge $\tilde{A}_{\bar{z}}=0$. In this gauge the interactions vanish and the relevant propagators are:

$$\begin{aligned}
\langle(\tilde{A}_z)^i_j(z)(\tilde{A}_z)^k_l(w)\rangle &= -\frac{g_{2d}^2}{2\pi}\delta^i_l\delta^k_j\frac{1}{1+z\bar{z}}\frac{1}{1+w\bar{w}}\frac{\bar{z}-\bar{w}}{z-w}\,,\\
\langle(i^*\tilde{F}^i_j(z))(i^*\tilde{F}^k_l(w))\rangle &= -\delta^i_l\delta^k_j\left(\frac{g_{2d}^2}{8\pi}-\frac{ig_{2d}^2}{4}(1+z\bar{z})^2\delta^{(2)}(z-w)\right)\,,\\
\langle(i^*\tilde{F}^i_j(z))(\tilde{A}_z)^k_l(w)\rangle &= -\frac{g_{2d}^2}{4\pi}\delta^i_l\delta^k_j\frac{1}{1+w\bar{w}}\frac{1+z\bar{w}}{z-w}\,.
\end{aligned}\tag{6.23}$$

When computing the above propagators for points lying on the edge C_1 ($z=t$) and on the edge C_2 ($w=e^{i\delta}s$), they reduce to

$$\begin{aligned}
&\langle(\tilde{A}_z)^i_j(z)(\tilde{A}_z)^k_l(w)\rangle = -\frac{g_{2d}^2}{2\pi}\delta^i_l\delta^k_j\frac{1}{1+t^2}\frac{1}{1+s^2}\,\frac{t-e^{-i\delta}s}{t-e^{i\delta}s}\,,\\
&\langle(i^*\tilde{F}^i_j(0))(\tilde{A}_z)^k_l(z)\rangle = \frac{g_{2d}^2}{4\pi}\delta^i_l\delta^k_j\frac{1}{1+t^2}\frac{1}{t}\,,\qquad \langle(i^*\tilde{F}^i_j(0))(\tilde{A}_z)^k_l(w)\rangle = \frac{g_{2d}^2}{4\pi}\delta^i_l\delta^k_j\frac{1}{1+s^2}\frac{e^{-i\delta}}{s}\,,\\
&\langle(i^*\tilde{F}^i_j(\infty))(\tilde{A}_z)^k_l(z)\rangle = -\frac{g_{2d}^2}{4\pi}\delta^i_l\delta^k_j\frac{t}{1+t^2}\,,\qquad \langle(i^*\tilde{F}^i_j(\infty))(\tilde{A}_z)^k_l(w)\rangle = -\frac{g_{2d}^2}{4\pi}\delta^i_l\delta^k_j\frac{e^{-i\delta}s}{1+s^2}\,.
\end{aligned}\tag{6.24}$$

These Feynman rules can be checked by computing the first two non trivial orders for the standard wedge in YM_2, *i.e.* $L=0$. One quickly finds:

$$\begin{aligned}
\langle W^{(2d)}_{\text{1-loop}}\rangle &= \frac{g_{2d}^2N}{2\pi}\left(\frac{\pi^2}{4}-\frac{1}{2}(2\pi-\delta)\delta\right)\,,\\
\langle W^{(2d)}_{\text{2-loop}}\rangle &= -\frac{g_{2d}^4N^2}{96\pi^2}(2\pi-\delta)^2\delta^2\,.
\end{aligned}\tag{6.25}$$

Using (6.22) one gets

$$\mathcal{H}^{(1)}(\lambda,\varphi)=\frac{\lambda\varphi}{8\pi^2},\qquad\qquad \mathcal{H}^{(2)}(\lambda,\varphi)=-\frac{\lambda^2\varphi(\pi^2-\varphi^2)}{192\pi^4}, \tag{6.26}$$

which is exactly the result of [131].

6.3.2 Operator insertions of length $L=1$

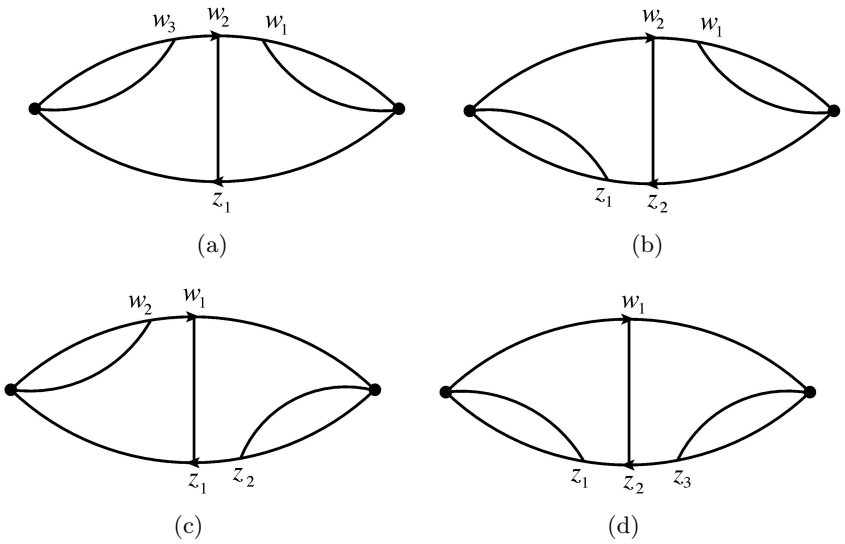

Figure 6.3: All the δ-dependent diagrams at order λ^2 in YM_2

The first non-trivial contribution in this case appears at order λ^2: we need at least one propagator connecting the two halves of the wedge, to carry the dependence on the opening angle δ. Then we have to consider the effect of the operator insertions, which should be connected to the contour, respecting planarity, in all possible ways. The relevant choices are represented in Figure 6.3. We remark that every diagram has the same weight: in fact the operator we study is single-trace and every diagram arises from an unique set of Wick contractions. Furthermore there are some obvious symmetries between the different diagrams, that imply the following representation:

$$\begin{aligned}
&\text{(a)}+\text{(d)}=2\frac{g_{2d}^6N^4}{32\pi^3}\int_0^\infty ds_1\int_0^{s_1}ds_3\frac{1}{(s_1^2+1)(s_3^2+1)}\frac{s_1}{s_3}\,\mathcal{F}_\delta(\infty,0;s_3,s_1)\,,\\
&\text{(b)}+\text{(c)}=\frac{g_{2d}^6N^4}{32\pi^3}\int_\infty^0 dt_1\int_0^\infty ds_1\frac{1}{(t_1^2+1)(s_1^2+1)}\frac{s_1}{t_1}\Big[\mathcal{F}_\delta(\infty,t_1;0,s_1)+\mathcal{F}_{-\delta}(\infty,t_1;0,s_1)\Big]\,,
\end{aligned} \tag{6.27}$$

where we have introduced the function $\mathcal{F}_\delta(a,b;c,d)$

$$\mathcal{F}_\delta(a,b;c,d)=\int_a^b dt\int_c^d ds\,\frac{1}{(t^2+1)(s^2+1)}\,\frac{e^{i\delta}t-s}{t-e^{i\delta}s}\,. \tag{6.28}$$

Using the identity $\frac{1}{(s^2+1)(t^2+1)}\frac{s}{t}=\frac{1}{4}\partial_s\partial_t[\log\left(s^2+1\right)\log\left(t^2/(t^2+1)\right)]$ and integrating by parts, we obtain

$$\begin{aligned}(\mathrm{a})+(\mathrm{d})=&\frac{g_{2d}^6N^4}{32\pi^3}\Bigg[2\log^2\epsilon\mathcal{F}_\delta(\infty,0;0,\infty)+\log\epsilon\int_0^\infty ds_1\log(s_1^2+1)\frac{d}{ds_1}\mathcal{F}_\delta(\infty,0;0,s_1)+\\&+\log\epsilon\int_0^\infty ds_3\log\left(\frac{s_3^2}{s_3^2+1}\right)\frac{d}{ds_3}\mathcal{F}_\delta(\infty,0;s_3,\infty)+\\&+\frac{1}{2}\int_0^\infty ds_1\log(s_1^2+1)\log\left(\frac{s_1^2}{s_1^2+1}\right)\left[\frac{d}{ds_3}\mathcal{F}_\delta(\infty,0;s_3,s_1)\right]_{s_3=s_1}+\\&+\frac{1}{2}\int_0^\infty ds_1\int_0^{s_1}ds_3\log(s_1^2+1)\log\left(\frac{s_3^2}{s_3^2+1}\right)\frac{d}{ds_3}\frac{d}{ds_1}\mathcal{F}_\delta(\infty,0;s_3,s_1)\Bigg]\end{aligned} \tag{6.29}$$

and

$$\begin{aligned}(\mathrm{b})+(\mathrm{c})=&\frac{g_{2d}^6N^4}{32\pi^3}\Bigg[-\log^2\epsilon\Big[\mathcal{F}_\delta(\infty,0;0,\infty)+\mathcal{F}_{-\delta}(\infty,0;0,\infty)\Big]+\\&+\frac{1}{2}\log\epsilon\int_\infty^0 dt_1\log\left(\frac{t_1^2}{t_1^2+1}\right)\frac{d}{dt_1}\Big[\mathcal{F}_\delta(\infty,t_1;0,\infty)+\mathcal{F}_{-\delta}(\infty,t_1;0,\infty)\Big]-\\&-\frac{1}{2}\log\epsilon\int_0^\infty ds_1\log\left(s_1^2+1\right)\frac{d}{ds_1}\Big[\mathcal{F}_\delta(\infty,0;0,s_1)+\mathcal{F}_{-\delta}(\infty,0;0,s_1)\Big]+\\&+\frac{1}{4}\int_\infty^0 dt_1\int_0^\infty ds_1\log\left(s_1^2+1\right)\log\left(\frac{t_1^2}{t_1^2+1}\right)\frac{d}{dt_1}\frac{d}{ds_1}\Big[\mathcal{F}_\delta(\infty,t_1;0,s_1)+\mathcal{F}_{-\delta}(\infty,t_1;0,s_1)\Big]\,,\end{aligned} \tag{6.30}$$

where ϵ is a regulator that cuts the contour in a neighborhood of the operator insertions and it will be send to zero at the end of the computation. Now using that

$$\frac{d}{da}\mathcal{F}_{\pm\delta}(a,0;0,\infty)=\frac{d}{da}\mathcal{F}_{\mp\delta}(\infty,0;0,a)\,,\qquad \frac{d}{da}\mathcal{F}_{\pm\delta}(\infty,0;a,\infty)=\frac{d}{da}\mathcal{F}_{\mp\delta}(\infty,a;0,\infty) \tag{6.31}$$

and the definition (6.21), we can sum up all the contributions in (6.29) and (6.30) obtaining

$$\begin{aligned}\mathcal{M}_1^{(1)}=&-\frac{g_{2d}^4N^2}{4\pi^2}\Bigg\{\frac{1}{2}\int_0^\infty ds_1\log(s_1^2+1)\log\left(\frac{s_1^2}{s_1^2+1}\right)\left[\frac{d}{ds_3}\mathcal{F}_\delta(\infty,0;s_3,s_1)\right]_{s_3=s_1}\\&-\frac{1}{4}\int_0^\infty dt_1\int_0^\infty ds_1\log\left(s_1^2+1\right)\log\left(\frac{t_1^2}{t_1^2+1}\right)\frac{d}{dt_1}\frac{d}{ds_1}\Big[\mathcal{F}_\delta(\infty,t_1;0,s_1)+\mathcal{F}_{-\delta}(\infty,t_1;0,s_1)\Big]\Bigg\}\,,\end{aligned} \tag{6.32}$$

where we have defined $\mathcal{M}_L^{(l)}$ as the sum of the δ-dependent part of $\langle \mathcal{W}_L^{(2d)}(\delta)\rangle$ at loop order l. To derive the above equation we have taken advantage of the useful relations

$$\begin{aligned}
&\mathcal{F}_\delta(\infty,0;0,\infty) = \mathcal{F}_{-\delta}(\infty,0;0,\infty)\,, \qquad\qquad \frac{d}{da}\frac{d}{db}\mathcal{F}_{\pm\delta}(\infty,0;a,b) = 0\,,\\
&\int_0^\infty da \log\left(\frac{a^2}{a^2+1}\right)\frac{d}{da}\mathcal{F}_{\pm\delta}(\infty,a;0,\infty) = \int_0^\infty db \log\left(b^2+1\right)\frac{d}{db}\mathcal{F}_{\pm\delta}(\infty,0;0,b)\,.
\end{aligned} \tag{6.33}$$

We remark that the dependence on the cutoff ϵ disappears: as expected we end up with a finite result. We further observe that turning $\delta \to -\delta$ is the same as taking complex conjugation, then we can rewrite (6.32) as follows

$$\begin{aligned}
\mathcal{M}_1^{(1)} = -\frac{g_{2d}^4 N^2}{16\pi^2}\Bigg\{&\int_0^\infty ds_1 \log(s_1^2+1)\log\left(\frac{s_1^2}{s_1^2+1}\right)\left[\frac{d}{ds_3}\mathcal{F}_\delta(\infty,0;s_3,s_1)\right]_{s_3=s_1}\\
&-\int_0^\infty dt_1\int_0^\infty ds_1 \log\left(s_1^2+1\right)\log\left(\frac{t_1^2}{t_1^2+1}\right)\frac{d}{dt_1}\frac{d}{ds_1}\mathcal{F}_\delta(\infty,t_1;0,s_1)\Bigg\}+\text{c.c.}
\end{aligned} \tag{6.34}$$

and performing the derivatives (6.34) becomes

$$\mathcal{M}_1^{(1)} = -\frac{g_{2d}^4 N^2}{16\pi^2}\int_0^\infty ds dt \frac{\log(s^2+1)}{(t^2+1)(s^2+1)}\frac{e^{i\delta}t-s}{t-e^{i\delta}s}\left[\log\left(\frac{s^2}{s^2+1}\right)-\log\left(\frac{t^2}{t^2+1}\right)\right]+\text{c.c.} \tag{6.35}$$

The function $\mathcal{H}_1$ is then obtained with the help of (6.22), then at one-loop order we have

$$\mathcal{H}_1^{(1)}(\lambda,\varphi) = \frac{1}{2}\partial_\delta \mathcal{M}_1^{(1)}\Big|_{\substack{\delta=\pi-\varphi\\ g_{2d}^2=-2g^2/A}}\,. \tag{6.36}$$

Exploiting the simple decomposition

$$\frac{e^{i\delta}t-s}{t-e^{i\delta}s} = -\frac{t}{s}+\frac{1}{s}\frac{s^2+1}{e^{i\delta}s-t}-\frac{1}{s}\frac{t^2+1}{e^{i\delta}s-t}\,, \tag{6.37}$$

the derivative of (6.35) becomes

$$\frac{g_{2d}^4 N^2}{16\pi^2}\int_0^\infty ds dt \frac{\log(s^2+1)}{s}\left[\frac{1}{(t^2+1)}-\frac{1}{(s^2+1)}\right]\left[\log\left(\frac{s^2}{s^2+1}\right)-\log\left(\frac{t^2}{t^2+1}\right)\right]\partial_\delta\left(\frac{1}{e^{i\delta}s-t}\right)+\text{c.c.} \tag{6.38}$$

Using

$$\partial_\delta\left(\frac{1}{e^{i\delta}s-t}\right) = -is\,e^{i\delta}\partial_t\left(\frac{1}{e^{i\delta}s-t}\right)\,, \tag{6.39}$$

the integral (6.38) takes the form:

$$\frac{ig_{2d}^4N^2}{16\pi^2}\int_0^\infty ds\Big\{\log(s^2+1)\log\left(\frac{s^2}{s^2+1}\right)\frac{s}{s^2+1}- \tag{6.40}$$
$$-2\int_0^\infty dt\left[\log\left(\frac{s^2}{s^2+1}\right)\frac{t\log(s^2+1)}{(t^2+1)^2}\frac{e^{i\delta}}{e^{i\delta}s-t}-\log\left(\frac{t^2}{t^2+1}\right)\frac{1-t^2}{1+t^2}\frac{s}{1+s^2}\frac{1}{e^{i\delta}s-t}\right]\Big\}+\text{c.c.}$$

Summing up the integrands with their complex conjugate (the first term vanishes) and changing variables $s\to\sqrt{\omega\rho}$ and $t\to\sqrt{\omega/\rho}$, we obtain:

$$\begin{aligned}\partial_\delta\mathcal{M}_1^{(1)} &= -\frac{g_{2d}^4N^2}{8\pi^2}\int_0^\infty d\omega d\rho\frac{\sin\delta\,[(\rho+\omega)(\rho\omega-1)+\rho(1+\rho\omega)\log(1+\rho\omega)]\log\left(\frac{\rho\omega}{1+\rho\omega}\right)}{(1+\rho\omega)(\rho+\omega)^2(\rho^2-2\rho\cos\delta+1)}\\ &= \frac{g_{2d}^4N^2}{4\pi^2}\sin\delta\int_0^\infty d\rho\frac{\log^2\rho}{(\rho^2-1)(\rho^2-2\rho\cos\delta+1)}\,.\end{aligned} \tag{6.41}$$

The integration domain is easily restricted to $[0,1]$ and we arrive at

$$\partial_\delta\mathcal{M}_1^{(1)} = -\frac{g_{2d}^4N^2}{4\pi^2}\sin\delta\int_0^1 d\rho\frac{\log^2\rho}{\rho^2-2\rho\cos\delta+1} = -g_{2d}^4N^2\,\frac{\pi}{3}\,B_3\left(\frac{\delta}{2\pi}\right), \tag{6.42}$$

where the $B_n(x)$ are the Bernoulli polynomials defined as

$$B_{2n+1}(x) = \frac{(-1)^{n+1}2(2n+1)\sin(2\pi x)}{(2\pi)^{2n+1}}\int_0^1 dt\,\frac{\log^{2n}t}{t^2-2t\cos(2\pi x)+1}. \tag{6.43}$$

Finally, using (6.36), we find the desired result

$$\mathcal{H}_1^{(1)}(\lambda,\varphi) = -\frac{\lambda^2}{24\pi}\,B_3\left(\frac{\pi-\varphi}{2\pi}\right). \tag{6.44}$$

6.3.3 Operator insertions of length L

We are now ready to compute the leading weak coupling contribution to the Lüscher term, using YM_2 perturbation theory. We have to consider all possible planar diagrams with one single line connecting the right and left sides of the wedge, in presence of length L operator insertions (see Figure 6.4). As remarked in the previous Section, every diagram has the same weight.

We construct the generic term of the relevant perturbative order by introducing the auxiliary function g_n, that contains the contribution of all the propagators connecting the operators with contour in each of the four sectors represented in Figure 6.4:

$$\mathcal{M}_L^{(1)} = \frac{(-1)^{L+1}2^{3L}\,\pi^L}{g_{2d}^{2L}\,N^L}\sum_{n,m=0}^{L}\int_0^\infty dsdt\,(-1)^{n+m}g_n(t,\epsilon)g_{L-n}(s,\epsilon)I_\delta(s,t)g_m(1/s,\epsilon)g_{L-m}(1/t,\epsilon) \tag{6.45}$$

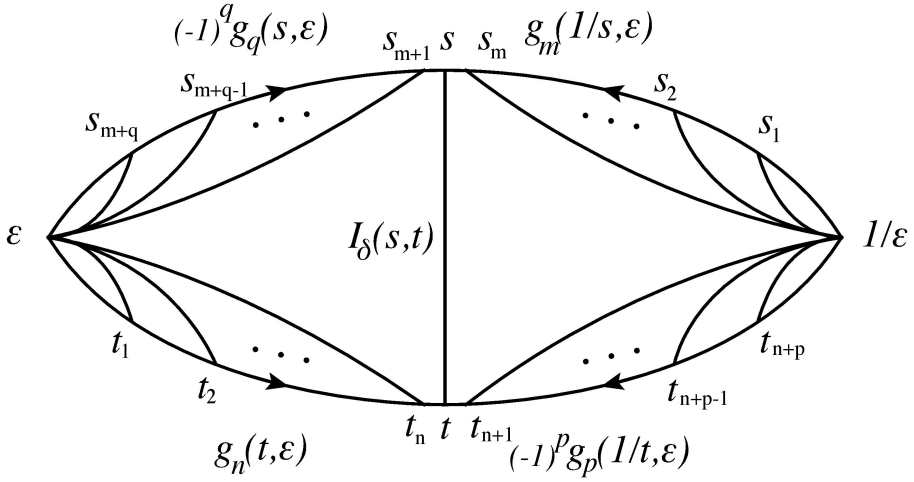

Figure 6.4: Schematic representation of an arbitrary diagram contributing to the first non-trivial order of $\mathcal{B}_L(\lambda, \varphi)$

where

$$I_\delta(s,t) = \left(-\frac{g_{2d}^2}{2\pi}\right) \frac{1}{(t^2+1)(s^2+1)} \frac{te^{i\delta} - s}{t - e^{i\delta}s} \tag{6.46}$$

and

$$g_n(t,\epsilon) = \left(-\frac{g_{2d}^2 N}{4\pi}\right)^n \int_\epsilon^t dt_n \int_\epsilon^{t_n} dt_{n-1} \ldots \int_\epsilon^{t_2} dt_1 \prod_{i=1}^n \Delta(t_i), \tag{6.47}$$

being $\Delta(t) = \frac{1}{t}\frac{1}{t^2+1}$ the propagator from the origin to the contour (up to a constant factor, see (6.24)). Obviously the number of lines on the right and on the left side of the central propagator is equal to L. Moreover we have introduced an explicit cutoff $\epsilon \to 0$ to avoid intermediate divergencies. A recurrence relation for g_n and its derivative follows directly from its definition:

$$\begin{aligned} g_n(t,\epsilon) &= \left(-\frac{g_{2d}^2 N}{4\pi}\right) \int_\epsilon^t dt_n \, \Delta(t_n) \, g_{n-1}(t_n,\epsilon)\,, \\ \frac{d}{dt} g_n(t,\epsilon) &= \left(-\frac{g_{2d}^2 N}{4\pi}\right) \Delta(t) \, g_{n-1}(t,\epsilon)\,. \end{aligned} \tag{6.48}$$

As shown in the Appendix C, we can combine these two equations into a single recurrence relation, involving just $g_n(t,\epsilon)$

$$g_n(t,\epsilon) = -\sum_{k=1}^n \frac{(-\alpha)^k}{k!} \log^k\left(\frac{t^2}{t^2+1}\right) g_{n-k}(t,\epsilon) - (t \to \epsilon), \tag{6.49}$$

where $\alpha = -\frac{g_{2d}^2 N}{8\pi}$. We can solve the recurrence relation by finding the related generat-

ing function $G(t,\epsilon,z)$

$$g_n(t,\epsilon)=\frac{1}{2\pi i}\oint_\gamma \frac{dz}{z^{n+1}}G(t,\epsilon,z)\,, \tag{6.50}$$

for a suitable closed curve γ around the origin. We have obtained (see Appendix C for the details)

$$G(t,\epsilon,z)=\left(\frac{t^2}{t^2+1}\frac{\epsilon^2+1}{\epsilon^2}\right)^{\alpha z}\,. \tag{6.51}$$

Then (6.45) becomes

$$\mathcal{M}_L^{(1)}=\frac{(-1)^{L+1}}{(2\pi i)^4}\frac{2^{3L}\,\pi^L}{g_{2d}^{2L}\,N^L}\sum_{n,m=0}^{L}\int_0^\infty dsdt\oint\frac{G(t,\epsilon,z)}{z^{n+1}}\frac{G^{-1}(s,\epsilon,w)}{w^{L-n+1}}I_\delta(s,t)\frac{G(1/s,\epsilon,v)}{v^{m+1}}\frac{G^{-1}(1/t,\epsilon,u)}{u^{L-m+1}}. \tag{6.52}$$

The sums over m and n are done explicitly

$$\sum_{n=0}^{L}\frac{1}{z^{n+1}w^{L-n+1}}=\frac{z^{-(L+1)}-w^{-(L+1)}}{w-z} \tag{6.53}$$

and using the observations in Appendix C and in particular the formula (C.18), we obtain

$$\begin{aligned}\mathcal{M}_L^{(1)}=&\frac{(-1)^{L+1}}{(2\pi i)^2}\frac{2^{3L}\,\pi^L}{g_{2d}^{2L}\,N^L}\left(\frac{-g_{2d}^2}{2\pi}\right)\times\\&\times\int_0^\infty dsdt\oint\frac{dz}{z^{L+1}}\frac{dv}{v^{L+1}}\left[\left(\frac{t^2(1+s^2)}{s^2(1+t^2)}\right)^{\alpha z}\left(\frac{(1+t^2)}{(1+s^2)}\right)^{\alpha v}\frac{1}{(t^2+1)(s^2+1)}\frac{te^{i\delta}-s}{t-e^{i\delta}s}\right].\end{aligned} \tag{6.54}$$

Notice that the ϵ-dependence has disappeared: the cancellation of the intermediate divergencies is a non-trivial bonus of our method.

Computing the residues, (6.54) takes the following compact form

$$\mathcal{M}_L^{(1)}=\frac{(-1)^{L+1}\alpha^{2L}}{(L!)^2}\frac{2^{3L}\,\pi^L}{g_{2d}^{2L}\,N^L}\left(\frac{-g_{2d}^2}{2\pi}\right)\int_0^\infty dsdt\frac{\left[\log\left(\frac{t^2(1+s^2)}{s^2(1+t^2)}\right)\log\left(\frac{(1+t^2)}{(1+s^2)}\right)\right]^L}{(t^2+1)(s^2+1)}\frac{te^{i\delta}-s}{t-e^{i\delta}s}\,. \tag{6.55}$$

We are interested in calculating the Bremsstrahlung function, so we take the derivative of the VEV of the Wilson loop as seen in the equation (6.8). Using (6.39), after some algebra, we find

$$\begin{aligned}\mathcal{H}_L^{(1)}=i\frac{(-1)^{L+1}\alpha^{2L}}{2(L!)^2}\frac{2^{3L}\,\pi^L}{g_{2d}^{2L}\,N^L}\left(\frac{-g_{2d}^2}{2\pi}\right)\int_0^\infty dsdt\Bigg\{&\left[\log\left(\frac{t^2(1+s^2)}{s^2(1+t^2)}\right)\log\left(\frac{(1+t^2)}{(1+s^2)}\right)\right]^L\\&\times\left[\frac{1}{t^2+1}\partial_s\left(\frac{1}{e^{i\delta}s-t}\right)+\frac{e^{i\delta}}{s^2+1}\partial_t\left(\frac{1}{e^{i\delta}s-t}\right)\right]\Bigg\}\Bigg|_{\substack{\delta=\pi-\varphi\\ g_{2d}^2=-2g^2/A}}.\end{aligned} \tag{6.56}$$

Performing some integration by parts and transformations $s \leftrightarrow t$ and $s,t \to \frac{1}{s,t}$, the change of variables $s \to \sqrt{\omega\rho}$ and $t \to \sqrt{\omega/\rho}$ gives

$$\mathcal{H}_L^{(1)} = -\frac{(-1)^{L+1}\alpha^{2L}}{L!(L-1)!}\frac{2^{3L}\,\pi^L}{g_{2d}^{2L}\,N^L}\left(\frac{-g_{2d}^2}{2\pi}\right)\sin\delta \tag{6.57}$$
$$\times\int_0^1 d\rho\int_0^\infty d\omega\left[\log\left(\frac{\rho(\rho+\omega)}{\rho\omega+1}\right)\log\left(\frac{\rho(\rho\omega+1)}{\rho+\omega}\right)\right]\frac{(\rho^2-1)\log\rho}{(\rho+\omega)(1+\rho\omega)(\rho^2-2\rho\cos\delta+1)}\Bigg|_{\substack{\delta=\pi-\varphi\\ g_{2d}^2=-2g^2/A}}^{L-1}.$$

Using the expansion

$$\left[\log\left(\frac{\rho(\rho+\omega)}{\rho\omega+1}\right)\log\left(\frac{\rho(\rho\omega+1)}{\rho+\omega}\right)\right]^{L-1} = \sum_{k=0}^{L-1}\binom{L-1}{k}(-1)^k\log^{2(L-1-k)}\rho\log^{2k}\left(\frac{\rho+\omega}{\rho\omega+1}\right), \tag{6.58}$$

the integration over ω is straightforward since

$$\int d\omega\frac{\log^{2k}\left(\frac{\rho+\omega}{\rho\omega+1}\right)}{(\rho+\omega)(1+\rho\omega)} = -\frac{\log^{2k+1}\left(\frac{\rho+\omega}{\rho\omega+1}\right)}{(\rho^2-1)(2k+1)}. \tag{6.59}$$

Then we obtain

$$\mathcal{H}_L^{(1)} = -\frac{(-1)^{L+1}\alpha^{2L}}{L!(L-1)!}\frac{2^{3L}\,\pi^L}{g_{2d}^{2L}\,N^L}\left(\frac{-g_{2d}^2}{2\pi}\right)\beta\left(\frac{1}{2},L\right)\left\{\sin\delta\int_0^1 d\rho\frac{\log^{2L}\rho}{\rho^2-2\rho\cos\delta+1}\right\}\Bigg|_{\substack{\delta=\pi-\varphi\\ g_{2d}^2=-2g^2/A}}, \tag{6.60}$$

where $\beta(a,b)$ is the Euler Beta function. The integral in (6.60) is basically the standard representation (6.43) of the Bernoulli polynomials. Therefore $\mathcal{H}_L^{(1)}$ becomes:

$$\mathcal{H}_L^{(1)} = -\frac{(-1)^{L+1}\alpha^{2L}}{L!(L-1)!}\frac{2^{3L}\,\pi^L}{g_{2d}^{2L}\,N^L}\left(\frac{-g_{2d}^2}{2\pi}\right)\beta\left(\frac{1}{2},L\right)\frac{(2\pi)^{2L+1}(-1)^{L+1}}{2(2L+1)}B_{2L+1}\left(\frac{\pi-\varphi}{2\pi}\right). \tag{6.61}$$

Finally inserting the expression for α and using (6.5), we obtain the desired result

$$\mathcal{H}_L^{(1)} = -\frac{(-1)^L\lambda^{L+1}}{4\pi(2L+1)!}B_{2L+1}\left(\frac{\pi-\varphi}{2\pi}\right). \tag{6.62}$$

6.4 The $L=1$ case from perturbative $\mathcal{N}=4$ SYM

In order to check the above results, in this Section we compute the one-loop Feynman diagrams associated to the Bremsstrahlung function for the operator insertion with $L=1$. It can be considered also as further test of the correspondence between $\mathcal{N}=4$ BPS observables on S^2 and two-dimensional Yang-Mills theory on the sphere. We are

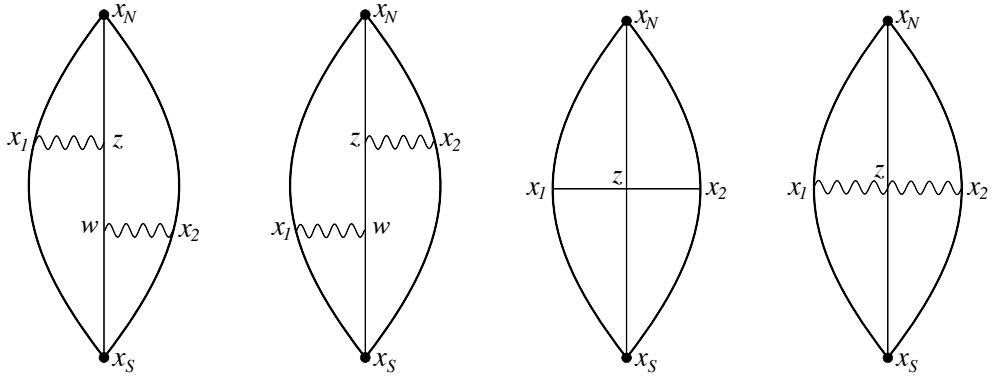

(a) H_1 (b) H_2 (c) X_1 (d) X_2

Figure 6.5: All the δ-dependent diagrams at order λ^2

interested only in the δ-dependent contributions, then we have to consider just diagrams which connect the right and left sides of the wedge, at the first non-trivial order. In Figure 6.5 we represent all the δ-dependent Feynman graphs we can draw at order λ^2.

The diagram (a) of Figure 6.5 is given by

$$[3.(\mathrm{a})] = \frac{\lambda^2}{4}\int_0^\pi d\tau_1 \int_\pi^{2\pi} d\tau_2\, \dot{x}_1^\mu \dot{x}_2^\nu \left(\partial_{x_1^\mu}\partial_{x_2^\nu} + 2\partial_{x_1^\mu}\partial_{x_S^\nu} + 2\partial_{x_N^\mu}\partial_{x_2^\nu} + 4\partial_{x_N^\mu}\partial_{x_S^\nu}\right)\mathcal{H}(x_1, x_N; x_2, x_S)\,, \tag{6.63}$$

where

$$\mathcal{H}(x_1, x_2; x_3, x_4) \equiv \int \frac{d^4z\, d^4w}{(2\pi)^8} D(x_1 - z)D(x_2 - z)D(w - z)D(x_3 - w)D(x_4 - w) \tag{6.64}$$

with $D(x-y) = 1/(x-y)^2$. All but the last term in (6.63) contain at least one derivative with respect to τ_1 or τ_2: these terms, after the integration over τ, are δ-independent. Therefore we are left with

$$\begin{aligned} H_1 &= \lambda^2 \int_0^\pi d\tau_1 \int_\pi^{2\pi} d\tau_2\, \dot{x}_1^\mu \dot{x}_2^\nu\, \partial_{x_N^\mu}\partial_{x_S^\nu}\mathcal{H}(x_1, x_N; x_2, x_S) \\ &= \frac{\lambda^2}{(2\pi)^2}\int_0^\pi d\tau_1 \int_\pi^{2\pi} d\tau_2 \int d^4z\, (\dot{x}_1\cdot\partial_{x_N})\, D(x_1 - z)D(x_N - z)(\dot{x}_2\cdot\partial_{x_S})\, \mathcal{I}_1(x_S - z, x_2 - z)\,, \end{aligned} \tag{6.65}$$

where

$$\mathcal{I}_1(x_1 - x_3, x_2 - x_3) \equiv \frac{1}{(2\pi)^6}\int d^4w\, D(x_1 - w)D(x_2 - w)D(x_3 - w)\,. \tag{6.66}$$

To compute one of the Feynman integrals in (6.65), we apply the trick used in [109]. In particular we add to the integrand a term which becomes δ-independent after the τ integration

$$(\dot{x}_1\cdot\partial_{x_N})\, D(x_1-z)D(x_N-z)(\dot{x}_2\cdot\partial_{x_2})\, \mathcal{I}_2(x_S-z,x_2-z)\,, \tag{6.67}$$

where $\mathcal{I}_2$ is defined in [109]. Therefore we can recast the δ-dependence of (6.65) as

$$\frac{\lambda^2}{(2\pi)^2}\int_0^\pi d\tau_1\!\!\int_\pi^{2\pi} d\tau_2\!\!\int d^4z\,(\dot{x}_1\cdot\partial_{x_N})\, D(x_1-z)D(x_N-z)\;\dot{x}_2\cdot V(x_S-z,x_2-z)\,, \tag{6.68}$$

where

$$V^\mu(x,y)\equiv\partial_{x^\mu}\mathcal{I}_1(x,y)-\partial_{y^\mu}\mathcal{I}_2(x,y). \tag{6.69}$$

Using the explicit representation for V^μ (see [109]), we can write

$$\begin{aligned}\dot{x}_2\cdot V(x_S-z,x_2-z)=\frac{D(x_S-z)}{32\pi^4}\Bigg\{\frac{d}{d\tau_2}\Bigg[\mathrm{Li}_2\left(1-\frac{(x_S-x_2)^2}{(x_2-z)^2}\right)+\frac{1}{2}\log^2\left(\frac{(x_S-x_2)^2}{(x_2-z)^2}\right)\\ -\frac{1}{2}\log^2\left(\frac{(x_S-x_2)^2}{(x_S-z)^2}\right)\Bigg]-2\dot{x}_2\cdot(x_S-x_2)D(x_S-x_2)\log\left(\frac{(x_2-z)^2}{(x_S-z)^2}\right)\Bigg\}.\end{aligned} \tag{6.70}$$

Again the total derivative gives a δ-independent contribution, then we have

$$\begin{aligned}H_1=-\frac{\lambda^2}{(2\pi)^6}\int_0^\pi d\tau_1\!\!\int_\pi^{2\pi} d\tau_2\,(\dot{x}_2\cdot x_S)D(x_S-x_2)\int d^4z\,(\dot{x}_1\cdot\partial_{x_N})\,D(x_1-z)\\ D(x_N-z)D(x_S-z)\,\log\!\left(\frac{(x_2-z)^2}{(x_S-z)^2}\right)+\text{“}\delta\text{-ind. terms”}\,.\end{aligned} \tag{6.71}$$

The δ-dependent part of the diagram in Figure 6.5.(b) is easily obtained from H_1 by exchanging $x_N\leftrightarrow x_S$.

The diagrams (c) and (d) of Figure 6.5 are given by

$$\begin{aligned}[3.(c)]=X_1=-\frac{\lambda^2}{4}\cos\delta\int_0^\pi d\tau_1\int_\pi^{2\pi} d\tau_2\;\mathcal{X}(1,1,1,1)\,,\\ [3.(d)]=X_2=-\frac{\lambda^2}{4}\int_0^\pi d\tau_1\int_\pi^{2\pi} d\tau_2\;\dot{x}_1\cdot\dot{x}_2\;\mathcal{X}(1,1,1,1)\,,\end{aligned} \tag{6.72}$$

where $\mathcal{X}$ is the scalar component of a more general class of tensorial Feynman integrals $\mathcal{X}^{\mu_1\cdots\mu_n}$ defined as follows

$$\mathcal{X}^{\mu_1\cdots\mu_n}(\nu_1,\nu_2,\nu_3,\nu_4)\equiv\int\frac{d^4z}{(2\pi)^6}\;z^{\mu_1}...z^{\mu_n}\,D(x_S-z)^{\nu_1}D(x_1-z)^{\nu_2}D(x_N-z)^{\nu_3}D(x_2-z)^{\nu_4}. \tag{6.73}$$

Now, recalling the definition (6.16) and denoting with the prime the derivative respect to δ (notice that x_2, x_2' and $\dot{x}_2$ form an orthogonal basis), we have

$$\begin{aligned}
H_1' =& 4\lambda^2 \int_0^{\pi} d\tau_1 \int_{\pi}^{2\pi} d\tau_2 \, (\dot{x}_2 \cdot x_S) D(x_S - x_2) \, x_2'^{\mu} \, \dot{x}_1^{\nu} \; (x_N^{\nu} \mathcal{X}^{\mu}(1,1,2,1) - \mathcal{X}^{\mu\nu}(1,1,2,1)) \; , \\
H_2' =& 4\lambda^2 \int_0^{\pi} d\tau_1 \int_{\pi}^{2\pi} d\tau_2 \, (\dot{x}_2 \cdot x_N) D(x_N - x_2) \, x_2'^{\mu} \, \dot{x}_1^{\nu} \; (x_S^{\nu} \mathcal{X}^{\mu}(2,1,1,1) - \mathcal{X}^{\mu\nu}(2,1,1,1)) \; , \\
X_1' =& \frac{\lambda^2}{4} \int_0^{\pi} d\tau_1 \int_{\pi}^{2\pi} d\tau_2 \; \left(\sin\delta \, \mathcal{X}(1,1,1,1) - 2\cos\delta \, x_2'^{\mu} \, \mathcal{X}^{\mu}(1,1,1,2) \right) \; , \\
X_2' =& \frac{\lambda^2}{4} \int_0^{\pi} d\tau_1 \int_{\pi}^{2\pi} d\tau_2 \; \left(-(\dot{x}_1 \cdot x_2') \, \mathcal{X}(1,1,1,1) + 2(\dot{x}_1 \cdot \dot{x}_2) \, x_2'^{\mu} \, \mathcal{X}^{\mu}(1,1,1,2) \right) \; .
\end{aligned} \tag{6.74}$$

Finally, summing up all the different contributions in $\mathcal{N} = 4$ SYM, we obtain the function $\mathcal{H}_1^{(1)}$ defined in (6.16)

$$\mathcal{H}_1^{(1)} = \frac{1}{2}(H_1' + H_2' + X_1' + X_2') \Big|_{\delta = \pi - \varphi} \; . \tag{6.75}$$

In order to check the results of the previous sections, it is enough to perform the integrals numerically. The result of the numerical computation is shown in Figure 6.6.

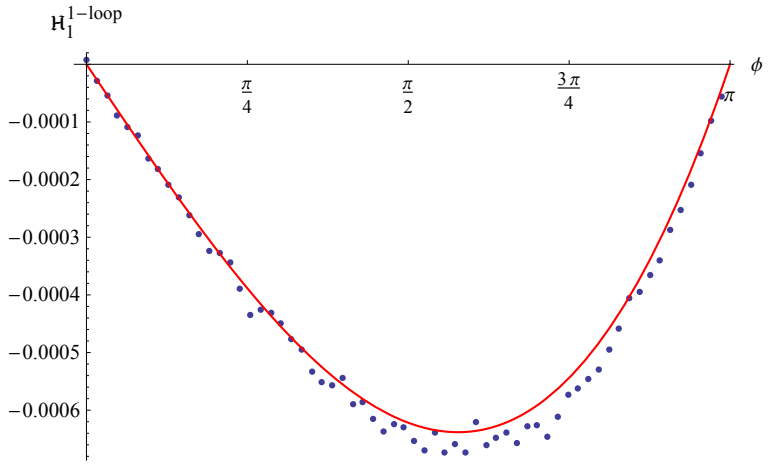

Figure 6.6: Numerical computation of $\mathcal{H}_1^{(1)}$. The blue dots are the numerical data and the red line is the expected curve.

The numerical data are the average of several Montecarlo integrations. The data error is bigger when φ is closed to $\pi/2$ because the integrals in the (6.75) are oscillatory.

In principle we could also compute analytically the integrals in (6.75) with the help of usual Feynman integral techniques. Indeed, in the dual conformal symmetry picture,

the quantities $\mathcal{X}$ are the so-called "*box*" integrals. Decomposing tensorial boxes in combinations of scalar ones, one should expand the result on a basis of the Master Integrals. Finally the tricky part would consist in computing the remaining integrals over the loop parameters. These quite technical computations are beyond the aim of this thesis and we leave them to further developments in a may be more general setting.

Chapter 7

Ladder diagrams resummation in the ABJ(M) cusp anomalous dimension

The duality between $\mathcal{N} = 6$ Super Chern-Simons theory with matter and string theory on $AdS_4 \times \mathbb{CP}^3$ represents one the most interesting possibilities to explore AdS/CFT correspondence beyond the original paradigm (see Section 2.1.5 and 2.2). Although it seems to share many similarities with the cousin $\mathcal{N} = 4$ Super Yang-Mills theory in four dimensions, there are still many aspects calling for a better comprehension. Supersymmetric Wilson loops, in particular, provide a rich class of BPS observables [77, 78, 79, 80, 81, 87, 172] that can be computed exactly through localization technique in the simplest situations [38]. While their quantum behavior is still rather mysterious in the general case [82], the well-understood 1/2 BPS and 1/6 BPS circles, presented in Section 3.2 and more explicitly in Section 3.3.2, exhibit an intriguing non-trivial interpolation between weak and strong coupling regime [111, 110, 173, 174]. A careful study of the relevant matrix models [174] has also unveiled a variety of phenomena of string/M-theory origin [175, 176, 177]. This contrasts with the relative simplicity of $\mathcal{N} = 4$ SYM, where the gaussian matrix model that we have seen in Section 3.4.1 describes exactly the dynamics of 1/2 BPS Wilson loops [37].

Wilson loops are relevant in gauge theories because they encode important properties of scattering amplitudes and infrared radiation: the cusp anomalous dimension $\Gamma(\varphi, \theta)$, presented in Chapter 4, appears in fact in many interesting physical situations as we have seen.

As anticipated before, even for the simple circular 1/2 BPS Wilson loop the interpolation between weak and strong regimes for ABJ(M) theory appears to be non-trivial. Integrability itself has been explored here in a somehow limited range of situations [178, 179, 180, 181, 182]: when established it still depends on an elusive interpolating

function, $h(\lambda)$ [183, 184, 185]. Recently a proposal for the functional form of $h(\lambda)$ has been advanced [186] and checked at two-loop level in string theory [187], under suitable assumptions. Alternatively $h(\lambda)$ could be determined by computing exactly some quantity by integrability and confronting with the same calculation by localization (or by other QFT techniques in which unknown functions are absent). A candidate quantity is the ABJM Bremsstrahlung function, for which all-order proposal exists [85], but integrability has not been yet applied to its determination. For this reason we think it is important to study $\Gamma(\varphi, \theta)$ in $\mathcal{N} = 6$ Super Chern-Simons theory: it would be useful to obtain exact QFT results to be compared with the integrability approach and, at strong coupling, with string theory. $\Gamma(\varphi, \theta)$ has been briefly discussed in ABJ(M) theory in Section 4.2.2.1. The resulting cusped Wilson loop is not globally supersymmetric and its exact evaluation seems very challenging.

Fortunately, the analogous system in $\mathcal{N} = 4$ SYM can be tackled in a particular limit through Feynman diagrams resummation. In [141] a new scaling limit involving the complexified angle θ was introduced,

$$i\theta >> 1, \quad \lambda << 1, \quad \hat{\lambda} = \lambda \exp(i\theta/4) \text{ fixed.} \tag{7.1}$$

In this limit the leading order contribution is simply given by ladder diagrams, where the rungs are made by scalar exchanges. The ladder diagrams can be summed up efficiently using a Bethe-Salpeter equation that can be solved exactly in the small φ limit. The strong coupling behavior has been also examined, finding agreement with the corresponding string theory calculation [141]. Later it was also performed an analysis at next-to-leading order, generalizing the original Bethe-Salpeter equation and computing the relevant corrections at strong coupling [142]. Remarkably these corrections have been also obtained from string theory and successfully compared each other. As repeatedly stressed in the original analysis [141], the matching of the strong coupling limit of the Bethe-Salpeter solution with the string theory computation is a bit surprising. The ladders limit, $\lambda \to 0$ with $\hat{\lambda}$ fixed, is different from the strong coupling limit $\lambda \to \infty$ with $i\theta >> 1$ fixed and the result could in principle depend on their order: nevertheless they agree at leading and subleading level.

In this Chapter we will consider a similar limit in three-dimensional ABJ(M) theory, obtaining some exact results for $\Gamma(\varphi, \hat{\lambda}_i)$. Here $\lambda_1 = \frac{N}{k}, \lambda_2 = \frac{M}{k}$ are the 't Hooft couplings of the ABJ(M) theory with gauge group $U(N) \times U(M)$, while κ is the Chern-Simons level. The presence of fermionic couplings to the cusped loop inherits a surprising supersymmetric structure in the relevant Bethe-Salpeter equation and then we will be able to solve the associated effective Schroedinger problem exactly for any value of φ. This is in sharp contrast with the $\mathcal{N} = 4$ SYM case, where an analytic solution for the Bethe-Salpeter equation exists only at $\varphi = 0$ (that in this case is the only supersymmetric point of the associated Schroedinger equation [141]).

The Chapter is structured in the following way: in Section 7.1 we recall the main features of the cusped Wilson loop in ABJ(M) theory presented in Section 4.2.2.1. We

also consider the quantum behavior of the straight-line and its divergences. The limit in which the ladder diagrams dominate is described in Section 7.2, where we also discuss how to derive the cusp anomalous dimension both in the explicit cut-off scheme and in dimensional regularization. In Section 7.3 we derive the relevant Bethe-Salpeter equation and, after diagonalization, we obtain the associated Schroedinger equation. We solve the supersymmetric Schroedinger equations for generic opening angle φ, in the cut-off scheme, and for $\varphi = 0$ in dimensional regularization. In Section 7.4 we obtain the cusp anomalous dimension at leading order and discuss the operator mixing for the cusped Wilson loops. In passing we also propose the all-order exponentiation structure for the cusped 1/2 BPS Wilson loop. This Chapter is based on [188].

7.1 The 1/2 BPS generalized cusped Wilson line in ABJ(M) theory

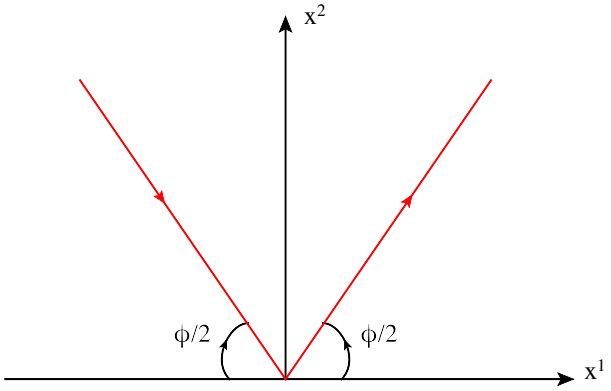

Figure 7.1: The planar cusp

We consider the theory on the Euclidean space-time and take the contour depicted in Figure 7.1. The two rays are in the plane $(1, 2)$, intersect at the origin and are given, as anticipated in Section 4.2.2.1, by

$$x^\mu = \{0, \tau \cos\frac{\varphi}{2}, |\tau| \sin\frac{\varphi}{2}\} \qquad -\infty \geq \tau \leq \infty \tag{7.2}$$

The angle between the rays is $\pi - \varphi$, thus $\varphi = 0$ gives the continuous straight line.

Let us now analyze more deeply the scalar and fermion couplings already sketched in Section 4.2.2.1. In order to define the generalized cusp, one have to consider different scalar and fermion couplings on the two segments of the cusp (but constant on each segment). The fermionic couplings are of the form

$$\eta^\alpha_{iM} = n_{iM}\eta^\alpha_i \qquad \text{and} \qquad \bar{\eta}^M_{i\alpha} = n^M_i \bar{\eta}_{i\alpha} \tag{7.3}$$

where the index $i = 1, 2$ specifies which edge of the cusp we are considering. As discussed in [83] we can take:

$$\eta_{1\alpha} = \begin{pmatrix} e^{-i\frac{\varphi}{4}} & e^{i\frac{\varphi}{4}} \end{pmatrix}, \qquad \bar{\eta}_{1\alpha} = i \begin{pmatrix} e^{i\frac{\varphi}{4}} \\ e^{-i\frac{\varphi}{4}} \end{pmatrix} \tag{7.4}$$

and

$$\eta_{2\alpha} = \begin{pmatrix} e^{i\frac{\varphi}{4}} & e^{-i\frac{\varphi}{4}} \end{pmatrix}, \qquad \bar{\eta}_{2\alpha} = i \begin{pmatrix} e^{-i\frac{\varphi}{4}} \\ e^{i\frac{\varphi}{4}} \end{pmatrix} \tag{7.5}$$

The $R-$symmetry part of the couplings is totally unconstrained and we choose

$$n_{1M} = \begin{pmatrix} \cos\frac{\theta}{4} & \sin\frac{\theta}{4} & 0 & 0 \end{pmatrix} \qquad \text{and} \qquad n_{2M} = \begin{pmatrix} \cos\frac{\theta}{4} & -\sin\frac{\theta}{4} & 0 & 0 \end{pmatrix} \tag{7.6}$$

(and we denote by $\bar{n}_i^M$ the transpose of n_{iM}). The two matrices which couple the scalars are built in terms of n and $\bar{n}$. On the two edges we have

$$M_1{}^I_J = \hat{M}_1{}^I_J = \begin{pmatrix} -\cos\frac{\theta}{2} & -\sin\frac{\theta}{2} & 0 & 0 \\ -\sin\frac{\theta}{2} & \cos\frac{\theta}{2} & 0 & 0 \\ 0 & 0 & 1 & 0 \\ 0 & 0 & 0 & 1 \end{pmatrix} \quad \text{and} \quad M_2{}^I_J = \hat{M}_2{}^I_J = \begin{pmatrix} -\cos\frac{\theta}{2} & \sin\frac{\theta}{2} & 0 & 0 \\ \sin\frac{\theta}{2} & \cos\frac{\theta}{2} & 0 & 0 \\ 0 & 0 & 1 & 0 \\ 0 & 0 & 0 & 1 \end{pmatrix}. \tag{7.7}$$

In general this configuration is not supersymmetric unless $\theta = \pm\varphi$ [83].

The vacuum expectation value of the Wilson loop is defined by (3.86). In order to do a perturbative evaluation at weak coupling of (3.86), we have to distinguish the upper left $N \times N$ and the lower right $M \times M$ blocks of the super-matrix as explained in Section 3.3.2. For these sub-sectors the trace is obviously taken in the fundamental representation $\mathbf{N}$ or $\mathbf{M}$ of the gauge group respectively.

7.1.1 The structure of the divergences and the straight-line exponentiation

We are of course interested in the quantum expectation value of the generalized cusped Wilson loop previously introduced. In particular we need a complete understanding of its singularities to properly extract the cusp anomalous dimension. In four-dimensional $\mathcal{N} = 4$ SYM, the perfect balance between the gauge and scalar contributions cancels all the infinities related to integrations along the smooth part of the contour. Only the singularities associated to the discontinuous behavior at the cusp appear and one immediately singles out the relevant diagrams to be computed. In three dimensions the story is a little bit more subtle: the presence of fermionic contributions breaks that equilibrium and we have to deal with divergent contributions [1] that persist even in absence of the cusp: the supersymmetric straight-line itself, although being BPS,

[1] As discussed in [83] one has to resort to a renormalization procedure suitable for open Wilson lines

is not finite in perturbation theory, at least in dimensional regularization [83]. This type of singularities shows up, in general, in diagrams that lie on a single halve of the cusped loop: the scaling limit considered in the rest of this Chapter selects only ladder diagrams, then we do not have to face these divergences. Nevertheless we find useful to discuss them in the context of the straight-line and we will also learn something about their exponentiation properties.

We will evaluate the straight-line of length $2L$ for $\theta = 0$ up to two-loops in ABJ(M), guessing the all-loop behavior. We employ dimensional regularization shifting the dimension to $d = 3 - 2\epsilon$ while keeping the Dirac algebra and $\epsilon^{\mu\nu\rho}$ tensor strictly in 3 dimensions. Note that this breaks the conformal invariance introducing a mass scale $\mu^{2\epsilon}$ that keeps the action dimensionless. At a given perturbative order, we need to sum the contributions lying the upper-left and the lower-right blocks and we normalize the Wilson line as follows

$$\langle \mathcal{W}_{sl} \rangle_{\pm}^{(l)} = \frac{\langle \mathcal{W}_{sl} \rangle_{\uparrow}^{(l)} \pm \langle \mathcal{W}_{sl} \rangle_{\downarrow}^{(l)}}{N \pm M} \tag{7.8}$$

where $\uparrow$ and $\downarrow$ specify the upper-left sector $N \times N$ and the lower-right sector $M \times M$ respectively, l the perturbative order and $\pm$ the loop constructed with the trace or supertrace as in (3.56).

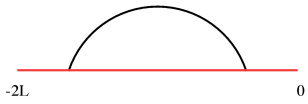

Figure 7.2: The fermion exchange

The perturbative expansion for the straight-line follows from the (3.86) and it is a particular case of the one considered in [83]. The only non-vanishing diagram at one-loop is the fermion exchange in Figure 7.2. Its value is given by:

$$\begin{aligned} \langle \mathcal{W}_{sl} \rangle_{+}^{(1)} =& - \left(\frac{2\pi}{\kappa} \right) \frac{2MN}{M+N} \frac{\Gamma\left(\frac{1}{2} - \epsilon\right)}{4\pi^{3/2-\epsilon}} \frac{(2\mu L)^{2\epsilon}}{\epsilon} \\ \langle \mathcal{W}_{sl} \rangle_{-}^{(1)} =& 0 \end{aligned} \tag{7.9}$$

At two-loop, it is easy to check that all the bosonic diagrams vanish. The only non-vanishing two-loop diagrams are summarized in Figure 7.3. We first consider the diagrams 7.3.(a) and 7.3.(b): they have been computed in [83] and their value in dimensional regularization is the following

$$\begin{aligned} [7.3.(a)]_{\uparrow} =& \left(\frac{2\pi}{\kappa} \right)^2 M^2 N \frac{\Gamma\left(\frac{1}{2} - \epsilon\right)^2}{16\pi^{3-2\epsilon}} \frac{\sqrt{\pi}}{2^{4\epsilon}} \frac{\Gamma(2\epsilon+1)}{\Gamma\left(2\epsilon + \frac{1}{2}\right)} \frac{(2\mu L)^{4\epsilon}}{\epsilon^2} \\ [7.3.(b)]_{\uparrow} =& \left(\frac{2\pi}{\kappa} \right)^2 M N^2 \frac{\Gamma\left(\frac{1}{2} - \epsilon\right)^2}{16\pi^{3-2\epsilon}} \frac{(2\epsilon - 1)}{2(4\epsilon - 1)} \frac{(2\mu L)^{4\epsilon}}{\epsilon^2} \end{aligned} \tag{7.10}$$

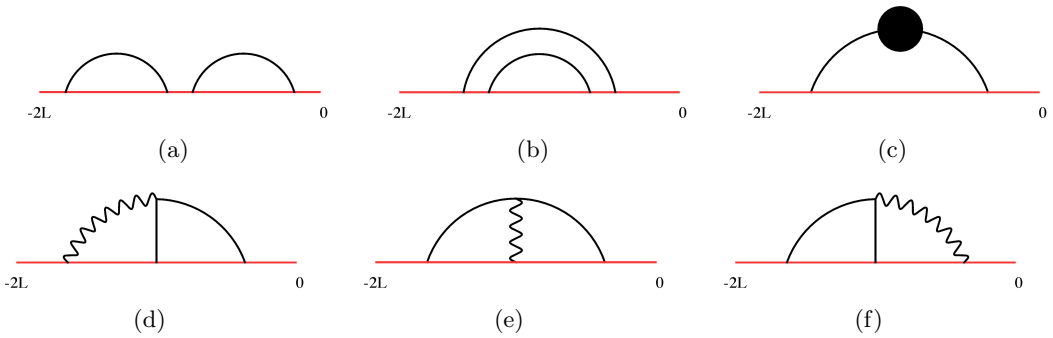

Figure 7.3: Non-vanishing two loop diagrams for the straight-line.

The one-loop correction to the fermion exchange 7.3.(c) drops out when we take the trace (we have opposite contributions from the two blocks) but is relevant in the supertrace and it is given by

$$[7.3.(c)]_{\uparrow} = \left(\frac{2\pi}{\kappa}\right)^2 MN(N-M)\frac{\Gamma\left(\frac{1}{2}-\epsilon\right)^2}{16\pi^{3-2\epsilon}}\frac{(2\mu L)^{4\epsilon}}{\epsilon(1-4\epsilon)} \tag{7.11}$$

We consider now the diagrams involving the gauge-vertex interaction: disregarding the group theoretical factor, one can prove that $7.3.(d)+7.3.(e) = 7.3.(f)$. Exploiting then the result of [83] we get:

$$[7.3.(d)]_{\uparrow}+[7.3.(e)]_{\uparrow}+[7.3.(f)]_{\uparrow} = -\left(\frac{2\pi}{\kappa}\right)^2 MN(M+N)\frac{\Gamma^2\left(\frac{1}{2}-\epsilon\right)}{2^{6+4\epsilon}\pi^{3-2\epsilon}}\frac{4\sqrt{\pi}\Gamma(2\epsilon)-2^{4\epsilon}\Gamma\left(2\epsilon-\frac{1}{2}\right)}{\Gamma(2\epsilon+\frac{1}{2})}\frac{(2\mu L)^{4\epsilon}}{\epsilon} \tag{7.12}$$

Summing up all the contributions, we can extract the complete two-loop result for the trace:

$$\langle \mathcal{W}_{sl}\rangle_{+}^{(2)} = \frac{1}{2}\left(\frac{2\pi}{\kappa}\right)^2 MN\frac{\Gamma\left(\frac{1}{2}-\epsilon\right)^2}{16\pi^{3-2\epsilon}}\frac{(2\mu L)^{4\epsilon}}{\epsilon^2} \tag{7.13}$$

and for the supertrace

$$\langle \mathcal{W}_{sl}\rangle_{-}^{(2)} = \frac{1}{2}\left(\frac{2\pi}{\kappa}\right)^2 MN\frac{\Gamma\left(\frac{1}{2}-\epsilon\right)^2}{16\pi^{3-2\epsilon}}\frac{(2\mu L)^{4\epsilon}}{\epsilon^2}\left(\frac{1}{1-4\epsilon}-\frac{\Gamma(2\epsilon)\Gamma(1+2\epsilon)}{\Gamma(4\epsilon)}\right) \tag{7.14}$$

Notice that for the traced operator, in the ABJM case ($M=N$), we have

$$\langle \mathcal{W}_{sl}\rangle_{+}^{(2)} = \frac{1}{2}\left(\langle \mathcal{W}_{sl}\rangle_{+}^{(1)}\right)^2. \tag{7.15}$$

This is the hallmark of abelian exponentiation, namely up to two-loop we can write

$$\langle \mathcal{W}_{sl}\rangle_{+}^{\text{ABJM}} = \exp\left(-\frac{2\pi}{\kappa}N\frac{\Gamma\left(\frac{1}{2}-\epsilon\right)}{4\pi^{3/2-\epsilon}}\frac{(2\mu L)^{2\epsilon}}{\epsilon}\right) \tag{7.16}$$

Actually, we are able to guess the exponentiation also in the ABJ case ($M \neq N$): indeed, focusing on the gauge group part, up to two-loop we can write for the trace:

$$\begin{aligned}\langle \mathcal{W}_{sl} \rangle_{+}^{\text{ABJ}} =& \cosh V_{\epsilon}^{+} + \frac{2\sqrt{MN}}{M+N} \sinh V_{\epsilon}^{+} \\ =& \frac{(\sqrt{M}+\sqrt{N})^2}{2(M+N)} e^{V_{\epsilon}^{+}} + \frac{(\sqrt{M}-\sqrt{N})^2}{2(M+N)} e^{-V_{\epsilon}^{+}}\end{aligned} \tag{7.17}$$

where

$$V_{\epsilon}^{+} = -\left(\frac{2\pi}{\kappa}\right) \sqrt{MN} \frac{\Gamma\left(\frac{1}{2}-\epsilon\right)}{4\pi^{3/2-\epsilon}} \frac{(2\mu L)^{2\epsilon}}{\epsilon} \tag{7.18}$$

Equations (7.16) and (7.17) naturally suggest to conjecture that this is the exact value for the traced straight-line in dimensional regularization: if so, the divergent contribution would be just a one-loop effect, which propagates to higher loops to preserve exponentiation. Let us notice that, in the ABJM case, the cusped Wilson loop would be cured at all-order from spurious single-line divergence by simply subtracting the one-loop contribution of the straight-line: only the genuine anomalous cusp divergence should survive in the final result [83]. On the other hand, for $M \neq N$ our straight-line conjecture would suggest a peculiar exponentiation structure, that should be valid also for non-trivial opening angles. Eq. (7.17) implies a double-exponentiation that is different from the one proposed in [83] and predicts precise mixing coefficients between the two exponential factors. Nicely we will recover the same pattern and the same mixing coefficients in the ladder-resummed result.

We end the Section with some remarks concerning the supertrace. One can imagine that the supertrace operator could have a similar double exponentiation behavior of the traced operator. Since the one-loop expectation value of $\mathcal{W}_{-}$ vanishes, it is reasonable to make the following ansatz

$$\langle \mathcal{W}_{sl} \rangle_{-}^{\text{ABJ}} = \cosh V_{\epsilon}^{-} = \frac{1}{2} e^{V_{\epsilon}^{-}} + \frac{1}{2} e^{-V_{\epsilon}^{-}} \tag{7.19}$$

where

$$V_{\epsilon}^{-} = -\left(\frac{2\pi}{\kappa}\right) \sqrt{MN} \frac{\Gamma\left(\frac{1}{2}-\epsilon\right)}{4\pi^{3/2-\epsilon}} \frac{(2\mu L)^{2\epsilon}}{\epsilon} \sqrt{\frac{\Gamma(2\epsilon)\Gamma(1+2\epsilon)}{\Gamma(4\epsilon)} - \frac{1}{1-4\epsilon}} \tag{7.20}$$

have been obtained from the two-loop result (7.14). Notice that in this case we cannot check the ansatz because the first non-zero contribution arises from a four-loop computation. The quantities V_{ϵ}^{+} and V_{ϵ}^{-} differ only by finite terms. Indeed, by expanding the square root in (7.20), we obtain

$$V_{\epsilon}^{-} = -\left(\frac{2\pi}{\kappa}\right) \sqrt{MN} \frac{\Gamma\left(\frac{1}{2}-\epsilon\right)}{4\pi^{3/2-\epsilon}} \frac{(2\mu L)^{2\epsilon}}{\epsilon} \left[1 - 2\epsilon + \mathcal{O}(\epsilon^2)\right] = V_{\epsilon}^{+} + \mathcal{O}(1) \tag{7.21}$$

7.2 The cusp anomalous dimension in ABJ(M) theory and its computation through ladder diagrams

In this Section we discuss the definition of the cusp anomalous dimension in general ABJ(M) theories and its computation in a limit in which ladder diagrams dominate. New features in the $N \neq M$ will emerge due to the exponentiation properties of our cusped loops, as suggested from the straight-line example and confirmed in the ladder limit.

7.2.1 The cusp anomalous dimension in ABJ(M) theory

We start by recalling the four-dimensional story: the generalized cusp anomalous dimension is defined by the divergent behavior of a cusped Wilson loop [114]

$$\langle \mathcal{W}_{\text{cusp}} \rangle \simeq e^{-\Gamma_{\text{cusp}}(\varphi,\theta) \log \frac{\Lambda_{UV}}{\Lambda_{IR}}} .$$

Here Λ_{IR} and Λ_{UV} are the infrared and ultraviolet cut-offs respectively, that regularize the specific divergencies associated to the cusp angle. Typically one takes $\Lambda_{IR} = 1/L$, where L is the (finite) length of the two rays and $\Lambda_{UV} = 1/\varepsilon$, with ε being a short-length scale cutting out the the cusp singularity. An alternative, but completely equivalent, definition can be obtained in dimensional regularization [117], considering the renormalization of the cusped Wilson loop operator. After the usual renormalization of the gauge theory[2], the relevant Wilson loop must be still multiplicatively renormalized by means of a renormalization constant Z_{cusp}

$$\mathcal{W}^R_{\text{cusp}} = Z^{-1}_{\text{cusp}} \mathcal{W}^B_{\text{cusp}}$$

where B and R refer to the bare and renormalized operator respectively. Z_{cusp} introduces the usual mass scale μ, associated to the dimensional regularization, into the game and the cusp anomalous dimension is defined as

$$\Gamma_{\text{cusp}} = -\mu \frac{d}{d\mu} \log Z_{\text{cusp}}. \tag{7.22}$$

We remark that in this language Γ_{cusp} really plays the role of the anomalous dimension of a (non-local) quantum operator. At perturbative level it is easy to trace back the origin of this divergence: it comes from diagrams connecting both rays of the cusp and its exponentiation is governed by their maximal non-abelian part [117].

Il the ABJ(M) case the situation is a little bit different: we have two gauge groups and the fermionic interactions, that live in the off-diagonal sector of the super-connection, mix non-trivially the $U(N)$ and $U(M)$ structures. We expect therefore a non-standard

[2] In $\mathcal{N} = 4$ SYM this step is superfluous, being the β-function vanishing

exponentiation result for the cusped Wilson loop, as already hinted by the straight-line computation presented before. Moreover the absence of a non-abelian exponentiation theorem in this case forces us to make some assumption on the all-order structure of the cusp divergences. Based on the two-loop computation of [83] and the straight-line result we expect, in the general $N \neq M$ case and in dimensional regularization, that the quantum expectation value of our cusped Wilson loop organizes itself as

$$\langle \mathcal{W}_+ \rangle = c_1 \tilde{Z}_1 Z^{(1)}_{\text{cusp}} W_1^F + c_2 \tilde{Z}_2 Z^{(2)}_{\text{cusp}} W_2^F, \tag{7.23}$$

where $\tilde{Z}_1$ and $\tilde{Z}_2$ take into account the divergences coming from diagrams inserted on a single halve and we assume they are obtained from eq.(7.17)

$$\begin{aligned} \tilde{Z}_1 =& e^{V_\epsilon^+} = \exp\left[-\sqrt{MN} \left(\frac{2\pi}{\kappa}\right) \frac{\Gamma\left(\frac{1}{2}-\epsilon\right)}{4\pi^{3/2-\epsilon}} \frac{(2\mu L)^{2\epsilon}}{\epsilon} \right] \\ \tilde{Z}_2 =& e^{-V_\epsilon^+} = \exp\left[\sqrt{MN} \left(\frac{2\pi}{\kappa}\right) \frac{\Gamma\left(\frac{1}{2}-\epsilon\right)}{4\pi^{3/2-\epsilon}} \frac{(2\mu L)^{2\epsilon}}{\epsilon} \right] \end{aligned} \tag{7.24}$$

The mixing coefficients c_1, c_2 are as well guessed from eq. (7.17)

$$c_1 = \frac{(\sqrt{M}+\sqrt{N})^2}{2(M+N)}, \quad c_2 = \frac{(\sqrt{M}-\sqrt{N})^2}{2(M+N)} \tag{7.25}$$

while $Z^{(1)}_{\text{cusp}}$ and $Z^{(2)}_{\text{cusp}}$ contain the true singularities associated to the cusp. The factors W_1^F and W_2^F are instead finite contributions to the quantum expectation value that are irrelevant for the computation of the cusp anomalous dimension. The above structure, that will be exactly reproduced in the limit in which ladder diagrams are resummed, suggests that we actually have two different cusp anomalous dimensions

$$\Gamma^{(1)}_{\text{cusp}} = -\mu \frac{d}{d\mu} \log Z^{(1)}_{\text{cusp}}, \quad \Gamma^{(2)}_{\text{cusp}} = -\mu \frac{d}{d\mu} \log Z^{(2)}_{\text{cusp}} \tag{7.26}$$

This apparently unexpected fact has a natural interpretation: the cusped Wilson loop $\mathcal{W}_+$, constructed through the 1/2 BPS lines and defined with the trace, mixes under cusp renormalization with $\mathcal{W}_-$, the analogous operator defined through the super-trace!

As usual in the theory of renormalization of composed local operators we would expect the arising, in our case, of a matrix-valued set of renormalization constants: the independent anomalous dimensions can be extracted from the eigenvalues of this matrix. Let us see how the same happens in the present, non-local, situation. We start by expressing $\mathcal{W}_+^B$ and $\mathcal{W}_-^B$, seen as bare quantum operator, by means of two other bare operators

$$\begin{aligned} \mathcal{W}_+^B =& \mathcal{A}_{11} \mathcal{W}_1^B + \mathcal{A}_{12} \mathcal{W}_2^B \\ \mathcal{W}_-^B =& \mathcal{A}_{21} \mathcal{W}_1^B + \mathcal{A}_{22} \mathcal{W}_2^B \end{aligned} \tag{7.27}$$

that we assume to be diagonal under cusp renormalization

$$\begin{aligned}\mathcal{W}_1^B &= \mathcal{Z}_1\, \mathcal{W}_1^R \\ \mathcal{W}_2^B &= \mathcal{Z}_2\, \mathcal{W}_2^R\end{aligned} \tag{7.28}$$

These relations can be written using the coefficient matrix $\mathcal{A}_{ij}$

$$\begin{pmatrix}\mathcal{W}_+^B \\ \mathcal{W}_-^B\end{pmatrix} = \mathcal{A}\, \begin{pmatrix}\mathcal{W}_1^B \\ \mathcal{W}_2^B\end{pmatrix} \tag{7.29}$$

and the diagonal matrix $\mathcal{Z}$ containing the renormalization factors

$$\begin{pmatrix}\mathcal{W}_1^B \\ \mathcal{W}_2^B\end{pmatrix} = \begin{pmatrix}\mathcal{Z}_1 & 0 \\ 0 & \mathcal{Z}_2\end{pmatrix} \begin{pmatrix}\mathcal{W}_1^R \\ \mathcal{W}_2^R\end{pmatrix} \qquad \Rightarrow \qquad \begin{pmatrix}\mathcal{W}_1^B \\ \mathcal{W}_2^B\end{pmatrix} = \mathcal{Z}\, \begin{pmatrix}\mathcal{W}_1^R \\ \mathcal{W}_2^R\end{pmatrix} \tag{7.30}$$

The renormalized operators $\mathcal{W}_+^R$ and $\mathcal{W}_-^R$ are then expressed back from the bare ones using the matrix $\tilde{\mathcal{Z}} = \mathcal{A}\,\mathcal{Z}\,\mathcal{A}^{-1}$

$$\begin{pmatrix}\mathcal{W}_+^B \\ \mathcal{W}_-^B\end{pmatrix} = \tilde{\mathcal{Z}} \begin{pmatrix}\mathcal{W}_+^R \\ \mathcal{W}_-^R\end{pmatrix} \tag{7.31}$$

The quantum result eq. (7.23) is recovered identifying

$$\begin{aligned}\mathcal{Z}_1 &= \tilde{Z}_1\, Z_{\text{cusp}}^{(1)} \\ \mathcal{Z}_2 &= \tilde{Z}_2\, Z_{\text{cusp}}^{(2)}\end{aligned} \tag{7.32}$$

Based on the explicit two-loop calculation of [83] and the straight-line result we expect that for $N = M$ a simplification generally occurs: in both cases in fact, we observe the arising of a single exponential, signaling that the traced operator $\mathcal{W}_+$ does not mix and its renormalization is associated to a single cusp anomalous dimension.

7.2.2 The scaling limit selecting ladder diagrams

In [141] it was considered a scaling limit in $\mathcal{N} = 4$ SYM that allows an exact computation of the cusp anomalous dimension, by simply resumming an infinite class of ladder diagrams. The limit consists in complexifying the R-symmetry angle θ and taking

$$i\theta >> 1, \quad \lambda << 1, \quad \hat{\lambda} = \lambda \exp(i\theta/4) \text{ fixed.} \tag{7.33}$$

Pure scalar exchanges between the rungs of the cusped Wilson loop become dominant and can be resummed by means of a Bethe-Salpeter equation [141]. Subleading corrections can be also systematically included in this scheme and consistency at strong coupling with semiclassical string computations has been found [142].

In our case we want to consider a similar limit: upon a quick inspection of the perturbative diagrams we recognize two types of relevant contributions (we refer to [83]

for details on the perturbative expansion and related computations). At one-loop we have the single fermionic exchange,

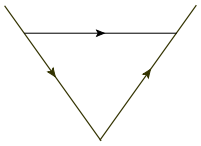

$$= \left(\frac{2\pi}{\kappa}\right) MN \frac{\Gamma\left(\frac{1}{2}-\epsilon\right)}{4\pi^{3/2-\epsilon}} (\mu L)^{2\epsilon} \frac{1}{\epsilon} \frac{\cos\frac{\theta}{2}}{\cos\frac{\varphi}{2}} \,.$$

We notice that the fermionic exchange is proportional to $\lambda \cos\frac{\theta}{2}$, suggesting to perform the scaling limit as

$$i\theta >> 1, \quad \lambda << 1, \quad \hat{\lambda} = \lambda \exp(i\theta/2) \text{ fixed.} \tag{7.34}$$

At two-loop we observe that the above limit suppresses all the diagrams in which internal interactions are present. Obviously the double-fermionic exchange survives but also a pure scalar exchange comes into the game

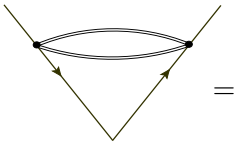

$$= -\left(\frac{2\pi}{\kappa}\right)^2 MN^2 \frac{\Gamma^2\left(\frac{1}{2}-\epsilon\right)}{16\pi^{3-2\epsilon}} (\mu L)^{4\epsilon} \cos^2\frac{\theta}{2} \frac{1}{\epsilon} \frac{\varphi}{\sin\varphi} \,.$$

This last contribution has exactly the same form of the one-loop scalar exchange in $\mathcal{N} = 4$ SYM, except that here it appears at two-loop and the scaling behavior is different.

It is not difficult to realize that, at leading order, the generic diagrams surviving the limit consist of ladders made by fermionic and scalar exchanges, that should therefore summed up to obtain the complete result. We remark that the contributions coming from diagrams ending on a single line, and so leading to divergences not related to the cusp renormalization constant, are automatically suppressed in our limit: we do not have to take into account the subtraction associated to $\tilde{Z}_1$ and $\tilde{Z}_2$. In the next Section we will derive an efficient way to sum up all the relevant ladder diagrams.

7.3 Bethe-Salpeter equation for the generalized cusp in ABJ(M) at leading order in the scaling limit

To calculate the n-th order correction to the cusp anomalous dimension, in principle it is enough to identify all diagrams that have order $O(\hat{\lambda}^n)$ in the scaling limit (7.34). But the number of such diagrams is infinite, and a better way to organize the calculation is to first compute the kernel diagrams and then generate all other diagrams with the help of the Bethe-Salpeter equation. The number of diagrams in the kernel at each order is finite. In addition, the Bethe-Salpeter equation automatically exponentiates the result, making it easy to extract Γ_{cusp}.

We denote the sum of the ladder diagrams by $F_a{}^b(s,t)$ where s and t are the positions on the cusp and a, b are group indices that can be $\{(i,j),(\hat{i},\hat{j})\}$ for $U(N)$ and $U(M)$,

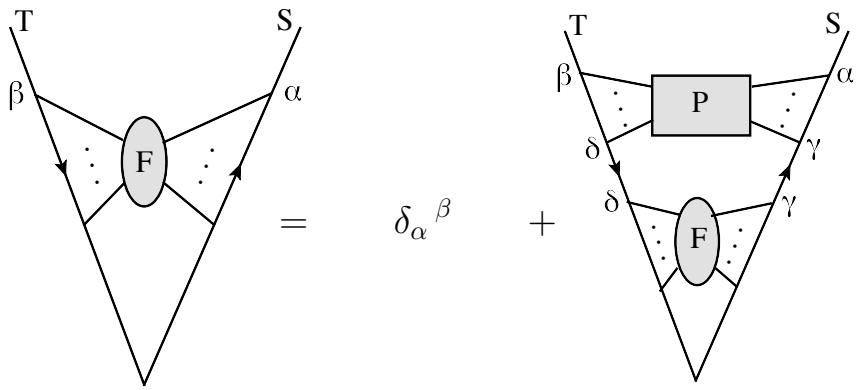

Figure 7.4: Bethe-Salpeter equation at leading order

respectively. $F_a{}^b(s,t)$ satisfies a Bethe-Salpeter equation

$$F_a{}^b(S,T) = \delta_a{}^b + \int_0^S ds \int_0^T dt\; F_c{}^d(s,t) P_a{}^c{}_d{}^b(s,t) \tag{7.35}$$

that is shown schematically in Figure 7.4. In the scaling limit (7.34) the scalar and the fermionic couplings of the loop dominate and one has to consider only exchanges of these fields between the two segments of the Wilson loop. The indices sequence follows the path-ordering of the Wilson loop and the scalar and fermionic propagators fix the kernel indices as follow:

$$P_a{}^c{}_d{}^b(s,t) \simeq \delta_a{}^b\, \delta^c{}_d \times (\text{a "scalar" function of } s \text{ and } t), \tag{7.36}$$

with

$$\begin{aligned}
P_i{}^k{}_l{}^j(s,t) &= M\delta_i{}^j \delta^k{}_l P^{(B)}(s,t) \\
P_i{}^{\hat{k}}{}_{\hat{l}}{}^j(s,t) &= \delta_i{}^j \delta^{\hat{k}}{}_{\hat{l}} P^{(F)}(s,t) \\
P_{\hat{i}}{}^k{}_l{}^{\hat{j}}(s,t) &= \delta_{\hat{i}}{}^{\hat{j}} \delta^k{}_l P^{(F)}(s,t) \\
P_{\hat{i}}{}^{\hat{k}}{}_{\hat{l}}{}^{\hat{j}}(s,t) &= N\delta_{\hat{i}}{}^{\hat{j}} \delta^{\hat{k}}{}_{\hat{l}} P^{(B)}(s,t)
\end{aligned} \tag{7.37}$$

where $P^{(F)}(s,t)$ is the fermionic propagator and $P^{(B)}(s,t)$ the scalar effective propagator (double exchange) defined by [83]:

$$\begin{aligned}
P^{(F)}(s,t) &= -\left(\frac{2\pi}{k}\right) \frac{\Gamma(1/2-\epsilon)\mu^{2\epsilon}}{4\pi^{3/2-\epsilon}} \frac{\cos\theta/2}{\cos\varphi/2}\, (\partial_s + \partial_t) \frac{1}{(s^2+t^2+2st\cos\varphi)^{\frac{1}{2}-\epsilon}} \\
P^{(B)}(s,t) &= \left(\frac{2\pi}{k}\right)^2 \frac{\Gamma^2(1/2-\epsilon)\mu^{4\epsilon}}{4\pi^{3-2\epsilon}} \frac{\cos^2\theta/2}{\cos^2\varphi/2}\, \frac{\cos^2\varphi/2}{(s^2+t^2+2st\cos\varphi)^{1-2\epsilon}}
\end{aligned} \tag{7.38}$$

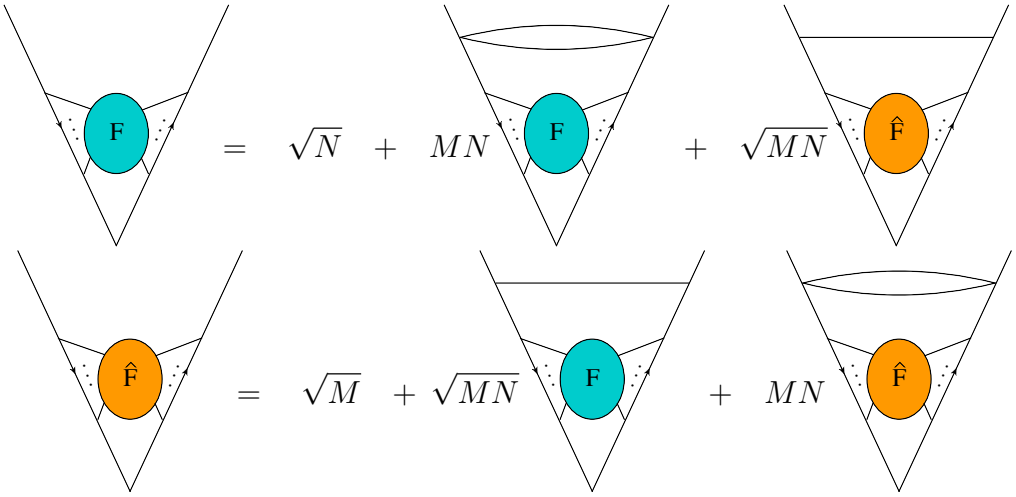

Figure 7.5: Bethe-Salpeter equation at leading order

According to $U(N)$ or $U(M)$ indices (7.35) splits into

$$\begin{aligned} F_i{}^j(S,T) &= \delta_i{}^j + \int_0^S ds \int_0^T dt \left(M F_k{}^l(s,t)\delta_i{}^j \delta^k{}_l P^{(B)}(s,t) + F_{\hat{k}}{}^{\hat{l}}(s,t)\delta_i{}^j \delta^{\hat{k}}{}_{\hat{l}} P^{(F)}(s,t) \right) \\ F_{\hat{i}}{}^{\hat{j}}(S,T) &= \delta_{\hat{i}}{}^{\hat{j}} + \int_0^S ds \int_0^T dt \left(F_k{}^l(s,t)\delta_{\hat{i}}{}^{\hat{j}} \delta^k{}_l P^{(F)}(s,t) + N F_{\hat{k}}{}^{\hat{l}}(s,t)\delta_{\hat{i}}{}^{\hat{j}} \delta^{\hat{k}}{}_{\hat{l}} P^{(B)}(s,t) \right). \end{aligned} \tag{7.39}$$

Thus, defining

$$\begin{aligned} F(S,T) &= \frac{1}{\sqrt{N}} \mathrm{Tr}_{\mathbf{N}}[F_i{}^j(S,T)] \\ \hat{F}(S,T) &= \frac{1}{\sqrt{M}} \mathrm{Tr}_{\mathbf{M}}[F_{\hat{i}}{}^{\hat{j}}(S,T)] \end{aligned} \tag{7.40}$$

we get

$$\begin{aligned} F(S,T) &= \sqrt{N} + \int_0^S ds \int_0^T dt \left(MNF(s,t)P^{(B)}(s,t) + \sqrt{MN}\hat{F}(s,t)P^{(F)}(s,t) \right) \\ \hat{F}(S,T) &= \sqrt{M} + \int_0^S ds \int_0^T dt \left(\sqrt{MN}F(s,t)P^{(F)}(s,t) + MN\hat{F}(s,t)P^{(B)}(s,t) \right). \end{aligned} \tag{7.41}$$

Changing variables according to $s = Le^{\sigma'}$, $t = Le^{\tau'}$, where L is an arbitrary length

scale, we get

$$F(\sigma,\tau) = \sqrt{N} + \int_{-\infty}^{\sigma} d\sigma' \int_{-\infty}^{\tau} d\tau' \left(MNF(\sigma',\tau')P^{(B)}(\sigma',\tau') + \sqrt{MN}\hat{F}(\sigma',\tau')P^{(F)}(\sigma',\tau') \right)$$
$$\hat{F}(\sigma,\tau) = \sqrt{M} + \int_{-\infty}^{\sigma} d\sigma' \int_{-\infty}^{\tau} d\tau' \left(\sqrt{MN}F(\sigma',\tau')P^{(F)}(\sigma',\tau') + MN\hat{F}(\sigma',\tau')P^{(B)}(\sigma',\tau') \right). \tag{7.42}$$

with

$$P^{(F)}(\sigma,\tau) = -\left(\frac{2\pi}{k}\right) \frac{\Gamma(1/2-\epsilon)(\mu L)^{2\epsilon}}{2^{5/2-\epsilon}\pi^{3/2-\epsilon}} \frac{\cos\theta/2}{\cos\varphi/2} \, (e^{\tau}\partial_\sigma + e^{\sigma}\partial_\tau) \frac{e^{-\frac{1}{2}(\sigma+\tau)} e^{\epsilon(\sigma+\tau)}}{(\cosh(\sigma-\tau)+\cos\varphi)^{\frac{1}{2}-\epsilon}}$$
$$P^{(B)}(\sigma,\tau) = \left(\frac{2\pi}{k}\right)^2 \frac{\Gamma^2(1/2-\epsilon)(\mu L)^{4\epsilon}}{2^{3-2\epsilon}\pi^{3-2\epsilon}} \frac{\cos^2\theta/2}{\cos^2\varphi/2} \, \frac{\cos^2\varphi/2 \; e^{2\epsilon(\sigma+\tau)}}{(\cosh(\sigma-\tau)+\cos\varphi)^{1-2\epsilon}}. \tag{7.43}$$

F and $\hat{F}$ obey the differential equations

$$\begin{aligned} \partial_\sigma\partial_\tau F(\sigma,\tau) &= MNF(\sigma,\tau)P^{(B)}(\sigma,\tau) + \sqrt{MN}\hat{F}(\sigma,\tau)P^{(F)}(\sigma,\tau) \\ \partial_\sigma\partial_\tau \hat{F}(\sigma,\tau) &= \sqrt{MN}F(\sigma,\tau)P^{(F)}(\sigma,\tau) + MN\hat{F}(\sigma,\tau)P^{(B)}(\sigma,\tau) \end{aligned} \tag{7.44}$$

with boundary conditions $F(-\infty,\tau) = F(\sigma,-\infty) = \sqrt{N}$ and $\hat{F}(-\infty,\tau) = F(\sigma,-\infty) = \sqrt{M}$. Then we write $x = \sigma - \tau$ and $y = (\sigma+\tau)/2$ and obtain

$$\begin{aligned} \left(\frac{1}{4}\partial_y^2 - \partial_x^2\right) F(x,y) &= MNF(x,y)\tilde{P}^{(B)}(x,y) + \sqrt{MN}\hat{F}(x,y)\tilde{P}^{(F)}(x,y) \\ \left(\frac{1}{4}\partial_y^2 - \partial_x^2\right) \hat{F}(x,y) &= \sqrt{MN}F(x,y)\tilde{P}^{(F)}(x,y) + MN\hat{F}(x,y)\tilde{P}^{(B)}(x,y). \end{aligned} \tag{7.45}$$

with

$$\tilde{P}^{(F)}(x,y) = \left(\frac{2\pi}{k}\right) \frac{\Gamma(1/2-\epsilon)\mu^{2\epsilon}}{(2\pi)^{3/2-\epsilon}} \frac{\cos\theta/2}{\cos\varphi/2} e^{2\epsilon y} \left\{ \frac{d}{dx}\left[\frac{\sinh x/2}{(\cosh x+\cos\varphi)^{\frac{1}{2}-\epsilon}} \right] - \epsilon \frac{\cosh x/2}{(\cosh x+\cos\varphi)^{\frac{1}{2}-\epsilon}} \right\}$$
$$\tilde{P}^{(B)}(x,y) = \left(\frac{2\pi}{k}\right)^2 \frac{\Gamma^2(1/2-\epsilon)\mu^{4\epsilon}}{(2\pi)^{3-2\epsilon}} \frac{\cos^2\theta/2}{\cos^2\varphi/2} e^{4\epsilon y} \left\{ \frac{(\cosh x+\cos\varphi)^{2\epsilon}}{2} - \frac{\sinh^2 x/2}{(\cosh x+\cos\varphi)^{1-2\epsilon}} \right\}. \tag{7.46}$$

7.3.1 General solution in $d = 3$

For $\epsilon = 0$ equations (7.45) can be decoupled easily since the kernels (7.46) are independent of y. Indeed, by introducing

$$\mathcal{H}(x,y) = F(x,y) + \hat{F}(x,y), \qquad \mathcal{K}(x,y) = F(x,y) - \hat{F}(x,y), \tag{7.47}$$

(7.45) are equivalent to

$$\begin{aligned}\left(\frac{1}{4}\partial_y^2 - \partial_x^2\right)\mathcal{H}(x,y) &= \left(aW'(x) - a^2W^2(x) + \frac{a^2}{2}\right)\mathcal{H}(x,y)\\ \left(\frac{1}{4}\partial_y^2 - \partial_x^2\right)\mathcal{K}(x,y) &= \left(-aW'(x) - a^2W^2(x) + \frac{a^2}{2}\right)\mathcal{K}(x,y).\end{aligned} \tag{7.48}$$

with

$$a = \left(\frac{2\pi}{k}\right)\frac{\sqrt{MN}}{2^{3/2}\pi}\frac{\cos\theta/2}{\cos\varphi/2}\,, \tag{7.49}$$

and

$$W(x) = \frac{\sinh x/2}{(\cosh x + \cos\varphi)^{\frac{1}{2}}}\,. \tag{7.50}$$

These equations can be solved using the separation variable method. Setting

$$\mathcal{H}(x,y) = h(y)\psi_+(x) \qquad \mathcal{K}(x,y) = k(y)\psi_-(x), \tag{7.51}$$

we get

$$\begin{aligned}\partial_y^2 h(y) &= 4(-E + \frac{a^2}{2})h(y)\\ \partial_y^2 k(y) &= 4(-\tilde{E} + \frac{a^2}{2})k(y)\end{aligned} \tag{7.52}$$

and

$$\begin{aligned}\left(-\partial_x^2 + a^2W^2(x) - aW'(x)\right)\psi_+(x) &= E\psi_+(x)\\ \left(-\partial_x^2 + a^2W^2(x) + aW'(x)\right)\psi_-(x) &= \tilde{E}\psi_-(x)\end{aligned} \tag{7.53}$$

The solution of the y dependent equations is simply

$$\begin{aligned}h(y) &= C_1 e^{2\sqrt{-E+\frac{a^2}{2}}y} + C_2 e^{-2\sqrt{-E+\frac{a^2}{2}}y}\\ k(y) &= C_3 e^{2\sqrt{-\tilde{E}+\frac{a^2}{2}}y} + C_4 e^{-2\sqrt{-\tilde{E}+\frac{a^2}{2}}y}\end{aligned} \tag{7.54}$$

with $C_{1,2,3,4}$ constants which have to be fixed by imposing the boundary conditions as we will discuss in the following. The $x-$dependent equations (7.53) can be seen as the two Schroedinger equations of a supersymmetric quantum mechanical system [189], therefore E and $\tilde{E}$ are non-negative. In principle one could solve for these equations. However we are only interested to consider the case in which the edges of the cusp extend to infinity, i.e. S and T very large. In this limit $x \sim 0$ and y is very large, thus we make the ansatz $E = \tilde{E} = 0$ [3] and we set $\psi_+(0) = \psi_-(0) = 1$ since they can be reabsorbed in the normalization constants $C_1, \ldots, C_4$.

[3] In the weak coupling limit for positive energy values the solutions of (7.54) become oscillatory.

Using (7.51), (7.54) and (7.47) we get

$$\begin{aligned} F(0,y) &= \frac{C_1+C_3}{2}e^{\sqrt{2}ay} + \frac{C_2+C_4}{2}e^{-\sqrt{2}ay} \\ \hat{F}(0,y) &= \frac{C_1-C_3}{2}e^{\sqrt{2}ay} + \frac{C_2-C_4}{2}e^{-\sqrt{2}ay}. \end{aligned} \tag{7.55}$$

We fix the constants $C_1, \ldots, C_4$ by matching the perturbative result. In $d = 3$ there are UV divergences coming from the integration regions close to the cusps. To isolate this divergence we set $s_{min} = t_{min} = \varepsilon$ which means $y_{min} = \log \varepsilon \equiv -L_0$. Obviously,

$$F(0,-L_0) = \sqrt{N}, \qquad \text{and} \qquad \hat{F}(0,-L_0) = \sqrt{M}. \tag{7.56}$$

Inserting these conditions in (7.55) we obtain

$$\begin{aligned} F(0,y) &= \sqrt{N}e^{\sqrt{2}a(y+L_0)} - \frac{C_2+C_4}{2}\sinh\sqrt{2}a(y+L_0)e^{\sqrt{2}aL_0} \\ \hat{F}(0,y) &= \sqrt{M}e^{\sqrt{2}a(y+L_0)} - \frac{C_2-C_4}{2}\sinh\sqrt{2}a(y+L_0)e^{\sqrt{2}aL_0} \end{aligned} \tag{7.57}$$

The two remaining constants are determined by matching the first order in the coupling (which is contained in a) of our solution (7.57) with the first iteration of the Bethe-Salpeter equations (7.42) at the same order

$$\begin{aligned} F^{(1)}(\tau,\tau) &= M\sqrt{N}\int_{-L_0}^{\tau} d\sigma' \int_{-L_0}^{\tau} d\tau' P^F(\sigma',\tau') \\ \hat{F}^{(1)}(\tau,\tau) &= N\sqrt{M}\int_{-L_0}^{\tau} d\sigma' \int_{-L_0}^{\tau} d\tau' P^F(\sigma',\tau') \end{aligned} \tag{7.58}$$

which gives

$$\begin{aligned} C_2 &= \frac{\sqrt{N}+\sqrt{M}}{2}(1-A) \\ C_4 &= \frac{\sqrt{N}-\sqrt{M}}{2}(1+A) \end{aligned} \tag{7.59}$$

where

$$A = \lim_{\substack{y\to\infty \\ L_0\to\infty}} \frac{\sqrt{MN}}{\alpha(y+L_0)}\int_{-L_0}^{y} d\sigma' \int_{-L_0}^{y} d\tau' P^F(\sigma',\tau') \tag{7.60}$$

In the appendix D we compute this integral and we find that $A = 1$, thus $C_2 = 0$ and $C_4 = \sqrt{N} - \sqrt{M}$. Inserting this result in (7.57) we finally obtain

$$\begin{aligned} \langle \mathcal{W}^{+}_{\text{cusp}} \rangle &= \frac{\sqrt{N}F + \sqrt{M}\hat{F}}{N+M} = \cosh\sqrt{2}a(y+L_0) + \frac{2\sqrt{MN}}{N+M}\sinh\sqrt{2}a(y+L_0) \\ \langle \mathcal{W}^{-}_{\text{cusp}} \rangle &= \frac{\sqrt{N}F - \sqrt{M}\hat{F}}{N-M} = \cosh\sqrt{2}a(y+L_0) \end{aligned} \tag{7.61}$$

7.3.2 Solution for $\epsilon \neq 0$ and $\varphi = 0$

In the particular case of $\varphi = 0$ eqs. (7.45) can be exactly solved also for $\epsilon \neq 0$. To show this fact we first perform the change of variable $x \to ix'$ and $y \to \frac{1}{2}y'$. Then using (7.47), eqs. (7.45) become

$$\begin{aligned}\Box\mathcal{H}(x',y') &= \left[\vec{\nabla}\tilde{\mathcal{W}}(x',y')\cdot\vec{\nabla}\tilde{\mathcal{W}}(x',y') - \Box\tilde{\mathcal{W}}(x',y')\right]\mathcal{H}(x',y')\\ \Box\mathcal{K}(x',y') &= \left[\vec{\nabla}\tilde{\mathcal{W}}(x',y')\cdot\vec{\nabla}\tilde{\mathcal{W}}(x',y') + \Box\tilde{\mathcal{W}}(x',y')\right]\mathcal{K}(x',y').\end{aligned} \tag{7.62}$$

with $\vec{\nabla} = (\partial_{x'}, \partial_{y'})$, $\Box = \partial^2_{x'} + \partial^2_{y'}$ and

$$\tilde{\mathcal{W}}(x',y') = \frac{2^{\epsilon-1/2}a_\epsilon}{\epsilon}e^{\epsilon y'}\cos^{2\epsilon}\frac{x'}{2}\,, \qquad a_\epsilon = \left(\frac{2\pi}{k}\right)\sqrt{MN}\frac{\Gamma(1/2-\epsilon)\mu^{2\epsilon}}{(2\pi)^{3/2-\epsilon}}\cos\theta/2\,. \tag{7.63}$$

These equations are the Schroedinger equations of the two bosonic sectors of a two-dimensional $\mathcal{N} = 2$ supersymmetric quantum mechanics. The wave function of the ground state can be exactly found and gives

$$\begin{aligned}\mathcal{H}(x,y) =& C_1 e^{-\tilde{\mathcal{W}}(-ix,2y)} = C_1 e^{-\frac{2^{\epsilon-1/2}a_\epsilon}{\epsilon}e^{2\epsilon y}\cosh^{2\epsilon}\frac{x}{2}}\\ \mathcal{K}(x,y) =& C_2 e^{\tilde{\mathcal{W}}(-ix,2y)} = C_2 e^{\frac{2^{\epsilon-1/2}a_\epsilon}{\epsilon}e^{2\epsilon y}\cosh^{2\epsilon}\frac{x}{2}}\end{aligned} \tag{7.64}$$

with C_1 and C_2 normalization constants. Thus, using (7.47), one finds

$$\begin{aligned}F(x,y) =& \frac{C_1}{2}e^{-\frac{2^{\epsilon-1/2}a_\epsilon}{\epsilon}e^{2\epsilon y}\cosh^{2\epsilon}\frac{x}{2}} + \frac{C_2}{2}e^{\frac{2^{\epsilon-1/2}a_\epsilon}{\epsilon}e^{2\epsilon y}\cosh^{2\epsilon}\frac{x}{2}}\\ \hat{F}(x,y) =& \frac{C_1}{2}e^{-\frac{2^{\epsilon-1/2}a_\epsilon}{\epsilon}e^{2\epsilon y}\cosh^{2\epsilon}\frac{x}{2}} - \frac{C_2}{2}e^{\frac{2^{\epsilon-1/2}a_\epsilon}{\epsilon}e^{2\epsilon y}\cosh^{2\epsilon}\frac{x}{2}}\end{aligned} \tag{7.65}$$

Here too we use the boundary conditions

$$F(0,-\infty) = \sqrt{N} \quad \text{and} \qquad \hat{F}(0,-\infty) = \sqrt{M} \tag{7.66}$$

to fix the constants in (7.65), getting

$$\begin{aligned}C_1 =& \sqrt{N} + \sqrt{M}\\ C_2 =& \sqrt{N} - \sqrt{M}\,.\end{aligned} \tag{7.67}$$

Finally, we can write

$$\begin{aligned}\langle\mathcal{W}^+_{\varphi=0}\rangle =& \frac{\sqrt{N}F + \sqrt{M}\hat{F}}{N+M} = \cosh V_\epsilon(x,y) + \frac{2\sqrt{MN}}{M+N}\sinh V_\epsilon(x,y)\,,\\ \langle\mathcal{W}^-_{\varphi=0}\rangle =& \frac{\sqrt{N}F - \sqrt{M}\hat{F}}{N-M} = \cosh V_\epsilon(x,y)\,,\end{aligned} \tag{7.68}$$

where

$$V_\epsilon(x,y) = -\tilde{\mathcal{W}}(-ix,2y) = -\frac{2^{\epsilon-1/2}a_\epsilon}{\epsilon}e^{2\epsilon y}\cosh^{2\epsilon}\frac{x}{2} \tag{7.69}$$

Setting $x=0$ and $y=\log L$, we restore the physical variables obtaining

$$V_\epsilon(0,\log L) = -\left(\frac{2\pi}{\kappa}\right)\sqrt{MN}\frac{\Gamma\left(\frac{1}{2}-\epsilon\right)}{4\pi^{3/2-\epsilon}}\frac{(2\mu L)^{2\epsilon}}{\epsilon}\cos\frac{\theta}{2} \tag{7.70}$$

The resummation of the divergent part of the traced and supertraced loops in the (7.68) seems to confirm our guesses made in Section 7.1.1. Indeed, with the substitution $\hat{\lambda}_i \to \lambda_i$, we have

$$V_\epsilon(0,\log L) \overset{\hat{\lambda}_i\to\lambda_i}{=} V_\epsilon^+ = V^-_{\epsilon,\text{div.}} \tag{7.71}$$

where $V^-_{\epsilon,\text{div.}}$ is the divergent part of V_ϵ^- that is equal to V_ϵ^+ as shown in (7.21). We can conclude that at leading order in the scaling limit (7.34) the cusp divergence of the Wilson loops $\mathcal{W}^\pm_{\varphi=0}$ is the same of the divergence associated to the a Wilson line of length $2L$.

7.4 The determination of $\Gamma_{\text{cusp}}(\varphi)$

We want to extract $\Gamma_{\text{cusp}}(\varphi)$ from the solutions of Bethe-Salpeter equation: we have simply to recast them in a suitable form to single out the logarithmic divergence. Going back to the original (dimensionful) variables, we have to define

$$\begin{aligned} T = S = \Lambda_{IR}^{-1} = Le^{y} \quad &\to \quad y = -\log L\Lambda_{IR} = \log\frac{T}{L}; \\ \varepsilon = \Lambda_{UV}^{-1} = Le^{-L_0} \quad &\to \quad L_0 = \log L\Lambda_{UV} = \log\frac{L}{\varepsilon} \end{aligned} \tag{7.72}$$

where Λ_{IR} is the natural IR cut-off (associated to the length of the cusp) and $\Lambda_{UV} = \frac{1}{\varepsilon}$ is the UV cut-off (cutting-off the cusp, where ladders collapse). We have also introduced a scale length L for dimensional reason (that will not play any role in the following). With the above definitions we get

$$(y + L_0) = \log\frac{T}{\varepsilon} = \log\frac{\Lambda_{UV}}{\Lambda_{IR}} \tag{7.73}$$

We can finally rewrite the expectation value of the Wilson loop, as determined in the previous section, in the suggestive form as follows:

$$\begin{aligned} \langle\mathcal{W}^+_{\text{cusp}}\rangle^{ABJ} =& \frac{(\sqrt{M}+\sqrt{N})^2}{2(M+N)}e^{-\alpha\log\frac{\Lambda_{UV}}{\Lambda_{IR}}} + \frac{(\sqrt{M}-\sqrt{N})^2}{2(M+N)}e^{\alpha\log\frac{\Lambda_{UV}}{\Lambda_{IR}}} \\ \langle\mathcal{W}^-_{\text{cusp}}\rangle^{ABJ} =& \frac{1}{2}e^{-\alpha\log\frac{\Lambda_{UV}}{\Lambda_{IR}}} + \frac{1}{2}e^{\alpha\log\frac{\Lambda_{UV}}{\Lambda_{IR}}} \end{aligned} \tag{7.74}$$

We have exactly reproduced the double-exponential structure found for the straight-line in Section 7.1.1: it is also consistent with the two-loop calculation of [83] and corrects the exponentiation proposed there. We remark that this result comes from an all-order computation, although in a particular limit, and strongly supports the mixing picture that we have developed in Section 7.2.1. Let us discuss the cusp anomalous dimension obtained here.

We first consider the ABJM case ($N = M$). As already announced in Section 7.2.1 we observe a drastic simplification with the disappearing of one of the two exponentials. The definition of the $\Gamma_{\text{cusp}}(\varphi, \hat{\lambda})$ is the usual one and we have:

$$\langle \mathcal{W}^{+}_{\text{cusp}} \rangle^{ABJM} = e^{-\alpha \log \frac{\Lambda_{UV}}{\Lambda_{IR}}} \qquad \Rightarrow \qquad \Gamma_{\text{cusp}}(\varphi) = \alpha = \frac{N}{\kappa} \frac{\cos \theta/2}{\cos \varphi/2} = \frac{\hat{\lambda}}{\cos \frac{\varphi}{2}} \tag{7.75}$$

with $\hat{\lambda}_1 = \hat{\lambda}_2 = \hat{\lambda}$ in this case. As a matter of fact, we have seen in solving the Bethe-Salpeter equation that $F = \hat{F}$ and the effective Schroedinger equations decouple.

In the general situation, when $N \neq M$, we need more attention: the expectation value of $\mathcal{W}_{\pm}$ contains a double exponential, so we have to resort to eq. (7.31). The entries of the mixing matrix can be read from (7.74). The coefficients of the divergent logarithms in the exponentials are identified with $\Gamma^{(1,2)}_{\text{cusp}}(\varphi)$

$$\begin{aligned} \Gamma^{(1)}_{\text{cusp}}(\varphi) =& \frac{\sqrt{\hat{\lambda}_1 \hat{\lambda}_2}}{\cos \frac{\varphi}{2}} \\ \Gamma^{(2)}_{\text{cusp}}(\varphi) =& - \frac{\sqrt{\hat{\lambda}_1 \hat{\lambda}_2}}{\cos \frac{\varphi}{2}} \end{aligned} \tag{7.76}$$

and appear effectively as the eigenvalues of a mixing matrix. Notice that in the BPS limit $\varphi = \theta = i\infty$, $\Gamma^{(1,2)}_{\text{cusp}}$ vanish as expected!

We can also apply the definition of cusp anomalous dimension for the $\varphi = 0$ case derived from dimensional regularization

$$\begin{aligned} \Gamma^{(1)}_{\text{cusp}} =& - \mu \frac{\partial}{\partial \mu} Z^{(1)}_{\text{cusp}} = \frac{\sqrt{MN}}{\kappa} \cos \frac{\theta}{2} = \sqrt{\hat{\lambda}_1 \hat{\lambda}_2} \\ \Gamma^{(2)}_{\text{cusp}} =& - \mu \frac{\partial}{\partial \mu} Z^{(2)}_{\text{cusp}} = - \frac{\sqrt{MN}}{\kappa} \cos \frac{\theta}{2} = - \sqrt{\hat{\lambda}_1 \hat{\lambda}_2} \end{aligned} \tag{7.77}$$

finding perfect consistency with the previous analysis.

Our final result deserves a certain number of comments. A first remark concerns the structure of the exponentiation in the ABJ case: looking at our explicit calculation, one could expect that only the lower cusp anomalous dimensions should dominate, the other giving a subleading contribution. On the other hand they appear on the same footing in our computations and, much more crucially, consistency with perturbative results

needs both of them. At this order, in the scaling limit, we have $\Gamma^{(1)}_{\rm cusp}(\varphi) = -\Gamma^{(2)}_{\rm cusp}(\varphi)$: we think that subleading corrections should change this relations, generating a non-symmetric function of the scaled 't Hooft coupling. A second important observation concerns the actual functional form of $\Gamma_{\rm cusp}(\varphi)$. Let us concentrate for the moment on the $N = M$ case. We see that the final expression is just the exponentiation of the one-loop result: in the ladder limit the leading cusp divergence undergoes to an abelian exponentiation! This property was absolutely unexpected and it is completely different from the analogous $\mathcal{N} = 4$ SYM resummation, where an highly non-trivial function appears at this order, even for $\varphi = 0$. The reason relies of course in the supersymmetric structure of the effective Schroedinger equation but it has also a perturbative explanation: fermionic and bosonic diagrams do not exponentiate in an abelian way by themselves and it is their delicate balance that, order by order in the coupling constant, generates this nice behavior. We have checked explicitly at three-loop in perturbation theory this fact. The $N \neq M$ situation presents instead a slightly more involved structure: we have still an abelian-like exponentiation at this order, but when expressed in terms of the two (scaled) 't Hooft couplings $\hat{\lambda}_1,\ \hat{\lambda}_2$ it appears through a square root of their product. This is a further effect of the diagonalization process and at moment we do not have a satisfying explanation from general principles. We stress that from the point of view of the original CS level k the exponentiation is one-loop as well. A third and, may be, more interesting remark, is related to the strong-coupling limit and the connection with string theory. To fix the ideas let us consider the more simple ABJM case: because of the abelian-like exponentiation we do not have any non-trivial interpolation between weak and strong-coupling and the scaling limit does not match the expected $\sqrt{\hat{\lambda}}$ behavior of string theory. At variance with $\mathcal{N} = 4$ SYM the scaling limit does not seem to commute with the strong-coupling limit, a fact that in four-dimensions was not expected a priori (see the comments in the original computation [141]).

Chapter 8

Conclusions and discussion

In this thesis we have studied observables involving Wilson loops and local operators in supersymmetric gauge theories as $\mathcal{N} = 4$ SYM and ABJ(M) theories. We have used perturbation theory in the weak-coupling expansion at large N and, when it was possible, we have resummed all the perturbative series obtaining exact results. AdS/CFT correspondence, localization and integrability techniques allow us to compare our results with the strong-coupling regime and with some matrix-model or Y-system results. In the following we comment the main outputs of our original work presented in chapters 5, 6 and 7 and discuss possible further developments.

In Chapter 5 we have studied correlation functions of Wilson loops and local operators on the sphere S^2 in $\mathcal{N} = 4$ SYM theory. A matrix-model for these observables has been proposed and the different configurations we have examined reproduce its results. In particular we have considered a chiral operator inserted on the north-pole of S^2 and a Wilson loop placed on a latitude. The resummation of the ladder perturbative series is easily performed, leading to the expected result. The interaction diagrams sums to zero up to order λ^2 and we expect the same behavior at any perturbative order. A more involved situation arises when the operator is inserted in an arbitrary point of one of the two hemispheres. In this case the interaction diagrams do not sum to zero and they nicely interplay with the ladder ones to reproduces the matrix-model result.

It would be possible to extend the present computation to the case of two chiral primaries and one Wilson loop, checking in this way the expression derived in [153]. More generally one could try to develop an analogous supersymmetric system in three-dimensional ABJM theory [16], where a family of 1/6 BPS Wilson loops living on the two-sphere S^2 with the same properties of the 1/8 BPS operators considered here has been recently derived [82] and studied at quantum level [85]. Chiral primaries sharing part of the supersymmetries should be constructed and, at least at perturbative level, the correlation functions could be studied.

In Chapter 6 we have explored the possibility to study the near-BPS expansion of

the generalized cusp anomalous dimension with L units of R-charge by means of supersymmetric localization. The R-charge is provided by the insertion of certain scalar operators into a cusped Wilson loop, according to the original proposal of [139], [140]. The relevant generalized Bremsstrahlung function $\mathcal{B}_L(\lambda, \varphi)$ has been computed by solving a set of TBA equations in the near-BPS limit [167, 168] and, more recently, using QSC approach [166]. We have proposed here a generalization of the method discussed in [131], relating the computation to the quantum average of some BPS Wilson loops with local operator insertions along the contour. The system should localize into perturbative YM_2 on S^2, in the zero-instanton sector, suggesting the possibility to perform exact calculations in this framework. We have checked our proposal, reproducing the leading Lüscher correction to the generalized cusp anomalous dimension at weak coupling. We have further tested our strategy in the case $L = 1$, using Feynman diagrams directly in $\mathcal{N} = 4$ Super Yang-Mills theory.

Our investigations represent only a first step in connecting integrability results with localization outputs: we certainly would like to derive the complete expression for $\mathcal{B}_L(\lambda, \varphi)$ in this framework. Two-dimensional Yang-Mills theory on the sphere has an exact solution, even at finite N [159, 160]: on the other hand, the construction of the vacuum expectation values of Wilson loops with local operator insertions has not been studied in the past, at least to our knowledge. The matrix model [169], computing the generalized Bremsstrahlung function, strongly suggests that these two-dimensional observables, in the zero-instanton sector, should be obtained by extending the techniques of [153]. One could expect that also a finite N answer is possible, as in the case of $L = 0$.

A further direction could be to develop an efficient technique to explore this kind of observable directly in four-dimensions, by using perturbation theory. It would be interesting to go beyond the near-BPS case and to study the anomalous dimensions for more general local operator insertions. The construction of similar systems in three-dimensional ABJM theory should also be feasible and could provide new insights to get exact results.

In Chapter 7 we have studied a cusped Wilson loop in $\mathcal{N} = 6$ Super Chern-Simons theory, constructed with lines that are 1/2 BPS. We have computed the associated cusp anomalous dimension in a scaling limit in which ladder diagrams dominate: because of the 1/2 BPS character of the two halves, we have both bosonic and fermionic ladder exchanges and their resummation is encoded into a coupled Bethe-Salpeter equation. We have seen that this problem can be mapped into a supersymmetric Schroedinger equation whose ground state solution provides an exact expression for the cusp anomalous dimensions. Actually we found that, in the general $N \neq M$ case, the traced Wilson loop undergoes through a double-exponentiation, that we have interpreted as an operator mixing under cusp renormalization: we have associated to the eigenvalues of the mixing matrix two independent cusp anomalous dimensions. The final result is very simple and the exponentiations are abelian, the cusp anomalous dimensions are

one-loop exact up diagonalization. The strong-coupling limit is therefore trivial and we do not find consistency with string theory computation [138]: we argue that the scaling limit considered here does not commute with the strong-coupling limit. Concerning abelian exponentiation, a similar phenomenon has been observed recently [190] in studying $\mathcal{N} = 4$ SYM cusped Wilson loops in k-symmetric representations: at large N and k planar diagrams dominate and the exponentiation is of abelian type.

The obvious follow-up of the present work is to take into account the subleading corrections to the scaling limit: in [142] a systematic approach to this computation has been developed in the $\mathcal{N} = 4$ SYM case and it should be possible to perform an analogous investigation here. Preliminary results seem promising. It would be interesting to see if the supersymmetric structure we have found is preserved beyond leading order: in any case we expect a non-trivial modification of the relation $\Gamma^{(1)}_{\text{cusp}}(\varphi) = -\Gamma^{(2)}_{\text{cusp}}(\varphi)$. Another direction of work consists in checking the exponential structure at three-loop: the mixing we have observed here prescribes an exponentiation with definite group-dependent coefficients (see eq. (7.74)), that appear to be the same both in the scaling limit and in the general two-loop result [83]. It would be of course nice to have a deeper understanding for the occurrence of the mixing coefficients: a closer look at the supersymmetric quantum mechanics discussed in [87], where the 1/2 BPS line is obtained from a Higgsing procedure, should be probably useful for this task.

More ambitiously, one would like to approach the generalized cusp anomalous dimension in ABJ(M) theory from a general point of view, with the hope that other all-order results can be obtained. In four-dimensions a particularly powerful approach has been pushed forward recently [166, 144], applying to cusped Wilson loop the technique of the quantum spectral curve. Beautiful results have been obtained for the Bremsstrahlung function and the quark-anti-quark potential. It would be nice to extended this approach in the ABJ(M) case, in which the quantum spectral curve has been already studied [191]. It should be also possible to extend the TBA equations derived in [139, 140] in the three-dimensional context, taking advantage of the investigations presented in [192, 193, 194]

Acknowledgments

First and foremost, I am very deeply grateful to my advisor, Luca Griguolo, for initiating me to this interesting area of research and for sharing his knowledge. Special thanks are also due to Marisa Bonini and Domenico Seminara for numerous collaborations, discussions and encouragement.

I gratefully acknowledge financial support for the participation in schools and conferences from the INFN research group GAST and the LACES organizers. Furthermore, I would like to thank the european network COST and in particular Silvia Penati for the COST action "The string theory universe" MP1210.

Finally it is a pleasure to acknowledge the warm hospitality extended to me by the "Emmy Noether Research Group" of the Humboldt University, where part of this work was done. Special thanks are due to Valentina Forini for his hospitality and enlightening discussions.

Appendix A

Notation and conventions

A.1 $\mathcal{N} = 4$ SYM

Feynman rules

We shall briefly review the Euclidean Feynman rules relevant for our computations. We use the position-space propagators, which are obtained from those in momentum space (see *e.g.* [89]) by means of the following master integral

$$\int \frac{d^{2\omega}p}{(2\pi)^{2\omega}} \frac{e^{ip\cdot x}}{(p^2)^s} = \frac{\Gamma(\omega - s)}{4^s \pi^\omega \Gamma(s)} \frac{1}{(x^2)^{\omega - s}}. \tag{A.1}$$

Defining the quantity

$$D(x-y) \equiv \frac{\Gamma(\omega-1)}{2(2\pi)^{2\omega}} \frac{1}{[(x-y)^2]^{\omega-1}}\,, \tag{A.2}$$

in Landau gauge, we have the following propagators

$$\begin{aligned} \left\langle A_\mu^{ij}(x), A_\nu^{kl}(y) \right\rangle &= \lambda\, \frac{\delta^{il}\delta^{jk}}{N} \delta_{\mu\nu} D(x-y) \\ \left\langle \Phi_I^{ij}(x), \Phi_J^{kl}(y) \right\rangle &= \lambda \frac{\delta^{il}\delta^{jk}}{N} \delta_{IJ} D(x-y) \end{aligned} \tag{A.3}$$

The one-loop corrections to the scalar propagators (A.3) in coordinate space was compute in [89] and takes the form

$$\left\langle \Phi_I^{ij}(x), \Phi_J^{kl}(y) \right\rangle^{(1)} = -\frac{\delta^{il}\delta^{jk}}{N} \lambda^2 \frac{\Gamma^2(\omega-1)}{2^5 \pi^{2\omega} (2-\omega)(2\omega-3)} \frac{\delta_{IJ}}{[(x-y)^2]^{2\omega-3}} \tag{A.4}$$

The integrals $\mathcal{I}_1(\mathbf{x},\mathbf{y})$ and $\mathcal{I}_2(\mathbf{x},\mathbf{y})$

The integral $\mathcal{I}_1(x,y)$, defined in (5.25), has been evaluated [109] in momentum space representation and using dimensional regularization ($\omega = 2+\epsilon$)

$$\begin{aligned}\mathcal{I}_1(x,y) &\equiv \int \frac{d^{2\omega}p_1 d^{2\omega}p_2}{(2\pi)^{4\omega}} \frac{e^{ip_1x+ip_2y}}{p_1^2 p_2^2 (p_1+p_2)^2} \\ &= \frac{\Gamma(2\omega-3)}{64\pi^{2\omega}(\omega-1)} \int_0^1 d\alpha \;\; \frac{[\alpha(1-\alpha)]^{\omega-2}}{[\alpha(x-y)^2+(1-\alpha)y^2]^{2\omega-3}} \\ &\qquad \times {}_2F_1\left(1, 2\omega-3, \omega, \frac{(y-\alpha x)^2}{\alpha(x-y)^2+(1-\alpha)y^2}\right).\end{aligned} \tag{A.5}$$

From this representation, one obtains the behavior of $\mathcal{I}_1$ near $x=0$

$$\mathcal{I}_1(0,y) = \frac{\Gamma^2(\omega-1)}{64\pi^{2\omega}(2\omega-3)(2-\omega)} \frac{1}{[y^2]^{2\omega-3}}. \tag{A.6}$$

Since (A.5) is manifestly symmetric under the exchange $x \leftrightarrow y$ and $x \leftrightarrow y-x$, the behavior at $y=0$ and $y=x$ is similar. The integral $\mathcal{I}_2(x,y)$ is defined as follows [109]

$$\begin{aligned}\mathcal{I}_2(x,y) = -\frac{\Gamma(2\omega-3)}{64\pi^{2\omega}(\omega-1)} \int_0^1 d\alpha \frac{\alpha^{\omega-1}(1-\alpha)^{\omega-2}}{[\alpha(1-\alpha)x^2+(y-\alpha x)^2]^{2\omega-3}} \\ \times {}_2F_1\left(1, 2\omega-3, \omega, \frac{(y-\alpha x)^2}{(y-\alpha x)^2+\alpha(1-\alpha)x^2}\right).\end{aligned} \tag{A.7}$$

Here we quote its behavior at $x=0$, $y=0$ and $y=x$.

At $x=0$:

$$\mathcal{I}_2(0,y) = -\frac{\Gamma^2(\omega-1)}{128\pi^{2\omega}(2-\omega)(2\omega-3)\,[(y)^2]^{2\omega-3}}. \tag{A.8}$$

At $y=0$:

$$\mathcal{I}_2(x,0) = -\frac{\Gamma(2\omega-3)\Gamma(3-\omega)\Gamma(\omega-1)}{64\pi^{2\omega}\,[x]^{2\omega-3}} \frac{(\Gamma(\omega-2)-2\Gamma(3-\omega)\Gamma(2\omega-4))}{4(\omega-2)^3\Gamma(2-\omega)\Gamma(2\omega-4)}. \tag{A.9}$$

At $y=x$:

$$\mathcal{I}_2(x,x) = -\frac{\Gamma(2\omega-3)\Gamma(2-\omega)\Gamma(\omega)}{64\pi^{2\omega}(\omega-1)[x^2]^{2\omega-3}} \frac{1-\frac{\Gamma(\omega-1)}{\Gamma(3-\omega)\Gamma(2\omega-2)}}{2(\omega-2)}. \tag{A.10}$$

In Section 5.2 we introduced the following combination of the derivatives of $\mathcal{I}_1$ and $\mathcal{I}_2$:

$$V^\mu(x,y) \equiv \frac{\partial \mathcal{I}_1(x,y)}{\partial x_\mu} - \frac{\partial \mathcal{I}_2(x,y)}{\partial y_\mu}. \tag{A.11}$$

Taking the derivative of (A.5) and (A.7), V^μ can be expressed as [109]

$$V^\mu(x,y) = -\frac{\Gamma(2\omega-2)x^\mu}{32\pi^{2\omega}(\omega-1)(x^2)^{2\omega-2}}\int_0^1 d\alpha[\alpha(1-\alpha)]^{1-\omega}{}_2F_1(1,2\omega-2;\omega;\xi)(1-\xi)^{2\omega-2}, \tag{A.12}$$

where

$$\xi = \frac{(y-\alpha x)^2}{(y-\alpha x)^2+\alpha(1-\alpha)x^2}. \tag{A.13}$$

In particular, setting $\omega = 2$ one has

$$\begin{aligned} V^\mu(x,y) &= -\frac{x^\mu}{32\pi^4x^2}\int_0^1 d\alpha\frac{1}{\alpha(1-\alpha)x^2+(y-\alpha x)^2} \\ &= \frac{x^\mu}{32\pi^4x^2}\frac{\log\left[\frac{y^2}{(x-y)^2}\right]}{(x-y)^2-y^2} \end{aligned} \tag{A.14}$$

For our purposes, however, it is more useful to rewrite V^μ as

$$\begin{aligned} V^\mu(x,y) =& \frac{1}{32\pi^4x^2}\left\{\frac{\partial}{\partial y_\mu}\left[\mathrm{Li}_2\left(1-\frac{(x-y)^2}{y^2}\right)+\frac{1}{2}\log^2\left(\frac{(x-y)^2}{y^2}\right)\right.\right. \\ &\left.\left. -\frac{1}{2}\log^2\left(\frac{(x-y)^2}{x^2}\right)\right]-\frac{2(x-y)^\mu}{(x-y)^2}\log\left(\frac{y^2}{x^2}\right)\right\}. \end{aligned} \tag{A.15}$$

A.2 ABJ(M)

Feynman rules

We shall briefly review the Euclidean Feynman rules relevant for our computations. We use the position-space propagators, which are obtained from those in momentum space (see *e.g.* [78]) by means of the following master integral

$$\int\frac{d^{3-2\epsilon}p}{(2\pi)^{3-2\epsilon}}\frac{e^{ip\cdot x}}{(p^2)^s} = \frac{\Gamma\left(\frac{3}{2}-s-\epsilon\right)}{4^s\pi^{\frac{3}{2}-\epsilon}\Gamma(s)}\frac{1}{(x^2)^{\frac{3}{2}-s-\epsilon}}. \tag{A.16}$$

Defining the quantity

$$D(x-y) \equiv \frac{\Gamma\left(\frac{1}{2}-\epsilon\right)}{4\pi^{\frac{3}{2}-\epsilon}}\frac{1}{((x-y)^2)^{\frac{1}{2}-\epsilon}}\,, \tag{A.17}$$

in Landau gauge, we have the following propagators

$$\begin{aligned}
\langle (A_\mu)_i{}^j(x)(A_\nu)_k{}^l(y)\rangle =&\delta_i^l\delta_k^j\left(\frac{2\pi i}{\kappa}\right)\epsilon_{\mu\nu\rho}\partial_x^\rho D(x-y),\\
\langle (\hat{A}_\mu)_{\hat{i}}{}^{\hat{j}}(x)(\hat{A}_\nu)_{\hat{k}}{}^{\hat{l}}(y)\rangle =&-\delta_{\hat{i}}^{\hat{l}}\delta_{\hat{k}}^{\hat{j}}\left(\frac{2\pi i}{\kappa}\right)\epsilon_{\mu\nu\rho}\partial_x^\rho D(x-y).\\
\langle (C_I)_i{}^{\hat{j}}(x)(\bar{C}^J)_{\hat{k}}{}^l(y)\rangle =&\delta_I^J\ \delta_i^l\ \delta_{\hat{k}}^{\hat{j}}D(x-y),\\
\langle (\psi_I)_{\hat{i}}{}^j(x)(\bar{\psi}^J)_k{}^{\hat{l}}(y)\rangle =&\delta_I^J\ \delta_{\hat{i}}^{\hat{l}}\ \delta_k^j i\gamma^\mu\partial_\mu D(x-y).
\end{aligned}\tag{A.18}$$

The one-loop corrections to the propagators (A.18) in coordinate space was compute in [78]. The one loop two-point function for the gauge field takes the form

$$\langle (A_\mu)_i{}^j(x)(A_\nu)_k{}^l(y)\rangle^{(1)}=\delta_i^l\delta_k^j\left(\frac{2\pi}{\kappa}\right)^2\frac{M\Gamma^2\left(\frac{1}{2}-\epsilon\right)}{4\pi^{3-2\epsilon}}\left(\frac{\delta_{\mu\nu}}{((x-y)^2)^{1-2\epsilon}}-\partial_\mu\partial_\nu\left(\frac{((x-y)^2)^\epsilon}{4\epsilon(1+2\epsilon)}\right)\right).\tag{A.19}$$

The correction to the gauge propagator of $\hat{A}$ is very similar to (A.19): we have simply to replace M with N and $\delta_i^l\ \delta_k^j$ with $\delta_{\hat{i}}^{\hat{l}}\ \delta_{\hat{k}}^{\hat{j}}$. The one-loop correction to the fermion propagator in coordinate space is given by

$$\langle (\psi_I)_{\hat{i}}{}^j(x)(\bar{\psi}^J)_k{}^{\hat{l}}(y)\rangle^{(1)}=-i\delta_{\hat{i}}^{\hat{l}}\delta_k^j(N-M)\frac{\Gamma^2\left(\frac{1}{2}-\epsilon\right)}{16\pi^{3-2\epsilon}}\frac{1}{((x-y)^2)^{1-2\epsilon}}.\tag{A.20}$$

Gamma matrices and bilinears

When computing the *fermionic diagrams* contributing to the Wilson loop defined by the super-connection (3.50) we often encounter bilinears constructed with the spinors η and $\bar{\eta}$ defined by the two relations

$$(\dot{x}^\mu\gamma_\mu)_\alpha{}^\beta=\frac{1}{2i}|\dot{x}|(\eta^\beta\bar{\eta}_\alpha+\eta_\alpha\bar{\eta}^\beta)\qquad(\eta^\beta\bar{\eta}_\alpha-\eta_\alpha\bar{\eta}^\beta)=2i\delta_\alpha^\beta,\tag{A.21}$$

For instance, the most common is

$$\eta_1\gamma^\mu\bar{\eta}_2,\tag{A.22}$$

where the superscripts 1 and 2 denote two different points on the contour. We can determine its value up to an overall factor by means of the following corollary of (A.21)

$$\bar{\eta}_\alpha\eta^\beta=i\left(\mathbb{1}+\frac{\dot{x}^\lambda\gamma_\lambda}{|\dot{x}|}\right)_\alpha{}^\beta.\tag{A.23}$$

Consider in fact the product $(\eta_1\bar{\eta}_2)(\eta_1\gamma^\mu\bar{\eta}_2)$. We can rewrite it as

$$(\eta_1\bar{\eta}_2)(\eta_1\gamma^\mu\bar{\eta}_2)=\bar{\eta}_{2\alpha}\eta_2^\beta(\gamma^\mu)_\beta{}^\rho\bar{\eta}_{1\rho}\eta_1^\alpha=-\mathrm{Tr}\left[\left(1+\frac{\dot{x_2}^\lambda\gamma_\lambda}{|\dot{x}_2|}\right)\gamma^\mu\left(1+\frac{\dot{x_1}^\nu\gamma_\nu}{|\dot{x}_1|}\right)\right],\tag{A.24}$$

where we used (A.23) in order to eliminate the spinors from the expression. Thus

$$(\eta_2\gamma^\mu\bar{\eta}_1) = -\frac{2}{(\eta_1\bar{\eta}_2)}\left[\frac{\dot{x_1}^\mu}{|\dot{x}_1|}+\frac{\dot{x_2}^\mu}{|\dot{x}_2|}-i\frac{\dot{x_2}^\lambda}{|\dot{x}_2|}\frac{\dot{x_1}^\nu}{|\dot{x}_1|}\epsilon_{\lambda\nu}{}^\mu\right]. \tag{A.25}$$

The only undetermined factor in (A.25) is the scalar contraction $(\eta_1\bar{\eta}_2)$. The condition (A.23) however determines its *norm*, *i.e* the product $(\eta_1\bar{\eta}_2)(\eta_2\bar{\eta}_1)$

$$(\eta_1\bar{\eta}_2)(\eta_2\bar{\eta}_1) = -\operatorname{Tr}\left[\left(1+\frac{\dot{x_2}^\lambda}{|\dot{x}_2|}\gamma_\lambda\right)\left(1+\frac{\dot{x_1}^\nu}{|\dot{x}_1|}\gamma_\nu\right)\right] = -2\left[1+\frac{(\dot{x}_1\cdot\dot{x}_2)}{|\dot{x}_1||\dot{x}_2|}\right]. \tag{A.26}$$

There is a second bilinear that will be relevant, namely the one containing three Dirac matrices

$$\eta_1\gamma^\lambda\gamma^\mu\gamma^\nu\bar{\eta}_2. \tag{A.27}$$

Its evaluation reduces to the previous case because of the following identity

$$\gamma^\rho\gamma^\mu\gamma^\sigma = \delta^{\rho\mu}\gamma^\sigma+\delta^{\mu\sigma}\gamma^\rho-\delta^{\rho\sigma}\gamma^\mu+i\epsilon^{\rho\mu\sigma}\mathbb{1}, \tag{A.28}$$

which holds for three-dimensional Euclidean gamma matrices.

For completeness, we shall also give all the possible scalar contractions for our specific circuit

$$\begin{aligned}&\eta_1\bar{\eta}_1 = \eta_2\bar{\eta}_2 = 2i, \qquad \eta_1\bar{\eta}_2 = \eta_2\bar{\eta}_1 = 2i\cos\frac{\varphi}{2},\\ &\eta_2\eta_1 = -2i\sin\frac{\varphi}{2}, \qquad \bar{\eta}_1\bar{\eta}_2 = 2i\sin\frac{\varphi}{2}.\end{aligned} \tag{A.29}$$

Here the indices 1 and 2 indicates the two different edges of the cusp.

Appendix B

Relevant integrals for correlation functions in $\mathcal{N} = 4$ SYM

B.1 Summing up interactions I: the details

The evaluation of P_1

Using the integral representation of $\mathcal{I}_1$ given in (A.5), we get

$$\begin{aligned} P_1 =& \oint d\tau_1\, d\tau_2\ \ \mathcal{I}_1(x_1 - x_2, x_N - x_2)\ (x_1 - x_2)^2 \\ =& \frac{\Gamma(2\omega-3)}{2^5\pi^{2\omega}(\omega-1)} \frac{\sin^2\theta_0}{(1-\cos\theta)^{2\omega-3}} \oint d\tau_1 d\tau_2 \int_0^1 d\alpha\ \frac{[\alpha(1-\alpha)]^{\omega-2}(1-\cos\tau_{12})}{2^{2\omega-3}} \\ & \times\ {}_2F_1\bigg(1, 2\omega-3; \omega; 1-\alpha(1-\alpha)\frac{\sin^2\theta_0}{(1-\cos\theta_0)}(1-\cos\tau_{12})\bigg). \end{aligned} \tag{B.1}$$

With the help of the following identity

$$\begin{aligned} {}_2F_1(\alpha,\beta;\gamma;z) =& \frac{\Gamma(\gamma)\Gamma(\gamma-\alpha-\beta)}{\Gamma(\gamma-\alpha)\Gamma(\gamma-\beta)}\ {}_2F_1(\alpha,\beta;\alpha+\beta-\gamma+1;1-z) \\ & + (1-z)^{\gamma-\alpha-\beta}\frac{\Gamma(\gamma)\Gamma(\alpha+\beta-\gamma)}{\Gamma(\alpha)\Gamma(\beta)}\ {}_2F_1(\gamma-\alpha,\gamma-\beta;\gamma-\alpha-\beta+1;1-z), \end{aligned} \tag{B.2}$$

and the series representation of the hypergeometric function, P_1 becomes

$$\begin{aligned} & \frac{1}{2^{6+2\epsilon}\pi^{4+2\epsilon}} \sum_{k=0}^{\infty} \oint d\tau_1 d\tau_2 \int_0^1 d\alpha \bigg[\frac{(\sin^2\theta_0)^{1-\epsilon+k}}{(1-\cos\theta_0)^{1+\epsilon+k}} \Gamma(\epsilon) \frac{\Gamma(1+\epsilon+k)}{\Gamma(k+1)} [\alpha(1-\alpha)]^k (1-\cos\tau_{12})^{1-\epsilon+k} \\ & \quad + \frac{(\sin^2\theta_0)^{1+k}}{(1-\cos\theta_0)^{1+2\epsilon+k}}\ \frac{\Gamma(-\epsilon)}{\Gamma(1-\epsilon)} \frac{\Gamma(1+2\epsilon+k)\Gamma(1+\epsilon)}{\Gamma(1+\epsilon+k)} [\alpha(1-\alpha)]^{\epsilon+k} (1-\cos\tau_{12})^{k+1} \bigg]. \end{aligned} \tag{B.3}$$

The integrations can now be performed easily, and we obtain

$$\frac{\sqrt{\pi}}{2^{6+2\epsilon}\pi^{3+2\epsilon}}\sum_{k=0}^{\infty}\Bigg[2^{3+k}\frac{(\sin^2\theta_0)^{1+k}}{(1-\cos\theta_0)^{1+2\epsilon+k}}\frac{\Gamma(-\epsilon)}{\Gamma(1-\epsilon)}\frac{\Gamma(1+2\epsilon+k)\Gamma(1+\epsilon)\Gamma(1+\epsilon+k)\Gamma(3/2+k)}{\Gamma(2+2\epsilon+2k)\Gamma(k+2)} \\ + 2^{3-\epsilon+k}\frac{(\sin^2\theta_0)^{1-\epsilon+k}}{(1-\cos\theta_0)^{1+\epsilon+k}}\Gamma(\epsilon)\frac{\Gamma(1+\epsilon+k)\Gamma(k+1)\Gamma(3/2-\epsilon+k)}{\Gamma(2k+2)\Gamma(2-\epsilon+k)}\Bigg]. \tag{B.4}$$

Taking the limit $\epsilon \to 0$ we see that divergences cancel, and the sum over k gives

$$P_1 = \frac{1}{8\pi^2}\left[\frac{\pi^2}{6} - \mathrm{Li}_2\left(\sin^2\frac{\theta}{02}\right)\right]. \tag{B.5}$$

The evaluation of P_2

Using the integral representation of $\mathcal{I}_1$ and $\mathcal{I}_2$ given in (A.5) and (A.7), we get

$$\begin{aligned} P_2 =& \oint d\tau_1\, d\tau_2 \left[\mathcal{I}_1(x_1-x_N, x_2-x_N) + \mathcal{I}_2(x_2-x_N, x_1-x_N)\right] \\ =& \frac{1}{2^{2\omega+3}}\frac{\Gamma(2\omega-3)}{\pi^{2\omega}(\omega-1)}\frac{1}{(1-\cos\theta_0)^{2\omega-3}}\oint d\tau_1 d\tau_2 \int_0^1 d\alpha \;\; \frac{(1-\alpha)[\alpha(1-\alpha)]^{\omega-2}}{\left[1+\alpha\cos\theta_0-\alpha(1+\cos\theta_0)\cos\tau_{21}\right]^{2\omega-3}} \\ & \times {}_2F_1\left(1, 2\omega-3, \omega, 1-\frac{\alpha(1-\alpha)}{1+\alpha\cos\theta_0-\alpha(1+\cos\theta_0)\cos\tau_{21}}\right). \end{aligned} \tag{B.6}$$

With the help of the identity

$${}_2F_1(\alpha,\beta;\gamma;z) = (1-z)^{-\beta}\,{}_2F_1\left(\beta, \gamma-\alpha;\gamma;\frac{z}{z-1}\right), \tag{B.7}$$

we arrive to the following expression

$$\begin{aligned} P_2 =& \frac{1}{2^{2\omega+3}}\frac{\Gamma(2\omega-3)}{\pi^{2\omega}(\omega-1)}\frac{1}{(1-\cos\theta_0)^{2\omega-3}}\oint d\tau_1 d\tau_2 \int_0^1 d\alpha \;\; \alpha^{1-\omega}(1-\alpha)^{2-\omega} \\ & \times {}_2F_1\left(2\omega-3, \omega-1, \omega, -\frac{1-\alpha}{\alpha} - \frac{(1+\cos\theta_0)(1-\cos\tau_{21})}{1-\alpha}\right). \end{aligned} \tag{B.8}$$

Exploiting the Mellin-Barnes representation of the hypergeometric function, we recast P_2 as

$$\begin{aligned} & \frac{1}{2^{2\omega+4}}\frac{1}{\pi^{2\omega+1}\,i}\frac{1}{(1-\cos\theta_0)^{2\omega-3}}\oint d\tau_1 d\tau_2 \int_0^1 d\alpha \;\; \alpha^{1-\omega}(1-\alpha)^{2-\omega} \\ & \quad \times \int_{-i\infty}^{i\infty} dt\, \frac{\Gamma(2\omega-3+t)\Gamma(\omega-1+t)\Gamma(-t)}{\Gamma(\omega+t)}\left(\frac{1-\alpha}{\alpha} + \frac{(1+\cos\theta_0)(1-\cos\tau_{21})}{1-\alpha}\right)^t. \end{aligned} \tag{B.9}$$

We perform a Mellin-Barnes transform also of last factor in (B.9), obtaining

$$-\frac{1}{2^{2\omega+5}}\frac{1}{\pi^{2\omega+2}}\frac{1}{(1-\cos\theta_0)^{2\omega-3}}\int_{-i\infty}^{i\infty}dt\int_{-i\infty}^{i\infty}ds\,\frac{\Gamma(2\omega-3+t)\Gamma(s)\Gamma(-t-s)}{(\omega-1+t)}(1+\cos\theta_0)^{-s}$$
$$\times\oint d\tau_1\,d\tau_2\,(1-\cos\tau_{21})^{-s}\int_0^1 d\alpha\quad\alpha^{1-\omega-t-s}(1-\alpha)^{2-\omega+t+2s}. \tag{B.10}$$

Evaluating the integrals over τ_1, τ_2 and α and setting $\omega=2+\epsilon$, we get

$$-\frac{1}{2^{7+2\epsilon}}\frac{\sqrt{\pi}}{\pi^{5+2\epsilon}}\int_{-i\infty}^{i\infty}dt\int_{-i\infty}^{i\infty}ds\frac{(1+\cos\theta_0)^{-s}}{(1-\cos\theta_0)^{1+2\epsilon}}\,2^{-s}\frac{\Gamma(1+2\epsilon+t)\Gamma(s)\Gamma(-t-s)\Gamma(\frac{1}{2}-s)}{(1+\epsilon+t)\Gamma(1-s)\Gamma(s-2\epsilon+1)}$$
$$\times\Gamma(-\epsilon-t-s)\Gamma(1+t+2s-\epsilon). \tag{B.11}$$

Analyzing the singularity structure of the integrand, it is possible to choose a contour of integration for s and t that allows us to take $\epsilon=0$ and satisfies

$$0<Re(s)<1/2,\qquad -1<Re(t)<-Re(s). \tag{B.12}$$

Shifting $t\to t-s$ and expressing everything in terms of Γ-functions (B.11) becomes

$$-\frac{1}{2^7}\frac{\sqrt{\pi}}{\pi^5}\int_{-i\infty}^{i\infty}ds\,\frac{(1+\cos\theta_0)^{-s}}{(1-\cos\theta_0)}\frac{2^{-s}\sin(\pi s)\Gamma\left(\frac{1}{2}-s\right)\Gamma(s)}{\pi s}$$
$$\times\int_{-i\infty}^{i\infty}dt\,\left[\Gamma(t-s)\Gamma(-t)^2\Gamma(s+t+1)-\frac{\Gamma(t-s)\Gamma(-t)^2\Gamma(s+t+1)\Gamma(t-s+1)}{\Gamma(t-s+2)}\right]. \tag{B.13}$$

The integral over t can be performed using the two Barnes lemmas, obtaining

$$\frac{i}{2^6}\frac{\sqrt{\pi}}{\pi^4}\int_{-i\infty}^{i\infty}ds\,\frac{(1+\cos\theta_0)^{-s}}{(1-\cos\theta_0)}2^{-s}\Gamma\left(\frac{1}{2}-s\right)\Gamma(s)^2\Gamma(-s)\left(1-\frac{\Gamma(1-s)^2}{\Gamma(1-2s)}\right). \tag{B.14}$$

Finally the integral over s is easily done through residue theorem, and we get

$$P_2=\frac{1}{96\pi^2}\frac{1}{1-\cos\theta_0}\left[\pi^2-3\,\mathrm{Li}_2\left(\sin^2\frac{\theta_0}{2}\right)-6\left(\log^2\left(\cos\frac{\theta_0}{2}\right)+\arctan^2\left(\sqrt{1+2\cos\theta_0}\right)\right)\right]. \tag{B.15}$$

The evaluation of P_3

The evaluation of P_3 is straightforward: taking $\omega=2+\epsilon$ we get

$$\begin{aligned}P_3&=\oint d\tau_1\,d\tau_2\,\left[\mathcal{I}_2(x_2-x_N,x_2-x_N)+\mathcal{I}_1(0,x_2-x_N)\right]\\&=-\frac{\csc(\pi\epsilon)(\Gamma(\epsilon)-2\Gamma(1-\epsilon)\Gamma(2\epsilon))}{2^{6+2\epsilon}\pi^{1+2\epsilon}(1-\cos\theta_0)^{1+2\epsilon}\Gamma(1-\epsilon)}\\&=\frac{1}{192}\frac{1}{1-\cos\theta_0}\qquad\epsilon\to0.\end{aligned} \tag{B.16}$$

The evaluation of P_4

We have

$$\begin{aligned} P_4 =& \oint d\tau_1 d\tau_3 \, \mathrm{Li}_2 \left(1 - \frac{\sin^2\theta_0}{1-\cos\theta_0}(1-\cos\tau_{31})\right) \\ =& 8\pi \int_0^{\pi/2} d\tau \, \mathrm{Li}_2 \left(1 - K(\theta_0)\sin^2\tau\right), \end{aligned} \tag{B.17}$$

where $K(\theta_0) = 4\cos^2\frac{\theta_0}{2}$. Using the integral representation of the dilogarithm and changing variable to $x = \sin\tau$, we obtain

$$\begin{aligned} P_4 =& -8\pi \int_0^1 ds \int_0^1 dx \frac{\log\left[1 - s(1-K(\theta_0)x^2)\right]}{s\sqrt{1-x^2}} \\ =& \frac{2}{3}\pi^4 - 8\pi^2 \int_0^1 \frac{ds}{s} \log\left[\frac{1}{2}\left(1 + \sqrt{1 + \frac{K(\theta_0)s}{1-s}}\right)\right] \\ =& \frac{\pi^4}{6} - 2\pi^2\log^2(2) - 8\pi^2 \int_2^K dK' \, \frac{d}{dK'} \int_0^1 \frac{ds}{s} \log\left[\frac{1}{2}\left(1 + \sqrt{1 + \frac{K'[\theta_0]s}{1-s}}\right)\right]. \end{aligned} \tag{B.18}$$

Taking the derivative and interchanging the order of integration we get

$$P_4 = \frac{2}{3}\pi^4 - 8\pi^2 \left[\log^2\left(\cos\frac{\theta_0}{2}\right) + \arctan^2\left(\sqrt{1+2\cos\theta_0}\right)\right]. \tag{B.19}$$

B.2 Some useful integrals

In this appendix we give the integrals $\mathcal{J}_n$ and $\tilde{\mathcal{J}}$ needed to evaluate (5.49):

$$\mathcal{J}_n = \int_0^{2\pi} d\tau \, \tau^n \, f(\tau), \qquad \tilde{\mathcal{J}} = \int_0^{2\pi} d\tau_1 \, \tau_1 \, f(\tau_1) \int_{\tau_1}^{2\pi} d\tau_2 \, f(\tau_2), \tag{B.20}$$

with $f(\tau)$ given in (5.46) (henceforth we set $\sin\phi = b$, thus $\sigma = \sqrt{\frac{1+b}{1-b}}$).

The integral $\mathcal{J}_0$ and $\mathcal{J}_1$ are straightforward. Making the change of variables $\tan\frac{\tau}{2} = x$, $\mathcal{J}_0$ becomes

$$\mathcal{J}_0 = \frac{2}{1-b}\int_0^\infty \frac{dx}{1+\sigma^2x^2} + (b \to -b) = \frac{2\pi}{\sqrt{1-b^2}}. \tag{B.21}$$

For $\mathcal{J}_1$, periodicity of $f(\tau)$ allows us to write

$$\mathcal{J}_1 = \pi \int_{-\pi}^{\pi} d\tau \, \frac{1}{1+b\cos\tau} = \pi\mathcal{J}_0. \tag{B.22}$$

The evaluation of $\mathcal{J}_2$ is a bit tricky. Again using periodicity and the change of variables $\tan\frac{\tau}{2} = x$, we can write

$$\mathcal{J}_2 = \pi^2\mathcal{J}_0 + \frac{16}{\sqrt{1-b^2}}\mathcal{F}(\sigma), \tag{B.23}$$

where

$$\mathcal{F}(\sigma) = \int_0^\infty dx \frac{\arctan^2 \sigma x}{1+x^2}. \tag{B.24}$$

First we evaluate the derivative of $\mathcal{F}(\sigma)$

$$\mathcal{F}'(\sigma) = \frac{1}{\sigma^2}\int_{-\infty}^{\infty} dx \frac{x \arctan \sigma x}{(1+x^2)(1/\sigma^2+x^2)} = \frac{\pi}{\sigma^2-1}\log\left(\frac{1+\sigma}{2}\right), \tag{B.25}$$

and then we write

$$\begin{aligned}\mathcal{F}(\sigma) =& \mathcal{F}(1) + \int_1^\sigma d\sigma' \mathcal{F}'(\sigma') \\ =& \frac{1}{3}\left(\frac{\pi}{2}\right)^3 - \frac{\pi}{2}\left[\frac{1}{2}\log^2\left(\frac{1+\sigma}{2}\right) + \mathrm{Li}_2\left(\frac{1-\sigma}{2}\right)\right].\end{aligned} \tag{B.26}$$

Finally, substituting this result in (B.23), we obtain:

$$\mathcal{J}_2 = \frac{4\pi}{\sqrt{1-b^2}}\left[\frac{2}{3}\pi^2 - 2\mathrm{Li}_2\left(\frac{1-\sigma}{2}\right) - \log^2\left(\frac{1+\sigma}{2}\right)\right]. \tag{B.27}$$

The integral $\tilde{\mathcal{J}}$ can be treated in a similar way, with the change of variables $x_{1,2} = \cot\left(\frac{\tau_{1,2}}{2}\right)$, one has

$$\tilde{\mathcal{J}} = \frac{8}{(1+b)^2}\int_{-\infty}^{\infty} dx_1 \frac{\mathrm{arccot}(x_1)}{1+\frac{x_1^2}{\sigma^2}} \int_{-\infty}^{x_1} dx_2 \frac{1}{1+\frac{x_2^2}{\sigma^2}}. \tag{B.28}$$

Performing the integration over x_2 and integrating by parts we get:

$$\begin{aligned}\tilde{\mathcal{J}} =& \frac{\pi^3}{1-b^2} + \frac{8}{1-b^2}\int_{-\infty}^{\infty} dx_1 \frac{\arctan(x_1/\sigma)^2}{1+x_1^2} \\ =& \frac{\pi^3}{1-b^2} - \frac{8}{1-b^2}\mathcal{F}\left(\frac{1}{\sigma}\right),\end{aligned} \tag{B.29}$$

where $\mathcal{F}(\sigma)$ is given in (B.26).

B.3 Summing up interactions II: the details

In this appendix we evaluate the contribution to (5.60), called A, i.e.

$$\begin{aligned}\mathrm{A} =& -\frac{\lambda^2\cos^2\phi}{2^3\sqrt{2}N}\oint d\tau_1 d\tau_2\, f(\tau_1)\, f(\tau_2)\;\; \mathcal{I}_1(x_1-x_2, x_{\mathcal{O}}-x_2)\,(x_1-x_2)^2 \\ &+ \frac{\lambda^2\cos^2\phi}{2\sqrt{2}N}\oint d\tau_1 d\tau_2\, f(\tau_1)\left[\mathcal{I}_1(x_1-x_{\mathcal{O}}, x_2-x_{\mathcal{O}}) + \mathcal{I}_2(x_2-x_{\mathcal{O}}, x_1-x_{\mathcal{O}})\right] \\ &- \frac{\lambda^2\cos^2\phi}{2^8\pi^4\sqrt{2}N}\oint d\tau_1 d\tau_2\, f(\tau_1)\, f(\tau_2)\left[\mathrm{Li}_2\Big(1-(1-\cos\tau_{21})f(\tau_1)\Big)\right],\end{aligned} \tag{B.30}$$

with $\mathcal{I}_1$ and $\mathcal{I}_2$ given in(A.5) and (A.7). The new feature of this contribution with respect to the integrals evaluated in appendix B.1 is the appearance of the functions $f(\tau_i)$ (also in the argument of the dilogarithm and the hypergeometric function). Because of this fact, we are not able to compute (B.30) analytically and we have to resort to its numerical evaluation for different values of the angle $\phi \in [0, \pi/2]$, which identifies the position of the operator on the sphere. The results are shown in Figure B.1.

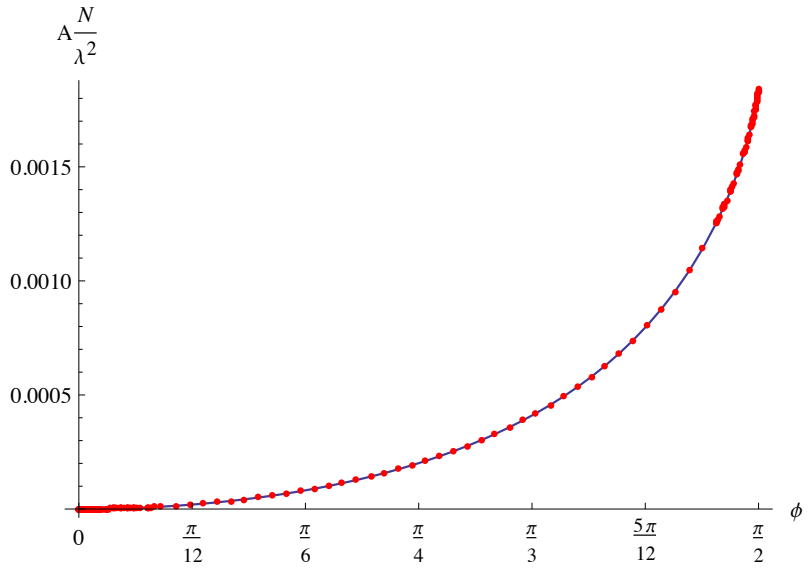

Figure B.1: Numerical evaluation of the quantity $\mathrm{A}\frac{N}{\lambda^2}$ as a function of the angle ϕ obtained with Wolfram Mathematica routine NIntegrate.

In particular, the vanishing of A at $\phi = 0$ (i.e. the operator on the north-pole) is consistent with analytic results of Section 5.2.

The last integral in (5.60), i.e. the term B, is

$$B = \frac{\lambda^2 \cos^2\phi}{2^9 \pi^4 \sqrt{2} N} \oint d\tau_1 d\tau_2 d\tau_3 \, \epsilon(\tau_1, \tau_2, \tau_3) \, f(\tau_1) \, f(\tau_3) \, F(\tau_3, \tau_2), \tag{B.31}$$

with

$$F(\tau_3, \tau_2) = F(\tau_2, \tau_3) = \cot\left(\frac{\tau_{32}}{2}\right) \log\left(\frac{f(\tau_3)}{f(\tau_2)}\right). \tag{B.32}$$

It is useful to express $f(\tau)$ in terms of its primitive $g(\tau)$

$$g(\tau) = \frac{2}{\sqrt{1-b^2}} \mathrm{arccot}\left(\frac{1}{\sigma} \cot\frac{\tau_i}{2}\right), \tag{B.33}$$

with

$$g(0) = \lim_{\tau \to 0^+} g(\tau) = 0, \qquad g(2\pi) = \lim_{\tau \to 2\pi^-} g(\tau) = \frac{2\pi}{\sqrt{1-b^2}}. \tag{B.34}$$

Then using the integration by parts and (5.32) and (5.30), we can evaluate one of the three integrals, obtaining

$$B = \frac{\lambda^2 \cos^2\phi}{2^8\pi^4\sqrt{2}N} \oint d\tau_2 \Bigg\{ \oint d\tau_3 \left(g(\tau_3) - g(\tau_2)\right) f(\tau_3)\, F(\tau_3,\tau_2) \\ + \frac{1}{2} g(2\pi) \left[\int_0^{\tau_2} d\tau_3\, f(\tau_3)\, F(\tau_3,\tau_2) - \int_{\tau_2}^{2\pi} d\tau_3\, f(\tau_3)\, F(\tau_3,\tau_2) \right] \Bigg\}. \tag{B.35}$$

With the usual change of variables $x = \cot\frac{\tau}{2}$, in both integrals, we can evaluate one of the two integrals, obtaining

$$B = \frac{\lambda^2}{2^4\pi^2\sqrt{2}N} \left\{ \log^2\left(\frac{2\sigma}{\sigma+1}\right) - \frac{1}{2\pi} \int_0^\infty dy\, \frac{\sigma\, \log^2\left(\frac{1+y^2}{\sigma^2+y^2}\right)}{\sigma^2+y^2} \right\}. \tag{B.36}$$

The integral in (B.36) is done by expanding the integrand in power series in σ at $\sigma = 1$

$$\int_0^\infty dy\, \frac{\sigma\, \log^2\left(\frac{1+y^2}{\sigma^2+y^2}\right)}{\sigma^2+y^2} = \int_{-\infty}^\infty dy \sum_{n=2}^\infty \sum_{j=1}^{n-1} \frac{i^{n+1}}{2(n-j)\left(y^2+1\right)^{n+1}} \left((i-y)^{n-j} + (i+y)^{n-j}\right) \\ \times (i-y)^{j+1} \left(H_j - \beta_{\frac{i+y}{i-y}}(1+j,0) - \log\left(\frac{2y}{y-i}\right) \right) (\sigma-1)^n, \tag{B.37}$$

where $H_n = \sum_{k=1}^n \frac{1}{k}$ are the harmonic numbers and $\beta_z(a,b) = z^a \sum_{n=0}^\infty \frac{(1-b)_n}{n!(a+n)} z^n$ is the incomplete β-function.

Given the following series expansion

$$\left(H_j - \beta_{\frac{i+y}{i-y}}(1+j,0) - \log\left(\frac{2y}{y-i}\right) \right) = \sum_{k=1}^j \frac{1}{k} \left(\frac{(i+y)^k}{(i-y)^k} + 1 \right), \tag{B.38}$$

(B.37) becomes

$$
\begin{aligned}
&\sum_{n=2}^{\infty}\sum_{j=1}^{n-1}\sum_{k=1}^{j}\int_{-\infty}^{\infty} dy\ \frac{i^{n+1}}{2(n-j)\,(y^2+1)^{n+1}}((i-y)^{n-j}+(i+y)^{n-j})\frac{1}{k}\left(\frac{(i+y)^k}{(i-y)^k}+1\right)(\sigma-1)^n\\
=&\sum_{n=2}^{\infty}\sum_{j=1}^{n-1}\sum_{k=1}^{j}\frac{(\sigma-1)^n}{\pi^2 k\Gamma(k+1)(n-j)\Gamma(k+n-j)}\Bigg[ie^{-i\pi k}2^{-n-2}\sin(\pi j)\sin(\pi(k-j))\\
&\quad\times\Bigg(\pi^2(-k)\csc(\pi j)\csc(\pi(k-j))\Gamma(k+n-j)\left(\pi e^{i\pi k}(-2)^n\csc(\pi k)\,{}_2\tilde{F}_1\left(1,1-n;2-k;\frac{1}{2}\right)\right.\\
&\quad\left.+2\left(-1+e^{2i\pi k}\right)\Gamma(n)\Gamma(k-n)\right)-\pi e^{i\pi k}\Gamma(k+1)\sin(\pi j)\left(\pi\csc^2(\pi j)\csc(\pi(k-j))\right.\\
&\quad\times\left(\pi 2^n\csc(\pi(k-j))\,{}_2\tilde{F}_1\left(1,1-n;-k-n+j+2;\frac{1}{2}\right)+2(-1)^n\Gamma(k+n-j)\right.\\
&\quad\left.\times\left(\beta_{\frac{1}{2}}(k-j,-k-n+j+1)+\beta_{\frac{1}{2}}(k-n,1-k)+\beta_{\frac{1}{2}}(-j,-n+j+1)+\beta_{\frac{1}{2}}(-n+j+1,-j)\right)\right)\\
&\quad\left.+4i\Gamma(n)\left(\pi(-1)^n\csc^2(\pi j)\Gamma(k-j)+\Gamma(-j)\csc(\pi(k-j))\Gamma(-n+j+1)\Gamma(k+n-j)\right)\right)\Bigg]\\
=&\sum_{n=2}^{\infty}\frac{2^{-n}\pi e^{i\pi n}}{n^2}\Bigg[2^n n\left(n\,{}_3F_2\left(1,1,1-n;2,2;\frac{1}{2}\right)+2(\Phi(2,1,n)+\psi^{(0)}(n)+\gamma)-\log(4)\right)\\
&\qquad\qquad+2n\Phi\left(\frac{1}{2},1,n\right)+2i\pi n-2\Bigg](\sigma-1)^n\\
=&-\pi\left[2\mathrm{Li}_2\left(\frac{1-\sigma}{2}\right)+2\mathrm{Li}_2\left(\frac{\sigma-1}{2\sigma}\right)-\log(\sigma)(\log(\sigma)-2\log(\sigma+1)+\log(4))\right],
\end{aligned}
\tag{B.39}
$$

where γ is the Eulero-Mascheroni constant, ${}_2\tilde{F}_1(a,b,c,z)=\frac{{}_2F_1(a,b,c,z)}{\Gamma(c)}$ is the regularized hypergeometric function, $\Phi(z,a,s)=\sum_{n=0}^{\infty}\frac{z^n}{(a+n)^s}$ is the Lerch transcendent function and $\psi^{(0)}(z)=\frac{d}{dz}\log\Gamma(z)$ is the digamma function.

Finally, including the result (B.39) in (B.36), we obtain

$$
\begin{aligned}
B=&\frac{\lambda^2}{2^4\pi^2\sqrt{2}N}\left\{\log^2\left(\frac{2\sigma}{\sigma+1}\right)+\mathrm{Li}_2\left(\frac{1-\sigma}{2}\right)+\mathrm{Li}_2\left(\frac{\sigma-1}{2\sigma}\right)-\frac{1}{2}\log(\sigma)\log\left(\frac{4\sigma}{(\sigma+1)^2}\right)\right\}\\
=&\frac{\lambda^2}{2^5\pi^2\sqrt{2}N}\left[\log^2\left(\frac{2\sigma}{1+\sigma}\right)+\log^2\left(\frac{1+\sigma}{2}\right)+2\mathrm{Li}_2\left(\frac{1-\sigma}{2}\right)+2\mathrm{Li}_2\left(\frac{\sigma-1}{2\sigma}\right)\right]\\
=&-2\mathbf{L}.
\end{aligned}
\tag{B.40}
$$

where $\mathbf{L}$ is defined in (5.51).

Appendix C

The generating function $G(t, \epsilon, z)$ and some related properties

We present here the derivation of some results that have been used in computing the Lüscher term from YM_2 perturbation theory: in particular we will examine the derivation of the generating function $G(t, \epsilon, z)$. We start from the two relations (6.48)

$$g_n(t,\epsilon) = \left(-\frac{g_{2d}^2 N}{4\pi}\right) \int_\epsilon^t dt_n \, \Delta(t_n) \, g_{n-1}(t_n, \epsilon) \,, \tag{C.1}$$

$$\frac{d}{dt} g_n(t,\epsilon) = \left(-\frac{g_{2d}^2 N}{4\pi}\right) \Delta(t) \, g_{n-1}(t,\epsilon) \tag{C.2}$$

with $g_0(t, \epsilon) = 1$. Using the identity

$$\Delta(t) = \frac{1}{2} \frac{d}{dt} \log\left(\frac{t^2}{t^2+1}\right) \tag{C.3}$$

into the recurrence relation (C.1) and integrating by parts we obtain

$$\begin{aligned} g_n(t,\epsilon) &= \left(-\frac{g_{2d}^2 N}{8\pi}\right) \left\{ \log\left(\frac{t^2}{t^2+1}\right) g_{n-1}(t,\epsilon) - \log\left(\frac{\epsilon^2}{\epsilon^2+1}\right) g_{n-1}(\epsilon,\epsilon) - \right. \\ &\qquad \left. - \int_\epsilon^t dt_n \, \log\left(\frac{t_n^2}{t_n^2+1}\right) \, \frac{d}{dt_n} g_{n-1}(t_n,\epsilon) \right\} \\ &= \left(-\frac{g_{2d}^2 N}{8\pi}\right) \left\{ \log\left(\frac{t^2}{t^2+1}\right) g_{n-1}(t,\epsilon) - \log\left(\frac{\epsilon^2}{\epsilon^2+1}\right) g_{n-1}(\epsilon,\epsilon) - \right. \\ &\qquad \left. - \left(-\frac{g_{2d}^2 N}{4\pi}\right) \int_\epsilon^t dt_n \, \log\left(\frac{t_n^2}{t_n^2+1}\right) \, \Delta(t_n) \, g_{n-2}(t_n,\epsilon) \right\} . \end{aligned} \tag{C.4}$$

We rewrite the product in the last line as

$$\log\left(\frac{t_n^2}{t_n^2+1}\right)\,\Delta(t_n) = \frac{1}{4}\frac{d}{dt_n}\log^2\left(\frac{t_n^2}{t_n^2+1}\right) \tag{C.5}$$

and integrating by parts again we obtain

$$\begin{aligned} g_n(t,\epsilon) =& \Bigg\{\Bigg[\left(-\frac{g_{2d}^2 N}{8\pi}\right)\log\left(\frac{t^2}{t^2+1}\right) g_{n-1}(t,\epsilon) - \frac{1}{2}\left(-\frac{g_{2d}^2 N}{8\pi}\right)^2 \log^2\left(\frac{t^2}{t^2+1}\right) g_{n-2}(t,\epsilon) \\ & - (t\to\epsilon)\Bigg] + \frac{1}{2}\left(-\frac{g_{2d}^2 N}{8\pi}\right)^2 \int_\epsilon^t dt_n\, \log^2\left(\frac{t_n^2}{t_n^2+1}\right)\, \frac{d}{dt_n} g_{n-2}(t_n,\epsilon)\Bigg\}. \end{aligned} \tag{C.6}$$

The procedure can be iterated $n-1$ times and, defining $\alpha = -\frac{g_{2d}^2 N}{8\pi}$, we arrive at

$$g_n(t,\epsilon) = -\sum_{k=1}^{n}\frac{(-\alpha)^k}{k!}\log^k\left(\frac{t^2}{t^2+1}\right) g_{n-k}(t,\epsilon) - (t\to\epsilon)\,. \tag{C.7}$$

We can solve the recurrence by finding the generating function: given the sequence $g_n(t,\epsilon)$ we define

$$G(t,\epsilon,z) = \sum_{n=0}^{\infty} g_n(t,\epsilon)\, z^n \qquad \text{with} \quad z\in\mathbb{C}\,, \tag{C.8}$$

then using Cauchy's formula

$$g_n(t,\epsilon) = \frac{1}{2\pi i}\oint_\gamma \frac{dz}{z^{n+1}} G(t,\epsilon,z) \tag{C.9}$$

with γ a closed curve around the origin.

Going back to the equation (C.7), we notice that $g_{n-k}(\epsilon,\epsilon) = 0$ for $k\neq n$. Then we get:

$$\begin{aligned} G(t,\epsilon,z) - 1 =& \sum_{n=1}^{\infty} g_n(t,\epsilon) z^n = -\sum_{n=1}^{\infty} z^n \sum_{k=1}^{n}\frac{(-\alpha)^k}{k!}\log^k\left(\frac{t^2}{t^2+1}\right) g_{n-k}(t,\epsilon) + \\ & + \sum_{n=1}^{\infty}\frac{(-\alpha z)^n}{n!}\log^n\left(\frac{\epsilon^2}{\epsilon^2+1}\right) \\ =& -\sum_{k=1}^{\infty} z^k \frac{(-\alpha)^k}{k!}\log^k\left(\frac{t^2}{t^2+1}\right)\sum_{n=k}^{\infty} g_{n-k}(t,\epsilon) z^{n-k} + e^{-\alpha z\log\left(\frac{\epsilon^2}{\epsilon^2+1}\right)} - 1 \\ =& -\left(e^{-\alpha z\log\left(\frac{t^2}{t^2+1}\right)} - 1\right) G(t,\epsilon,z) + e^{-\alpha z\log\left(\frac{\epsilon^2}{\epsilon^2+1}\right)} - 1\,. \end{aligned} \tag{C.10}$$

Finally the generating function is:

$$G(t,\epsilon,z) = \left(\frac{t^2}{t^2+1}\frac{\epsilon^2+1}{\epsilon^2}\right)^{\alpha z}. \tag{C.11}$$

Following the same steps, we can find that the generating function associated to the sequence $(-1)^n g_n(s,\epsilon)$ is $G^{-1}(s,\epsilon,w)$.

Let us now consider the expression (6.52) and (6.53): we have to evaluate a double-integral of the following type

$$A \equiv \frac{1}{(2\pi i)^2}\oint dzdw \frac{z^{-(L+1)} - w^{-(L+1)}}{w-z} F(z,w) \tag{C.12}$$

with $F(z,w)$ analytic around $z, w = 0$ and symmetric in $w \leftrightarrow z$

$$F(z,w) = \sum_{n=0}^{\infty}\sum_{m=0}^{\infty} a_{n,m} z^n\, w^m\,, \tag{C.13}$$

where $a_{n,m} = a_{m,n}$. Redefining $z \to zw$ we have

$$A = \frac{1}{(2\pi i)^2}\oint dzdw \frac{1}{w^{L+1}}\frac{z^{-(L+1)}-1}{1-z}\sum_{m,n=0}^{\infty} a_{n,m} z^n w^{n+m}\,. \tag{C.14}$$

Performing the integral over w, we obtain

$$A = \frac{1}{(2\pi i)}\sum_{n=0}^{L} a_{n,L-n}\oint \frac{dz}{z^{L+1-n}}\frac{1-z^{L+1}}{1-z} = \sum_{n=0}^{L} a_{n,L-n}\,. \tag{C.15}$$

Notice that the function $F(w,z)$ at $w = z$ has the form

$$F(z,z) = \sum_{n=0}^{\infty}\sum_{m=0}^{\infty} a_{n,m} z^{n+m} = \sum_{k=0}^{\infty} b_k z^k \tag{C.16}$$

whit $b_k = \sum_{n=0}^{k} a_{n,k-n}$. Then

$$A = b_L = \frac{1}{2\pi i}\oint \frac{dz}{z^{L+1}} F(z,z), \tag{C.17}$$

i.e.

$$\oint dzdw \frac{z^{-(L+1)} - w^{-(L+1)}}{w-z} F(z,w) = 2\pi i \oint \frac{dz}{z^{L+1}} F(z,z)\,. \tag{C.18}$$

Appendix D

The integral of the fermionic kernel

In the following we want to compute the quantity A appearing in the Section 7.3.1 and defined by

$$A = \lim_{\substack{y\to\infty \\ L_0\to\infty}} \frac{\sqrt{MN}}{\sqrt{2}a(y+L_0)} \int_{-L_0}^{y} d\tau' \int_{-L_0}^{y} d\sigma' P^{(F)}(\sigma',\tau'). \tag{D.1}$$

For the moment we choose different upper bounds for the integrals. Using the definition of $P^{(F)}$ given by (7.38), we have:

$$\begin{aligned}\int_{-L_0}^{\tau} d\tau' \int_{-L_0}^{\sigma} d\sigma' P^{(F)}(\sigma',\tau') &= -\frac{\cos\theta/2}{\sqrt{2}k}\frac{1}{\cos\varphi/2}\int_{-L_0}^{\tau} d\tau' \int_{-L_0}^{\sigma} d\sigma' \frac{d}{d\sigma'}\left(\frac{e^{\frac{1}{2}(\tau'-\sigma')}}{(\cosh(\sigma'-\tau')+\cos\varphi)^{\frac{1}{2}}}\right) \\ &= -\frac{\cos\theta/2}{\sqrt{2}k}\frac{1}{\cos\varphi/2}\Big(I(\sigma,\tau) - I(-L_0,\tau)\Big)\end{aligned} \tag{D.2}$$

where we have computed the first integral using the total derivative and where we have defined:

$$I(\sigma,\tau) \equiv \int_{-L_0}^{\tau} d\tau' \frac{e^{\frac{1}{2}(\tau'-\sigma)}}{(\cosh(\sigma-\tau')+\cos\varphi)^{\frac{1}{2}}}. \tag{D.3}$$

We can take the change of variable $z = e^{\sigma-\tau'}$ and solve the first integral:

$$\begin{aligned} I(\sigma,\tau) =& \sqrt{2}\int_{-L_0}^{\tau} d\tau' \frac{1}{\left[e^{2(\sigma-\tau')} + 2e^{(\sigma-\tau')}\cos\varphi + 1\right]^{1/2}} \\ =& -\sqrt{2}\int_{e^{(\sigma+L_0)}}^{e^{(\sigma-\tau)}} \frac{dz}{z}\frac{1}{\left[z^2+2z\cos\varphi+1\right]^{1/2}} \\ =& -\sqrt{2}\Big[-\log\left(\frac{1+z\cos\varphi+\sqrt{z^2+2z\cos\varphi+1}}{z}\right)\Big]_{e^{(\sigma+L_0)}}^{e^{(\sigma-\tau)}}. \end{aligned} \tag{D.4}$$

The second contribution is:

$$I(-L_0,\tau) = -\sqrt{2}\Big[-\log\left(\frac{1+z\cos\varphi+\sqrt{z^2+2z\cos\phi+1}}{z}\right)\Big]_1^{e^{-(\tau+L_0)}} \tag{D.5}$$

Summing up, we obtain:

$$I(\sigma,\tau) - I(-L_0,\tau) = \sqrt{2}\Big[G(\sigma-\tau) - G(\sigma+L_0) - G(-\tau-L_0) + G(0)\Big] \tag{D.6}$$

where

$$G(x) = \log\left(1+e^x\cos\varphi+\sqrt{e^{2x}+2e^x\cos\varphi+1}\right) \tag{D.7}$$

Now setting $\tau=\sigma=y$, we have

$$I(y,y) - I(-L_0,y) = \sqrt{2}\Big[2G(0) - G(-y-L_0) - G(y+L_0)\Big] \tag{D.8}$$

and taking the limit $y,\ L_0\to\infty$, we can write the following expansion:

$$I(y,y) - I(-L_0,y) \simeq -\sqrt{2}(y+L_0) + \text{const} + \mathcal{O}(e^{-(y+L_0)}). \tag{D.9}$$

Therefore

$$\sqrt{MN}\int_{-L_0}^{y} d\tau' \int_{-L_0}^{y} d\sigma' P^{(F)}(\sigma',\tau') \simeq \frac{\cos\theta/2}{\cos\varphi/2}\frac{\sqrt{MN}}{k}(y+L_0) = \sqrt{2}a(y+L) \tag{D.10}$$

Recalling the definition (D.1), we obtain:

$$A = 1 \tag{D.11}$$

Bibliography

[1] S. R. Coleman and J. Mandula, "All Possible Symmetries of the S Matrix," *Phys. Rev.* **159** (1967) 1251–1256.

[2] R. Haag, J. T. Lopuszanski, and M. Sohnius, "All Possible Generators of Supersymmetries of the s Matrix," *Nucl. Phys.* **B88** (1975) 257.

[3] W. Nahm, "Supersymmetries and their Representations," *Nucl. Phys.* **B135** (1978) 149.

[4] B. I. Zwiebel, "Two-loop Integrability of Planar N=6 Superconformal Chern-Simons Theory," *J. Phys.* **A42** (2009) 495402, `arXiv:0901.0411 [hep-th]`.

[5] G. Papathanasiou and M. Spradlin, "The Morphology of N=6 Chern-Simons Theory," *JHEP* **07** (2009) 036, `arXiv:0903.2548 [hep-th]`.

[6] V. K. Dobrev and V. B. Petkova, "On the group theoretical approach to extended conformal supersymmetry: classification of multiplets," *Lett. Math. Phys.* **9** (1985) 287–298.

[7] D. Bailin and A. Love, *Supersymmetric gauge field theory and string theory.* 1994.

[8] L. Brink, J. H. Schwarz, and J. Scherk, "Supersymmetric Yang-Mills Theories," *Nucl. Phys.* **B121** (1977) 77.

[9] F. Gliozzi, J. Scherk, and D. I. Olive, "Supersymmetry, Supergravity Theories and the Dual Spinor Model," *Nucl. Phys.* **B122** (1977) 253–290.

[10] D. J. Gross and F. Wilczek, "Asymptotically Free Gauge Theories. 1," *Phys. Rev.* **D8** (1973) 3633–3652.

[11] M. T. Grisaru, M. Rocek, and W. Siegel, "Zero Three Loop beta Function in N=4 Superyang-Mills Theory," *Phys. Rev. Lett.* **45** (1980) 1063–1066.

[12] S. Mandelstam, "Light Cone Superspace and the Ultraviolet Finiteness of the N=4 Model," *Nucl. Phys.* **B213** (1983) 149–168.

[13] L. Brink, O. Lindgren, and B. E. W. Nilsson, "The Ultraviolet Finiteness of the N=4 Yang-Mills Theory," *Phys. Lett.* **B123** (1983) 323.

[14] C. Montonen and D. I. Olive, "Magnetic Monopoles as Gauge Particles?," *Phys. Lett.* **B72** (1977) 117.

[15] G. 't Hooft, "A Planar Diagram Theory for Strong Interactions," *Nucl. Phys.* **B72** (1974) 461.

[16] O. Aharony, O. Bergman, D. L. Jafferis, and J. Maldacena, "N=6 superconformal Chern-Simons-matter theories, M2-branes and their gravity duals," *JHEP* **10** (2008) 091, arXiv:0806.1218 [hep-th].

[17] O. Aharony, O. Bergman, and D. L. Jafferis, "Fractional M2-branes," *JHEP* **11** (2008) 043, arXiv:0807.4924 [hep-th].

[18] M. A. Bandres, A. E. Lipstein, and J. H. Schwarz, "Studies of the ABJM Theory in a Formulation with Manifest SU(4) R-Symmetry," *JHEP* **09** (2008) 027, arXiv:0807.0880 [hep-th].

[19] J. M. Maldacena, "The Large N limit of superconformal field theories and supergravity," *Int. J. Theor. Phys.* **38** (1999) 1113–1133, arXiv:hep-th/9711200 [hep-th]. [Adv. Theor. Math. Phys.2,231(1998)].

[20] H. Ooguri and C. Vafa, "World sheet derivation of a large N duality," *Nucl. Phys.* **B641** (2002) 3–34, arXiv:hep-th/0205297 [hep-th].

[21] G. 't Hooft, "Dimensional reduction in quantum gravity," in *Salamfest 1993:0284-296*, pp. 0284–296. 1993. arXiv:gr-qc/9310026 [gr-qc].

[22] L. Susskind, "The World as a hologram," *J. Math. Phys.* **36** (1995) 6377–6396, arXiv:hep-th/9409089 [hep-th].

[23] J. D. Bekenstein, "Black holes and entropy," *Phys. Rev.* **D7** (1973) 2333–2346.

[24] S. W. Hawking, "Black Holes and Thermodynamics," *Phys. Rev.* **D13** (1976) 191–197.

[25] J. Polchinski, "Dirichlet Branes and Ramond-Ramond charges," *Phys. Rev. Lett.* **75** (1995) 4724–4727, arXiv:hep-th/9510017 [hep-th].

[26] E. Witten, "Anti-de Sitter space and holography," *Adv. Theor. Math. Phys.* **2** (1998) 253–291, arXiv:hep-th/9802150 [hep-th].

[27] S. S. Gubser, I. R. Klebanov, and A. M. Polyakov, "Gauge theory correlators from noncritical string theory," *Phys. Lett.* **B428** (1998) 105–114, arXiv:hep-th/9802109 [hep-th].

[28] J. H. Schwarz, "Superconformal Chern-Simons theories," *JHEP* **11** (2004) 078, arXiv:hep-th/0411077 [hep-th].

[29] J. Bagger and N. Lambert, "Modeling Multiple M2's," *Phys. Rev.* **D75** (2007) 045020, arXiv:hep-th/0611108 [hep-th].

[30] J. Bagger and N. Lambert, "Gauge symmetry and supersymmetry of multiple M2-branes," *Phys. Rev.* **D77** (2008) 065008, arXiv:0711.0955 [hep-th].

[31] A. Gustavsson, "Algebraic structures on parallel M2-branes," *Nucl. Phys.* **B811** (2009) 66–76, arXiv:0709.1260 [hep-th].

[32] M. Van Raamsdonk, "Comments on the Bagger-Lambert theory and multiple M2-branes," *JHEP* **05** (2008) 105, arXiv:0803.3803 [hep-th].

[33] J. Bagger and N. Lambert, "Three-Algebras and N=6 Chern-Simons Gauge Theories," *Phys. Rev.* **D79** (2009) 025002, arXiv:0807.0163 [hep-th].

[34] J. Polchinski, *String theory. Vol. 1: An introduction to the bosonic string.* Cambridge University Press, 2007.

[35] N. A. Nekrasov, "Seiberg-Witten prepotential from instanton counting," *Adv. Theor. Math. Phys.* **7** no. 5, (2003) 831–864, arXiv:hep-th/0206161 [hep-th].

[36] N. Nekrasov and A. Okounkov, "Seiberg-Witten theory and random partitions," *Prog. Math.* **244** (2006) 525–596, arXiv:hep-th/0306238 [hep-th].

[37] V. Pestun, "Localization of gauge theory on a four-sphere and supersymmetric Wilson loops," *Commun. Math. Phys.* **313** (2012) 71–129, arXiv:0712.2824 [hep-th].

[38] A. Kapustin, B. Willett, and I. Yaakov, "Exact Results for Wilson Loops in Superconformal Chern-Simons Theories with Matter," *JHEP* **03** (2010) 089, arXiv:0909.4559 [hep-th].

[39] J. Gomis, T. Okuda, and V. Pestun, "Exact Results for 't Hooft Loops in Gauge Theories on $S * *4$," *JHEP* **05** (2012) 141, arXiv:1105.2568 [hep-th].

[40] N. Drukker, T. Okuda, and F. Passerini, "Exact results for vortex loop operators in 3d supersymmetric theories," *JHEP* **07** (2014) 137, arXiv:1211.3409 [hep-th].

[41] F. Passerini and K. Zarembo, "Wilson Loops in N=2 Super-Yang-Mills from Matrix Model," *JHEP* **09** (2011) 102, arXiv:1106.5763 [hep-th]. [Erratum: JHEP10,065(2011)].

[42] J. G. Russo and K. Zarembo, "Large N Limit of N=2 SU(N) Gauge Theories from Localization," *JHEP* **10** (2012) 082, arXiv:1207.3806 [hep-th].

[43] F. Bigazzi, A. L. Cotrone, L. Griguolo, and D. Seminara, "A novel cross-check of localization and non conformal holography," *JHEP* **03** (2014) 072, arXiv:1312.4561 [hep-th].

[44] J. A. Minahan and K. Zarembo, "The Bethe ansatz for N=4 superYang-Mills," *JHEP* **03** (2003) 013, arXiv:hep-th/0212208 [hep-th].

[45] N. Beisert, "The complete one loop dilatation operator of N=4 superYang-Mills theory," *Nucl. Phys.* **B676** (2004) 3–42, arXiv:hep-th/0307015 [hep-th].

[46] N. Beisert and M. Staudacher, "The N=4 SYM integrable super spin chain," *Nucl. Phys.* **B670** (2003) 439–463, arXiv:hep-th/0307042 [hep-th].

[47] N. Beisert, C. Kristjansen, and M. Staudacher, "The Dilatation operator of conformal N=4 superYang-Mills theory," *Nucl. Phys.* **B664** (2003) 131–184, arXiv:hep-th/0303060 [hep-th].

[48] N. Beisert, "The Dilatation operator of N=4 super Yang-Mills theory and integrability," *Phys. Rept.* **405** (2004) 1–202, arXiv:hep-th/0407277 [hep-th].

[49] C. Sieg, "Review of AdS/CFT Integrability, Chapter I.2: The spectrum from perturbative gauge theory," *Lett. Math. Phys.* **99** (2012) 59–84, arXiv:1012.3984 [hep-th].

[50] C. Sieg, "Superspace computation of the three-loop dilatation operator of N=4 SYM theory," *Phys. Rev.* **D84** (2011) 045014, arXiv:1008.3351 [hep-th].

[51] H. Bethe, "On the theory of metals. 1. Eigenvalues and eigenfunctions for the linear atomic chain," *Z. Phys.* **71** (1931) 205–226.

[52] N. Beisert, V. Dippel, and M. Staudacher, "A Novel long range spin chain and planar N=4 super Yang-Mills," *JHEP* **07** (2004) 075, arXiv:hep-th/0405001 [hep-th].

[53] N. Beisert and M. Staudacher, "Long-range psu(2,2—4) Bethe Ansatze for gauge theory and strings," *Nucl. Phys.* **B727** (2005) 1–62, arXiv:hep-th/0504190 [hep-th].

[54] F. Fiamberti, A. Santambrogio, C. Sieg, and D. Zanon, "Wrapping at four loops in N=4 SYM," *Phys. Lett.* **B666** (2008) 100–105, arXiv:0712.3522 [hep-th].

[55] F. Fiamberti, A. Santambrogio, C. Sieg, and D. Zanon, "Anomalous dimension with wrapping at four loops in N=4 SYM," *Nucl. Phys.* **B805** (2008) 231–266, arXiv:0806.2095 [hep-th].

[56] Z. Bajnok and R. A. Janik, "Four-loop perturbative Konishi from strings and finite size effects for multiparticle states," *Nucl. Phys.* **B807** (2009) 625–650, arXiv:0807.0399 [hep-th].

[57] N. Gromov, V. Kazakov, A. Kozak, and P. Vieira, "Exact Spectrum of Anomalous Dimensions of Planar N = 4 Supersymmetric Yang-Mills Theory: TBA and excited states," *Lett. Math. Phys.* **91** (2010) 265–287, arXiv:0902.4458 [hep-th].

[58] N. Gromov, V. Kazakov, and P. Vieira, "Exact Spectrum of Anomalous Dimensions of Planar N=4 Supersymmetric Yang-Mills Theory," *Phys. Rev. Lett.* **103** (2009) 131601, arXiv:0901.3753 [hep-th].

[59] D. Bombardelli, D. Fioravanti, and R. Tateo, "Thermodynamic Bethe Ansatz for planar AdS/CFT: A Proposal," *J. Phys.* **A42** (2009) 375401, arXiv:0902.3930 [hep-th].

[60] G. Arutyunov and S. Frolov, "On String S-matrix, Bound States and TBA," *JHEP* **12** (2007) 024, arXiv:0710.1568 [hep-th].

[61] G. Arutyunov and S. Frolov, "String hypothesis for the AdS(5) x S**5 mirror," *JHEP* **03** (2009) 152, arXiv:0901.1417 [hep-th].

[62] G. Arutyunov and S. Frolov, "Thermodynamic Bethe Ansatz for the AdS(5) x S(5) Mirror Model," *JHEP* **05** (2009) 068, arXiv:0903.0141 [hep-th].

[63] A. B. Zamolodchikov, "Thermodynamic Bethe Ansatz in Relativistic Models. Scaling Three State Potts and Lee-yang Models," *Nucl. Phys.* **B342** (1990) 695–720.

[64] A. B. Zamolodchikov, "On the thermodynamic Bethe ansatz equations for reflectionless ADE scattering theories," *Phys. Lett.* **B253** (1991) 391–394.

[65] K. G. Wilson, "Confinement of Quarks," *Phys. Rev.* **D10** (1974) 2445–2459.

[66] J. M. Maldacena, "Wilson loops in large N field theories," *Phys. Rev. Lett.* **80** (1998) 4859–4862, arXiv:hep-th/9803002 [hep-th].

[67] S.-J. Rey and J.-T. Yee, "Macroscopic strings as heavy quarks in large N gauge theory and anti-de Sitter supergravity," *Eur. Phys. J.* **C22** (2001) 379–394, arXiv:hep-th/9803001 [hep-th].

[68] G. W. Semenoff and K. Zarembo, "Wilson loops in SYM theory: From weak to strong coupling," *Nucl. Phys. Proc. Suppl.* **108** (2002) 106–112, arXiv:hep-th/0202156 [hep-th]. [,106(2002)].

[69] N. Drukker, D. J. Gross, and H. Ooguri, "Wilson loops and minimal surfaces," *Phys. Rev.* **D60** (1999) 125006, arXiv:hep-th/9904191 [hep-th].

[70] K. Zarembo, "Supersymmetric Wilson loops," *Nucl. Phys.* **B643** (2002) 157–171, arXiv:hep-th/0205160 [hep-th].

[71] Z. Guralnik and B. Kulik, "Properties of chiral Wilson loops," *JHEP* **01** (2004) 065, arXiv:hep-th/0309118 [hep-th].

[72] Z. Guralnik, S. Kovacs, and B. Kulik, "Less is more: Non-renormalization theorems from lower dimensional superspace," *Int. J. Mod. Phys.* **A20** (2005) 4546–4553, arXiv:hep-th/0409091 [hep-th].

[73] A. Dymarsky, S. S. Gubser, Z. Guralnik, and J. M. Maldacena, "Calibrated surfaces and supersymmetric Wilson loops," *JHEP* **09** (2006) 057, arXiv:hep-th/0604058 [hep-th].

[74] N. Drukker, S. Giombi, R. Ricci, and D. Trancanelli, "More supersymmetric Wilson loops," *Phys. Rev.* **D76** (2007) 107703, arXiv:0704.2237 [hep-th].

[75] N. Drukker, S. Giombi, R. Ricci, and D. Trancanelli, "Supersymmetric Wilson loops on S**3," *JHEP* **05** (2008) 017, arXiv:0711.3226 [hep-th].

[76] N. Drukker, "1/4 BPS circular loops, unstable world-sheet instantons and the matrix model," *JHEP* **09** (2006) 004, arXiv:hep-th/0605151 [hep-th].

[77] D. Gaiotto and X. Yin, "Notes on superconformal Chern-Simons-Matter theories," *JHEP* **08** (2007) 056, arXiv:0704.3740 [hep-th].

[78] N. Drukker, J. Plefka, and D. Young, "Wilson loops in 3-dimensional N=6 supersymmetric Chern-Simons Theory and their string theory duals," *JHEP* **11** (2008) 019, arXiv:0809.2787 [hep-th].

[79] B. Chen and J.-B. Wu, "Supersymmetric Wilson Loops in N=6 Super Chern-Simons-matter theory," *Nucl. Phys.* **B825** (2010) 38–51, arXiv:0809.2863 [hep-th].

[80] S.-J. Rey, T. Suyama, and S. Yamaguchi, "Wilson Loops in Superconformal Chern-Simons Theory and Fundamental Strings in Anti-de Sitter Supergravity Dual," *JHEP* **03** (2009) 127, arXiv:0809.3786 [hep-th].

[81] N. Drukker and D. Trancanelli, "A Supermatrix model for N=6 super Chern-Simons-matter theory," *JHEP* **02** (2010) 058, arXiv:0912.3006 [hep-th].

[82] V. Cardinali, L. Griguolo, G. Martelloni, and D. Seminara, "New supersymmetric Wilson loops in ABJ(M) theories," *Phys. Lett.* **B718** (2012) 615–619, arXiv:1209.4032 [hep-th].

[83] L. Griguolo, D. Marmiroli, G. Martelloni, and D. Seminara, "The generalized cusp in ABJ(M) N = 6 Super Chern-Simons theories," *JHEP* **05** (2013) 113, arXiv:1208.5766 [hep-th].

[84] N. Kim, "Supersymmetric Wilson loops with general contours in ABJM theory," *Mod. Phys. Lett.* **A28** (2013) 1350150, arXiv:1304.7660 [hep-th].

[85] M. S. Bianchi, L. Griguolo, M. Leoni, S. Penati, and D. Seminara, "BPS Wilson loops and Bremsstrahlung function in ABJ(M): a two loop analysis," *JHEP* **06** (2014) 123, arXiv:1402.4128 [hep-th].

[86] D. H. Correa, J. Aguilera-Damia, and G. A. Silva, "Strings in $AdS_4 \times \mathbb{CP}^3$ Wilson loops in $\mathcal{N}$ =6 super Chern-Simons-matter and bremsstrahlung functions," *JHEP* **06** (2014) 139, arXiv:1405.1396 [hep-th].

[87] K.-M. Lee and S. Lee, "1/2-BPS Wilson Loops and Vortices in ABJM Model," *JHEP* **09** (2010) 004, arXiv:1006.5589 [hep-th].

[88] E. Witten, "Quantum Field Theory and the Jones Polynomial," *Commun. Math. Phys.* **121** (1989) 351–399.

[89] J. K. Erickson, G. W. Semenoff, and K. Zarembo, "Wilson loops in N=4 supersymmetric Yang-Mills theory," *Nucl. Phys.* **B582** (2000) 155–175, arXiv:hep-th/0003055 [hep-th].

[90] N. Drukker and D. J. Gross, "An Exact prediction of N=4 SUSYM theory for string theory," *J. Math. Phys.* **42** (2001) 2896–2914, arXiv:hep-th/0010274 [hep-th].

[91] M. S. Bianchi, G. Giribet, M. Leoni, and S. Penati, "The 1/2 BPS Wilson loop in ABJ(M) at two loops: The details," *JHEP* **10** (2013) 085, arXiv:1307.0786 [hep-th].

[92] M. S. Bianchi, G. Giribet, M. Leoni, and S. Penati, "1/2 BPS Wilson loop in N=6 superconformal Chern-Simons theory at two loops," *Phys. Rev.* **D88** no. 2, (2013) 026009, arXiv:1303.6939 [hep-th].

[93] L. Griguolo, G. Martelloni, M. Poggi, and D. Seminara, "Perturbative evaluation of circular 1/2 BPS Wilson loops in N = 6 Super Chern-Simons theories," *JHEP* **09** (2013) 157, arXiv:1307.0787 [hep-th].

[94] E. Guadagnini, M. Martellini, and M. Mintchev, "Wilson Lines in Chern-Simons Theory and Link Invariants," *Nucl. Phys.* **B330** (1990) 575.

[95] N. Drukker, S. Giombi, R. Ricci, and D. Trancanelli, "Wilson loops: From four-dimensional SYM to two-dimensional YM," *Phys. Rev.* **D77** (2008) 047901, arXiv:0707.2699 [hep-th].

[96] A. A. Migdal, "Recursion Equations in Gauge Theories," *Sov. Phys. JETP* **42** (1975) 413. [Zh. Eksp. Teor. Fiz.69,810(1975)].

[97] B. E. Rusakov, "Loop averages and partition functions in U(N) gauge theory on two-dimensional manifolds," *Mod. Phys. Lett.* **A5** (1990) 693–703.

[98] M. Staudacher and W. Krauth, "Two-dimensional QCD in the Wu-Mandelstam-Leibbrandt prescription," *Phys. Rev.* **D57** (1998) 2456–2459, arXiv:hep-th/9709101 [hep-th].

[99] A. Bassetto and L. Griguolo, "Two-dimensional QCD, instanton contributions and the perturbative Wu-Mandelstam-Leibbrandt prescription," *Phys. Lett.* **B443** (1998) 325–330, arXiv:hep-th/9806037 [hep-th].

[100] E. Witten, "Two-dimensional gauge theories revisited," *J. Geom. Phys.* **9** (1992) 303–368, arXiv:hep-th/9204083 [hep-th].

[101] V. Pestun, "Localization of the four-dimensional N=4 SYM to a two-sphere and 1/8 BPS Wilson loops," *JHEP* **12** (2012) 067, arXiv:0906.0638 [hep-th].

[102] A. A. Gerasimov and S. L. Shatashvili, "Higgs Bundles, Gauge Theories and Quantum Groups," *Commun. Math. Phys.* **277** (2008) 323–367, arXiv:hep-th/0609024 [hep-th].

[103] A. A. Gerasimov and S. L. Shatashvili, "Two-dimensional gauge theories and quantum integrable systems," in *Proceedings of Symposia in Pure Mathematics, May 25-29 2007, University of Augsburg, Germany*. 2007. arXiv:0711.1472 [hep-th].
http://inspirehep.net/record/767222/files/arXiv:0711.1472.pdf.

[104] G. W. Moore, N. Nekrasov, and S. Shatashvili, "Integrating over Higgs branches," *Commun. Math. Phys.* **209** (2000) 97–121, arXiv:hep-th/9712241 [hep-th].

[105] N. A. Nekrasov and S. L. Shatashvili, "Quantization of Integrable Systems and Four Dimensional Gauge Theories," in *Proceedings, 16th International Congress on Mathematical Physics (ICMP09)*. 2009. arXiv:0908.4052 [hep-th].
http://inspirehep.net/record/829640/files/arXiv:0908.4052.pdf.

[106] S. Giombi and V. Pestun, "Correlators of local operators and 1/8 BPS Wilson loops on S**2 from 2d YM and matrix models," *JHEP* **10** (2010) 033, arXiv:0906.1572 [hep-th].

[107] S. Giombi, V. Pestun, and R. Ricci, "Notes on supersymmetric Wilson loops on a two-sphere," *JHEP* **07** (2010) 088, arXiv:0905.0665 [hep-th].

[108] A. Bassetto, L. Griguolo, F. Pucci, D. Seminara, S. Thambyahpillai, and D. Young, "Correlators of supersymmetric Wilson-loops, protected operators and matrix models in N=4 SYM," *JHEP* **08** (2009) 061, arXiv:0905.1943 [hep-th].

[109] A. Bassetto, L. Griguolo, F. Pucci, and D. Seminara, "Supersymmetric Wilson loops at two loops," *JHEP* **06** (2008) 083, arXiv:0804.3973 [hep-th].

[110] N. Drukker, M. Marino, and P. Putrov, "From weak to strong coupling in ABJM theory," *Commun. Math. Phys.* **306** (2011) 511–563, arXiv:1007.3837 [hep-th].

[111] M. Marino and P. Putrov, "Exact Results in ABJM Theory from Topological Strings," *JHEP* **06** (2010) 011, arXiv:0912.3074 [hep-th].

[112] N. Drukker, M. Marino, and P. Putrov, "Nonperturbative aspects of ABJM theory," *JHEP* **11** (2011) 141, arXiv:1103.4844 [hep-th].

[113] J.-L. Gervais and A. Neveu, "The Slope of the Leading Regge Trajectory in Quantum Chromodynamics," *Nucl. Phys.* **B163** (1980) 189.

[114] A. M. Polyakov, "Gauge Fields as Rings of Glue," *Nucl. Phys.* **B164** (1980) 171–188.

[115] V. S. Dotsenko and S. N. Vergeles, "Renormalizability of Phase Factors in the Nonabelian Gauge Theory," *Nucl. Phys.* **B169** (1980) 527.

[116] R. A. Brandt, F. Neri, and M.-a. Sato, "Renormalization of Loop Functions for All Loops," *Phys. Rev.* **D24** (1981) 879.

[117] G. P. Korchemsky and A. V. Radyushkin, "Renormalization of the Wilson Loops Beyond the Leading Order," *Nucl. Phys.* **B283** (1987) 342–364.

[118] R. A. Brandt, A. Gocksch, M. A. Sato, and F. Neri, "LOOP SPACE," *Phys. Rev.* **D26** (1982) 3611.

[119] A. V. Belitsky, A. S. Gorsky, and G. P. Korchemsky, "Gauge / string duality for QCD conformal operators," *Nucl. Phys.* **B667** (2003) 3–54, arXiv:hep-th/0304028 [hep-th].

[120] Y. Makeenko, P. Olesen, and G. W. Semenoff, "Cusped SYM Wilson loop at two loops and beyond," *Nucl. Phys.* **B748** (2006) 170–199, arXiv:hep-th/0602100 [hep-th].

[121] N. S. Craigie and H. Dorn, "On the Renormalization and Short Distance Properties of Hadronic Operators in QCD," *Nucl. Phys.* **B185** (1981) 204.

[122] I. I. Balitsky and V. M. Braun, "Evolution Equations for QCD String Operators," *Nucl. Phys.* **B311** (1989) 541–584.

[123] G. P. Korchemsky and G. Marchesini, "Structure function for large x and renormalization of Wilson loop," *Nucl. Phys.* **B406** (1993) 225–258, arXiv:hep-ph/9210281 [hep-ph].

[124] S. J. Brodsky, Y. Frishman, G. P. Lepage, and C. T. Sachrajda, "Hadronic Wave Functions at Short Distances and the Operator Product Expansion," *Phys. Lett.* **B91** (1980) 239.

[125] Yu. M. Makeenko, "Conformal operators in quantum chromodynamics," *Sov. J. Nucl. Phys.* **33** (1981) 440. [Yad. Fiz.33,842(1981)].

[126] T. Ohrndorf, "Constraints From Conformal Covariance on the Mixing of Operators of Lowest Twist," *Nucl. Phys.* **B198** (1982) 26.

[127] N. Drukker and S. Kawamoto, "Small deformations of supersymmetric Wilson loops and open spin-chains," *JHEP* **07** (2006) 024, arXiv:hep-th/0604124 [hep-th].

[128] N. Beisert *et al.*, "Review of AdS/CFT Integrability: An Overview," *Lett. Math. Phys.* **99** (2012) 3–32, arXiv:1012.3982 [hep-th].

[129] N. Beisert, "The SU(2—2) dynamic S-matrix," *Adv. Theor. Math. Phys.* **12** (2008) 948–979, arXiv:hep-th/0511082 [hep-th].

[130] D. M. Hofman and J. M. Maldacena, "Reflecting magnons," *JHEP* **11** (2007) 063, arXiv:0708.2272 [hep-th].

[131] D. Correa, J. Henn, J. Maldacena, and A. Sever, "An exact formula for the radiation of a moving quark in N=4 super Yang Mills," *JHEP* **06** (2012) 048, arXiv:1202.4455 [hep-th].

[132] B. Fiol, B. Garolera, and A. Lewkowycz, "Exact results for static and radiative fields of a quark in N=4 super Yang-Mills," *JHEP* **05** (2012) 093, arXiv:1202.5292 [hep-th].

[133] L. F. Alday and J. M. Maldacena, "Gluon scattering amplitudes at strong coupling," *JHEP* **06** (2007) 064, arXiv:0705.0303 [hep-th].

[134] L. F. Alday and J. Maldacena, "Comments on gluon scattering amplitudes via AdS/CFT," *JHEP* **11** (2007) 068, arXiv:0710.1060 [hep-th].

[135] J. M. Drummond, G. P. Korchemsky, and E. Sokatchev, "Conformal properties of four-gluon planar amplitudes and Wilson loops," *Nucl. Phys.* **B795** (2008) 385–408, arXiv:0707.0243 [hep-th].

[136] V. Forini, "Quark-antiquark potential in AdS at one loop," *JHEP* **11** (2010) 079, arXiv:1009.3939 [hep-th].

[137] N. Drukker and V. Forini, "Generalized quark-antiquark potential at weak and strong coupling," *JHEP* **06** (2011) 131, arXiv:1105.5144 [hep-th].

[138] V. Forini, V. G. M. Puletti, and O. Ohlsson Sax, "The generalized cusp in AdS_4 x CP^3 and more one-loop results from semiclassical strings," *J. Phys.* **A46** (2013) 115402, arXiv:1204.3302 [hep-th].

[139] D. Correa, J. Maldacena, and A. Sever, "The quark anti-quark potential and the cusp anomalous dimension from a TBA equation," *JHEP* **08** (2012) 134, arXiv:1203.1913 [hep-th].

[140] N. Drukker, "Integrable Wilson loops," *JHEP* **10** (2013) 135, arXiv:1203.1617 [hep-th].

[141] D. Correa, J. Henn, J. Maldacena, and A. Sever, "The cusp anomalous dimension at three loops and beyond," *JHEP* **05** (2012) 098, arXiv:1203.1019 [hep-th].

[142] J. M. Henn and T. Huber, "Systematics of the cusp anomalous dimension," *JHEP* **11** (2012) 058, arXiv:1207.2161 [hep-th].

[143] J. M. Henn and T. Huber, "The four-loop cusp anomalous dimension in $\mathcal{N} = 4$ super Yang-Mills and analytic integration techniques for Wilson line integrals," *JHEP* **09** (2013) 147, arXiv:1304.6418 [hep-th].

[144] N. Gromov and F. Levkovich-Maslyuk, "Quark–anti-quark potential in N=4 SYM," arXiv:1601.05679 [hep-th].

[145] J. M. Henn, J. Plefka, and K. Wiegandt, "Light-like polygonal Wilson loops in 3d Chern-Simons and ABJM theory," *JHEP* **08** (2010) 032, arXiv:1004.0226 [hep-th]. [Erratum: JHEP11,053(2011)].

[146] A. Lewkowycz and J. Maldacena, "Exact results for the entanglement entropy and the energy radiated by a quark," *JHEP* **05** (2014) 025, arXiv:1312.5682 [hep-th].

[147] M. Bianchi, L. Griguolo, A. Mauri, S. Penati, M. Preti, and D. Seminara, "ABJ(M) Bremsstrahlung function at three loops and beyond," *In progress* (2016) .

[148] D. Young, "BPS Wilson Loops on S**2 at Higher Loops," *JHEP* **05** (2008) 077, arXiv:0804.4098 [hep-th].

[149] A. Bassetto, L. Griguolo, F. Pucci, D. Seminara, S. Thambyahpillai, and D. Young, "Correlators of supersymmetric Wilson loops at weak and strong coupling," *JHEP* **03** (2010) 038, arXiv:0912.5440 [hep-th].

[150] S. Giombi and V. Pestun, "The 1/2 BPS 't Hooft loops in N=4 SYM as instantons in 2d Yang-Mills," *J. Phys.* **A46** (2013) 095402, arXiv:0909.4272 [hep-th].

[151] G. W. Semenoff and K. Zarembo, "More exact predictions of SUSYM for string theory," *Nucl. Phys.* **B616** (2001) 34–46, arXiv:hep-th/0106015 [hep-th].

[152] G. W. Semenoff and D. Young, "Exact 1/4 BPS Loop: Chiral primary correlator," *Phys. Lett.* **B643** (2006) 195–204, arXiv:hep-th/0609158 [hep-th].

[153] S. Giombi and V. Pestun, "Correlators of Wilson Loops and Local Operators from Multi-Matrix Models and Strings in AdS," *JHEP* **01** (2013) 101, arXiv:1207.7083 [hep-th].

[154] K. Zarembo, "Holographic three-point functions of semiclassical states," *JHEP* **09** (2010) 030, arXiv:1008.1059 [hep-th].

[155] M. S. Costa, R. Monteiro, J. E. Santos, and D. Zoakos, "On three-point correlation functions in the gauge/gravity duality," *JHEP* **11** (2010) 141, arXiv:1008.1070 [hep-th].

[156] J. Escobedo, N. Gromov, A. Sever, and P. Vieira, "Tailoring Three-Point Functions and Integrability," *JHEP* **09** (2011) 028, arXiv:1012.2475 [hep-th].

[157] M. Bonini, L. Griguolo, and M. Preti, "Correlators of chiral primaries and 1/8 BPS Wilson loops from perturbation theory," *JHEP* **09** (2014) 083, arXiv:1405.2895 [hep-th].

[158] N. Drukker and J. Plefka, "Superprotected n-point correlation functions of local operators in N=4 super Yang-Mills," *JHEP* **04** (2009) 052, arXiv:0901.3653 [hep-th].

[159] A. A. Migdal, "Gauge Transitions in Gauge and Spin Lattice Systems," *Sov. Phys. JETP* **42** (1975) 743. [Zh. Eksp. Teor. Fiz.69,1457(1975)].

[160] E. Witten, "On quantum gauge theories in two-dimensions," *Commun. Math. Phys.* **141** (1991) 153–209.

[161] N. Beisert, C. Kristjansen, J. Plefka, G. W. Semenoff, and M. Staudacher, "BMN correlators and operator mixing in N=4 superYang-Mills theory," *Nucl. Phys.* **B650** (2003) 125–161, arXiv:hep-th/0208178 [hep-th].

[162] N. Gromov, V. Kazakov, S. Leurent, and D. Volin, "Quantum Spectral Curve for Planar $\mathcal{N}$ = Super-Yang-Mills Theory," *Phys. Rev. Lett.* **112** no. 1, (2014) 011602, arXiv:1305.1939 [hep-th].

[163] N. Beisert, B. Eden, and M. Staudacher, "Transcendentality and Crossing," *J. Stat. Mech.* **0701** (2007) P01021, arXiv:hep-th/0610251 [hep-th].

[164] Z. Bern, M. Czakon, L. J. Dixon, D. A. Kosower, and V. A. Smirnov, "The Four-Loop Planar Amplitude and Cusp Anomalous Dimension in Maximally Supersymmetric Yang-Mills Theory," *Phys. Rev.* **D75** (2007) 085010, arXiv:hep-th/0610248 [hep-th].

[165] S. S. Gubser, I. R. Klebanov, and A. M. Polyakov, "A Semiclassical limit of the gauge / string correspondence," *Nucl. Phys.* **B636** (2002) 99–114, arXiv:hep-th/0204051 [hep-th].

[166] N. Gromov and F. Levkovich-Maslyuk, "Quantum Spectral Curve for a Cusped Wilson Line in N=4 SYM," arXiv:1510.02098 [hep-th].

[167] N. Gromov and A. Sever, "Analytic Solution of Bremsstrahlung TBA," *JHEP* **11** (2012) 075, arXiv:1207.5489 [hep-th].

[168] N. Gromov, F. Levkovich-Maslyuk, and G. Sizov, "Analytic Solution of Bremsstrahlung TBA II: Turning on the Sphere Angle," *JHEP* **10** (2013) 036, arXiv:1305.1944 [hep-th].

[169] G. Sizov and S. Valatka, "Algebraic Curve for a Cusped Wilson Line," *JHEP* **05** (2014) 149, arXiv:1306.2527 [hep-th].

[170] M. Bonini, L. Griguolo, M. Preti, and D. Seminara, "Bremsstrahlung function, leading Luscher correction at weak coupling and localization," arXiv:1511.05016 [hep-th].

[171] N. Gromov, V. Kazakov, S. Leurent, and D. Volin, "Solving the AdS/CFT Y-system," *JHEP* **07** (2012) 023, arXiv:1110.0562 [hep-th].

[172] D. Berenstein and D. Trancanelli, "Three-dimensional N=6 SCFT's and their membrane dynamics," *Phys. Rev.* **D78** (2008) 106009, arXiv:0808.2503 [hep-th].

[173] A. Klemm, M. Marino, M. Schiereck, and M. Soroush, "Aharony-Bergman-Jafferis–Maldacena Wilson loops in the Fermi gas approach," *Z. Naturforsch.* **A68** (2013) 178–209, arXiv:1207.0611 [hep-th].

[174] M. Marino and P. Putrov, "ABJM theory as a Fermi gas," *J. Stat. Mech.* **1203** (2012) P03001, arXiv:1110.4066 [hep-th].

[175] Y. Hatsuda, S. Moriyama, and K. Okuyama, "Instanton Effects in ABJM Theory from Fermi Gas Approach," *JHEP* **01** (2013) 158, arXiv:1211.1251 [hep-th].

[176] F. Calvo and M. Marino, "Membrane instantons from a semiclassical TBA," *JHEP* **05** (2013) 006, arXiv:1212.5118 [hep-th].

[177] Y. Hatsuda, M. Marino, S. Moriyama, and K. Okuyama, "Non-perturbative effects and the refined topological string," *JHEP* **09** (2014) 168, arXiv:1306.1734 [hep-th].

[178] J. A. Minahan and K. Zarembo, "The Bethe ansatz for superconformal Chern-Simons," *JHEP* **09** (2008) 040, arXiv:0806.3951 [hep-th].

[179] G. Arutyunov and S. Frolov, "Superstrings on AdS(4) x CP**3 as a Coset Sigma-model," *JHEP* **09** (2008) 129, arXiv:0806.4940 [hep-th].

[180] B. Stefanski, jr, "Green-Schwarz action for Type IIA strings on AdS(4) x CP**3," *Nucl. Phys.* **B808** (2009) 80–87, arXiv:0806.4948 [hep-th].

[181] N. Gromov and P. Vieira, "The AdS(4) / CFT(3) algebraic curve," *JHEP* **02** (2009) 040, arXiv:0807.0437 [hep-th].

[182] N. Gromov and P. Vieira, "The all loop AdS4/CFT3 Bethe ansatz," *JHEP* **01** (2009) 016, arXiv:0807.0777 [hep-th].

[183] T. Nishioka and T. Takayanagi, "On Type IIA Penrose Limit and N=6 Chern-Simons Theories," *JHEP* **08** (2008) 001, arXiv:0806.3391 [hep-th].

[184] D. Gaiotto, S. Giombi, and X. Yin, "Spin Chains in N=6 Superconformal Chern-Simons-Matter Theory," *JHEP* **04** (2009) 066, arXiv:0806.4589 [hep-th].

[185] G. Grignani, T. Harmark, and M. Orselli, "The SU(2) x SU(2) sector in the string dual of N=6 superconformal Chern-Simons theory," *Nucl. Phys.* **B810** (2009) 115–134, arXiv:0806.4959 [hep-th].

[186] N. Gromov and G. Sizov, "Exact Slope and Interpolating Functions in N=6 Supersymmetric Chern-Simons Theory," *Phys. Rev. Lett.* **113** no. 12, (2014) 121601, arXiv:1403.1894 [hep-th].

[187] L. Bianchi, M. S. Bianchi, A. Bres, V. Forini, and E. Vescovi, "Two-loop cusp anomaly in ABJM at strong coupling," *JHEP* **10** (2014) 13, arXiv:1407.4788 [hep-th].

[188] M. Bonini, L. Griguolo, M. Preti, and D. Seminara, "Surprises from the resummation of ladders in the ABJ(M) cusp anomalous dimension," *To appear* (2016) .

[189] F. Cooper, A. Khare, and U. Sukhatme, "Supersymmetry and quantum mechanics," *Phys. Rept.* **251** (1995) 267–385, arXiv:hep-th/9405029 [hep-th].

[190] D. H. Correa, F. I. S. Massolo, and D. Trancanelli, "Cusped Wilson lines in symmetric representations," *JHEP* **08** (2015) 091, arXiv:1506.01680 [hep-th].

[191] A. Cavaglià, D. Fioravanti, N. Gromov, and R. Tateo, "Quantum Spectral Curve of the $\mathcal{N} = 6$ Supersymmetric Chern-Simons Theory," *Phys. Rev. Lett.* **113** no. 2, (2014) 021601, arXiv:1403.1859 [hep-th].

[192] D. Bombardelli, D. Fioravanti, and R. Tateo, "TBA and Y-system for planar AdS(4)/CFT(3)," *Nucl. Phys.* **B834** (2010) 543–561, arXiv:0912.4715 [hep-th].

[193] N. Gromov and F. Levkovich-Maslyuk, "Y-system, TBA and Quasi-Classical strings in AdS(4) x CP3," *JHEP* **06** (2010) 088, arXiv:0912.4911 [hep-th].

[194] A. Cavaglia, D. Fioravanti, and R. Tateo, "Discontinuity relations for the AdS_4/CFT_3 correspondence," *Nucl. Phys.* **B877** (2013) 852–884, arXiv:1307.7587 [hep-th].